Computational Synthetic Biology for Molecular Communications

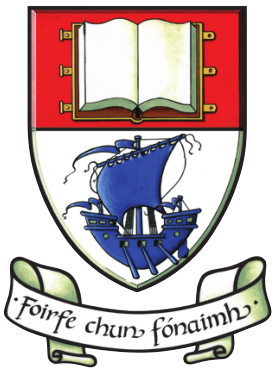

Daniel Perez Martins, MSc

School of Science and Computing

Waterford Institute of Technology

This dissertation is submitted for the degree of

Doctor of Philosophy

Supervisors: Dr Sasitharan BALASUBRAMANIAM
Dr Michael Taynan BARROS

Submitted to Waterford Institute of Technology, October 2019

DECLARATION

I hereby certify that this material, which I now submit for assessment on the programme of study leading to the award of Doctor of Philosophy, is entirely my own work and has not been taken from the work of others save to the extent that such work has been cited and acknowledged within the text of my work.

Signed: _____ ID: 20069724

To my wife Larissa Perez Cavalcante.

To my mother Virgínia de Fátima Perez Martins.

ACKNOWLEDGMENT

I would like to express my deep gratitude and appreciation to Dr Sasitharan Balasubramaniam and Dr Michael Barros, my research supervisors, for their patient guidance, enthusiastic encouragement and useful critiques during the development of this PhD research. Sasi, your passion, ambition and work ethics taught me that to be able to do high-level research you have to aim high, push the boundaries, and to not rest until producing the best possible result. Michael, your drivenness, ambition and mindfulness taught me that the research career is built by small steps that have always aim to the same goal and that regardless how hard the research life is, you should keep your head high and enjoy the process. I thank both of you for shaping me as a better professional.

I would also like to extend my thanks to all of the TSSG community, for giving me this opportunity to pursue the highest level of education. TSSG is a great place to work that I was blessed to be part of it during these years.

I would like to acknowledge the support from Lee Coffey, Pharmaceutical Molecular and Biotechnology Research Centre (PMBRC) at Waterford Institute of Technology, Ireland; Prof. Arinthip Thamchaipenet and Kantinan Leetanasaksakul, Kasetsart University, Thailand; Massimiliano Pierobon, University of Nebraska-Lincoln; and Pietro Lió, University of Cambridge, UK for their collaboration and invaluable support to develop this PhD research.

I would like to thank my wife for her unconditional support and encouragement to become a better professional. Your love and caring eased the tough moments during these four years of PhD. I am very happy and lucky to have you by my side. I would like to express my gratitude and love to you.

I would also like to thank my family, especially my mother, Virginia, for the education and teachings that enabled me to have the ethic required to pursue a PhD degree.

”Thus, the task is, not so much to see what no one has yet seen; but to think what nobody has yet thought, about that which everybody sees.”

Erwin Schrödinger

”The real voyage of discovery consists not in seeking new lands but seeing with new eyes.”

Marcel Proust

Computational Synthetic Biology for Molecular Communications

D. P. Martins

Abstract

Bacteria-based synthetic biology systems have been proposed in the past twenty years as solutions for biotechnology and the design of novel therapeutics. In parallel to the field of synthetic biology, a new field has emerged where engineers can characterize and design communications systems through the exchange of molecules. This field is known as molecular communications, and has taken the paradigm from conventional communication networks and applied it to biological systems. This paradigm shift has numerous challenges, and in particular due to the characteristics of the molecular signal propagation behaviour that is very different from electromagnetic signals. Since the birth of this new field, numerous research works have concentrated on characterizing the communication channels and developing theoretical models to lay the groundwork for novel applications. Both Synthetic Biology and Molecular Communications fields have evolved since then, and the current challenges reside in the ability to combine these two fields together to create novel applications. The aim of integrating these two fields is to enable implementation of complex synthetic circuits that are able to autonomously operate in the long-term with high accuracy levels and reliability.

In this PhD thesis, synthetic biology and molecular communications systems are integrated through computational methods for a number of applications that utilizes bacteria as the main cell lines to be programmed. This novel combination can provide novel biotechnology solutions such as biofilm prevention, bio-sensor synthetic gates, as well as synthetic logic circuits. This synergistic integration was proven in this PhD thesis, and can provide a new direction for the molecular communications community.

LIST OF FIGURES

LIST OF TABLES

CONTENTS

CHAPTER 1

INTRODUCTION

1.1 SYNTHETIC BIOLOGY

The formal method for the design of artificial systems based on engineering of biological cells is known as Synthetic Biology. Currently, several synthetic designs and applications have been proposed to perform a variety of functions, such as novel theranostics (therapeutics plus diagnostics), and synthetic computing systems [1–4]. For example, a bacterial population used for a targeted drug delivery system can be controlled using a killing switch activated by their signalling process [3]. Their ultimate goal is to solve complex biotechnological problems that are not solvable using the tool sets provided by single disciplines. The interdisciplinary nature of this field is the fundamental approach taken to develop novel solutions.

Similar to the development of engineering systems, both bottom-up and top down approaches can be applied to the design of synthetic systems. However, scientists often prefer designing complex systems by first building their small components, which reduces the overall complexity of the entire systems. Electronic and communications systems are examples of complex systems built using a bottom-up approach. Nonetheless, this does not invalidate the top-down designs such as the works in [5–7]. For instance, computational tools that

aid the design of synthetic systems requires an overall understanding about the system's operation by the researchers [6]. Großkopf et al. reviewed the top-down designs of synthetic microbial communities built to understand the population's ecological interactions [5]. Using the top-down approach, researchers were also able to minimise the genome required for the design of a viable bacteria cell[1].

There are several implementations of synthetic systems based on prokaryotic cells. This is due to the extensive knowledge known about prokaryotic cells, allied with its simplicity compared to eukaryotic cells. Designs from simple logic gates to novel therapeutics can be developed using bacteria-based synthetic systems. For example, engineered *Escherichia coli* populations were interconnected to build different two-input Boolean logic gates [4]. In a more complex example, a combination of oral drugs and a substance produce by engineered *Lactobacilus lactis* bacteria can restore blood sugar levels [8]. Researchers have also developed synthetic systems based on the interactions of two different bacterial strains. For example, *Escherichia coli* cells were engineered to detect and produce specific antibiotics to target pathogenic *Pseudomonas aeruginosa* cells [9].

Methods and techniques often applied to engineering processes are considered in the design of synthetic biology systems. It is important, for example, to consider modular components when building a synthetic circuit to enhance its flexibility, which is similar to the approach taken to design electronic circuits [10]. Furthermore, synthetic systems should be controllable and have a certain degree of reliability to prevent unwanted effects that harm the cell, and their outputs should be predictable so models can be constructed and designed for applications.

Despite the similarities discussed above, designing biological systems poses several challenges that are not common to the typical engineering fields. Mutation, uncertainty originated from gene expression noise, and ever changing extracellular environments are issues only faced by synthetic systems, each of which affects the predictability as well as

[1] A cell is considered viable if they are able to grow and replicate [7]

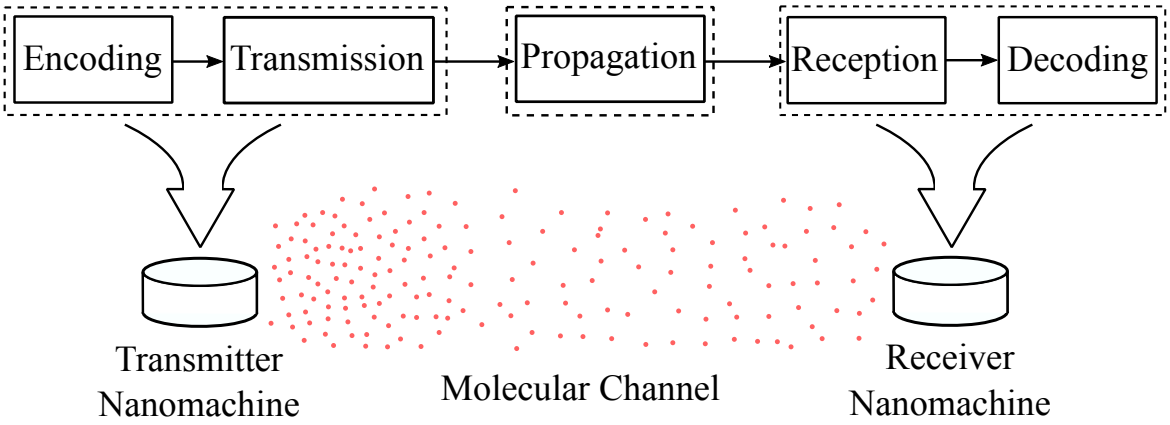

Fig. 1.1 Illustration of an end-to-end molecular communications system. The transmitter nanomachine encodes the information into a molecular signal, which may be through the concentration of molecules, and transmits it through a molecular channel. The receiver nanomachine will then retrieve the information from the received molecular signal.

reliability. Simplifying assumptions are often considered in order to create basic synthetic systems that are modular, therefore, reducing the number of uncertainties and enabling engineers to focus on aspects required for the design of these systems. An important aspect to take into account for the interoperability of these modules is their communications capability, as some of the current synthetic circuits are based on the exchange of molecules. This adds one more layer of complexity for the design of synthetic systems. Chapter 3 presents further details about the state-of-the-art and challenges in developing these systems.

1.2 MOLECULAR COMMUNICATIONS

A molecular communications system is an abstraction of the processes involved in the production, emission, transportation and reception of molecules by natural or artificial entities [11]. In this model, transmitter and reception nanomachines are the structures responsible for the production, emission and reception of a molecular signal (see Figure 1.1). The communications channel that interconnect these nanomachines is based on diffused propagation of molecules. In this case, the molecular mass can passively or actively move

from the nano transmitter to the nano receiver depending on the existence of an external force that induces their movement. [11, 12].

The study of natural cellular signalling processes is one of the research objectives in the field of molecular communications. Neurons, bacteria, and molecular motors have all been investigated in the design of molecular communications systems. The characteristics of each cellular system defines the molecular communications systems architecture. For instance, for a calcium signalling system, the molecular signal is the calcium ions that are transported between cells [13]. A very different example is the design of bacterial based systems, where bacteria can be the signal carrier, and can also be designed as the nano transmitter and receiver depending on the application [14].

This PhD work is focused on the design of bacteria-based molecular communications systems. In this case, the signal is the molecules produced, emitted, transported and received by the bacteria. In this communication paradigm, bacteria can be modelled as the nano transmitter and receiver or even the molecular signal carrier, depending on the communication architecture. Furthermore, these molecules are transported through free diffusion communications channel. Using these definitions, different bacteria-based molecular communications systems have been characterised and simulated over the past ten years [14–41]. Bacteria-based molecular communications systems enable a biocompatible exchange of molecules between the nanomachines [42], and have been proposed for a variety of applications, such as nanosensors and nanonetworks [21, 23, 26, 27, 32–34, 38]. A further description of bacteria-based molecular communications systems is presented in Chapter 4.

Even though there are high quantity of works describing and characterising the different molecular communications architectures, only a limited number of them lead to practical applications [43]. There is a gap between the molecular communications theory and its implementation towards real problems. Molecular communications systems have the potential to be pivotal in the development of novel theranostics technologies based on the communication

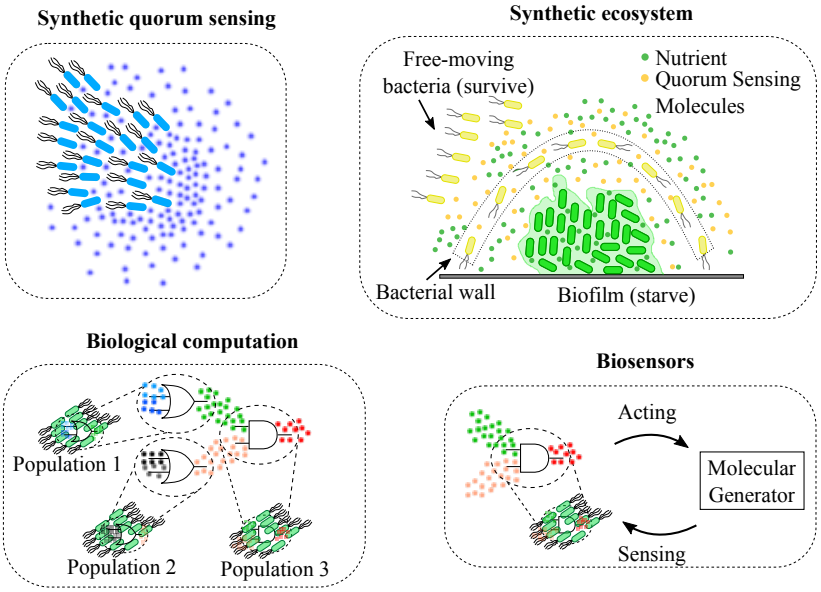

Fig. 1.2 Illustration of the bacteria-based molecular communications systems that are investigated in this research work.(a) Bacteria were engineered to produce quorum sensing molecules. (b) A predator-prey scenario can be built by exploiting the detection of quorum sensing molecules. In this case, bacteria were engineered to form a wall to consume the nutrients available around a biofilm. (c) Bacterial populations can be engineered to perform logic operations using different signalling molecules. By interconnecting these populations, synthetic circuits can be built, where each population will represent a logic gate. (d) Bacteria can sense specific molecules diffused into the environment and act to suppress them, or even produce biomarkers to notify their presence.

of nanomachines [43]. Therefore, it is important to narrow the gap between theory and practice by bringing synthetic biology and molecular communications together.

1.3 Engineering Communications Systems into Cells

A variety of artificial communications systems can be built using the natural bacterial signalling processes. Currently, there are several research avenues for the study of these engineered communications systems: synthetic quorum sensing systems, biological computation, synthetic ecosystems, bioprocessing, tissue engineering, synthetic pattern formation,

and biosensors [44]. In order to create these synthetic communications systems, researchers rewire bacterial quorum sensing systems to target the expression of genes specific to each desired application [44]. This rewiring often includes the design of custom plasmids that are injected into the bacterial cells that will change their functionalities. A similar result can be achieved by using specific inducers to activate the target genes. However, this approach is not always feasible due to the induction of higher molecular concentration requirements [44].

Bacteria can produce collective behaviours through quorum sensing (please refer to Chapter 2 for further details). Therefore, to investigate and exploit these behaviours for more complex applications, researchers engineer bacteria to produce specific molecules (e.g., autoinducers and chemoattractants). This is the minimum requirement for the development of an artificial communications system using bacteria, and this process is illustrated in Figure 1.2a [2–4, 8, 9, 45–50]. By exploiting the production and detection of signalling molecules, researchers were able to create synthetic bacterial communities to investigate ecosystems interactions like commensalism, predation and cooperation [5]. Figure 1.2b illustrates a scenario developed by Martins et al., where bacteria were engineered to identify the presence of a biofilm[2] and form a wall to surround it and consume the nutrients. The goal is to induce the biofilm disassembling process that can result from nutrient starvation [51].

The production of signalling molecules in response to the molecular concentrations in the environment can be applied to the design of bacteria-based systems capable of perform logic operations (see Figure 1.2c). These synthetic logic gates can be interconnected through diffusion channels to create circuits to produce a specific biomarker or molecules required for medical treatment [4, 45, 52–55]. Bacteria-based biosensor systems can be further enhanced to actuate the molecular source after sensing specific signalling molecules [38]. This process is illustrated in Figure 1.2d. This PhD thesis is focused on these four applications, and the following chapters provides further details for each of these applications.

[2]bacterial population surrounded by a polysaccharide matrix

1.4 RESEARCH SCOPE AND OBJECTIVES OF THE THESIS

The engineering of synthetic circuits in bacteria still poses numerous challenges. Currently, there are no complex bacteria-based therapeutics which can be used solely and don't rely on combinations with other drugs. Furthermore, these synthetic circuits cannot respond dynamically to pathogens and to environmental changes [2]. The lack of large synthetic circuits that can integrate safety switches to prevent the system from running unpredictably are also a major challenges for this type of application [2]. This PhD research work involves the analysis of biological behaviours and the modelling of molecular communications systems using bacteria. Moreover, it is focused on the interconnection of synthetic biology and molecular communications techniques to address the following challenges:

1. Establish a novel method for analysing the synthetic systems capable of communicating at the nanoscale

2. Model biological processes using conventional communications systems techniques

3. Shed light on cellular characteristics that are fundamental to the development of novel bacteria-based molecular communications systems

The close collaboration with a number of wet lab experimentalists, who have provided data required for the validation of the proposed computational models, will support the investigation and design of bacteria-based molecular communications system that addresses the aforementioned challenges. These collaborators include Prof. Arinthip Thamchaipenet from Department of Genetics, Kasetsart University, Thailand and Dr Lee Coffey from the Pharmaceutical and Molecular Biotechnology Research Centre, Waterford Institute of Technology, Ireland.

1.4.1 OBJECTIVES

The aim of this PhD research work is to investigate and model the molecular communications processes that support the operation of bacteria-based synthetic systems. This research is entirely dedicated to the modelling and analysis of bacteria-based molecular communications systems that will enhance the reliability and predictability of bacteria-based synthetic systems. Its ultimate goal is to lay the groundwork for the future development of novel theranostics systems. Therefore, the following specific objectives are defined to address the current limitations and challenges of this form of molecular communications system.

1. **Computational modelling of biotechnological applications based on common bacterial behaviours:** Computational models are a fundamental step used for the investigation of communications between bacteria, and to determine how this can be impacted when there are several species. They are less expensive compared to wet lab experiments [3] and can help in the identification of important characteristics that may not be possible to detect using the current technology **(focus on challenges 1 and 2)**.

2. **Enhancing the synthetic systems' reliability through bacteria-based molecular communications:** The current investigation on the reliability of synthetic systems is based on improving the genetic designs of the engineered cells. In particular for systems that apply signalling molecules to interconnect bacterial populations, the reliability analysis has not been properly investigated. The communications processes can introduce a series of uncertainties that can affect the overall reliability of the system. Therefore, it is important to evaluate the impact of the molecular communications systems on the reliable operation of the bacteria-based synthetic systems **(focus on challenges 1, 2 and 3)**.

[3] When compared to wet lab experiments

3. **Using bacteria-based molecular communications systems as novel theranostics tools:** New treatments and diagnostics are being investigated to improve the current medical practices in order to counter the emergence of antibiotic-resistant microbes, as well as other diseases. Bacteria-based synthetic systems supported by molecular communications can play a role for this new emerging application, as they can provide biocompatible solutions for these problems **(focus on challenges 1 and 3)**.

1.5 RESEARCH QUESTIONS

In the previous sections, a number of the challenges posed towards the development of practical bacteria-based communications systems were introduced (e.g., the impact from the dynamic environmental changes.) This research work aims to contribute towards the development of solutions for these aforementioned challenges. This is formally described through the following hypothesis:

Engineered bacteria-based molecular communications systems can guide and support synthetic engineering to enable the development of new biocompatible solutions for future theranostics tools.

These theranostics tools will have the bacteria-based molecular communications for sensing their enviroment and actuating on it, which in this thesis, is also studied in terms of possible closed-loop systems when bacteria is able to perform decision making, i.e. computation through synthetic logic circuits. Firstly, we will propose the use of bacteria-based molecular communications systems to investigate how to disassemble and prevent biofilms. Then we will expand towards designing bacteria-based computing devices, and finally, investigate the reliability of synthetic logic gates developed from bacteria-based molecular communications systems. This hypothesis has led to a number of research questions which were designed to fulfil all the required aspects for building synthetic communications systems.

First Research Question (RQ1) - *How can the communication functionalities of engineered bacteria through their genetics circuits be used for enhanced biological processes control?*

Synthetic biologists have been able to engineer bacteria to target several different biotechnological applications (e.g., logic computing of molecular signals) [3, 4, 56].

However, controlling biological functions is a lasting issue, which can lead to biocompatibility problems when designing bacteria-based molecular communication systems due to the lack of understanding and characterizing bacteria population interactions. The scientific literature on these systems concentrates on the modelling and performance analysis of communications processes of limited small-scale scenarios where control is a minor issue. Besides, more work is needed to drive molecular communication systems based on synthetic bacteria with enhanced communication capabilities for biological control and address its applicability in the biotechnology field. Therefore, one of the research tasks in this PhD thesis is to expand on modelling synthetic systems using molecular communications, in particular focusing on the communication performance when the engineered bacteria interact with the other populations. The goal is to model communication where different bacterial behaviours emerge from complex social interactions. Therefore, to assess these systems' performance, conventional communications metrics like noise, delay, signal power and path loss, are considered to give an appropriate quantification analysis of the bacteria population communication. This can be used for bacteria behaviour control, for example using quorum-sensing signals to coordinate bacteria by manipulating their movement, as well as using, again quorum-sensing signals, but now to interfere in the bacteria population communication to prevent biofilm formation **(focus on objectives 1 and 3)**.

Second Research Question (RQ2) - *How can the social interactions between bacteria influence the performance of their molecular communications systems?*

Bacteria are known to have very complex social structures, and they maintain these through complex molecular communication processes that do not only exist within their species but also between multiple different bacteria species. These social interactions and structures maintain bacteria community working under a certain hierarchy that is spatially distributed, where their position on the population reflects on the communication process with one another that is directly linked to the population chances of survival in an environment. For this research task, this PhD thesis will analyse social interactions among the bacterial cells, that represents the behaviours found in individual cells, which are much simpler. This is needed to measure how the interactions will impact on the noise, delay, signal power and path loss of the synthetic bacteria-based molecular communications system. This analyses will expand upon the RQ1 findings to modify and change some of the communication processes related to inducing positive or negative ecological relationships amongst the bacterial populations. This can allow the development of new approaches to curbing diseases (e.g. chronic infections and biofouling) that can arise from bacterial survival strategies, such as biofilms. To do this, concepts from conventional communications systems, such as sensing, actuating, jamming and interference, introduced by this work, can be adopted to counter these bacterial survival strategies **(focus on objectives 1 and 3)**.

Third Research Question (RQ3) - *How to design novel bacteria-on-a-chip devices using their embedded synthetic molecular communication functionalities for the development of future theranostics tools?*

Bacteria-on-a-chip devices emerge as the combination of living cells and electronics to develop a new range of sensors and actuators that exploits existing or engineered biological systems under a controlled micro-environment to allow novel operations in harsh or difficult environments. The most outstanding example is the ingestible bacteria-on-a-chip proposed by Mimee et al [57] that integrates living engineered

bacteria and low-power transceiver circuitry to wirelessly detect biological signals in the human gut and monitor its health. Another example is the bacteria population in a microfluidic device, which was used to develop a molecular diagnostics kit by analysing the concentration samples of the bacteria *Escherichia coli*'s XL1-blue and K12 strains propagation by Puchberger-Enengl et al [58].

This PhD thesis expands this concept and devise new type of systems under the bacteria-on-a-chip umbrella, the Bacterial Molecular Communications on a Chip and Bacterial Molecular Computing on a Chip devices. A throughout analysis of these two types of devices from the conceptual design, to modelling and their performance validation is a required step towards the development of future biotechnological applications, such as theranostics tools **(focus on objectives 2 and 3)**.

Fourth Research Question (RQ4) - *How can bacteria communication be engineered to build reliable bacteria-based synthetic logic circuits?*

Currently, synthetic biologists are able to engineer circuits into bacteria to perform tasks, like simple logic computing. However, numerous challenges have slowed down the development and application of more complex genetic circuits. The modelling of the communications processes (internal and external to the bacteria) is an important step towards the solution of those aforementioned challenges (see Section 1.4). Therefore, in this research we will model and analyse the molecular communications of engineered bacterial populations that are used to create synthetic logic circuits that are reliable despite being affected by unwanted effects, such as noise from the environment and delays from unsynchronised signals **(focus on objectives 2 and 3)**.

1.6 DOCUMENT ORGANIZATION

The rest of the thesis is organized as follows. Chapter 2 introduces the biological background that lay the foundation for modelling of bacteria-based molecular communications systems. Chapter 4 introduces, defines and characterises these systems, from a communications perspective. Therefore, this chapter is focused on relationships of biological systems and conventional communications systems, as well as metrics that can be applied for characterisation. Chapter 5 presents a summary of the research contribution, which is further detailed by the research papers generated from this thesis work and are found in Chapters 6 to 10. Following this, a discussion about the research papers findings is presented in Chapter 12. Finally, conclusion and future works are presented in Chapter 13.

CHAPTER 2

THE BIOLOGY OF BACTERIA AND THEIR COMMUNICATIONS PROCESSES

In this chapter the molecular biology fundamentals required to conduct this research is presented. The chapter will go through the basic fundamental knowledge of bacteria, which was the primary organism used in this research, the mechanism of communication, and corresponding computational rate equation models.

2.1 BACTERIA FUNDAMENTALS

Bacteria is a prokaryotic single-cellular organism and it is one of the oldest living things on Earth, where the first species appeared approximately four million years ago [59]. Prokaryotic cells do not have organelles that are functional components responsible for executing functions within the cell, including nutrients uptake and energy production. The organism also have two types of DNA molecules, which includes plasmids that are floating freely in the cytoplasm, as well as chromosomal DNA [59]. Furthermore, the DNA plamids can be shared between the cells upon physical contact (this process is further described in Section

2.1.2). These are the characteristics that differentiate prokaryotic from eukaryotic cells (e.g., mammalian cells).

Despite being a unicellular organism, bacteria perform complex tasks through the use of molecular signalling processes. These signalling mechanisms were not well-studied until the 1960s [60]. At that time, the researchers proposed the existence of external factors produced by bacteria which ensures their adaptation to environmental changes. Further investigation in later years improved this primitive characterisation and enabled the understanding of the collective behaviours controlled by these external factors [60]. One example is the process called *Quorum Sensing* and it is related to several important behaviours of bacteria. Section 2.1.3 provides an overall description of the quorum sensing system and Section 2.2.1 presents an example of a bacterial function that is controlled by this system.

2.1.1 BACTERIA MOTILITY

Bacteria can move in the environment using different mechanisms, including swarming and swimming [61]. As individual cells, bacteria can swim in a fluidic medium or follow a chemical gradient towards the emitting source. When grouped and living over a surface (semi-solid or solid), bacteria moves through the process of swarming. For this motility process, a specific structure called the *pili* is required to maintain the cells population which assists them to propel across the surface as a group [61].

When swimming, bacteria use their tails (also known as *flagella*), to propel themselves through the fluid environment. The flagella rotates both clockwise and counter-clockwise for the same period each, which results in a cycle of runs and tumbles [61, 62]. This movement is modelled as a random walk, where the average period for each cycle is modelled using an Exponential distribution based on the swim speed and the run duration, and the tumbling frequency is modelled as a Poisson distribution [62]. After tumbling, the bacteria returns to their straight movement and will do this by selecting a random direction that could be

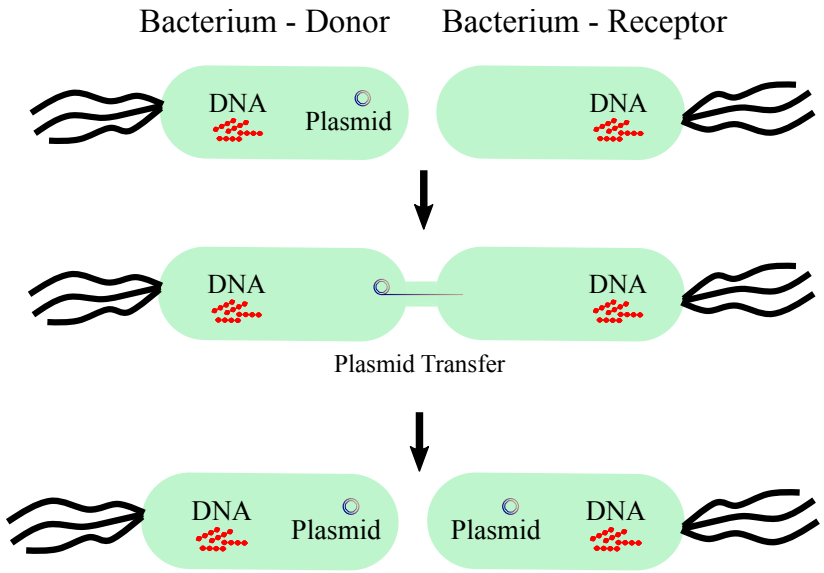

Fig. 2.1 Illustration of the plasmid transfer process through conjugation.

different from their previous run. This movement have been extensively studied and applied to the development of bacteria-based molecular communications simulation tools presented in this thesis (see Section 4.1).

2.1.2 PLASMID TRANSFER

A plasmid is a small circular double-stranded *naked* DNA molecule that can autonomously clone themselves. These genetic molecules are required for the bacterial survival and adaption against certain threats (e.g., antibiotics), and also enables their functions to be modified. At the same time, it also provides greater genetic variations for bacteria. An external gene, when integrated in the plasmid, is most likely to be retained in the cell for longer periods of time [63]. Plasmids can be exchanged between bacteria through a process known as *conjugation*. Through this mechanism, a bacterium can transfer their genes to another bacterium once they are in contact with each other (see Figure 2.1).

Bacterial conjugation has been considered for numerous biotechnological applications. As an example, Amos et al. proposed the use of *E. coli* to build synthetic genetic circuits [64]. They engineered a set of plasmids, where each one is a component of a circuit. As the bacteria

conjugates, the engineered plasmids are integrated into the plasmid of the recipient cell to form the circuit [64]. In another example, Hajimorad and Gralnick engineered plasmids to improve the interface between a bacteria species *Shewanella oneidensis* and a microbial sensor [65]. They were able to engineer the dynamic control of electron transfer from the bacteria to the sensor. By transferring these engineered plasmids, the bacterial population maintains the efficiency of the proposed system.

2.1.3 QUORUM SENSING AND MOLECULAR BINDING

Quorum sensing is a common bacterial process, whereby small molecules are used to produce collective behaviours. This process is regulated by certain genetic expression and is directly related to the cell-population density. Many bacterial physiological activities result from the quorum sensing communication, and they contribute to certain mechanisms such as the production of virulence factors and biofilms formation [66]. Different molecules are used in quorum sensing signals due to their specificity to different bacterial species. For example, Gram-positive bacteria uses processed oligo-peptides and Gram-negative bacteria uses autoinducers as quorum sensing molecules [67]. Furthermore, the Gram-negative quorum sensing systems are simpler than the mechanism used by the Gram-positive bacteria. The simplification comes from the direct regulation of gene expression in the Gram-negative bacteria, while the latter requires membrane sensor kinase proteins to bind to the quorum sensing molecules before they activate the related genes [68].

The focus of this PhD research is on the Gram-negative bacterial quorum sensing systems. The first discovery of this signalling system was through the study of a symbiotic relationship between the light organ of the Hawaiian squid *Euprymna scolopes* and a marine bacteria strain (*Vibrio fischeri*) [69]. Due to the high nutrient concentration in this organ, the *V. fischeri* bacteria can grow their population size, inducing the production of bioluminescent genes that helps the squid to become “invisible” to their predators. These genes are activated through

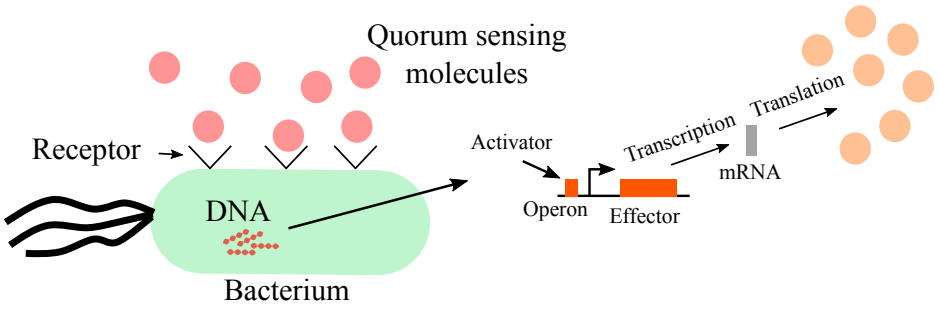

Fig. 2.2 Illustration of the binding process of quorum sensing molecules applied on the activation of specialised output signals.

a cluster of genes (also known as *operons*) *luxICDABE*, which gets activated by the transmembrane protein *LuxR*. A second protein *LuxI* is responsible for producing the autoinducer required for this process [69]. Figure 2.2 shows a general representation of this specific quorum sensing process that generates the molecular signals. Inside each bacterium cell, the operon promotes an array of genes (effector) to transcribe messenger RNAs (mRNAs), which translates the genetic commands into molecular signals, e.g. *V. fischeri* bioluminescence [69–71].

2.1.4 BIOFILMS

Bacteria and other microbes have a number of survival strategies in the natural environment [72]. Biofilm formation is a result from one of these strategies that is used for protecting bacteria from physical attacks, helping them to evolve and resist to antibiotic treatments [73]. To form a biofilm, bacteria needs to sense a surface and trigger their signalling pathways to produce proteins that enhance their adhesion to this particular surface [74]. Next, these bacteria will start to divide themselves to increase their population size and start to produce Extracellular Polymeric Substances (EPS) that will surround them, creating a protective medium. Lastly, bacteria will communicate to create specialised roles to maintain the biofilm [75].

In the recent years, biofilms are found to be related to the emergence of chronic infections and antibiotic resistant microbes [76]. Beyond the health-related issues, the environment can be impacted by biofilms, leading to biofouling, food and water contamination [77]. Therefore, numerous efforts to disassemble and prevent biofilms have been proposed through the use of drugs (antibiotics) and synthetically engineered systems [78–80]. In this PhD research, biofilms will also be investigated, as they are a common bacteria behaviour and can cause a great impact on the human health.

2.2 MATHEMATICAL MODELLING OF BIOLOGICAL PROCESSES

Biological systems are usually modelled using a set of mathematical equations that represents the chemical interactions among the substances of interest [81]. These models are defined as *Rate Reaction Equations* (*RRE*) [82]. The equations provide an approximate representation of a biological system by describing the speed of change in concentration of the output molecules with respect to the concentration of the chemicals used as the input. Consider the following example: a substance $[R_1]$ reacts with a substance $[R_2]$ to produce the compound $[R_1R_2]$. Then, this chemical substance ($[R_1R_2]$) can be associated with another substance ($[P_0]$) to activate a promoter $[P_1]$ that controls the production of a protein $[X]$. This description can be represented by the following chemical reactions [81]:

$$[R_1] + [R_2] \underset{k_2}{\overset{k_1}{\rightleftharpoons}} [R_1R_2], \tag{2.1}$$

$$[R_1R_2] + [P_0] \underset{k_4}{\overset{k_3}{\rightleftharpoons}} [P_1], \tag{2.2}$$

$$[\mathrm{P_1}] \xrightarrow{\mathrm{k_5}} [\mathrm{X}] + [\mathrm{P_1}], \tag{2.3}$$

$$[\mathrm{R_1}] \underset{\mathrm{k_7}}{\overset{\mathrm{k_6}}{\rightleftharpoons}} \varnothing, \tag{2.4}$$

$$[\mathrm{R_2}] \underset{\mathrm{k_8}}{\overset{\mathrm{k_6}}{\rightleftharpoons}} \varnothing, \tag{2.5}$$

$$[\mathrm{X}] \xrightarrow{\mathrm{k_6}} \varnothing, \tag{2.6}$$

$$[\mathrm{R_1R_2}] \xrightarrow{\mathrm{k_6}} \varnothing, \tag{2.7}$$

$$[\mathrm{P_1}] \xrightarrow{\mathrm{k_6}} \varnothing, \tag{2.8}$$

where k_1, k_3, k_5, k_7 and k_8 are the production rates; k_2, k_4 and k_6 are the dissociation rates of this system. The rate of these chemical reactions will be directly proportional to the product of the resulting molecular concentrations (which corresponds to the law of mass action). Therefore, the reactions (2.1)-(2.8) can be modelled using the following mathematical equations [81]:

$$\frac{d[\mathrm{R_1}]}{dt} = k_2[\mathrm{R_1R_2}] + k_7 - k_1[\mathrm{R_1}][\mathrm{R_2}] - k_6[\mathrm{R_1}] \tag{2.9}$$

$$\frac{d[\mathrm{R_2}]}{dt} = k_2[\mathrm{R_1R_2}] + k_8 - k_1[\mathrm{R_1}][\mathrm{R_2}] - k_6[\mathrm{R_2}] \tag{2.10}$$

$$\frac{d[\mathrm{R_1R_2}]}{dt} = -k_2[\mathrm{R_1R_2}] + k_1[\mathrm{R_1}][\mathrm{R_2}] - k_6[\mathrm{R_1R_2}] - k_3[\mathrm{P_0}][\mathrm{R_1R_2}] + k_4[\mathrm{P_1}] \tag{2.11}$$

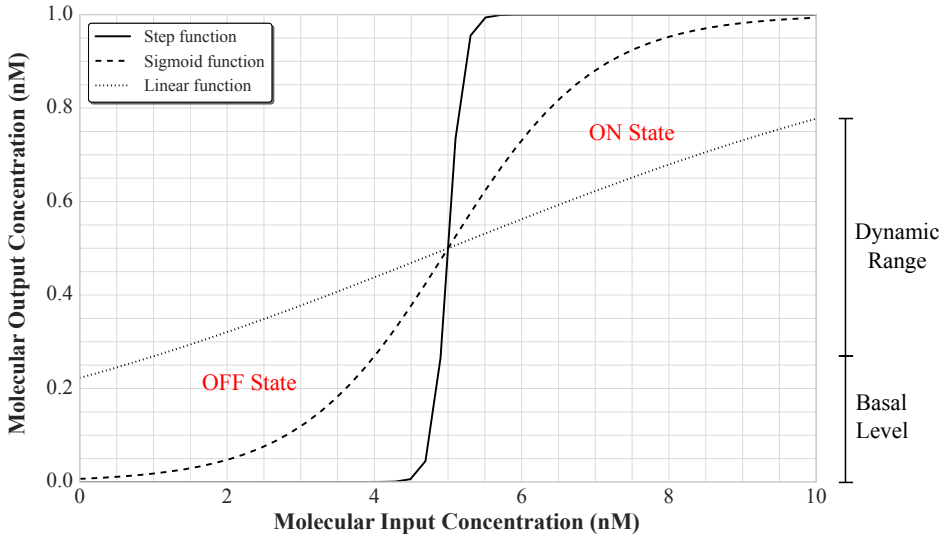

Fig. 2.3 Illustration of synthetic system responses to different molecular inputs.

$$\frac{d[\mathrm{X}]}{dt} = k_5[\mathrm{P}_1] - k_6[\mathrm{X}] \tag{2.12}$$

$$\frac{d[\mathrm{P}_0]}{dt} = -k_3[\mathrm{P}_0][\mathrm{R}_1\mathrm{R}_2] + k_4[\mathrm{P}_1] + k_6[\mathrm{P}_1] \tag{2.13}$$

$$\frac{d[\mathrm{P}_1]}{dt} = k_3[\mathrm{P}_0][\mathrm{R}_1\mathrm{R}_2] - k_4[\mathrm{P}_1] - k_6[\mathrm{P}_1]. \tag{2.14}$$

The rate reaction equations (2.9)–(2.14) describe the dynamics of the system specified by (2.1)–(2.8). This mathematical model may end up being too complex to analyse, due to the number of variables and non-linearities. Therefore, simplifications supported by wet lab experimental data are often considered to model these chemical reactions [81]. For example, certain substances can be considered as time-invariant, in other words, their concentration rates are equal to zero. Another possible simplification is to consider different reaction speeds at smaller timescales for the system. In this case, certain reactions would react almost instantly resulting in concentration rates equal to zero [81]. Based on these assumptions, the obtained molecular output concentration can be represented as the graph shown in Figure 2.3.

As shown in the Figure 2.3, the system response can range from a step to a linear function, which will dictate both its basal level as well as the dynamic range. The basal level will be the minimum amount of the output substance and the dynamic range is the difference between the maximum and minimum molecular concentrations. The system response can also dictate the ranges of the "ON" and "OFF" states which are the molecular concentration levels that can be measure readily or not easily attained, respectively.

In this research work, the RRE are considered for modelling different bacterial traits such as population growth and quorum sensing production. Moreover, the RRE are also considered to develop synthetic logic operations using bacteria. In the following sections, more elaborate details for these models are presented.

2.2.1 BACTERIAL POPULATION GROWTH AND QUORUM SENSING PRODUCTION

Once placed in a location with suitable conditions for their survival, bacteria divide themselves to produce offsprings [59]. This process occur in most bacterial species through the process of binary fission, whereby one large cell is divided into two smaller cells. However, they can also grow their numbers by budding, which creates appendages that will become newer cells, or produce several smaller cells at the same time [59]. If sub-optimal environmental conditions are detected, the bacteria shuts off all their process that are not essential, and this includes replication. Therefore, mathematical models that describe the functions of a bacterial population growth also considers the optimal environmental condition. An example of bacterial population growth model is described by the following RREs [83]:

$$\frac{d[\mathrm{S_{bac}}]}{dt} = -U_{bac}\left(\mu_{bac}\frac{[\mathrm{S_{bac}}]}{[\mathrm{S_{bac}}]+K_{bac}}\right)[\mathrm{N_{bac}}] \tag{2.15}$$

$$\frac{d[\mathrm{N_{bac}}]}{dt} = \left(\mu_{bac}\frac{[\mathrm{S_{bac}}]}{[\mathrm{S_{bac}}]+K_{bac}} - m_{bac}\right)[\mathrm{N_{bac}}] \tag{2.16}$$

where $[\mathrm{S_{bac}}]$ is the availability of nutrients to be consumed by the bacteria; $[\mathrm{N_{bac}}]$ is the bacterial density; μ_{bac} is the maximum growth rate; K_{bac} is the half-saturation constant for free-moving bacteria; m_{bac} is the maintenance rate of bacterial cells and U_{bac} is an utility parameter.

Another bacteria process that are often modelled using RREs are the quorum sensing system and Extracellular Polymeric Substances (EPS) production in biofilms. Whenever bacteria finds a suitable location to live and are attached to a surface, they can form a biological structure known as biofilm, which will protect their population from external attacks and enable them to survive longer in varying environmental conditions. Therefore, the EPS production is a fundamental aspect for bacterial survivability and this process is dependent on the quorum sensing system. As described in Section 2.1.3, using quorum sensing system, bacteria can produce and control their collective behaviours. Considering a *AHL-LuxR* system, the production of quorum sensing molecules and EPS can be mathematically described as follows [84]:

$$\frac{d[\mathrm{A}]}{dt} = c_A + \frac{k_A[\mathrm{C}]}{K_A+[\mathrm{C}]} - k_9[\mathrm{A}] - k_{10}[\mathrm{R}][\mathrm{A}] + k_{11}[\mathrm{RA}] \tag{2.17}$$

$$\frac{d[\mathrm{R}]}{dt} = c_R + \frac{k_R[\mathrm{C}]}{K_R+[\mathrm{C}]} - k_{12}[\mathrm{A}] - k_{10}[\mathrm{R}][\mathrm{A}] + k_{11}[\mathrm{RA}] \tag{2.18}$$

$$\frac{d[\mathrm{RA}]}{dt} = k_{10}[\mathrm{R}][\mathrm{A}] - k_{11}[\mathrm{RA}] - 2k_{13}[\mathrm{RA}]^2 + 2k_{14}[\mathrm{C}] \tag{2.19}$$

$$\frac{d[\mathrm{C}]}{dt} = k_{13}[\mathrm{RA}]^2 + k_{14}[\mathrm{C}] \tag{2.20}$$

$$\frac{d[\mathrm{A}_{m,e}(\hat{t})]}{dt} = (p_{out}[\mathrm{A}_m(\hat{t})] - p_{in}[\mathrm{A}_m(\hat{t})]) - D[\mathrm{A}_m(\hat{t})], \tag{2.21}$$

where [A], [R], [RA], [C], $[\mathrm{A}_{m,e}(\hat{t})]$ are the *AHL*, *LuxR*, *LuxR – AHL* complex, dimerized complex and external autoinducer concentrations, respectively; $k_0, k_1, k_2, k_3, k_4, k_5$ are the translation rates; c_A and c_R are the transcription basal levels for *AHL* and *LuxR*, respectively; k_A and k_R are the transcription rates; K_A and K_R are the degradation rates; D is the diffusion coefficient in water; p_{in} and p_{out} are the intracellular and extracellular transportation rates. The EPS produced by the quorum sensing process described by (2.17)-(2.21) is modelled as [29]

$$\frac{d[\mathrm{EPS}]}{dt} = k_{EPS}\frac{[\mathrm{C}]}{[\mathrm{C}] + K_C}, \tag{2.22}$$

where [EPS] is the EPS concentration, k_{EPS} is the maximum EPS production rate, and K_C is the dimerized complex degradation rate.

The bacterial population growth model presented in (2.15)-(2.16) can be modified to model a biofilm growth when producing quorum sensing molecules and EPS. Therefore [29, 83],

$$\frac{d[\mathrm{S_{bio}}]}{dt} = -U_2\left(\mu_2\frac{[\mathrm{S_{bio}}]}{K_{S2} + [\mathrm{S_{bio}}]}\right)[\mathrm{N}_2] - U_{AHL}\frac{d[\mathrm{A}]}{dt} - U_{LuxR}\frac{d[\mathrm{R}]}{dt} - U_{EPS}\frac{d[\mathrm{EPS}]}{dt}, \tag{2.23}$$

$$\frac{d[\mathrm{N}_2]}{dt} = \left(\mu_2\frac{[\mathrm{S_{bio}}]}{[\mathrm{S_{bio}}] + K_{S2}} - m_2\right)[\mathrm{N}_2], \tag{2.24}$$

where $[\mathrm{S_{bio}}]$ is the nutrient consumption by the biofilm, μ_2 are the maximum specific growth rate for the bacteria inside the biofilm; K_{S2} is the half-saturation constant for the biofilm;

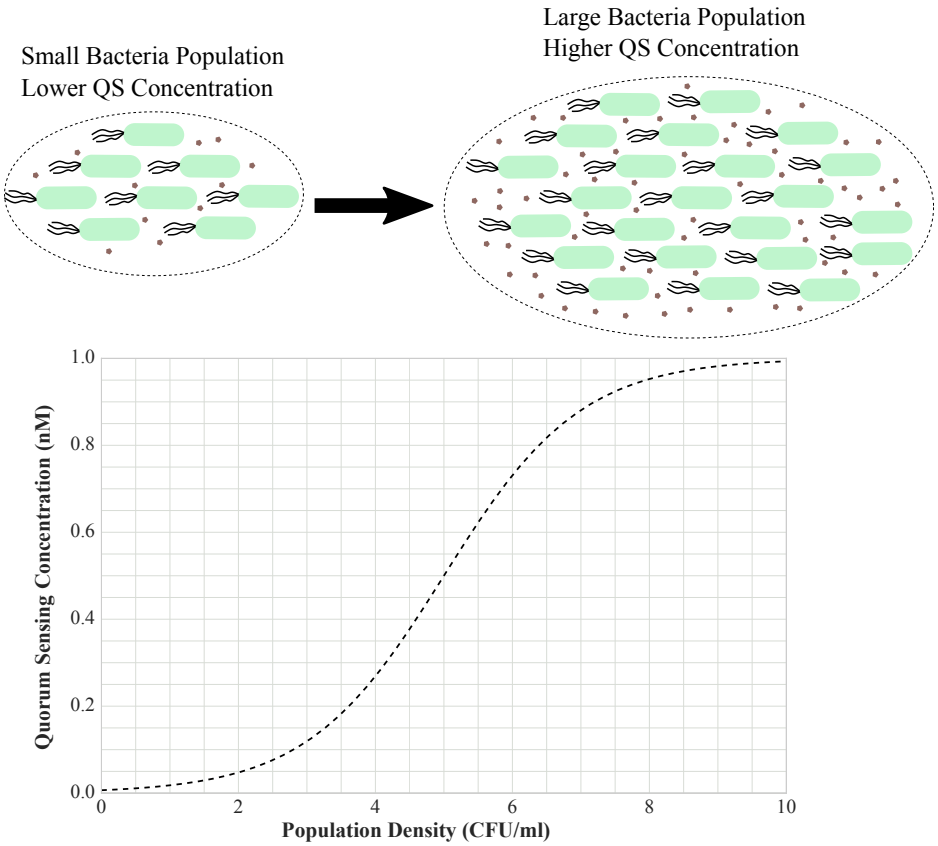

Fig. 2.4 Representation of the relationship between the bacterial population growth and quorum sensing production.

m_2 is the maintenance rate; k_{EPS} is the maximum EPS production rate; U_2, U_{AHL}, U_{LuxR}, U_{EPS} are the utility parameters; and $[N_2]$ is the biofilm population density. The relationship between the bacterial population size and the amount of quorum sensing that is produced by these cells is represented in Figure 2.4.

Both population growth and quorum sensing dynamics are important aspects to be studied for the development of bacteria-based systems, as they can directly affect the molecular communications performance of the systems. The bacteria population growth analysis can show the impact of ecological relationships and influence on the molecular concentration output by engineered bacteria. The study of the quorum sensing dynamics is fundamental for the description of any bacteria-based molecular communications system as their concentrations are the information that is exchanged in these systems.

2.2.2 ENGINEERING BACTERIA-BASED SYNTHETIC LOGIC GATES

Synthetic biology is a field that is focused on the development of synthetic systems using biological cells and abstracting their genetic functions that are similar to lumped-element model of electronics engineering [1]. Synthetic biologists have been proposing the use of bacterial and mammalian cells to perform logical operations, similar to Boolean digital devices. These artificial biological systems had been developed to create simple single synthetic logic gates to complex circuits, targeting several biotechnological applications. As an example, Hu et al. were able to engineer an AND gate in *Shewanella oneidensis* for microbial fuel cells [85]. In a more extensive analysis, Siuti et al. developed a simpler strategy to build 16 two-input logic gates in *Escherichia coli* cells [86]. This approach enables the synthetic biologists to propose a digital-to-analog converter. Each one of these applications have their own mathematical model that describes its function. Synthetic logic gates can also be described using RREs. For example, a synthetic OR gate can be characterised as a Hill logic function and represented as follows [87]

$$\frac{d[\mathrm{OR}]}{dt} = \frac{[\mathrm{E}]^{n_E}}{K_E^{n_E} + [\mathrm{E}]^{n_E}} + \frac{[\mathrm{F}]^{n_F}}{K_F^{n_F} + [\mathrm{F}]^{n_F}} - \gamma_{OR}[\mathrm{OR}] + N_{OR}(t), \tag{2.25}$$

where K_E and K_F define the rates of association constants by which [E] and [F] binds to the OR gate receptors, γ_{OR} is the decay constant for [OR], n_E, n_F are the Hill coefficients and $N_{OR}(t)$ is the noise resulting from the chemical reactions for this synthetic logic gate. This noise term is modeled as an Additive White Gaussian Noise (AWGN) and represents the internal fluctuations resulting from the production of the molecular output signals. Similarly, the synthetic AND gate can be represented as [87]

$$\frac{d[\mathrm{AND}]}{dt} = \frac{[\mathrm{G}]^{n_G}}{K_G^{n_G} + [\mathrm{G}]^{n_G}} \cdot \frac{[\mathrm{H}]^{n_H}}{K_H^{n_H} + [\mathrm{H}]^{n_H}} - \gamma_{AND}[\mathrm{AND}] + N_{AND}(t). \tag{2.26}$$

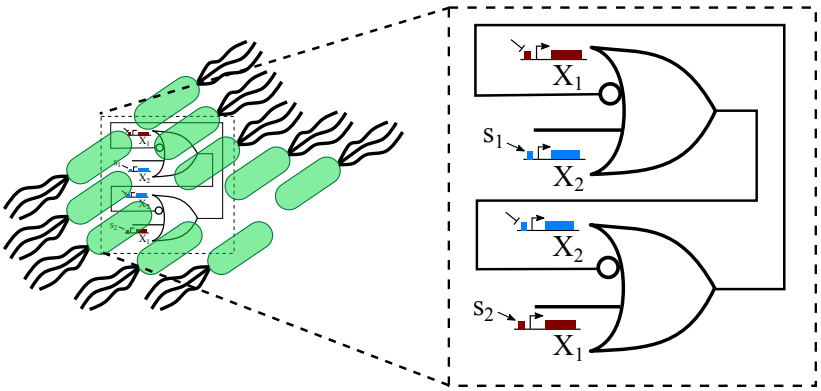

Fig. 2.5 Illustration of a bacteria-based toggle switch.

where K_G and K_H define the rates by which [G] and [H] binds to the AND gate receptors, γ_{AND} is the decay constant for [AND], n_G, n_H are the Hill coefficients and $N_{AND}(t)$ is the noise resulting from the chemical reactions for this synthetic logic gate (also modelled as a AWGN noise).

More complex devices have also been built using synthetic logic gates. For example, a toggle switch was created (see Figure 2.5) using engineered bacteria and modelled it using the following RREs [46]

$$\frac{d[\mathrm{I}]}{dt} = \frac{\beta}{1+K_J^{\alpha}} - \gamma_t[\mathrm{I}], \tag{2.27}$$

$$\frac{d[\mathrm{J}]}{dt} = \frac{\beta}{1+K_I^{\alpha}} - \gamma_t[\mathrm{J}], \tag{2.28}$$

where [I] and [J] represents the molecular signal concentrations that triggers and suppresses the operation of the synthetic logic gate, respectively; α and β are the repression constant, and the maximum production rates for both molecular signals [I] and [J]; s_I and s_J are the toggle switches' induction signals, $K_I = [\mathrm{I}]/(1+(s_I/K)^{n_t})$ and $K_J = [\mathrm{J}]/(1+(s_J/K)^{n_t})$ define the rates by which the molecular signals bind to the synthetic gate receptors, K is a constant that defines the equilibrium of the chemical reactions involved in the production of a molecular signal, γ_t is the decay constant for both molecular signals, and n_t is the

cooperativeness degree of the molecular signal with the synthetic gate receptor (this is also known as the *Hill* coefficient).

2.3 DISCUSSION

Through several years of research, biologists have laid the groundworks required to advance the development of biotechnological applications, such as new types of therapeutics. Hence, simple and complex synthetic biology systems have been proposed and modelled in the past twenty years [2–4, 45–49, 56, 65, 86]. As discussed in this chapter, mathematical models have been used to describe important aspects of biological processes and functions, and in particular how they can contribute towards collective behaviour in bacteria. More comprehensive models created from the combination of synthetic biology and other related fields (e.g., molecular communications) will allow researchers to expand their understanding of biological systems and develop novel applications.

Mathematical biology models are accurate representations of real systems. As presented in (2.17)-(2.24), a set of ordinary differential equations is used to represent a quorum sensing signalling system. To model a bacteria-based system designed to diffuse quorum sensing molecules through a fluid medium to a molecular receiver, for example, will require the combination of these models as well as other models that will represent the full end-to-end communications system. Multi-disciplinary approaches for the design and implementation of complex biotechnological systems has been considered, but some challenges still need to be addressed. For example, biological parts (smaller genetic functional units) are often custom designed for each application, and not all synthetic circuits are designed considering the orthogonality required to avoid unwanted impact on other cellular functions [47, 53, 88, 89]. Moreover, the current systems are investigated through their capacity to produce the required molecular output and not for their communications process, which can impact on the systems' reliability performance.

Preliminary studies combining both molecular communications and synthetic biology models have led to the theoretical design of molecular transmitters and receivers using bacteria [14, 26, 27, 33, 52, 90, 91]. However, research still need to be further pursued to fully investigate how communications channels can be integrated to interconnect the bacteria-based transmitters and receivers and develop end-to-end molecular communications systems. In this PhD thesis, the synthetic circuits will be applied to the design of biotechnological applications and evaluated through their communications capabilities. In the following chapters, more details and examples of systems combining synthetic biology with molecular communications are discussed.

CHAPTER 3

MOLECULAR COMMUNICATIONS AND SYNTHETIC BIOLOGY

In Chapter 2, the importance of quorum sensing system for the control of bacterial behaviours was discussed. Recent years has seen numerous research conducted in engineering of bacteria to produce quorum sensing molecules that can lead to biotechnological applications [4, 45–50]. This is achieved by engineering genetic circuits in bacteria through gene editing in order to activate a collective response of the bacterial population [2]. Researchers are taking this one step further, where they have been investigating the use of quorum sensing mechanism for designing communications systems [82, 92]. In this chapter, an in-depth description of the quorum sensing based molecular communications systems are presented.

3.1 TRANSDUCER DESIGN

Transducers are considered important devices in conventional communications systems as they can convert one type of signal into another form (e.g., mechanical into electrical signals) [93, 94]. Usually, transducers are placed inside the transmitters before modulation modules, and right after the demodulator in the receivers. In biological systems, transducers are found

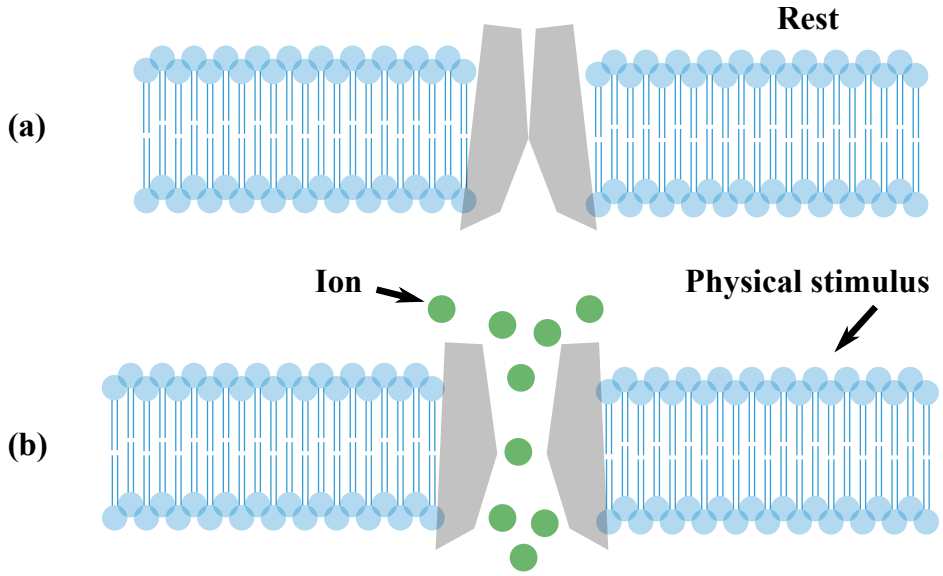

Fig. 3.1 Illustration of the bacteria ion gated channel. (a) This diagram shows no external or internal stimuli is applied on the cellular membrane, and therefore, the ion gated channel is at rest. (b) This diagram shows a physical stimulus is applied to the outer membrane, which trigger the channel to open, allowing ions to pass through the membrane (Adapted from [97]).

in the membranes of cells and can convert physical stimuli into either electrical or chemical signals, or both [95–97].

The cellular membrane have gated protein channels that regulate the exchange of molecules with the environment [95]. These channels are passive structures that are closed for majority of the time. If an external stimuli is applied onto the surface of the membrane, it will activate the opening of these gated protein channels (see Figure 3.1). These protein channels can be activated by heat, mechanical forces, molecules, voltage and transduce these stimuli into molecular concentrations or electrical signals [95, 96]. As an example of engineered membrane systems, Researchers engineered a *Bacillus subtilis* biofilm to study its internal electrical communication and found that bacteria can actively open the gate of potassium channel to amplify the molecular signal and counter the attenuation caused by the channel propagation [96].

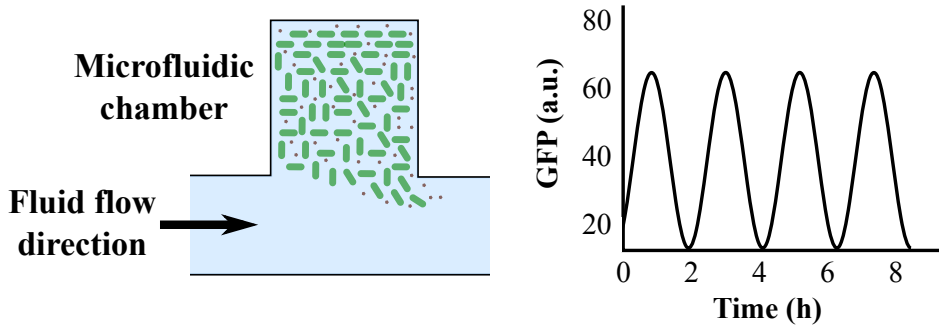

Fig. 3.2 Illustration of the bacteria-based genetic oscillator and of the periodic signal produced by it (figures are adapted from [104])

.

Bacteria uses these transduction channels (mechanical stimulus into chemical signals) to trigger their internal signalling pathways to produce proteins that increase their adhesion to surfaces and other cells [98–100]. This process has been studied for the development of surfaces that cannot be colonised by bacteria as their adhesion protein production is prevented upon contact to these particular surfaces [78, 99]. Moreover, the adhesion between bacteria and others cells have also been engineered to study this process and to propose biotechnological applications, such as in vivo colonisation of cancerous cells [101–103]. Biological transducers are, as shown by the applications introduced in this section, an important subsystem to investigate for the design of bacteria-based molecular communications systems.

3.2 OSCILLATOR DESIGN

Oscillators are devices that produce periodic signals and are applied to the generation of clock signals for digital systems and carriers for information signal modulators [105]. In nature, several systems and behaviours are controlled by periodic dynamics, such as the circadian rythmn and the synchronisation of bacterial behaviour inside a population [104, 106]. For example, a bacterial gene network was engineered to generate synchronised oscillations inside a microfluidic device [104]. In their experiment, the oscillations start after the bacterial population reaches a critical cellular density. The bacterial quorum sensing system outputs

a high molecular signal level (represented by a green fluorescent protein), and at the same time increase the production of the *AiiA* protein, which degrades quorum sensing molecules. This process is represented in Figure 3.2, where the molecular concentration rises once the population reaches critical density and the decline occurs when the AiiA protein degrades most of the quorum sensing molecules [104, 107]. In this case, the oscillation amplitude was modified by increasing the fluid flow inside the microfluidic device and modelled this bacteria-based genetic oscillator as follows [104]:

$$\frac{\partial[\mathrm{A}]}{\partial t} = C_A[1-(d/d_0)^4]P(\alpha,\tau) - \frac{\gamma_A[\mathrm{A}]}{1+f([\mathrm{A}]+[\mathrm{I}])}, \tag{3.1}$$

$$\frac{\partial[\mathrm{I}]}{\partial t} = C_I[1-(d/d_0)^4]P(\alpha,\tau) - \frac{\gamma_I[\mathrm{I}]}{1+f([\mathrm{A}]+[\mathrm{I}])}, \tag{3.2}$$

$$\frac{\partial[\mathrm{H}_i]}{\partial t} = \frac{b[\mathrm{I}]}{1+k[\mathrm{I}]} - \frac{\gamma_H[\mathrm{A}][\mathrm{H}_i]}{1+g[\mathrm{A}]} + D([\mathrm{H}_e]-[\mathrm{H}_i]), \tag{3.3}$$

$$\frac{\partial[\mathrm{H}_e]}{\partial t} = \frac{d}{1-d}D([\mathrm{H}_e]-[\mathrm{H}_i]) - \mu[\mathrm{H}_e] + D_1\frac{\partial^2[\mathrm{H}_e]}{\partial x^2}, \tag{3.4}$$

$$P(\alpha,\tau) = \frac{\delta+\alpha H_\tau^2}{1+k_1 H_\tau^2}, \tag{3.5}$$

where [A], [I], [H_i] and [H_e] are the molecular concentrations of AiiA, LuxI protein that activates green fluorescence, internal and external autoinducers, respectively; d is the cell density; d_0 is the initial cell density; τ is the considered delay for the chemical reactions; γ_A, γ_I and γ_H are the degradation rates for AiiA, LuxI and both internal and external autoinducers, respectively; D is the diffusion coefficient of the quorum sensing molecules through the cell membrane; D_1 is the diffusion constant; μ is the external quorum sensing molecules decay rate; δ is the leakiness of the promoter *luxI* required to produce LuxI; $H_\tau(t) = [\mathrm{H}_i](t-\tau)$ is

the concentration of the internal autoinducers produced in the previous time step; $P(\alpha, \tau)$ describes the delayed production of AiiA and LuxI; C_A, C_I, f, b, k, k_1, α and g are constants.

There are other examples of engineered biological oscillators. Elowitz and Leibler proposed the first genetic oscillator in 2000. They engineered three transcriptional repressor systems in *Escherichia coli* to build a genetic oscillator and termed it as the *repressilator* [108]. The repressilator is represented by the following model [108]:

$$\frac{dm_i}{dt} = -m_1 + \frac{a}{1+p_j^n} + a_0, \tag{3.6}$$

$$\frac{dp_j}{dt} = -\beta(p_j - m_i) \tag{3.7}$$

where m_i are the mRNA concentrations for the corresponding three repressor-proteins (i represents the proteins lacI, tetR, cI), p_j is the repressor-protein concentrations (j represents cI, lacI, tetR), a_0 is the protein copy number per cell that are produced from a specific promoter type based on a continuous growth for the bacterial population; β is the ratio between the protein and mRNA decay rates, and n is the Hill coefficient. In order to achieve shorter period pulses (minimum of thirteen minutes), a bacteria-based (*Escherichia coli*) tunable genetic oscillator was engineered using different proteins compared to the model proposed by [104] (Arabinose and IPTG, instead of AiiA and LuxI) [104, 109]. The proposed design was extremely robust, allowing to obtain oscillations for all IPTG levels (each one of these levels produced a different oscillation period) when using 0.7% arabinose at 37°C.

3.3 AMPLIFIER DESIGN

Amplifiers are electronic circuits that increase the power of a signal by a given factor. It is widely used in electronic and communications systems, where they are used to counter the effects of fading channels [110]. Similar to electronic devices, synthetic biology versions

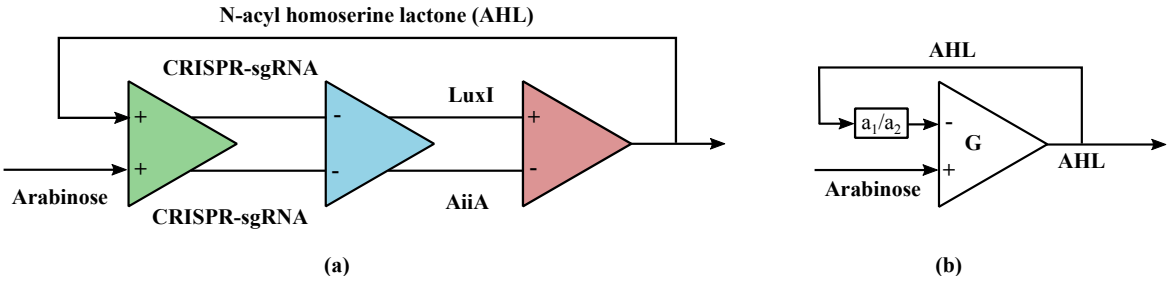

Fig. 3.3 Illustration of the the first synthetic operational amplifier. (a) Representation of the three stage synthetic operational amplifier with its respective molecular inputs and outputs. (b) The classical representation of an operational amplifier but using the quorum sensing molecules as inputs and outputs of the device, with an amplifying factor of $1/(a_1/a_2)$ (figures are adapted from [111])

.

of amplifiers have also been proposed. A negative feedback-based three-stage synthetic operational amplifier was designed by engineering a bacterial quorum sensing system [111]. In the first stage, the bacteria uses Arabinose and N-acyl homoserine lactones (AHL) to produce two CRISPR-sgRNA complexes. These outputs are then pushed through an amplifier which outputs AiiA and LuxI. In the last stage, the amplifier converts the difference between AiiA and LuxI to produce AHL, which is fed back to the first stage of this system (see Figure 3.3). Operational amplifiers can provide fine control of the output signal, which makes them suitable for the design of synthetic systems that require precise production of molecules. For example, diabetes is a systemic disease caused by the impairment in the blood glucose homeostasis, which is analogue to the synthetic system proposed by [111]. Therefore, this synthetic operational amplifier could be useful for controlling the production of insulin required for the balancing of the blood glucose levels.

Positive feedback-based synthetic amplifiers have also been researched and developed. A modular genetic amplifier in *Escherichia coli* bacteria was engineered to be coupled to any synthetic sensing system, where the molecular output signal activate the transcription of genes [112]. The proposed amplifier do not depend on exogenous inducers to operate as

it has a constitutively active variant of LuxR and was able to increase the sensitivity of the molecular input signals and amplify it accordingly [112].

Amplifiers are also considered for the design of comparators. These devices are often used in electronic systems to design analog-to-digital circuits [113]. Recently, a synthetic comparator that convert analog chemical signals into digital electrical/optical signals was developed by [114]. They engineered an electrogenic bacterial species, *Shewanella oneidensis*, which compares the continuous quorum sensing molecules produced by *Escherichia coli* and the output discrete digital electrical/optical signals [114].

3.4 FILTER DESIGN

Filters are devices that enable the selection of the wanted features of a signal [115]. This process often results in the removal of time or frequency bands of a signal. In communications systems, filters are widely used for the optimal detection of an unknown signal. When applied to wireless transmitters, filters can limit the signal bandwidth to adapt it to the communication channel requirements [116]. In biological systems, filters are often used to remove unwanted substances from fluids [117]. However, filters have been also proposed for applications that are similar to the ones considered for communications systems. They designed a bacteria-based bandpass filter by combining positive and negative genetic selections [118]. Their filter can be externally tuned by the addition of Amp or IPTG to affect the band selection for the β-lactamase and Amp activities, respectively. The external tuning of the enzyme band activity selection allows the bacterial population to grow into specific patterns, such as geometric shapes and letters [118]. It also eases the system optimisation as it only requires the addition of molecules into the system to modify its operation. A different approach was proposed for the design of a synthetic bandpass filter. They utilised terminators[1] as regulatory parts for the proposed genetic circuit [119]. The proposed circuit can act as a high band and

[1] Terminators are the section of DNA where the proteins transcritpion processes are ended.

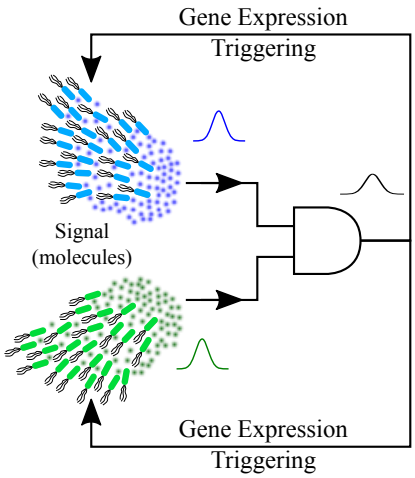

Fig. 3.4 Illustration of the microbial control device proposed by [120]

a bandpass filter at the same time as the terminator can affect the two fluorescence proteins used as reporters. In this case, a Red Fluorescence Protein (RFP) was chosen to be produced before the terminator, resulting in a high band filter, and a Green Fluorescence Protein (GFP) to be produced after the terminator, which will result in a bandpass filter [119]. Despite being more robust compared to the system proposed by [118], this circuit is simpler due to the exploitation of terminator nonlinear effects on the gene expression, compared to combining both a high and low pass filters to create a bandpass filter.

3.5 TRANSMITTER DESIGN

Bacteria are engineered to produce molecules that modify their stimulus responses as described in Chapter 2. These molecules are first encoded into biochemical (synthesis of other molecules) or physical stimuli to activate the collective bacterial response. The encoding process for a quorum sensing systems was investigated through a modular view of several cellular density diversity schemes, which they classified as basic and composed encoding systems [121]. This classification was based on their quorum sensing sensitivity profiles. They also experimentally verified their model to identify the *Vibrio harveyi* encoding network architecture [121]. In a different approach, a synthetic mammalian cell (HEK-293) was

designed to produce autoinducer-2 (AI-2) to control the behaviour of bacterial pathogen [122]. This microbial-control device has a complex signalling pathway that enables the sensing of pathogen-derived formyl peptides present in the environment, and triggering the production of AI-2 to prevent the virulence behaviour associated to quorum sensing signalling in pathogenic *Vibrio harveyi*. Bacteria can share the environment where they are placed with other microbial species or even other microorganisms. In this respect, the bacterial consensus based on the interchange of molecules was studied through the engineering of two *Escherichia coli* populations that diffuse signals to each other and express a specific gene depending on the molecular concentration levels produced by the microbes [120].

The natural cellular signalling processes can be engineered for programming different social interactions within a microbial consortia. For example, a synthetic predator-prey ecosystem was proposed by [123]. They engineered two *Escherichia coli* populations, one as the predator and the other as the prey, to create bi-directional communication and regulate the population survivability by the expression of a killer protein in the prey, and an antidote protein in the predator. This system was modeled as follows [123]:

$$\frac{dc_1}{dt} = k_{c1}c_1\left(1 - \frac{c_1 + c_2}{c_{max}}\right) - d_{c1}c_1\frac{K_1}{K_1 + A_{e2}^{\beta}} - Dc_1 + \varepsilon \cdot \xi, \tag{3.8}$$

$$\frac{dc_2}{dt} = k_{c2}c_2\left(1 - \frac{c_1 + c_2}{c_{max}}\right) - d_{c2}c_2\frac{A_{e1}^{\beta}}{K_2 + A_{e1}^{\beta}} - Dc_2 + \varepsilon \cdot \xi, \tag{3.9}$$

$$\frac{A_{e1}}{dt} = k_{A1}c_1 - (d_{Ae1} + D)A_{e1} + \varepsilon \cdot \xi, \tag{3.10}$$

$$\frac{A_{e2}}{dt} = k_{A2}c_2 - (d_{Ae2} + D)A_{e2} + \varepsilon \cdot \xi, \tag{3.11}$$

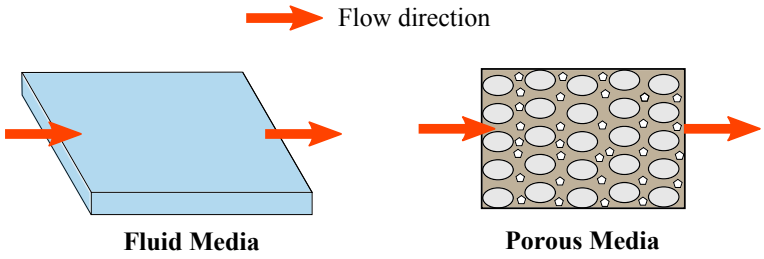

Fig. 3.5 Illustration the media channels modelled for the free-diffusion of signalling molecules.

where c_1 and c_2 are the predator and prey cell density, respectively; k_{c1} and k_{c2} are the specific cell growth rate constant for the predator and prey populations, respectively; c_{max} is the maximum cell growth; d_{c1} and d_{c2} are the cell death rates for the predator and prey populations, respectively; K_1 and K_2 are the required signalling molecule concentration to activate the promoter; D is the dilution rate; d_{Ae1} and d_{Ae2} are the decay rate constant of the signalling molecules for the predator and prey populations, respectively; A_{e1} and A_{e2} are the signalling molecule concentration in the environment around the predator and prey populations; ε is the noise amplitude; ξ is the Additive White Gaussian Noise (AWGN) with zero mean and unit variance (representing the fluctuations found in the experimental setup); and t is time. From a more complex perspective, [124] proposed six different two population consortia with well-defined social interactions by using modular signalling pathways. The bacteria signalling systems was engineered to transmit the required molecules and drive these ecosystems to have unidirectional and bidirectional social interactions.

3.6 COMMUNICATIONS CHANNELS

Liquid and porous media have been studied for the transport of molecules in several biochemical applications (see Figure 3.5), like the identification of biomarkers for periodontitis and how a bacterial micro-compartment organelle selects transport molecules [125, 126]. The extensive literature from the molecular communication researchers in recent years concentrate

on molecular diffusion studies that is used to support the design of diffusion-based synthetic systems. For example, in the Chapter 2, a number of reaction equations have a diffusion coefficient (usually represented as D) as a parameter for the evaluation of the molecular concentration that is able to reach the receptors after being transmitted from a source point using the Fick's diffusion model [127, 128].

The Fick's Law of diffusion is a mathematical model that describes the random movement of particles in space and time due to a concentration gradient [127–129]. In a free-diffusion system, the molecules transport themselves through the medium without any external force acting on them. If a force is applied to move the molecules, their concentration values can vary in space and time depending on the fluid flow or on the concentration gradient that is forcing their propagation. The Fick's Law of diffusion is defined as follows [129]

$$\frac{\partial c(x,t)}{\partial t} = -D(x,t)\frac{\partial^2 c(x,t)}{\partial x^2} \tag{3.12}$$

where $c(x,t)$ is the spatio-temporal molecular concentration, and D is the diffusion coefficient. In the case of homogenous media, the diffusion coefficient D become a constant value, and this is a common approach for many synthetic biologists [109, 123, 124, 129–132].

3.7 RECEIVER DESIGN

Specific molecular receptors can be engineered to improve the detection of signals for bacterial systems, and this could be used to develop receivers for molecular communication systems. For instance, chemotaxis receptors have been engineered to improve bacterial responses to chemoattractants, which are chemical molecules that are able to attract the motile cells [133, 134]. In the event that molecules bind onto the receptors, this will activate an internal pathway that enables the bacteria to adjust their movement so they can swim towards the chemoattractant source point. The chemotaxis receptors can be engineered to be

activated by quorum sensing molecules and drive a population of motile bacteria toward a second population of non-motile bacteria that emitted the quorum sensing molecules [133]. In a different approach, [134] engineered the hybrid chemotaxis receptors in *Escherichia coli*. They found that these hybrid receptors can be applied to characterise the molecular specificity of the chemotaxis receptors. A more complex design was proposed by [135], where they engineered bacterial strains to have specific responses to different environmental signals. For example, the engineered bacteria could detect the deficiency in the amount of oxygen around tissues, as this is a characteristic for tumour cells [135].

The specificities between the molecules that need to be sensed and the bacterial receptors drove researchers to investigate other designs for sensor proteins. A structure-based computational method was developed to enable the construction of highly selective receptors and engineer them into bacteria to regulate their gene expression based on the sensed molecules [136]. A more specific receptor design was proposed by [137], where they designed a zinc cation binding periplasmic [2] receptor that activates the *Escherichia coli* signal transduction pathway required for the β-galactosidase reporter gene regulation [137]. The performance of this computational design was measured by the molecular concentration of the reporter gene. A similar design could be applied for the detection of other metal that can be found on the bacteria extracellular space. Moreover, this could be extended for the construction of programmable bacteria-based sensors for different chemical threats [137]. These studies show the versatility of bacterial receptor engineering that can be used to design biotechnology applications.

3.8 DISCUSSION

Using a specific set of rules, biological parts, mathematical and computational models (as shown in the Chapter 2), synthetic biologists were capable of developing several devices that

[2]The periplasm is the region between the inner and outer cellular membranes.

mimic their electronic counterparts, similar to the devices described in this chapter [95, 96, 104, 108, 109, 111, 112, 118–124, 133–137]. As described in this chapter, synthetic biologists have been developing a number of elementary systems required for the full development of a conventional communications system. Nevertheless, these systems have not being formally applied to affect another bacterial population, and neither their communications performance were investigated.

From the molecular communications perspective, the construction of nanoscale systems capable of exchanging information in the form of molecules has been well supported by the advancements in synthetic biology systems. Therefore, the synthetic systems described in this chapter can be investigated in regards to their communications performance and further extended on the development of bacteria-based molecular communications devices that affect natural bacteria behaviours. For example, bacteria-based transmitters and receivers could be used to build a molecular MIMO communications system that control the biological processes related to bacterial virulence. Moreover, the synthetic engineering of the bacteria membrane could lead to the design of bandpass filters that selectively detect molecular signals, or of synthetic attenuators that remove certain molecular signals from the environment.

In this PhD research, different synthetic biology systems were applied to the design of bacteria-based molecular communications systems that directly affect other cells and bacterial natural behaviours. This approach aims to further extend the analysis of the synthetic systems described in this chapter and focuses on the evaluation of their communications performance.

CHAPTER 4

BACTERIA-BASED MOLECULAR COMMUNICATIONS SYSTEMS

Molecular communications systems are based on the exchange of molecular information, some of which can be engineered to carry encoded information. Depending on the application, the design of molecular communication system can be developed from different types of artificial and natural cells that are engineered to emit various types of molecules for communication [138]. For example, natural communication between bacteria have been used to develop diffusion-based molecular communications systems [14, 139]. Most of the bacteria-based systems that have been proposed uses the plasmid transfer (“wired") or the quorum sensing signalling (“wireless") mechanism to exchange molecular information [14, 139]. Therefore, in this section we have classified this into two broad modalities, which are ‘wired" and “wireless" systems. In this chapter, a brief description of the current simulation tools used and an in-depth description of the two modalities of bacteria-based molecular communications systems (and their applications) are provided.

4.1 SIMULATION TOOLS

Bacteria-based molecular communications systems are often simulated using Agent-Based Models (ABM) [140]. Through this computational simulator, the investigation of collective dynamics can be simplified into the study of the individual bacterium's behaviour. In this case, bacteria are placed into small environments, where they can move, share and deliver information to other organisms, which in this case can be engineered cells. BSim, BNSim, NanoNS, NanoNS3, N3Sim and BiNS2 are examples of simulation tools that have been proposed to investigate bacteria individual and collective dynamics [15–20]. From these simulators, only the BSim and the BNSim are agent-based simulators [16, 18]. The others are modified network simulators that represent the communications structures as network nodes, and are applied to analyse nanonetworks [15, 17, 19, 20].

Focusing on a diffusion-based molecular communications system, in [15] a computational framework was developed on top of a widely known network simulator (ns-2) to provide a better understanding of nanonetworks. The authors made a comprehensive validation of the NanoNS, but stopped short or developing concrete examples. The simulator for studying wireless bacteria-based molecular communications systems through physical contacts aspect, also known as conjugation, is not considered in the NanoNS design.

BSim was developed in 2012 by [16] to help analyse the relationship between the individual cells and population level behavioural dynamics. Despite the authors only providing scenarios for simulations of wireless bacteria-based communications systems, including logic operations and genetic oscillator, the tool can also be applied to the investigation of physical interaction amongst the bacteria. In [17] was proposed a nanonetwork simulator, where the transmitter and receivers were abstracted as nanomachines that emit and receive molecules. The tool, named BiNS2, was written in Java and it is agnostic to any application, nanomachine types and motility models. The authors implemented a collision detection

and management model for the diffusion of molecules in both two- and three-dimensional environments and the simulation performance was validated through a case study of the human immune system [17]. This simulation tool is currently on its seventeenth version and is still maintained by the authors and is freely available for the community.

To consider the bacterial intracellular processes for the ABM simulations in [18] was proposed a different tool, named BNSim. This simulation tool was written in C++ and uses the Gillespie algorithm to simulate the bacterial intracellular processes using mechanisms from populations dynamics [18]. Similar to the BSim, the BNSim is able to simulate bacterial population interactions in a three dimensional space. However, this software is no longer supported by the authors, where the last update was in 2015.

As a common design for molecular communications simulation tools, the abstraction of nanoscale transmitters and receivers was also considered for the development of the N3Sim [19]. This simulator has a number of differences compared to other tools discussed in this chapter. The authors implemented a collision detection algorithm and a harvester mechanism in the N3Sim [19]. Moreover, this tool is able to simulate two- and three-dimensional environments, where the molecules are subjected to free and anomalous diffusion molecular communications channels. In [19] no practical usage examples of the N3Sim were provided, where the only evaluation is based on analytically validation.

In a similar approach to the simulator proposed by [15], a bacterial nanonetwork simulator using the network simulator ns-3 was developed by [20] and named as nanoNS3. The authors implemented bacterial receivers and channel loss models for microfluidic systems in the network simulator. Moreover, modulation, source addressing, error and transfer rate analyses protocols were implemented in this simulator [20]. An experimental end-to-end molecular communication system was used to validate the signal reception in the nanoNS3, and the implemented protocols were analytically validated [20].

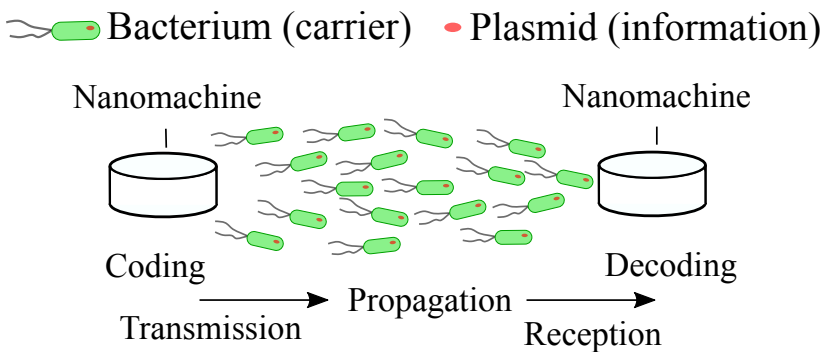

Fig. 4.1 Illustration of bacteria-based molecular communications system, where the plasmid stores the information and the bacteria mobility carries the encoded information.

Recently, a new simulation framework based on the standard IEEE 1906.1-2015 (IEEE Recommended Practice for Nanoscale and Molecular Communication Framework) was proposed by [141]. The authors implemented a two-dimensional environment where bacteria, acting as message carriers, exchanges plasmids among themselves through conjugation. This simulation framework was applied for the investigation of an infection scenario, where bacteria would swim within the bounded environment to infect other microbes through the transmission of plasmids [141]. Therefore, their analysis focused on the parameters that would affect this molecular communications system, including multiple infection sources, rate of infections, bacteria swim speed and dimensions [141].

4.2 "WIRED" BACTERIA-BASED MOLECULAR COMMUNICATIONS SYSTEMS

The first molecular communications system using bacteria was a single-hop nanonetwork [21]. In this model, flagellated bacteria were used to carry information between nanoscale devices (see Figure 4.1). The authors proposed encoding of information into the plasmid, and carrying it as is propagated through a fluid channel [21]. Later in the same year, in [14] a bacteria-based nanonetwork was designed considering the architecture proposed by

[21]. They evaluated the channel capacity and the received signal delay for a number of different scenarios. Other researchers then expanded the analytical models of the point-to-point molecular communications system to study multi-hop bacterial nanonetworks [26, 27]. In this expanded model, flagellated bacteria transported information through its plasmid between multiple nodes. When the bacteria arrives at the receiving node, the carrier microbe transfers the plasmids to other cells and does this based on random interactions. This process continues till the plasmid reaches the final node, where the information will be decoded [26, 27]. However, to maintain reliability, a medium-range nanonetwork will require several nodes to transmit information using this model.

The reliability analysis of this type of bacteria-based molecular communications system was investigated by [22]. The authors proposed a two-dimensional lattice where the bacteria would mobilize randomly between the transmitter and receiver to estimate the probability of successful delivery of plasmids during a period of time [22]. The authors validated their reliability analysis using the same simulation model from [37]. They found that for high reliability, a larger bacterial population size is needed. Moreover, an inverse relationship between the maximum delay and the reliability level was found [22].

The research works described so far considers a single transmitter that will emit the bacteria carrying the information in the form of plasmids to a nanoscale receiver. Expanding this architecture to consider multiple transmitters and receivers, [35] investigated the scheduling problem based on the presence of chemoattractants[1] in the environment. They formulated the total transmission time for this bacteria-based nanonetwork to analyse the impact of the total delay on the successful delivery of plasmids to the nano receivers. A carrier allocation problem can arise due to the use of multiple pairs of transmitters-receivers when considering a finite number of emitted bacteria. This issue was investigated by developing a transmission model similar to the one applied for ad hoc wireless networks and the transmission delay was minimised by adjusting the number of carriers considered in the network [36].

[1] These molecules, if detected by a bacterium, drive the bacterial movement towards their source.

A bacteria-based nanosensor network that incorporates bacterial properties and transports engineered plasmids between two nanomachines (one transmitter and one receiver) was proposed by [38]. They evaluated the probabilities of obtaining successful transformations (bacterial process of acquiring foreign plasmids) and plasmid delivery with respect to the time that the microbes were allowed to bind to the nano receiver. From the analysis, they found that there is an improvement on the successful plasmid delivery when the bacteria is allowed to be bound to the nano receiver for long durations [38]. It can be concluded from this work that the density of bacteria carriers and nano receivers has a major role on the system performance.

When bacteria exchange plasmids, only a fraction of this genetic material (message) is shared amongst them. This can lead to misinterpretation of the message by the nano receiver. To counter this effect, the messages were encoded using a forward and a reverse data transmission coding schemes [37]. For the forward encoding, the message is encoded into blocks from left to right in the plasmid. For the reverse encoding, the message is encoded from right to left in the same plasmid. In the case the forward-encoded section of the message is only delivered by one bacterium, a second bacterium can deliver the reverse-encoded portion allowing the full retrieval of the original message [37]. Their encoding technique resulted in improved performance in the successful decoding of the message, especially when there is a large distance between the nanomachines. Progressing from this model, [39] presented a comparative analysis of five different message encoding techniques for bacteria-based nanonetworks. For four of these techniques, the emitted bacteria will conjugate, and different message codings are used to improve the probability of successful delivery (on the last technique the bacteria do not conjugate and the message was not encoded either). The upper bound for this analysis was defined by the optimum encoding scheme[2]. The authors included in the comparative analysis their forward and reverse coding technique, and found that the four techniques considering the conjugation plus message encoding has a similar

[2]When the encoded message has the length similar to the original message

performance to the optimum encoding technique. Furthermore, the shift encoding (when the next message is shifted by one block in comparison with the previous block) was the best among the compared techniques.

Recently, a framework was developed to study the characteristics of a bacteria-based nanonetwork [23]. The authors considered single, and multiple, nanoscale transmitters and receivers communicating through motile information-carrier bacteria, and implemented an analytical model to evaluate the effects that could lower the nanonetwork's performance, which may be due to non-perfect conjugation [23]. Moreover, different scenarios were proposed to characterise the trade-offs and requirements of this bacteria-based nanonetwork. The authors found that the number of emitted bacteria improved the mean delivery time, and this gain is independent of the considered compartment sizes where the bacteria were placed [23].

Bacteria-based molecular communications using electrical signals have also been proposed [24, 25]. Bacteria have vital operations that are dependent of internal electron transfer, including the production of Adenosine Triphosphate (ATP), which is the energy used by the cells. Using this natural process, a queuing model was proposed to abstract microbial interactions [24]. In this model electrons are transferred from one bacterium to another as would occur in a conventional electric cable. The authors validated their continuous-time queuing model through simulations of open and closed space systems. They also performed wet-lab experiments for the closed space system to validate their model [24]. A year later, the same authors expanded the bacterial cable model to evaluate the channel capacity when bacteria have knowledge about the channel state information (CSI) [25]. In this case, they used a finite-state discrete-time Markov channel with Poisson inputs and outputs to describe this bacteria-based molecular communications system. Based on their model, they found the optimal binary Markov input distribution that balances the trade-off between the instanta-

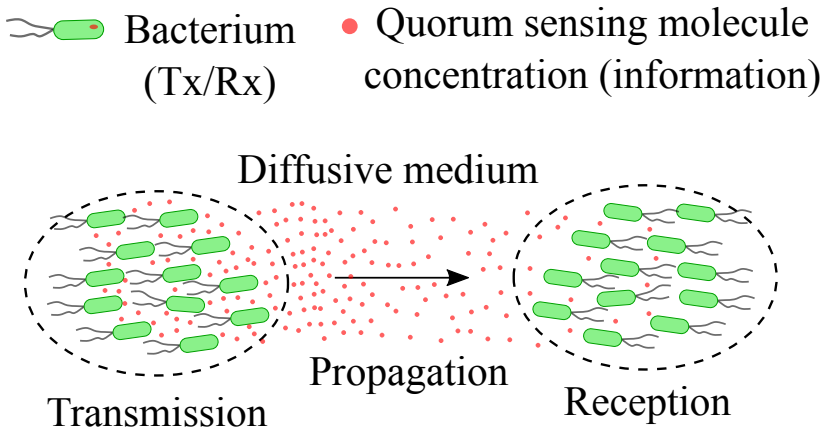

Fig. 4.2 Illustration of bacteria-based molecular communications system, where a group of bacteria encodes and transmits the information as concentration of *quorum sensing* molecules which will diffuse toward the neighbouring bacterial population.

neous mutual information rate, which is required for the channel capacity evaluation, and the steady-state distribution of the cable states [25].

4.3 "WIRELESS" BACTERIA-BASED MOLECULAR COMMUNICATIONS SYSTEMS

Despite bacteria being able to exchange information by transferring plasmids, they can also perform free diffusion molecular communications (see Figure 4.2). For this system, the information is the concentration of molecules diffused between the bacteria-based transceivers. A biological transceiver using integrated logic gate system was proposed to encode information that can transmit molecules with coded information [52]. This biotransceiver was composed of four components, which includes a transmitter, receiver, sensor and processor, and it was the first real design for a bacteria-based nanodevice [52]. The authors described each device's components using mathematical equations, including rate reaction equations for the signal processing, which was used to develop the synthetic logic gates. However, they did not validate their model but did investigate the biotransceiver operation numerically.

The reception performance of molecular signals by engineered bacteria have also been investigated [91]. To improve the detection of bacterial responses to pulse amplitude modulated (PAM) molecular signals an efficient sampling technique was proposed in [91]. The authors designed theoretical and experimental analyses for their proposal, where the bacteria is placed into a small chamber connected to a microfluidic channel. The PAM molecular signal is transported through the channel by a laminar flow, where they measured the fluorescense produced in response to this signal. The authors proposed four different sample strategies, and this includes total response duration, peak value, ramp-up and ramp-down slopes, and found that the ramp-up slope results in a lower probability of error compared to the other metrics [91]. This strategy could be further studied for the development of a modulation strategies for bacteria-based molecular communications system.

The dynamics that drive bacteria to interconnect and work collectively has been investigated using concepts from molecular communications [28, 29]. In [28], it was proposed the use of physico-chemical signals to drive the bacteria to a defined location, e.g. for drug delivery purposes. The authors found that the dynamics of attractions and repulsions imposed by the signals affect both the processes of finding the required destination and the probability of successful drug delivery. Expanding on this concept, the same authors studied the social interactions inside heterogeneous populations when bacteria used quorum sensing to stimulate collective behaviour [29]. They investigated the cooperative and competitive behaviours using a network-centric approach, and showed that their model have good correlation with the traditional metrics applied to studying population interactions.

Commonly used network protocols have been proposed for wireless bacteria-based molecular communications [30, 31]. For example, an error control method (automatic repeat request - ARQ) was designed for the transmission of quorum sensing molecules [30, 31]. The authors abstracted analogous electronic circuits to propose a similar way to engineer ARQ protocols into a bacterial population [30]. They simulated and analysed the communications

performance for three different ARQ protocols (go-back-N ARQ, selective-repeat ARQ, and stop-N-wait ARQ) and found that ARQ protocols can be applied to improve the performance of wireless bacteria-based nanonetworks despite producing different results compared to conventional wireless networks [31]. Nonetheless, this work lays the groundwork for the future implementations of other network protocols.

Researchers were able to design and characterise multihop wireless sensor nanonetworks using bacteria [32–34]. First, it was proposed the use of bacterial populations as nodes of a nanonetwork to investigate the communication process in this system [32]. They modelled the acquisition and relaying of molecular data by the bacterial population, and analysed the probability of error for this scenario [32]. The same authors expanded this work to study the performance of a wireless bacteria-based sensor network [33]. They evaluated the channel capacity, in terms of bit per channel use, by varying the maximum molecular concentration at the receiver, the number of bacteria in a node, and noise level [33]. From their analysis it is possible to observe that a communication process with low probability of error is achievable when considering a large number of bacteria in a node [33]. This result demonstrates the impact of individual molecular contributions for the performance of the wireless bacteria-based sensor network. As an extension to this work, the same authors studied different modulation schemes and provided a general discussion about the reliability of a bacteria-based wireless sensor nanonetwork [34]. They proposed the use of M-ary and quadrature amplitude modulation schemes for a network setup similar to their previous works. In this case, they compared different M-ary schemes and found that the best information rate was when they considered $M = 32$ [34]. The authors also found a linear relationship between the information rate (expressed in bits per sample) and the maximum transmission power.

Despite the similarity between conventional and bacteria-based molecular communications systems, the achievable information rate is much worse for the latter (if we compare

their absolute values[3]), due to the nature of molecular signalling [14, 40]. Therefore, limited information can be transmitted using a bacteria-based molecular communication system. Aiming to improve the information rate for these systems, an alternative encoding scheme was proposed by using the period when no signals is being transmitted to encode information[4], and named it as time elapse communication (TEC) [40, 41]. The authors first engineered bacteria to respond to a specific molecule emitted in a random ON-OFF pattern, and measured the amount of light produced by them. Then they implemented two TEC schemes for the molecular signals and again measured the output light. The authors found that the TEC scheme produces improved data rate compared to the simple On-Off Keying modulation. Furthermore, they compared the two TEC schemes, TEC-SIMPLE and TEC-SMART (simple and multiple error correction techniques, respectively), and found a better achievable data rate for the TEC-SMART scheme [40]. The authors then expanded their work to include a general discussion about the limitations of the TEC schemes and the channel capacity analysis [41].

4.4 DISCUSSION

In this chapter, several bacteria-based molecular communications systems and simulation tools used to study them are presented. Majority of the works described are focused on few aspects of an end-to-end communications system. A number of these works modelled the communications channels to understand how it affects bacterial signal carriers [14, 21–25], while others developed frameworks to account the interconnections within and between bacterial populations and investigated them based on metrics used in conventional networks [26–34]. Lastly, a number of these works evaluated the performance of simple bacteria-based molecular communications systems whose designs were not application-

[3] Bits per hour against bits per second, for the bacteria-based and conventional communications systems, respectively.

[4] This is a well-known technique for conventional wireless networks [142, 143]

driven [35–41]. These works focused on demonstrating the exchange of molecular signals in bacterial nanonetworks. Furthermore, they presented bacteria as a molecular communications transceiver (which is able to send and receive molecular signals), encoder and carrier of molecular signals.

The well-known characterisation of the diffusive channel allied with all the investigation presented in this chapter is an important step towards the design of a complete bacteria-based molecular communications system. This PhD work also contributes to this topic by not only adding more analyses and characterisations of bacteria-based communications systems, but also proposing different biotechnology applications. These applied systems are designed to fill the gaps presented in both Chapters 3 and 4, by interconnecting the fields of synthetic biology and molecular communications. The proposed applications are based on the wireless modality and focused on the collective interactions within and between bacterial populations. In the following subsections, the systems introduced in this chapter are discussed with respect to the bacteria-based molecular communications systems that are the basis of this PhD research.

4.4.1 DISASSEMBLING AND PREVENTING BIOFILMS

As aforementioned, the works described in this chapter did not focused on using bacteria-based molecular communications systems to tackle current biotechnological issues. For example, none of those works has proposed the disassembling, nor the prevention of biofilm formation. This structure has been related to severe chronic infections in humans (biofilms characteristics are discussed in Chapter 2) and its formation and maintenance is linked to the bacteria communications ability. Despite not targeting this application, the simulation tools presented in Section 4.1 could be modified and extended to interconnect bacteria and biofilms to analyse their relationship and propose solutions for biofilm formation, as an example.

4.4.2 DESIGN OF BACTERIA-BASED MOLECULAR COMMUNICATIONS DEVICES

Challenges need to be overcome before implementing a complete bacteria-based molecular communications device. For example, more studies are required to provide a better characterisation of the molecular signal production and reception, on more realistic scenarios. The bacteria-based molecular communications systems presented in this chapter abstracted the devices (e.g. transmitter and receiver) and focused on the analysis of the networking aspects and communications performance [30, 31, 37–39]. However, these works showed the feasibility of using bacteria to design molecular communications systems. Therefore, a more focused investigation, based on the integration between bacteria-based molecular communications systems and synthetic biology could enable the development of bacteria-based molecular communications devices, such as specific molecular biosensors or even transmitters that could interfere with another bacteria population.

4.4.3 BACTERIA-BASED SYNTHETIC LOGIC GATES

Some of the current works abstract the signal production and usage as simple mathematical models and focus on the study of the communications channel [14, 33] and molecular reception [90]. Others, use external devices and systems to generate modulated signals and investigated the bacterial response [40, 41, 52, 91]. Therefore, the study of how the molecular communications systems affects the bacteria behaviours is still an open challenge. A possible approach to overcome this challenge is to develop and analyse bacteria-based synthetic logic gates, which are one of the simplest synthetic biology systems. Logic gates often have one output that is the result of the Boolean operation of two inputs. Thus, the analysis of logic gate operation that integrates molecular communications system could provide the required insights for the development of more complex bacteria-based systems.

CHAPTER 5

THESIS RESEARCH SUMMARY

This chapter presents a complete list of research papers related to this thesis. The chapter will begin presenting a summary for each research paper, whilst mapping them to their respective research questions presented in Chapter 1. Next, these PhD thesis contributions are presented that address one or more research questions each (see Table 5.1).

Table 5.1 Association between the research questions and publications.

Questions	**Publications**
RQ1	NANOCOM, TNB_Bio
RQ2	NANOCOM, TNB_Bio
RQ3	TCBB, TNB_Logic, TCOM, TETC
RQ4	TNB_Logic, TETC

5.1 PUBLISHED PAPERS

NANOCOM (*Chapter 6*) - D. P. Martins, M. T. Barros, S. Balasubramaniam. Using Competing Bacterial Communication to Disassemble Biofilms. In *Proceedings of the 3rd ACM International Conference on Nanoscale Computing and Communication (NANOCOM 2016)*. 2016, USA, New York.

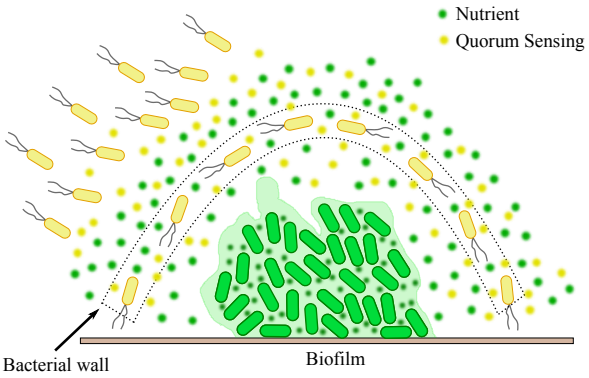

Fig. 5.1 Free-moving bacteria forms a wall and induces a nutrient competition with the biofilm. These bacteria attracts others to the wall using quorum sensing molecules and increase the wall's dimension [51].

Summary: Bacteria often group over surfaces as a survival strategy. In this form, bacteria produce an enclosure known as the extracellular polymeric substances, that surrounds them to protect against external physical attacks and controls the flow of molecules into the individual cells. The bacterial population when living under this structure is called biofilm and it has been related to chronic diseases and antibiotic resistance. This work proposed a technique to disassemble biofilms based on the starvation of the biofilm-forming bacteria. The *quorum sensing* communications controls the nutrient competition between two bacterial populations, where one would be engineered to surround the second population and deplete the nutrients required for the long-term maintenance of the biofilm. The obtained results showed the performance of the proposed technique, where the biofilm decays in 2 hours. Moreover, this work indicated the feasibility of using molecular communications and synthetic biology to design bacteria-based biotechnological applications.

This publication shows that the *quorum sensing* signals can effectively control the bacterial behaviour, like movement, nutrient consumption, and also provide them with the ability to form a wall around another bacterial population (see Figure 5.1). It also investigates the attraction of free-moving bacteria towards a biofilm-forming

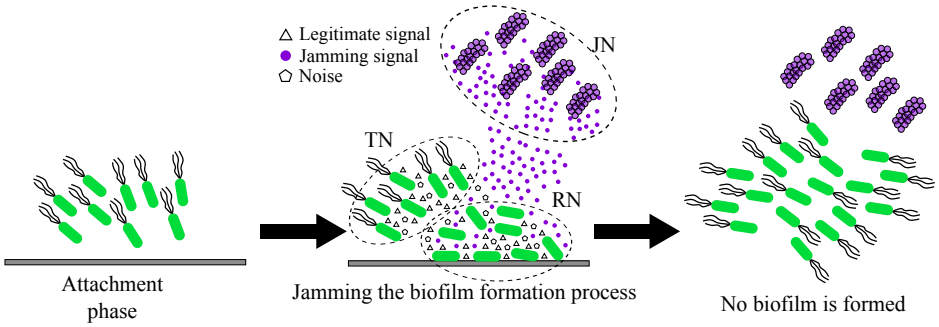

Fig. 5.2 An illustration of the pulse-based jamming system devised to prevent biofilm formation. The engineered jamming bacteria produces molecular signals that will interfere with the multi-stage communication process of the biofilm-forming bacteria [144].

bacteria population to promote its disassembling. Besides, engineered *quorum sensing* signalling is used to induce neighbouring bacteria to imitate the behaviour of a transmitter bacterium towards a fast nutrient consumption inside a micro-environment. This method leads to a new bacteria population that over time also leads to biofilm formation. However, the analysis results were centred only on the biofilm breakdown figures versus the engineered bacteria wall's growth, which highlights the potential usage of our proposed method in the control of biofilm formation as well as future treatments of bacterial infection.

TNB_Bio (*Chapter 7*) - D. P. Martins, K. Leetanasaksakul, M. T. Barros, A. Thamchaipenet, W. Donnelly, S. Balasubramaniam. Molecular Communications Pulse-Based Jamming Model for Bacterial Biofilm Suppression, *IEEE Transactions on Nanobioscience*, v. 17, no. 4, pp. 533–542, Oct. 2018.

Summary: The emergence of superbugs has led researchers to investigate novel techniques and treatments for bacteria-related diseases that do not enhance their antibiotic resistance. One of the targets for these approaches is to prevent bacteria to form the polysaccharide structure that protects them from environmental changes, which promote their resistance against antibiotics. This paper also targets this process, but instead of using chemicals, it proposes the use of a biological interference system

by an engineered bacterial population to affect the natural signalling required for the biofilm formation. This bacteria-based molecular communications system was inspired by a wet lab experiment, where a substance produced by *Streptomyces sp.* prevented the *Staphyloccocus aureus* biofilm formation. The proteomic data from this same experiment, performed by collaborators at Kasetsart University, Thailand, showed the suppression of the proteins involved in the biofilm formation and inspired the design of this pulse-based jamming system [145]. Furthermore, this publication analysed the effects of the delay and signal power on the jamming efficiency of these proteins.

Based on the knowledge acquired during the computational design of the biocompatible biofilm disassembling solution, this paper introduced the use of *quorum sensing* signals to interfere with the biofilm formation process of a second bacterial population. In this case, the biofilm-forming bacteria internal pathways were analysed to identify and target the proteins responsible for their activation to become the targets of an interfering signal produced by an engineered bacterial population (see Figure 5.2). This modelling partially addresses the RQ1 as it introduces the design of the interference signal as a pulse-based jamming bacteria-based system. The proposed solution disrupts the channel capacity of the legitimate transmission and consequently, affects the internal bacteria communications channels that control the biofilm formation process. In this paper, a negative social interaction between two bacterial populations was induced, and the analysis of the results from this relationship laid the groundwork required for the design of a fully operational pulse-based jamming system.

TCBB (*Chapter 8*) - D. P. Martins, M. T. Barros, M. Pierobon, M. Kandhvelu, P. Liò, S. Balasubramaniam, Computational Models for Trapping Ebola Virus Using Engineered Bacteria, *IEEE/ACM Transactions on Computational Biology and Bioinformatics*, v. 15, no. 6, pp. 2017–2027, Nov. 2018.

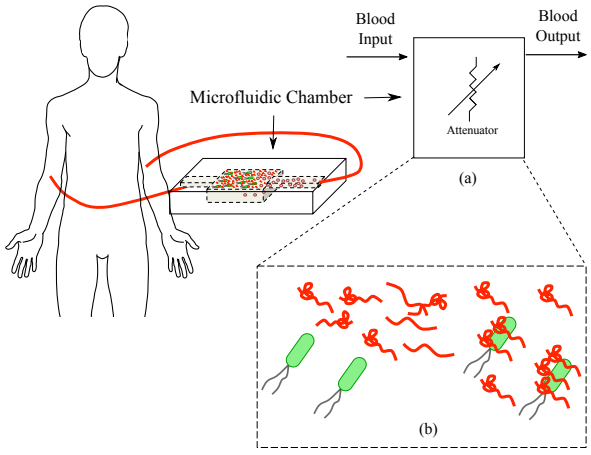

Fig. 5.3 Illustration of the microfluidic virus attenuator device that cycle Ebola contaminated blood the chamber containing engineered *E. coli* bacteria. (a) The microfluidic chamber emulates a conventional attenuator by reducing the amplitude of the molecular signal (Ebola distribution on the blood). (b) Bacteria binding the Ebola virus as they move inside the microfluidic chamber [146].

Summary: The scientific advancements in the last century have reduced the number of deadly virus outbreaks. Nonetheless, some of them are still concerning the scientific community, such as the Ebola virus that produces a haemorrhagic fever and is highly lethal, killing the patients in a few days after the infection. Ebola virus outbreaks have been recurrently occurring in Africa in the past 10 years, and worldwide efforts have been dedicated to finding a treatment for this disease. This work also aims for this goal and proposes a bio-compatible technique to reduce the number of virus in human blood. This technique is a dialysis-like medical procedure, where the patient's blood is cycled through a microfluidic chamber containing engineered bacteria responsible for binding to the virus, and reducing the number of virus in the blood. For this purpose,*Escherichia coli* had its surface engineered to trap the Ebola virus and this process was used to create a bacteria-based microfluidic virus attenuator, where the virus concentration in the blood is the molecular signal that has its amplitude reduced, see Figure 5.3.

The engineered bacteria was placed inside a microfluidic chamber to avoid direct contact with the patient and to allow them to have enough contact time with the patient's blood to ensure strong adhesion. Several parameters (blood velocity, different binding angle, patient's body temperature, binding tensions and blood viscosity) were investigated to ensure that the binding was strong enough to maintain the virus attached to the bacteria surface even under adverse situations. Furthermore, simulation scenarios were performed to investigate the virus pick-up dynamics and to evaluate the achievable attenuation ratio. Also, a mathematical equation based on the number of engineered bacteria placed inside of the microfluidic chamber was developed to predict the amount of Ebola virus that can be removed from the patient's blood. This results in a customisable microfluidic virus attenuator device that can be used to support the first stages of the Ebola fever disease treatment. The performance analysis showed that emulated molecular communications system was able to achieve a high trapping rate within 15 minutes. This work showed that the Ebola attenuator could retain a high number of the virus from returning to the patients' body, increasing their survival rate and is crucial for helping their post-exposure treatment.

TNB_Logic (*Chapter 9*) - D. P. Martins, M. T. Barros, S. Balasubramaniam. *Quality and Capacity Analysis of Molecular Communications in Bacterial Synthetic Logic Circuits*. IEEE Transactions on Nanobioscience, July 2019.

Summary: Bacteria can be engineered to act as a signal processing electronic device and manipulate molecular signals used in future human theranostics or agritech applications. They can be modelled as an analogue device, but are often referred to as digital logic gates. Nonetheless, due to the complexity of the biological processes, a complex circuitry built using either prokaryotic or eukaryotic cells is challenging. Therefore, flexible models that accurately describe these complex biological systems are needed. In this paper, we attempt to develop this type of modelling by integrating a model of

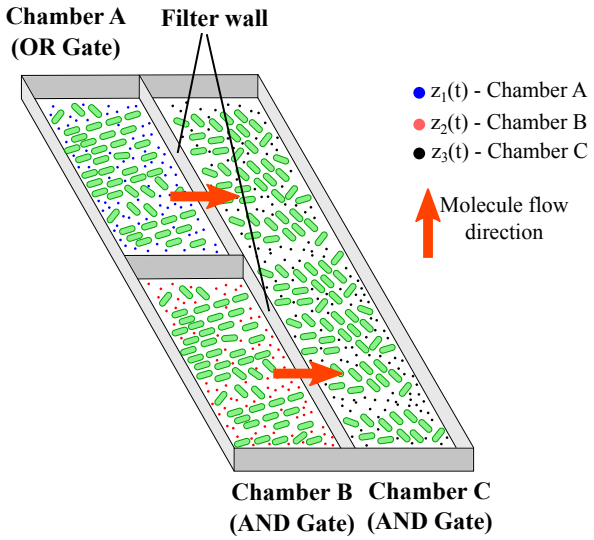

Fig. 5.4 Illustration of the proposed bacteria-based synthetic logic circuit. Each bacterial population is assigned to a compartment, becoming isolated from each other. The molecules produced at chambers A or B access chamber C by passing through a filter wall [147].

molecular communications and synthetic biology to describe a synthetic gate circuit composed of three gates. Each gate is an engineered bacterial population that can produce the response of a particular logic gate. These gates are interconnected through diffusion channels. Once the molecular input signal is processed on the first two synthetic logic gates it diffuses to the last gate.

Complex circuit design was proposed, where three bacterial populations were placed in a compartmented capsule to compute four molecular environmental signals and produce a single molecular output signal. This two-layer bacteria-based circuit also contained two diffusion channel as the connection bus between the first and the second layers of the circuit. Through the production of the molecular output signal concentration, the quality and channel capacity of the proposed circuit was assessed. Moreover, two external factors were considered in this paper's analysis: molecular-input delay and molecular concentration difference between the inputs of each logic gate of the circuit's first layer. The results showed that there is a trade-off between the circuit accuracy and its channel capacity, that is dependent on the number of bits emitted by the circuit.

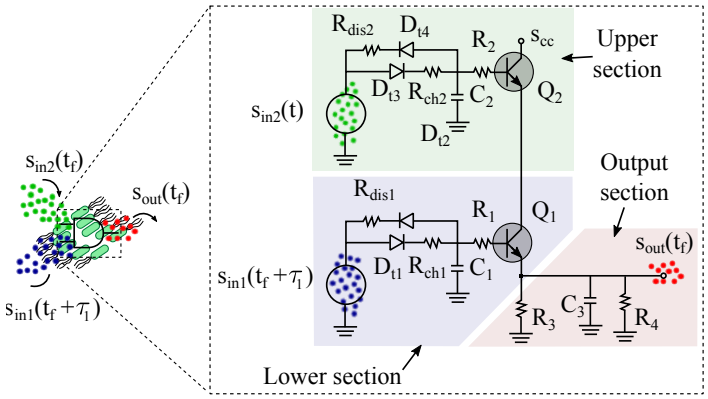

Fig. 5.5 Representation of the wireless bacteria-based biosensor using lumped components circuit, considering a time-independent bacterial population size variation [148].

Furthermore, the capsular bacteria-based synthetic logic circuit was more affected by the molecular input delay than the molecular concentration input gate difference. The RQ4 was partially addressed by the assessment of the circuit's reliability using five metrics, see 9, that determined how accurate and precise the systems was, under the presence of unwanted effects such as noise and delay.

5.2 SUBMITTED PAPERS

TCOM (*Chapter 10*) - D. P. Martins, M. T. Barros, L. Coffey, P. D. Cotter, D. P. Berry, and S. Balasubramaniam. *Frequency Analysis of Logic Computation for Bacteria-based Biosensor Molecular Communication System*. Submitted to IEEE Transactions on Communications, September 2019.

Summary: As shown before, electronics-analogous models support the development of synthetic biology systems. From detecting cancer cells to the prevention of biofilm formation, synthetic logic circuits are successfully being used in biotechnology applications. These systems are often analysed in the time domain, as a means of design validation analysis. Intending to expand the synthetic biologist toolset, this publication proposed a frequency domain analysis to study the impact of the molecular signal

spectrum on the operation of a bacteria-based biosensor. To be able to perform this frequency domain analysis, this work also provided an electronic equivalent circuit model for the transmission, processing and reception of molecular signals by the bacteria-based biosensor.

A generator device (for example, another group of bacteria in the microbiome) produces and propagates molecular signals to the bacteria-based biosensor, serving as the source of molecules that needs to be processed by the system. The bacteria-based biosensor device can detect nitrile ($R-C\equiv N$) emitted through the fluid channel and visually inform the amount of ammonia (NH_3) and acid (H^+) produced by the bacteria through a bioluminescent response signal. The performance of this bacteria-based molecular communications system was investigated in terms of the channel capacities (diffusion channel and circuit operation) and validated through a wet lab experiment.

The device circuitry operates using long pulse molecular signals, which results in a molecular output signal and a channel capacity highly dependent on lower molecular signal frequencies (around 10^{-5} Hz). The numerical analyses show that the biosensor quickly accumulates molecular environmental signal concentration if it has a higher amplitude and if their source is closer to the bacteria-based biosensor. Furthermore, the frequency domain analysis of the electronic equivalent circuit operation showed that the channel capacity quickly decreases for higher frequencies when higher molecular environmental signal amplitudes are applied, and slowly decreases when varying the distance between the molecular environmental signal source and the biosensor. This demonstrates that a fine-tuning of this molecular communications system was required to adapt the bacteria-based biosensor to the desired application scenario. The results in this paper also suggest that this electronic equivalent circuit model supports the development of more complex synthetic systems, as they uniquely can process molecular signals as a typical electronic circuit.

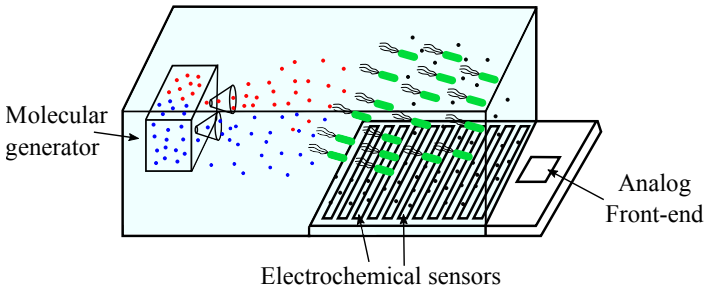

Fig. 5.6 Illustration of the integration of a bacteria-based molecular communications system with an electrochemical sensing device to detect the pH level change due to the molecular signal produced from the computing operation.

TETC (*Chapter 11*) - D. P. Martins, M. T. Barros, T. Sinkruasuan, B. O'Sullivan, A. O'Riordan, and S. Balasubramaniam. *A Reliability Analysis for Bacterial Molecular Computing on a Chip*. Submitted to IEEE Transactions on Emerging Topics in Computing, October 2019.

Summary: Synthetic biology systems operate using molecular signals, which are several magnitudes of power smaller than standard communications signals. Consequently, any small variation in the design parameters of a synthetic biology system caused by the environment or due to unexpected factors, like mutation, can have a great impact on its response. Reliability is then an important metric to be studied in these systems. In this paper, integration of bacteria-based molecular communications, synthetic biology and electrochemical sensing systems was introduced for the investigation of the reliability of bacterial molecular computing on a chip. This integration is enabled by the acidification of the fluid medium, where the bacteria-based molecular communications system is placed, due to the production of the engineered bacteria's molecular output signal. This publication also investigated the effect of the communications channel on the molecular output signal that is retrieved and evaluated at the electrochemical sensors as an electrical signal.

Results show that a small signal production delay can have a major impact on the computation reliability, i.e. the ability of the system to process such a signal. On the

other hand, the propagation delay is shown to improve the reliability of the proposed bacterial molecular computing on a chip system by compensating the impact of the production delay. Another important aspect of this paper was the investigation of the pH range of the fluid channel to define the detection threshold of the electrochemical sensors.

The proposal of bacterial molecular computing on a chip system (see Figure 5.6) and its reliability analysis is shown in this paper. Moreover, this publication is the first step towards further integration of molecular communications with electrochemical systems to support the future development of chips that can perform both biological and electronic computing of bio-electronic signals. Also, this publication shows the importance of fine-tuning the electrochemical sensors to avoid that the bio-electronic signal variations affect the pH level change detection.

5.3 CONTRIBUTIONS

This PhD thesis contributions build the basis of the extended analysis of computational synthetic biology that has been applied to the design of bacteria-based molecular communications systems.

Contribution 1: *Design and analysis of end-to-end bacteria-based molecular communications systems that use quorum sensing signalling to affect bacteria natural behaviours.*

Bacteria are almost everywhere and produce specific behaviours depending on the environmental conditions, like pH level and nutrient availability. For example, as a response to environmental changes, bacteria can form biofilms or move towards a better location to ensure their survivability. As these behaviours are tied to the bacteria communications capabilities, they became the focus for addressing the RQ1 in regards

to affecting its natural behaviour. For that, two applications (biofilm dissasembling and movement control) were theoretically analysed to demonstrate the use of bacteria communications capabilities as a synthetic system to manipulate the bacteria. First, several free-moving bacteria were attracted to a specific location and induced to consume all the nutrients available in their surroundings to break a biofilm due to starvation, see **NANOCOM** (Chapter 6). On average 53% of free moving bacteria were attracted to the surroundings of the biofilm creating a protective wall that induces this consumption. The attraction source was another group of the same free-moving bacteria that upon finding the biofilm location starts to diffuse *quorum sensing* molecules to attract nearby bacteria. Through the simulation of the bacteria movement and theoretical analysis of the nutrient consumption, both behaviours, bacteria movement and biofilm breakdown, were showed to be dependent on the number of free-moving bacteria that sits around the biofilm bacteria. However, a small action radius of quorum sensing molecules is needed to maximise bacteria attraction and contribute to the protective wall.

However, biofilm prevention can be an attractive method to develop infection therapies using purely synthetically engineered bacteria and its molecular communication system, which would powerfully contribute to combating the resistance to antibiotics at the same time. Therefore, in **TNB_Bio** a biofilm biocompatible prevention process was proposed, see Chapter 7. This technique involved a bacteria-based pulse-based jamming system that mimick the conventional radar interference scenario and directly attacks the bacteria signalling pathways responsible for biofilm formation. Bacteria have several signalling pathways that enable the performance of their natural process, such as the movement towards a nutrient gradient. From the experimental proteomic data analysis, performed by collaborators in the Kasetsart University (Thailand), I was able to develop models for these signalling pathways that compose the overall biofilm

formation mechanism, such pathways include as the defence, cellular stress and energy production. After that, an engineered bacteria population was developed that produces a *quorum sensing* molecular signal capable of reducing the levels of the main proteins of each one of those pathways. This means that the engineered bacteria population would interfere with the legitimate biofilm-forming communications, preventing its formation. This jamming process was showed to be dependent on the number of the engineered bacteria that produce the jamming signal, the synchronicity between the interference and legitimate transmissions, the power of the jamming signal and the distance between the engineered bacterial and the biofilm-forming populations. These are key parameters that ensure full operation of the jamming process. However, this can be classified as a synthetic end-end noisy bacteria-based molecular communication system that changes the natural biofilm formation using quorum sensing and hence addressing RQ1.

Contribution 2: *Investigation and performance evaluation of engineered bacteria using molecular signals to compete and interfere with other populations.*

Bacteria-based molecular communications systems can be modelled using single individuals as well as populations. For both modelling scenarios, positive or negative social interactions can affect the efficacy of those systems. Bacteria can compete for nutrients which can trigger their survival strategies and disrupt the correct operation of a bacteria-based molecular communications system. On the other hand, bacteria can cooperate to find better locations to live, improving their survivability. This PhD thesis contributed with the design and analysis of social interactions between bacterial populations for two bacteria-based molecular communications systems that are proposed solutions for the biofilm issue.

In **NANOCOM**, a bacterial competition was proposed to partially address the RQ2. This publication investigated a modified predator-prey scenario where the free-moving

bacteria was considered as the predator and the biofilm bacteria as the prey. For this interaction, however, the predator is not directly hunting the prey, but the nutrients available in the environment. At the same time, a cooperative interaction among the free-moving bacteria allowed them to quickly consume the available nutrients and speed up the disassembling process of a biofilm (two hours faster than the natural biofilm decay process). From the establishment of this cooperative interaction, was found that a smaller number of engineered bacteria was required to improve the bacterial walls' attraction probability.

A different type of competition was proposed in **TNB_Bio**, between a biofilm-forming bacteria and an engineered bacterial population. In this case, the two bacterial populations would compete against each other by using their communications systems, see Chapter 7. For a particular set of parameters and conditions, the negative interaction was showed to be more effective than the cooperative one (when the interfering signal affect the legitimate transmission). This negative effect was required to disrupt the production of the main proteins of the biofilm-related signalling pathways. From this perspective, the **TNB_Bio** publication also partially addresses RQ2 by providing a theoretical investigation about a negative social interaction between two bacterial populations that exchange molecular signals between each other.

Contribution 3: *Proposition, investigation and performance analysis of a bacteria-based microfluidic virus attenuator, synthetic logic circuit, biosensor and bio-electronic sensor.*

Bacteria-on-a-chip devices can be built using engineered bacteria and applied on several applications, especially as biotechnological solutions [43]. Four different bacteria-on-a-chip devices were proposed in this PhD thesis and had their performance investigated in the **TCBB**, **TNB_Logic**, **TCOM** and **TETC** publications. These four systems addressed the RQ3 by providing the groundwork required for the future development

of novel theranostic tools. The first proposed device targeted the attenuation of a viral signal inside of the human blood to increase the patient chance of survival during the treatment of the disease **TCBB**. In this case, the focused virus was Ebola, which is highly lethal as it produces a haemorrhagic fever that kills the patient within a few days after being infected [149]. For this reason, a bacteria-based microfluidic virus attenuator was proposed to support a faster removal of Ebola virus from the patient's blood, increasing the patient chance of survival. A mathematical model details how a genetically engineered bacterium binds to one or more viruses with modified chemical forces in the cell membrane that must be bigger than the hydrodynamic tension and drag forces produced while the bacterium is moving in the blood sample. Through the simulation of the bacteria movement and virus capture for some scenarios (see Chapter 8) it was found that the 5000 engineered bacteria were able to collect as much as 60% of the total number of virus confined in the microfluidic chamber. This publication also contributed with the analysis of the physical forces that could affect the bacteria-virus binding and the proposal of a mathematical formulation that allows the customisation of the device.

A Bacterial Molecular Computing on a chip was proposed in **TNB_Logic** to logically operate molecular signals, see Chapter 9. The molecular output of a synthetic logic circuit can be applied to identify cancerous cells or support the treatment of metabolic diseases [2, 47]. Here, three bacterial populations were placed inside a compartmented microfluidic chamber and interconnected through diffusion channels. Due to the nature of molecular signals and the propagation channel, different external factors including input concentration difference and molecular environment delay can affect these logic operations and lower the circuit's accuracy and precision. Thus, this device contributed to addressing the RQ3 by showing that both molecular-input delay and molecular-input signal concentration differences can affect the quality and communications

performance of the Bacterial Molecular Computing on a chip system. Moreover, it also identified a trade-off between these two metrics, which must be taken into account in the future design when applying this device in biomedical solutions.

The third proposed device was a bacteria-based biosensor for nitrile concentration in a fluid environment. This theoretical scenario could represent an environmental contamination process that would require a bioremediation technique to solve this problem. This publication, (**TCOM**), contributed to addressing RQ3 by providing an equivalent electronic model for the biological processes existent on this bacteria-based molecular communications systems, as well as, it investigated the impact of the communications channels over the signals transmitted through them using a frequency domain analysis, see Chapter 10. As synthetic systems often take several hours to produce molecular signals, the molecular signal frequency became a small value, which reflected on the system's channel capacity and amplitude of the molecular signal output being concentrated around this small value. Moreover, the proposed equivalent electronic circuit model was validated using the data obtained from a wet lab experiment performed by a collaborator at the Pharmaceutical and Molecular Biotechnology Research Centre - PMBRC. The obtained results showed that the proposed approach in this publication could be further extended to investigate other theranostic-related synthetic logic circuits.

Lastly, inspired by the aforementioned biosensor, in **TETC** a general Bacterial Molecular Computing on a chip device was proposed to detect two signals emitted by a molecular source and process it through a synthetic AND gate (see Chapter 11). This publication is based on the integration between molecular communications and electrochemical systems, where the molecular output signal produced by the engineered bacterial population changed the pH level of the fluid around it and, consequently, triggered the production of electrical signals by electrochemical sensors. As the biosensor

outputs a low molecular output signal concentrations, the consequent pH change might be subtle and the wrong definition of the electrochemical sensor would result in a wrong operation of this bacteria-based molecular communications system. Therefore, in **TETC**, the electrochemical sensors were designed to be the threshold for the correct operation of the bio-electronic sensor. This publication partially addressed the RQ3 by complementing the functionalities of the other three proposed devices. It added an electronic layer on a bacteria-based molecular communications system, which could support the development of devices that interface the nano and macroscale communications. This device is the basis for the future development of Bacterial Molecular Computing on a chip system for human and animal care that act upon the detection of specific molecular signals.

Contribution 4: *Reliable design and analysis of simple and complex "wireless" bacteria-based synthetic logic circuits.*

Bacteria-based sensing and actuation systems belong to a subset of the synthetic logic circuits that have been developed in the past years [47]. Sensors and actuators based in simple synthetic logic gates engineered into bacteria have been already designed to search for specific molecular concentration [150], to diagnose and treat cancer cells [151, 152], and to detect cadmium and lead in the environment [153]. The reliability of those designs depend on a careful engineering process and correct definition of the systems' parameters. Then, as the circuit becomes more complex, the reliability becomes more critical as more uncertainties (e.g., environmental changes, delays and noise) are added to the analysis. Therefore, in the publications **TNB_Logic** and **TETC**, different approaches were chosen for the investigation of the reliability analysis of Bacterial Molecular Computing on a chip system.

For **TNB_Logic**, the RQ4 was partially addressed by the assessment of the proposed circuit's quality. This metric was analysed in terms of the *accuracy_ratio*,

precision_ratio, *recall_ratio*, *false negative_ratio (FN_ratio)*, *false positive_ratio (FP_ratio)*. For the considered scenario, a high *precision_ratio* and *false negative_ratio (FN_ratio)* values were obtained, however, the *accuracy_ratio* lowered in respect with the increase of the circuit's the output bit-1 ratio. This result showed that the reception of the molecular output needs to be improved, meaning that it should be more sensitive to the molecules produced in the last chamber of the capsule. Additionally, in comparison with the channel capacity, it is showed that there is an inverse relationship between the *accuracy_ratio* and the channel capacity that is also dependent on the output bit-1 ratio.

For **TETC**, the reliability was analysed in terms of the number of correct detections of electrical signals by pH level electrochemical sensors that indirectly measured the molecular concentration output from the Bacterial Molecular Computing on a chip circuit. Using the pH 9 as the initial pH level for the fluid where the system was placed on, the investigated bacteria-based molecular communications systems were able to achieve the maximum reliable logic computation probability of 73% when no production delay was involved and 30% when considering a 5 hours production delay. It also is shown that the delayed communication could be improved by adding a propagation delay between the molecular source and the Bacterial Molecular Computing on a chip circuit and from it to the electrochemical sensors. This propagation delay would act as a buffer for the system adjusting the temporal measurement of the molecular output signal. This publication addressed the RQ4 by presenting design considerations and requirements for the implementation of a simple and reliable bio-electronic device, which could be further extended to more complex system designs.

CHAPTER 6

CONFERENCE PAPER: USING COMPETING BACTERIAL COMMUNICATION TO DISASSEMBLE BIOFILMS

Conference Title:	3rd ACM International Conference on Nanoscale Computing and Communication
Article Type:	Regular Paper
Complete Author List:	Daniel Perez Martins, Michael Taynnan Barros, Sasitharan Balasubramaniam
Keywords:	Biofilm; Synthetically engineered bacteria; Molecular communication.
Status:	Published: September 2016. doi: 10.1145/2967446.2967463

Using Competing Bacterial Communication to Disassemble Biofilms

Daniel P. Martins
Telecommunication Software & Systems Group (TSSG)
Waterford Institute of Technology (WIT)
Waterford , Ireland.
dpmartins@tssg.org

Michael T. Barros
Telecommunication Software & Systems Group (TSSG)
Waterford Institute of Technology (WIT)
Waterford , Ireland.
mbarros@tssg.org

Sasitharan Balasubramaniam
Nano Communications Center (NCC), Department of Electronics and Communication Engineering
Tampere University of Technology (TUT)
Tampere, Finland.
sasi.bala@tut.fi

ABSTRACT

In recent years, bacterial infections have become a major public health concern due to their ability to cooperate between single and multiple species resisting to various forms of treatments (e.g., antibiotics). One form of protection is through *biofilms*, where the bacteria produce a protective medium known as the *Extracellular Polymeric Substances* (*EPS*). Researchers are pursuing new multi-disciplinary approaches to treating and kerb the evolving process of these infections through the biofilms, to lower the humans' antibiotic dependence that can result in the so-called "*superbugs*". Although various solutions have been proposed to break biofilms, they are based on applying drugs or using nanoparticles. In this paper, we propose an alternative approach, where bacteria will cooperate and surround the biofilms to consume the nutrients. By hijacking the nutrients in the environment and blocking the flow from reaching the biofilms, this will lead to starvation, forcing them to break their structure. Preliminary simulations show that a small action radius of quorum sensing molecules is needed to maximise bacteria attraction to a particular location and create the protective wall. Therefore, this formation is capable of speeds up biofilm dispersal process by two hours.

CCS Concepts

•**Applied computing** → **Systems biology;** *Telecommunications; Computational biology; Systems biology;*

Keywords

Biofilm; Synthetically engineered bacteria; Molecular communication.

NANOCOM'16, September 28-30, 2016, New York, NY, USA

DOI: http://dx.doi.org/10.1145/2967446.2967463

1. INTRODUCTION

Bacterial infections are prevalent today and the continued resistance to various types of drugs has led them to emerge as super bugs [19]. The continued and evolved strength against antibiotics is due to their functionalities, which include their ability to interact, signal and communicate, move towards areas of favourable conditions, forming protective structures, as well mutation process that occurs in their DNAs [8, 26]. In this paper, we will focus on one particular functionality of bacteria that protects and enables them to evolve and resist to antibiotic treatment, and this is known as *biofilms*.

Biofilms are communities of bacteria that come together, attach to a surface and form a protective medium [8]. The formation of a biofilm begins when bacteria communicate with each other and receive signals from the environment triggering regulatory networks [8] to promote their attachment to a surface with favourable conditions (e.g., sufficient amount of nutrients). After performing the attachment, the signalling process will promote cell division to populate the surface, and production of a protective medium known as the *Extracellular Polymeric Substances* (*EPS*) [8]. After creating the EPS, bacteria within this protective medium perform complex communication processes to maintain the biofilm (e.g., division of labor) [10]. Protected by the EPS, the biofilm is hard to penetrate, leading the bacteria to evolve and survive in harsh environments.

Numerous chemical treatments have been developed to treat biofilms [26]. Those treatments will usually lead to dispersal of biofilms [4, 26]. Another solutions includes jamming the communication process between the bacteria to prevent them to signal in order to create EPS [11]. Also, probiotic bacteria have been used to treat certain biofilm-related diseases. For example, patients with bowel inflammation and oral mucositis have been subjected to bacteria-based treatments [13, 15]. In this paper, we propose an alternative mechanism that will disperse biofilms using molecular communication to induce a nutrient competition among different bacterial species. Molecular communication is a new paradigm where the communication system is constructed to represent the signalling process among cells [2, 6]. This new area of research also extends towards developing artificial communication systems [1, 3, 6].

The contributions of this paper include:

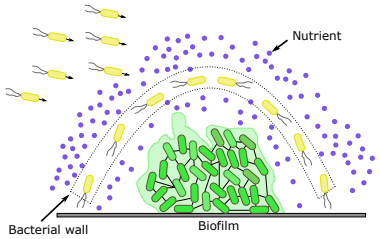

Figure 1: A bacterial wall is formed around the biofilm inducing a competition for available nutrients. Free-moving bacteria are attracted to the wall if their distance from the bacterial wall were smaller than the action radius of quorum sensing molecules.

- **Design of biocompatible technique to disperse biofilms:** The process concentrates on the natural signalling process between bacteria to induce competing behaviour. The bacteria swim towards an established biofilm, surrounds it and consume nutrients within the environment leading to biofilm starvation (the implicit objective is to trigger social competition within the biofilm that will lead to conflicts and breakage of the biofilm).
- **Simulation evaluation:** Simulation scenarios are proposed to show the effectiveness of breaking the biofilm through a population of bacteria that surrounds and intercepts the nutrients flowing towards the biofilm.

This paper is organised as follows. In Section 2, the biofilm dispersal process is characterized. The proposed system is formally characterized in Section 3. Section 4 presents the analysis and simulation of the bacterial competition that will lead to the breakage of the biofilm. Lastly, Section 5 presents the conclusion.

2. BIOFILM AND BREAKDOWN APPROACHES

Within the human body, biofilms can be formed between the edges of tissues that contain implantable devices [7]. After the biofilms are matured, the EPS protects the bacteria from physical attacks and drug treatments such as antibiotics. Bacteria inside biofilms constantly monitor the environment and induce specific phenotypes as response to any sensed signal [9]. As a response to harsh environments, the dispersal mechanism is activated. This mechanism, commonly used to assure community survival, can also be used to reach other surfaces and spread the biofilm further [19]. In certain cases, these dispersed cells (biofilm flocks or free-moving bacteria) are as harmful as the biofilm itself. For example, in air pipes, biofilm flocks can be carried by the air which can affect people who inhale them [7]. At the same time, biofilms in water pipes must be constantly monitored because they develop a high resistance to chlorine used to treat the water, resulting in high levels of contamination [7].

The current pharmaceutical products are capable of treating biofilms at the early formation stages [26]. However, drugs do not have the same efficiency to kill bacteria inside mature biofilms and, even worse, can promote the development of drug resistance genes. China have recently reported the emergence of "*superbugs*" that are resistant to all known antibiotics [14]. Therefore, numerous research efforts have been put into mechanisms of dispersing biofilms as a preventive measure for the superbugs [4, 16].

Current techniques to induce biofilm dispersal applies quorum sensing molecules and the use of nano particles. Researchers have investigated how disrupting quorum sensing could be used to disperse biofilms and have applied this technique towards the development of new antibiotics [4, 12]. Others are studying how to use nanoparticles as antimicrobials, as they can be lethal to free-moving bacteria [5]. Nanoparticles, as *silver ions*, can penetrate into biofilms and bond to EPS molecules disrupting it [25]. Although these novel approaches can break biofilms, they require an application of drugs or foreign materials which is not suitable for application in humans since they can result in harmful side effects. For example, nanoparticles need to be precisely injected close to the biofilm, and must not accumulate in specific areas of the tissue due to their high toxicity [21].

An alternative approach is proposed in this paper (see Figure 1). The basic idea is introduce a harsh environment by reducing the amount of available nutrients in order to affect the biofilm's capacity of maintaining the structure. The objective is to utilise bio-compatible mechanism of competing free-moving bacteria to hijack the nutrients. This will prevent the flow of nutrients into the biofilm and disrupt their upkeep leading to the breakage. The paper will present numerical evaluations to demonstrate how the blockage of consumed nutrients by free-moving bacteria can induce biofilm dispersal.

3. SYSTEM MODEL

We propose in this paper an induced ecological competition among engineered free-moving bacteria and biofilms. The competition analysis consist of two steps, which are illustrated in Figure 2. The first step consists of sensing biofilm within the environment. Engineered free-moving bacteria will detect a concentration level of QS molecules emitted by the biofilm, and terminate their movement once these levels indicate their proximity to the biofilm in order to form the protective wall. The free-moving bacteria will emit more QS molecules to attract other bacteria within the vicinity to increase the size as well as strengthen the wall. The biased movement results from the activation of their regulatory network once they sense a minimum level of QS molecules [18].

The second step is the nutrient consumption phase by the free-moving bacteria that results in the wall's growth. Due to the number of bacteria within the wall, after a certain period the nutrient consumption rate will be greater than the nutrient renewal process. Therefore, higher efficient nutrient consumption results in increased efficiency to disperse biofilms.

To analyse this process, we model the attraction of free-moving bacteria towards the biofilm to create the wall as a single event (see Subsection 3.1). In Subsection 3.2 we present the growth rate and nutrient consumption rate models for both biofilms and free-moving bacteria.

3.1 Attraction Model

To evaluate the attraction process of the free-moving bacteria to the wall we need to obtain the concentration levels of quorum sensing molecules (A_c) that are produced by the

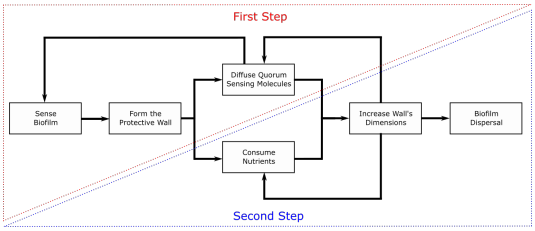

Figure 2: Flow diagram of proposed system. Free-moving bacteria are attracted to the wall and unbalancing the nutrient competition towards them and inducing biofilm to disperse.

wall. These levels can be evaluated as [20, 23]

$$A_c = \frac{D^2 N_{bac} r_v \beta}{(1+D)(1+D+DN_{bac}r_v)(\alpha+\beta)}, \quad (1)$$

where D is the diffusion coefficient, N_{bac} is the number of bacteria, r_v is the ratio of cell volume and the volume external to the cell, and α and β are the transcription rates. These molecules will be diffused into the environment and will decay exponentially with the distance from the origin,

$$A_D = A_c \exp\left(-\sqrt{(x-x_0)^2+(y-y_0)^2}\right), \quad (2)$$

where A_D is the autoinducer concentration at position (x, y) and (x_0, y_0) are the biofilm coordinates.

Considering the A_c as the maximum QS level, it is possible to specify the maximum action radius of the protective wall [9]. The action radius is the maximum distance that a bacterium can be with respect to the protective wall, in order for the attraction process to occur. This can be represented as follows

$$R_{QS} = \sqrt[3]{\frac{3c_{Aw}Ddt}{4\pi DdA_c - c_{Aw}}}, \quad (3)$$

where R_{QS} is the maximum action radius; d is the maximum distance achieved by the diffused molecules; c_{Aw} is the transcription basal level for AHL produced by free-moving bacteria at the wall and t is the diffusion time.

3.2 Growth Rate and Nutrient Consumption Rate Models

Mathematical models were used to study the effect of free-moving bacteria consumption of nutrients and its effect on the biofilm growth. For the free-moving bacteria, the nutrient consumption and biomass growth rate are represented by (4) and (5) [22]:

$$\frac{d[S_{bac}]}{dt} = -U_1\left(\mu_1 \frac{[S_{bac}]}{[S_{bac}]+K_{S1}}\right)[N_1] \quad (4)$$

$$\frac{d[N_1]}{dt} = \left(\mu_1 \frac{[S_{bac}]}{[S_{bac}]+K_{S1}} - m_1\right)[N_1] \quad (5)$$

where $[S_{bac}]$ is the nutrient consumption by the bacteria; $[N_1]$ is the bacterial concentration; μ_1 is the maximum growth rate; K_{S1} is the half-saturation constant for free-moving bacteria; m_1 is the maintenance rate of bacteria cells and U_1 is an utility parameter.

For the biofilms, other parameters are used to represent the growth and nutrient consumption. Quorum sensing system and EPS production have important roles in biofilm growth, and is highly related to the nutrient consumption rate. For the quorum sensing process, we considered the N-acyl-L-homoserine lactone (AHL) molecules and the $LuxR$ receptors, and their rates are described by (6)-(9) [17]

$$\frac{d[A]}{dt} = c_A + \frac{k_A[C]}{K_A+[C]} - k_0[A] - k_1[R][A] + k_2[RA] \quad (6)$$

$$\frac{d[R]}{dt} = c_R + \frac{k_R[C]}{K_R+[C]} - k_3[A] - k_1[R][A] + k_2[RA] \quad (7)$$

$$\frac{d[RA]}{dt} = k_1[R][A] - k_2[RA] - 2k_4[RA]^2 + 2k_5[C] \quad (8)$$

$$\frac{d[C]}{dt} = k_4[RA]^2 + k_5[C] \quad (9)$$

where $[A]$, $[R]$, $[RA]$, $[C]$ are the AHL, $LuxR$, $LuxR-AHL$ complex and dimerized complex concentration, respectively. The EPS production that results from the quorum sensing process is represented as [24]

$$\frac{d[EPS]}{dt} = k_{EPS}\frac{[C]}{[C]+K_C}. \quad (10)$$

The rate expression for the biofilm growth N_2, considering that bacteria has a limited growth and fixed maintenance rate (this is related to the nutrient consumption when bacteria is neither growing nor dividing) is represented as

$$\frac{d[N_2]}{dt} = \left(\mu_2 \frac{[S_{bio}]}{[S_{bio}]+K_{S2}} - m_2\right)[N_2]. \quad (11)$$

The nutrient consumption rate $[S_{bio}]$ function which is the weighted sum of all rate functions of this process [22, 24] is represented as follows

$$\frac{d[S_{bio}]}{dt} = -U_2\left(\mu_2 \frac{[S_{bio}]}{K_{S2}+[S_{bio}]}\right)N_2 - U_{AHL}\frac{d[A]}{dt} - U_{LuxR}\frac{d[R]}{dt} - U_{EPS}\frac{d[EPS]}{dt}, \quad (12)$$

where c_A and c_R are the transcription basal levels for AHL and $LuxR$, respectively; k_A and k_R are the transcription rates; K_A and K_R are the degradation rates; μ_2 are the maximum specific growth rate for the free-moving as well as bacteria inside the biofilm; $k_0, k_1, k_2, k_3, k_4, k_5$ are the translation rates; K_{S2} is the half-saturation constant for the biofilm; m_2 is the maintenance rate; k_{EPS} is the maximum EPS production rate; K_C is the dimerized complex degradation rate and U_2, U_{AHL}, U_{LuxR}, U_{EPS} are the utility parameters.

Considering that free-moving bacteria and biofilms are co-existing and competing for the same nutrients $[S]$, (5), (11) and (12) are modified as follows,

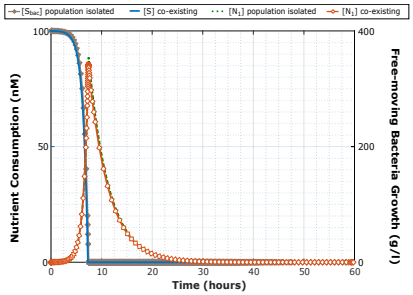

Figure 3: Numerical results of free-moving bacteria nutrient consumption and growth rate when isolated ($[S_{bac}]$ and $[N_1]$, respectively) and co-existing with the biofilm ($[S]$ and $[N_1]$, respectively).

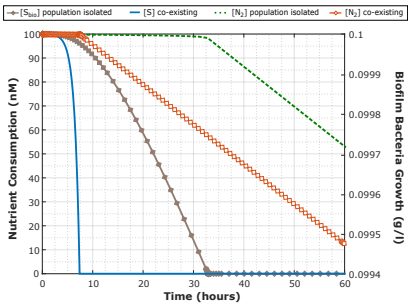

Figure 4: Numerical results of biofilm nutrient consumption and growth rate when isolated ($[S_{bio}]$ and $[N_2]$, respectively) and co-existing with free-moving bacteria ($[S]$ and $[N_2]$, respectively).

$$\frac{d[N_1]}{dt} = \left(\mu_1 \frac{[S]}{[S]+K_{S1}} - m_1\right)[N_1] \tag{13}$$

$$\frac{d[N_2]}{dt} = \left(\mu_2 \frac{[S]}{[S]+K_{S2}} - m_2\right)[N_2] \tag{14}$$

$$\begin{aligned}\frac{d[S]}{dt} = &-U_1\left(\mu_1 \frac{[S]}{K_{S1}+[S]}\right)[N_1] - \\ &- U_2\left(\mu_2 \frac{[S]}{K_{S2}+[S]}\right)N_2 - U_{AHL}\frac{d[A]}{dt} - \\ &- U_{LuxR}\frac{d[R]}{dt} - U_{EPS}\frac{d[EPS]}{dt}.\end{aligned} \tag{15}$$

The growth rate of free-moving bacteria attracted to the wall $[Ne]$ is

$$\frac{d[Ne]}{dt} = \mu_w[Ne], \tag{16}$$

where μ_w is the rate of free-moving bacteria that is attracted to the wall per hour.

Therefore, both (5) and (15) will be modified to consider (16), and is represented as follows

$$\frac{d[N_1]}{dt} = \left(\mu_1 \frac{[S]}{[S]+K_{S1}} - m_1\right)([N_1][Ne]) \tag{17}$$

$$\begin{aligned}\frac{d[S]}{dt} = &-U_1\left(\mu_1 \frac{[S]}{K_{S1}+[S]}\right)([N_1][Ne]) - \\ &- U_2\left(\mu_2 \frac{[S]}{K_{S2}+[S]}\right)N_2 - U_{AHL}\frac{d[A]}{dt} - \\ &- U_{LuxR}\frac{d[R]}{dt} - U_{EPS}\frac{d[EPS]}{dt}.\end{aligned} \tag{18}$$

4. BIOFILM DISPERSAL

In this section, we present the analysis of the biofilm's breakdown mechanism due to the starvation process. All equations shown in Section 3 are solved using the parameters presented in Table 1. The nutrient consumption rate, biofilm and free-moving bacteria growth rate are required to understand the biofilm's breaking process.

4.1 Numerical Results

We analysed the bacterial growth and nutrient consumption rates for the free-moving bacteria and biofilm when they are isolated as well as mixed (forming the wall) in the same environment using (4)–(15). The population of the free-moving bacteria, when isolated, will grow and consume the nutrients as shown in Figure 3. After growing for 7.4 hours, those free-moving bacteria will die due to insufficient nutrients. Figure 3 also shows that they have the same behaviour when they co-exists with the biofilm.

Figure 4 presents the biofilm growth rate over time. Nutrient concentration decays non-linearly over time towards zero producing a fast decaying process for the biofilm after 33 hours when isolated. However, when co-existing with free-moving bacteria, the biofilm decays with a higher rate than when isolated. Its take 10 hours to deplete the nutrients and start the decaying process. From Figures 3 and 4 we can observe that the decay rate of the biofilm is increased by the competition with the free-moving bacteria. Therefore, in order to quickly disperse the biofilm, it is necessary that most of the free-moving bacteria are attracted to the wall within 7.4 hours (this is of course with respect to the quantity of nutrients we have considered).

4.2 Simulation Results

Since our objective is to attract most of the free-moving bacteria from the environment towards the biofilm location, we simulated a scenario to determine the quantity of bacteria that will successfully arrive at that location within 7.4 hours. We placed one biofilm at a random position in a closed area ($1000 \times 1000 \mu m$), with 1000 free-moving bacteria swimming in the area. On average, **53% of free-moving bacteria were attracted to the wall.** We observed the attraction probability over time (five time steps from 1 to 5 hours) to evaluate the rate of free-moving bacteria that will

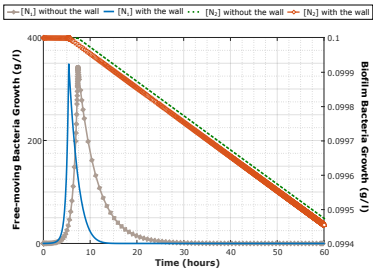

Figure 5: Comparison between free-moving bacteria and biofilm growth rate when co-existing ($[N_1]$ and $[N_2]$, respectively) within the same environment, and with the presence of the bacterial wall ($[N_1]$ and $[N_2]$, respectively).

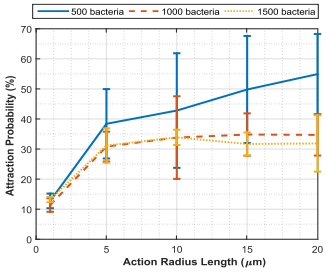

Figure 6: Simulation results for 5 different action radius lengths and three free-moving bacteria numbers (500, 1000, 1500).

continuously enter into the wall. Once the attraction probability of the five time steps are calculated, we used linear regression to obtain the rate of bacteria attraction to the wall $\mu_w = 0.11$, and this was used to evaluate (16) – (18). The results of integrating the rate of bacteria attraction is illustrated in Figure 5. As we can see from the figure, with continuous addition of free-moving bacteria to the wall, the biofilm started to **decay in 5.4 hours** making the natural competition process for the nutrients more efficient.

Figure 6 evaluates the attraction probability when the action radius is varied as well as the number of free-moving bacteria. Once again the biofilm was placed in a random position in a closed area of size $1000 \times 1000 \mu m$. The R_{QS} is varied between 1 and 20 μm and the number of free-moving bacteria is varied between 500, 1000 and 1500. The total simulation period is set at 1 hour. As shown in Figure 6, the attraction of free-moving bacteria increases accordingly to that action radius for all considered bacteria number. For 1000 and 1500, the system achieved its maximum attraction at $R_{QS} = 15\mu$m. However, the same does not occur for a few number of bacteria (e.g. 500) in which case a wider action radius is needed.

5. CONCLUSION

Over the years, researchers have been developing new solutions that can treat biofilms. The formation of the biofilm results from the bacteria's cooperative behaviour, and once they are formed will create a protective shield that makes them hard to kill. This can lead to infections within the human body as well as contamination within the environment (e.g., biofilms formed in water). Although solutions have been proposed to break and disperse the biofilms, they are based on using nanoparticles or drugs. This paper proposes the use of engineered free-moving bacteria that will cooperate and surround biofilms to hijack the nutrients within the environment. The consumption of the nutrients by free-moving bacteria will lead to minimum nutrients flowing into the biofilm leading to its breakdown. Our numerical analysis has shown how a certain quantity of bacteria that consume the nutrients can grow and populate, and at the same time the starvation of the biofilm can lead to negative growth. Our simulation have also shown that through the cooperative communication of autoinducers by the free-moving bacteria, this can lead to an attraction process that draws in a certain quantity of the microbes towards the biolfim. The proposed approach has shown the promise of using synthetic biology to engineer bacteria that can be used to breakdown and disperse biofilms.

Table 1: Parameters used to evaluate Eq. (1)-(18)

Variable	Value	Unit
c_A	2.7×10^{-2}	nM
c_{Aw}	2.7×10^{-2}	nM
c_R	2.7×10^{-2}	nM
k_A	2×10^{-3}	d^{-1}
k_R	2×10^{-3}	d^{-1}
k_0	1×10^{-2}	d^{-1}
k_1	0.1	d^{-1}
k_2	0.1	d^{-1}
k_3	1×10^{-2}	d^{-1}
k_4	0.1	d^{-1}
k_5	0.1	d^{-1}
k_{EPS}	1	d^{-1}
K_A	2×10^{-3}	gm^{-3}
K_R	2×10^{-3}	gm^{-3}
K_C	1	gm^{-3}
K_S	1	gm^{-3}
μ_{max}	1×10^{-4}	gm^{-3}
m	1×10^{-4}	gm^{-3}
U_X	0.6	–
U_{AHL}	2×10^{-2}	–
U_{EPS}	2×10^{-2}	–
γ	0.23	–
r	1.35	h^{-1}
N_{bac}	from 1000 to 10000	–
a	0.004	gm^{-3}
m_B	0.25	gm^{-3}
D	from 100 to 1000	m^2d^{-1}
α	6.93	$nM/(gm^{-3}d^{-1})$
β	2.93	$nM/(gm^{-3}d^{-1})$

6. ACKNOWLEDGMENT

This work has received support from the Science Foundation Ireland (SFI) via the CONNECT research centre under Grant 13/RC/2077, as well as the Academy of Finland FiDiPro program for the project "Nanocommunications Networks" 2012-2016, and the Finnish Academy Research Fel-

low program under Project no. 284531. This work has also been supported by EU funding from the European Union's Horizon 2020 research and innovation programme under the grant agreement No. 665564.

7. REFERENCES

[1] I. Akyildiz, M. Pierobon, S. Balasubramaniam, and Y. Koucheryavy. The internet of Bio-Nano things. *IEEE Communications Magazine*, 53(3):32–40, Mar 2015.

[2] I. F. Akyildiz, F. Brunetti, and C. Blázquez. Nanonetworks: A new communication paradigm. *Computer Networks*, 52(12):2260–2279, Aug 2008.

[3] S. Balasubramaniam and P. Lio'. Multi-Hop Conjugation Based Bacteria Nanonetworks. *IEEE Transactions on NanoBioscience*, 12(1):47–59, Mar 2013.

[4] N. Barraud, M. J. Kelso, S. A. Rice, and S. Kjelleberg. Nitric Oxide: A Key Mediator of Biofilm Dispersal with Applications in Infectious Diseases. *Current Pharmaceutical Design*, 21:31–42, Jan 2015.

[5] O. Choi, C. P. Yu, G. Esteban Fernández, and Z. Hu. Interactions of nanosilver with Escherichia coli cells in planktonic and biofilm cultures. *Water Research*, 44(20):6095–6103, Dec 2010.

[6] L. C. Cobo and I. F. Akyildiz. Bacteria-based communication in nanonetworks. *Nano Communication Networks*, 1(4):244–256, Dec 2010.

[7] J. W. Costerton and P. S. Stewart. Battling biofilms. *Scientific American*, 285(1):74–81, Jul 2001.

[8] C. de la Fuente-Núñez, F. Reffuveille, L. Fernández, and R. E. Hancock. Bacterial biofilm development as a multicellular adaptation: antibiotic resistance and new therapeutic strategies. *Current Opinion in Microbiology*, 16(5):580–589, 2013.

[9] S. J. Hagen. Swimming in Information? Physical Limits to Learning by Quorum Sensing. In S. J. Hagen, editor, *The Physical Basis of Bacterial Quorum Communication*, Biological and Medical Physics, Biomedical Engineering, chapter 7, pages 123–144. Springer New York, New York, NY, 2015.

[10] M. Hasan, E. Hossain, S. Balasubramaniam, and Y. Koucheryavy. Social behavior in bacterial nanonetworks: Challenges and opportunities. *IEEE Network*, 29(1):26–34, Jan 2015.

[11] M. Kalia, V. K. Yadav, P. K. Singh, D. Sharma, H. Pandey, S. S. Narvi, and V. Agarwal. Effect of Cinnamon Oil on Quorum Sensing-Controlled Virulence Factors and Biofilm Formation in Pseudomonas aeruginosa. *PLOS ONE*, 10(8):e0135495, Aug 2015.

[12] A. Kubacka, M. S. Diez, D. Rojo, R. Bargiela, S. Ciordia, I. Zapico, J. P. Albar, C. Barbas, V. a. P. Martins dos Santos, M. Fernández-García, and M. Ferrer. Understanding the antimicrobial mechanism of TiO2-based nanocomposite films in a pathogenic bacterium. *Scientific Reports*, 4:4134, Feb 2014.

[13] S. A. Limaye, R. I. Haddad, F. Cilli, S. T. Sonis, A. D. Colevas, M. T. Brennan, K. S. Hu, and B. A. Murphy. Phase 1b, multicenter, single blinded, placebo-controlled, sequential dose escalation study to assess the safety and tolerability of topically applied AG013 in subjects with locally advanced head and neck cancer receiving induction chemotherapy. *Cancer*, 119(24):4268–4276, Sep 2013.

[14] Y. Y. Liu, Y. Wang, T. R. Walsh, L. X. Yi, R. Zhang, J. Spencer, Y. Doi, G. Tian, B. Dong, X. Huang, L. F. Yu, D. Gu, H. Ren, X. Chen, L. Lv, D. He, H. Zhou, Z. Liang, J. H. Liu, and J. Shen. Emergence of plasmid-mediated colistin resistance mechanism MCR-1 in animals and human beings in China: A microbiological and molecular biological study. *The Lancet Infectious Diseases*, 16(2):161–168, Feb 2016.

[15] R. Martín, S. Miquel, J. Ulmer, N. Kechaou, P. Langella, and L. G. Bermúdez-Humarán. Role of commensal and probiotic bacteria in human health: a focus on inflammatory bowel disease. *Microbial cell factories*, 12:71, Jul 2013.

[16] D. McDougald, S. a. Rice, N. Barraud, P. D. Steinberg, and S. Kjelleberg. Should we stay or should we go: mechanisms and ecological consequences for biofilm dispersal. *Nature Reviews Microbiology*, 10(1):39–50, Jan 2012.

[17] P. Melke, P. Sahlin, A. Levchenko, and H. Jönsson. A cell-based model for quorum sensing in heterogeneous bacterial colonies. *PLoS Computational Biology*, 6(6):1–13, Jun 2010.

[18] J. G. Mitchell and K. Kogure. Bacterial motility: Links to the environment and a driving force for microbial physics. *FEMS Microbiology Ecology*, 55(1):3–16, Sep 2006.

[19] N. M. Oliveira, E. Martinez-Garcia, J. Xavier, W. M. Durham, R. Kolter, W. Kim, and K. R. Foster. Biofilm Formation As a Response to Ecological Competition. *PLOS Biology*, 13(7):e1002191, Jul 2015.

[20] A. Pai and L. You. Optimal tuning of bacterial sensing potential. *Molecular systems biology*, 5(286):211–286, May 2009.

[21] P. Ramesh and K. Gurunathan. Nanomaterials communication inside the living organism. *Nano Communication Networks*, 3(4):252–256, Dec 2012.

[22] D. Tilman. Tests of Resource Competition Theory Using Four Species of Lake Michigan Algae. *Ecology*, 62:802–815, Jun 1981.

[23] M. Weber and J. Buceta. Noise regulation by quorum sensing in low mRNA copy number systems. *BMC systems biology*, 5(1):11, Jan 2011.

[24] G. Wei, C. Walsh, I. Cazan, and R. Marculescu. Molecular tweeting. In *Proceedings of the 6th ACM Conference on Bioinformatics, Computational Biology and Health Informatics - BCB '15*, pages 366–375, New York, New York, USA, Sep 2015. ACM Press.

[25] S. M. Wirth, G. V. Lowry, and R. D. Tilton. Natural organic matter alters biofilm tolerance to silver nanoparticles and dissolved silver. *Environmental Science and Technology*, 46(22):12687–12696, Oct 2012.

[26] H. Wu, C. Moser, H.-Z. Wang, N. Høiby, and Z.-J. Song. Strategies for combating bacterial biofilm infections. *International Journal of Oral Science*, 7(1):1–7, Dec 2014.

CHAPTER 7

JOURNAL PAPER: MOLECULAR COMMUNICATIONS PULSE-BASED JAMMING MODEL FOR BACTERIAL BIOFILM SUPPRESSION

Conference Title:	IEEE Transactions on Communications
Article Type:	Regular Paper
Complete Author List:	Daniel Perez Martins, Kantinan Leetanasaksakul, Michael Taynnan Barros, Arinthip Thamchaipenet, William Donnelly, Sasitharan Balasubramaniam
Keywords:	Communication systems, Jamming, Digital circuits, Biological control systems
Status:	Published: v. 17, no. 4, p. 533-542, October 2018. doi: 10.1109/TNB.2018.2871276

This is the author's version of an article that has been published in this journal. Changes were made to this version by the publisher prior to publication.
The final version of record is available at http://dx.doi.org/10.1109/TNB.2018.2871276

Molecular Communications Pulse-based Jamming Model for Bacterial Biofilm Suppression

Daniel P. Martins, *Student Member, IEEE,* Kantinan Leetanasaksakul, Michael Taynnan Barros, *Member, IEEE,* Arinthip Thamchaipenet, William Donnelly, and Sasitharan Balasubramaniam, *Senior Member, IEEE*

***Abstract*—Studies have recently shown that the bacteria survivability within biofilms is responsible for the emergence of *superbugs*. The combat of bacterial infections, without enhancing its resistance to antibiotics, includes the use of nanoparticles to quench the *quorum sensing* of these biofilm-forming bacteria. Several sequential and parallel multi-stage communication processes are involved in the formation of biofilms. In this paper, we use proteomic data from a wet lab experiment to identify the communication channels that are vital to these processes. We also identified the main proteins from each channel and propose the use of jamming signals from synthetically engineered bacteria to suppress the production of those proteins. This biocompatible technique is based on synthetic biology and enables the inhibition of biofilm formation. We analyse the communications performance of the jamming process, by evaluating the path loss for a number of conditions that include different engineered bacterial population sizes, distances between the populations and molecular signal power. Our results show that sufficient molecular pulse-based jamming signals are able to prevent the biofilm formation by creating lossy communications channels (almost -3 dB for certain scenarios). From these results, we define the main design parameters to develop a fully operational bacteria-based jamming system.**

***Index Terms*—Communications systems, Jamming, Synthetic logic circuits, Biofilm suppression**

I. INTRODUCTION

IN recent years, the field of molecular communications has received considerable interests [1]–[3]. Its objective is to develop communications systems that are constructed from molecular biological components and systems found in nature [1], [3], [4]. One approach that has been proposed uses bacteria to perform molecular communications as carriers, transmitters or receivers. This includes the application of their motility behaviour to deliver DNA-encoded information [5]–[7], or engineering their diffusion-based signalling process between the cells [5], [7], [8]. For this case, the use of the bacteria signalling system (a.k.a *quorum sensing* – QS) allow communications engineers to synthetically coordinate the emission of molecules, whereby in a natural setting allow bacteria to perform certain functions, such as the formation of biofilms [9]. The coordination created by the QS signalling initiates a cascaded communications process within bacteria that lead to these behaviours.

Biofilms can lead to numerous resistant infections within the human body as well as environmental contamination. This is largely due to the protective surface that encapsulates the bacteria to allow them to survive through varying environmental conditions [10]. A recent concern has been raised about the role that biofilms have in protecting the bacteria from antibiotics. This protective mechanism has led to the emergence of the *superbug*, which are bacteria that have resistance to all current types of antibiotics [11]. Besides health issues, biofilms are also known to impact the environment, where they have led to contamination of fruits, vegetables and drinking water distribution systems [12], [13]. The formation of biofilms is triggered by a multi-stage communications process. Initially, bacteria will search for a suitable and favourable environment to form biofilms [14] (see Figure 1a). Once this location is found, bacteria will form a biofilm infrastructure that surrounds them and start to perform complex internal communication processes that help to maintain the whole infrastructure. This infrastructure is known as the *Extracellular Polymeric Substances* (*EPS*) matrix [15]. Numerous efforts have been dedicated for the dysregulation of bacteria resistance mechanisms [16], [17] and for the eradication of biofilms, including the use of chemical agents or synthetically engineered mechanisms [18]–

Daniel P. Martins, Michael T. Barros, William Donnelly and are with the Telecommunication Software & Systems Group (TSSG), Waterford Institute of Technology (WIT), Ireland. E-mail: dpmartins@tssg.org, mbarros@tssg.org, wdonnelly@tssg.org.

Kantinan Leetanasaksakul and Arinthip Thamchaipenet are with the Department of Genetics, Kasetsart University, Thailand. Email: kantinan.le@ku.th, arinthip.t@ku.ac.th.

Sasitharan Balasubramaniam is with the Telecommunication Software & Systems Group (TSSG), Waterford Institute of Technology (WIT), Ireland and with the Department of Electronic and Communication Engineering, Tampere University of Technology, Finland. Email: sasi.bala@tut.fi.

This is the author's version of an article that has been published in this journal. Changes were made to this version by the publisher prior to publication.
The final version of record is available at http://dx.doi.org/10.1109/TNB.2018.2871276

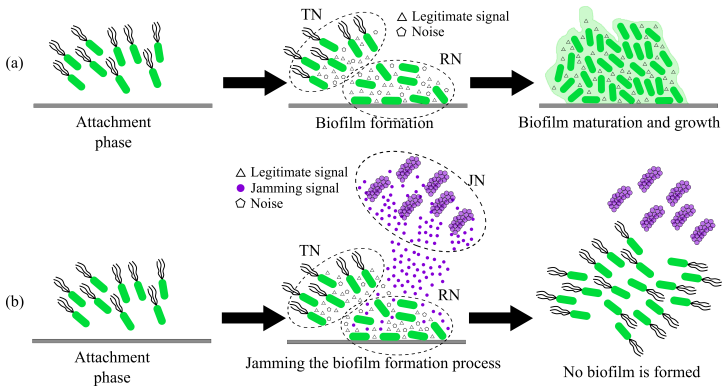

Fig. 1. A general illustration of the biofilm formation process in two different scenarios. (a) The biofilm bacteria within the transmitter node TN will produce different molecular protein signals to induce the receiver bacterial population to form the biofilm. (b) The case where engineered jamming bacteria node JN produces molecular protein signals that will interfere with the multi-stage communication process between TN and RN biofilm bacteria, inhibiting the biofilm formation.

[20]. In this paper, we will investigate an approach for preventing biofilm to form, based on interfering with its multi-stage and parallel communication processes.

We propose the use of synthetically engineered bacteria to transmit diffusion-based jamming signals to a group of bacteria that are aiming to produce a biofilm. The proposed model is based on jamming systems used in conventional wireless networks. This analogy mapping is illustrated in Figure 1b, where the engineered bacteria within the jamming node (JN), through the QS process, will emit concentrations of proteins to disrupt the communication process of the biofilm forming bacteria (contained within the transmitter node TN and receiver node RN). We focus on **how the interaction and communications process** between two bacterial populations, **will prevent the formation of the biofilm**. The objective of the molecular pulse based jamming signal is to degrade the performance (obtaining a high path loss) of the TN and RN bacteria communications link.

The modelling of molecular communications interference process has been proposed before [21]. However, there is no application of using natural bacteria signalling for disrupting molecular communications systems, and in particular for a biotechnology application, such as bacterial biofilm suppression. Our pulse based jamming model includes emulated digital toggle switches for the RN bacterial population, that change between states depending on a specific induction signal. For our model, we consider that **the molecular pulse-based jamming signal will induce the production of proteins that inhibit the biofilm formation**. We identified a number of channels used in the communication process for the biofilm formation and modelled each one as toggle switches [22]–[27]. The aim is to force the induction of suppressor molecules as the molecular pulse-based jamming signal that will prevent the formation of bacterial biofilms. We integrate the use of synthetic biology and molecular communications to develop this biocompatible solution. The main contributions of this paper are:

- **Identification of weak points within the biofilm formation multi-stage communications** to interfere using a molecular pulse-based jamming signal. We identify three main internal communication channels and their corresponding signalling proteins. For this paper, we used raw mass spectrometry proteomics data collected from wet lab experiments.
- **Design of a pulse-based jamming model to interfere an end-to-end bacteria-based molecular communications systems.** We use a bacterial population to emit *quorum sensing* molecules to disrupt and lower biofilm-related protein production. The path loss metric is used to determine the performance of the proposed model.
- **Actuation on a bacteria natural behaviour using synthetic biology and molecular communications.** The effectiveness of the proposed interfering system is dependent on the number of jamming molecules that reach the bacterial population and disrupt its intracellular signalling system. We emulate the internal bacterial process of activation (or deactivation) of the molecules to create the biofilm as toggle switches. The switching mechanism is then controlled by the molecular communications of proteins emitted by the engineered jamming

This is the author's version of an article that has been published in this journal. Changes were made to this version by the publisher prior to publication.
The final version of record is available at http://dx.doi.org/10.1109/TNB.2018.2871276

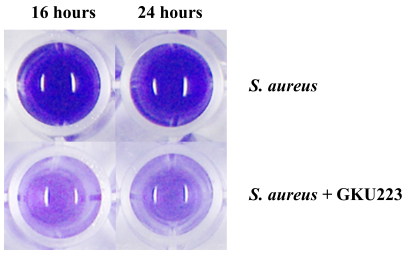

Fig. 2. Wet-lab demonstration of the *S. aureus* biofilm formation in a 96-well microtiter plate. The top row shows the isolated bacteria, leading to the biofilm formation. The bottom row shows the *S. aureus* after being treated with supernatant of *Streptomyces sp. GKU 223*, preventing the biofilm formation. Both cultures were cultivated in the 96-well microtiter plate at 37°C for 16 and 24 hours. The biofilm mass was stained using crystal violet. This result shows that the biofilm formation can be prevented based on applying supernatant, which in turn suppresses certain communication channels.

bacteria.

The rest of the paper is organised as follows. In Section II, we describe the *Staphyloccocus aureus* biofilm formation as a communications system and how it can be engineered to promote and suppress biofilm-related proteins. In Section III we present the physical model of the bacteria-based molecular communications system and the pulse-based jamming system. The analysis of different interfering scenarios for the proposed communications system is presented in Section IV. Lastly, in Section V we present our conclusions.

II. Background on Communications Process for Biofilm Formation

In order to determine the multi-stage communication process of biofilms, as well as deducing the types of proteins used in the signalling, wet lab experimental work was conducted. In the experiments, *Staphylococcus aureus* (we will refer to this as *S. aureus* for the remainder of the paper) was used as a biofilm-producer. Proteomic data were collected and compared between the stages during the full formation, and the case when a chemical agent is applied to prevent the formation. The proteomic data was deposited to jPOST (http://repository.jpostdb.org/, ID: JPST000480 and PXD010815). This chemical agent can be produced by a separate species known as a marine *Streptomyces sp.* GKU 223 [29]. Figure 2 demonstrates this comparison, where we can observe the difference in the biofilm mass after 16 and 24 hours when *S. aureus* was grown on its own (leading to biofilm formation) versus the case when biofilm was inhibited when in contact with the active chemicals produced by *Streptomyces sp.* GKU 223. Figure 3 shows the protein expression level of capsular biosynthesis, cellular stress, virulence, cell viability, and biofilm formation of *S. aureus*. The obtained data (see Figure 3) showed three different sets of proteins (*i.e.*, internal communications channels) that directly facilitated the multi-stage communication process for the biofilm formation. The internal communication channels are comprised of *cellular defence channel*, *cellular stress response channel*, and *energy supply channel*. For each of these channels, the proteins are triggered during different stages of the biofilm construction, as shown in Figure 4. Therefore, the objective of this paper is to piece out the relevant proteins for each of the channels and to disrupt their production through the jamming process. Detailed description for each of the channels will be presented in this section, as well as a description of the emulated toggle switch that controls the intra-cellular signalling for the protein production.

A. Cellular Defence Channel

Bacteria constantly monitor and respond accordingly to environmental changes. They coat their membranes using *Capsular Polysaccharides* (*CPS*) as a defence mechanism to these changes [22]. Each bacterial species can synthesize a number of different *CPS* serotypes. For example, *S. aureus* can synthesize up to thirteen different serotypes, which provide a better defence mechanism when compared to other bacterial strains [22]. Figure 5 presents the communications system involved in the *CPS* synthesis for *S. aureus*. The *CPS* starts to be produced when the bacteria sense specific environmental cues, including the culture medium's pH, iron limitation and CO_2 availability [10], [23]. These environmental signals trigger the expression of *CapM*, which induces the cascade production of other capsular polysaccharides (*CapL*, *Cap5I/Cap8H*, *Cap A/B* and *Cap5J/Cap8I*). Therefore, targeting the suppression of *CapM* will affect the entire defence channel and prevent biofilm formation [24].

B. Cellular Stress Channel

In response to cellular stress, bacteria can produce a matrix of *Extra Polymeric Substances* that protects them from physical attacks [25]. One of main components of the matrix is the *Polysaccharide Intercellular Adhesin* (*PIA*) [25]. In *S. aureus*, the *Agr quorum sensing* system induces the production of *PIA* mediated by *Staphylococcus acessory regulator A* (*SarA*) and *ica* pathway. The activation of the global regulator *SarA* also induces the production of other *Microbial Surface Components Recognizing Adhesive Matrix Molecules* (*MSCRAMMs*) like

This is the author's version of an article that has been published in this journal. Changes were made to this version by the publisher prior to publication.
The final version of record is available at http://dx.doi.org/10.1109/TNB.2018.2871276

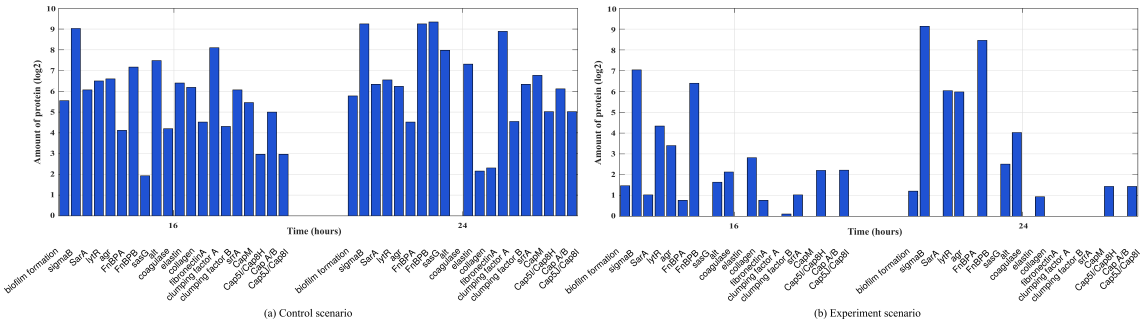

Fig. 3. A highlight of the most significant 19 proteins extracted from more than 1500 different types that were detected in the two experiment cases (*S. aureus* on its own and *S. aureus* mixed with the supernatant of *Streptomyces sp. GKU 223*). These concentration levels are important for characterising the three bacterial internal communication channels that are essential towards biofilm formation and maintenance: defence, energy supply and cell stress response.

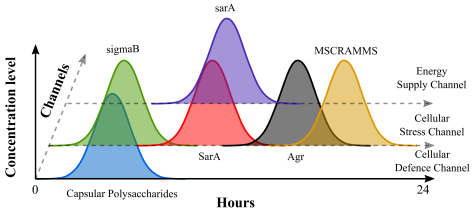

Fig. 4. Temporal illustration of the key proteins produced for the cellular defence, cellular stress response, and energy supply communication channel produced by the bacteria during the biofilm formation. Each of the proteins for the three communication channels is triggered at various stages of the biofilm lifetime.

lytR, *FnBPA*, *FnBPB*, *sasG* and *atl* (see Figure 6). These proteins are produced in response to any stress subjected onto the bacterial surface [25]. High concentration levels of these proteins within the bacterial cell will result in stronger adhesion to the substrate, as well as to other cells. Therefore, low levels of adhesins produced by *SarA* suppression can contribute towards the disassembling of the biofilm matrix structure. This particular protein molecule will be targeted for the jamming process.

C. Energy Supply Channel

The gene responsible for the respiratory response (*srrA*) in *S. aureus* acts as a global regulator of virulence factor and also has an important role in biofilm formation [26]. In environments with low oxygen, *srrA* is activated and promotes cellular adaptation for bacterial population maintenance (see Figure 7). In this case, the energy supply is provided through fermentation using the *ica* pathway and enzymes (*nrdD* and *nrdG*) [26]. However, low levels of *srrA* can lower the biofilm energy supply to a minimum level and contributes towards the biofilm disassembling process [27], which will also be another targeted protein for our proposed jamming process.

D. Toggle Switches Emulation

A molecular pulse-based jamming signal will trigger the production of specific suppressors, in order to reduce the production of the targeted proteins in each channel. This process can be emulated through the activation of toggle switches. In order to achieve this, we abstracted the protein production processes $h_{D1}(t)$, $h_{S1}(t)$ and $h_{F1}(t)$ (shown in Figure 5-7) as toggle switches that will trigger a cascade effect for each internal communication channel. As illustrated in Figure 8, the identified proteins *CapM*, *SarA*, *srrA* (target points along the communication process) will be one input for each of the toggle switches. Complementing these proteins, we have identified three other proteins that can be used as the second input to control the toggle switch. Effectively, these second inputs will lower the levels of the first inputs. The jamming signal will induce the production of *KdpDE*, interfering with *CapM* production, which has been suggested to decrease the transcription level of *CPS* [24]. In the case of the cellular stress toggle switch, the jamming signal will induce *SarR* production, which is a repressor for *SarA* production [30], and, for the energy supply toggle switch, *srrA* can be repressed by the induction of *pYJY4* protein [27].

We consider a fast and reversible binding process between the molecular pulse-based jamming signals and the bacterial receptors. The toggle switches will be induced by the jamming signal as shown in Figure 8. Therefore, each switch can be modelled based on the following Hill functions [31]

$$\frac{dX}{dt} = \frac{\beta}{1 + K_Y^{\alpha}} - \gamma X \tag{1}$$

This is the author's version of an article that has been published in this journal. Changes were made to this version by the publisher prior to publication.
The final version of record is available at http://dx.doi.org/10.1109/TNB.2018.2871276

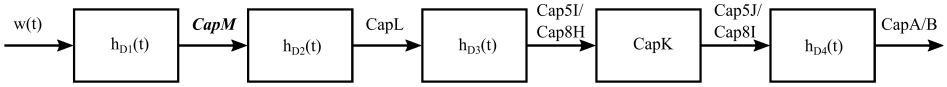

Fig. 5. The sequential stages of protein production, and their corresponding channel, during the cellular defence communications system. The selected protein highlighted in bold, *CapM*, is the molecular pulse-based jamming target. The signal $w_d(t)$ is the input signal that triggers the defence channel communication cascade

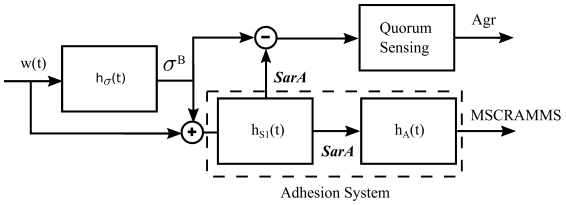

Fig. 6. The sequential and parallel stages of protein production, and their corresponding channel, during the cell stress response communications system (please note that certain channels are results of protein summations from previous stages). The selected protein highlighted in bold, *SarA*, is the molecular pulse-based jamming target. The signal $w_s(t)$ is the input signal that triggers the stress channel communication cascade.

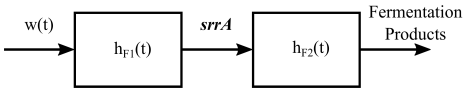

Fig. 7. The sequential stages of protein production, and their corresponding channel, during the cell energy production communications system. The selected protein highlighted in bold, *srrA*, is the molecular pulse-based jamming target. The signal $w_e(t)$ is the input signal that triggers the energy channel communication cascade

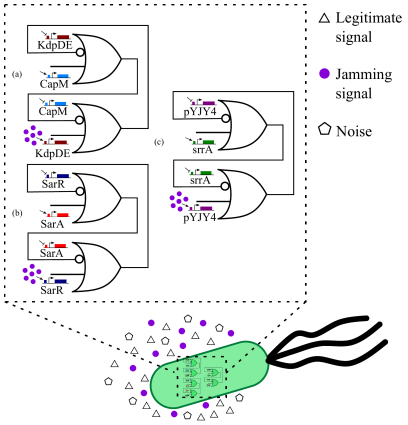

Fig. 8. The targeted protein production of *CapM*, *SarA*, *srrA* for the three internal communication channel, and its control can be represented as toggle switches. (a) The cellular defence system can be triggered by an increasing level of *CapM* and deactivated by an increasing level of *KdpDE*. (b) For the cellular stress response communications, *SarA* is deactivated by an increased level of *SarR*. (c) For the energy system, *srrA* is deactivated by an increased level of *pYJY4*.

and

$$\frac{dY}{dt} = \frac{\beta}{1 + K_X^{\alpha}} - \gamma Y \tag{2}$$

where X represents the protein levels of *CapM*, *SarA* or *srrA*, Y represents the protein levels of *KdpDE*, *SarR* or *pYJY4*, β is the maximum production rate for the selected inputs; α is the repression constant for the promoters X and Y, w_Y and w_X are the molecular pulse-based jamming signals that induce the toggle switches to work, $K_X = X/(1+(w_X/K)^n)$ and $K_Y = Y/(1+(w_Y/K)^n)$ are binding constants, γ is the first-order decay constant and n is the Hill coefficient.

III. THE PHYSICAL MODEL

The previous section described how biofilm inhibition can be achieved by suppressing specific proteins, and how this could be achieved through a toggle switch model that controls the intracellular signalling pathways controlling the protein production. Therefore, from a communication systems perspective, we must develop a model that will lead to the production of molecular pulse-based jamming signals that will interfere with the three internal communications channels, and suppressing the production of the targeted proteins. Our objective is to ensure the molecular protein jamming signals will reach the receiver biofilm bacteria population, bind to the bacterial membrane surfaces and block the cascade of sequential protein production events that will result in the inhibition of biofilm formation.

A general perspective of the proposed molecular communications system is presented in Figure 9. We consider a finite 2D aqueous environment with two bacterial populations (to recreate the environment of the wet-lab experiment). One will act as transmitter and receiver biofilm bacteria (placed in the transmitter and receiver nodes), TN and RN respectively and the other will be the engineered bacteria placed in the jamming node JN. The transmitter node TN is composed of n_t bacteria which will send a signal to the receiver node RN (with n_r bacteria). The jamming node JN, with n_j bacteria,

This is the author's version of an article that has been published in this journal. Changes were made to this version by the publisher prior to publication.
The final version of record is available at http://dx.doi.org/10.1109/TNB.2018.2871276

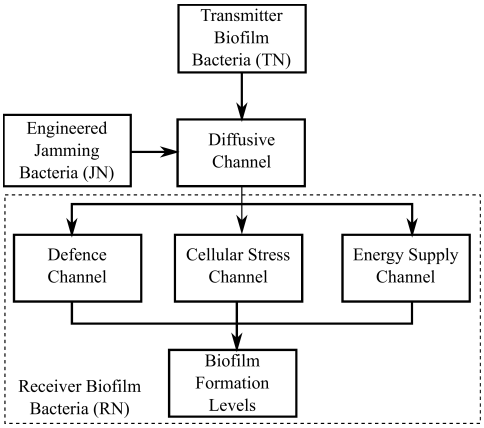

Fig. 9. Molecular communications system model to disrupt the biofilm formation.

will produce signals that influence the toggle switches of the receiver node RN bacteria in order to disrupt their internal communications channels (as presented in Section II). Each bacterium in TN and JN is considered as an emitting point source and is placed at random locations within a circle of radius r_{TN} and r_{JN} from the centre of the receiver node. Both the biofilm forming signalling molecules, as well as the jamming signalling molecules, propagates through free diffusion in the aqueous medium. We ignore the effects of collision that can occur among the molecules during the diffusion process.

The biofilm bacteria in the transmitter node are responsible for producing and diffusing a signal to induce the behaviour of the bacteria population in the receiver node to form a biofilm. The signal, denoted by $A_{TN,e}(\hat{t})$, is the QS signalling produced by the transmitter biofilm bacteria population. The jamming signal, $A_{JN,e}(\hat{t})$, is the time-related concentration of the proteins capable of activating the toggle switch for each internal communications channel of the receiver bacteria. In our model, both the communication for the biofilm formation and the molecular pulse-based jamming signal are described using the following set of differential equations [32]:

$$\begin{aligned}\frac{dA_m(\hat{t})}{dt} &= c_A + \frac{k_A C_m(\hat{t})}{K_A + C_m(\hat{t})} - k_0 A_m(\hat{t}) \\ &- k_1 R_m(\hat{t}) A_m(\hat{t}) + k_2 R A_m(\hat{t}) \\ &- p_{out} A_m(\hat{t}) + p_{in} A_{m,e}(\hat{t}),\end{aligned} \tag{3}$$

$$\begin{aligned}\frac{dR_m(\hat{t})}{dt} &= c_R + \frac{k_R C_m(\hat{t})}{K_R + C_m(\hat{t})} - k_3 A_m(\hat{t}) \\ &- k_1 R_m(\hat{t}) A_m(\hat{t}) + k_2 R A_m(\hat{t}),\end{aligned} \tag{4}$$

$$\begin{aligned}\frac{dRA_m(\hat{t})}{dt} &= k_1 R_m(\hat{t}) A_m(\hat{t}) - k_2 R A_m(\hat{t}) \\ &- 2k_4 R A_m(\hat{t})^2 + 2k_5 C_m(\hat{t}),\end{aligned} \tag{5}$$

$$\frac{dC_m(\hat{t})}{dt} = k_4 R A_m(\hat{t})^2 + k_5 C_m(\hat{t}), \tag{6}$$

$$\begin{aligned}\frac{dA_{m,e}(\hat{t})}{dt} &= (p_{out} A_m(\hat{t}) - p_{in} A_{m,e}(\hat{t})) \\ &- D A_{m,e}(\hat{t}),\end{aligned} \tag{7}$$

where $A_m(\hat{t})$, $A_{m,e}(\hat{t})$, $R_m(\hat{t})$, $RA_m(\hat{t})$, $C_m(\hat{t})$ are the internal and external autoinducer, receptor, complex and dimerized complex concentrations, respectively; c_A and c_R are the transcription basal levels for $A_m(\hat{t})$ and $R_m(\hat{t})$, respectively; k_A and k_R are the transcription rates; K_A and K_R are the degradation rates, $k_0 - k_5$ are the translation rates; p_{in} and p_{out} are transport rates inside and outside the bacteria, respectively; $\hat{t} = t - \tau_p$ and τ_p is the production delay; and $m = TN$ is when the molecular signals are emitted by the transmitter biofilm bacteria or $m = JN$ if the molecular signals are emitted by the engineered bacteria.

In absence of the molecular pulse-based jamming signal, the received signal $s(t)$ can be expressed as

$$s(t) = h_t(t) * (n_t A_{TN,e}(\hat{t})) + n(t) \tag{8}$$

where $n(t)$ is the Additive White Gaussian Noise, t is the time in hours and '$*$' denotes a convolution operation [33].

After reaching the receivers, the molecular pulse-based jamming signal will affect the protein production related to the initial steps of each internal communications processes. To interfere with the legitimate transmission, all engineered bacteria in the jamming node JN will diffuse molecules at the same time towards the receiver biofilm bacteria population. However, there are cases where parts of the bacterial population in JN are synchronised, and others are not, compromising the jamming effectiveness (see Figure 10). We evaluate this scenario by considering that the bacteria population in the jamming node JN can have v partitions with each starting to produce jamming molecules at different time periods. Therefore, these partitions can suffer from

This is the author's version of an article that has been published in this journal. Changes were made to this version by the publisher prior to publication.
The final version of record is available at http://dx.doi.org/10.1109/TNB.2018.2871276

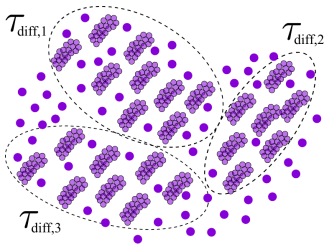

Fig. 10. An illustration of the jamming bacterial population partitions that represent segmented bacterial populations which will diffuse molecules at different time periods. Since in this example $v = 3$, the jamming node JN will have three random $\tau_{d,v}$ values.

different delays in the system and (8) can be represented as

$$s_j(t) = h_t(t) * (n_t[A_{TN,e}(\hat{t})]) + \overbrace{\sum_{i=1}^{v} h_j(t-\tau_{d,v}) * (n_{j,v}[A_{JN,e}(\hat{t})])}^{w(t)} + n(t), \tag{9}$$

where τ_d is the propagation delay for a signal produced by the engineered bacteria in the jamming node JN (in hours), and r_{JN} is the Euclidean distance between the JN and RN populations.

Bacteria diffuse molecules into the environment when signalling between each other [9]. These molecules propagate by Brownian motion and can be represented through Fick's law [34]. The received signal will vary according to time and the distance between the TN-RN and JN-RN populations. The channel for both the transmitter biofilm bacteria and the engineered bacteria can be defined as [35]

$$h_t(t) = \frac{1}{1 + e^{((r_{TN} - vt)/\sqrt{2})}} \tag{10}$$

$$h_j(t-\tau_{d,v}) = \frac{1}{1 + e^{((r_{JN} - v(t-\tau_{d,v}))/\sqrt{2})}} \tag{11}$$

where r_{TN} and r_{JN} are the average Euclidean distances from the centre of the transmitter node TN and jamming node JN to the centre of the receiver node RN and v is the velocity of the wave formed by the molecular pulse-based jamming signal propagation.

To measure the impact of the interference on the legitimate transmission we evaluate the path loss P_L in this system. Using equations (3)-(10), the path loss measured at receiver node RN when there are no engineered bacteria present can be expressed as

TABLE I
PARAMETERS USED FOR THE EVALUATION OF THE EQUATIONS (3)-(13). THE VALUES WERE OBTAINED FROM [32]. THE VALUES FOR β, K, n AND α WERE OBTAINED BY FITTING EQUATION (1) AND (2) TO THE EXPERIMENT RESULTS SHOWED IN FIGURE 3.

Variable	Value	Unit
c_A, c_R	2.7×10^{-2}	nM
k_A, k_R	2×10^{-3}	d^{-1}
k_0	1×10^{-2}	d^{-1}
k_1, k_2, k_4, k_5	0.1	d^{-1}
k_3	1×10^{-2}	d^{-1}
K_A, K_R	2×10^{-3}	gm^{-3}
p_{in}, p_{out}	0.1	d^{-1}
$[A_{TN}]_{initial}$	2	nM
$[R_{TN}]_{initial}$, $[R_{JN}]_{initial}$	0.15	nM
$[RA_{TN}]_{initial}$, $[RA_{JN}]_{initial}$	0	nM
$[C_{TN}]_{initial}$, $[C_{JN}]_{initial}$	0	nM
$[A^e_{TN}]_{initial}$, $[A^e_{JN}]_{initial}$	0.1	nM
β	80000	nM
σ_n^2	1	W
D	4.9	cm^2/h
α	1	–
K	10	–
n	2	–

$$P_L = \frac{P_t}{P_r} = \frac{n_t}{T^2} \int_{t=1}^{T} \frac{|A_{TN,e}(\hat{t})|^2}{|s(t)|^2}, \tag{12}$$

where T is the duration of the transmitted signal. When the engineered bacteria start to produce the molecular pulse-based jamming signal, the path loss P_{LJ} at the receiver for this scenario can be evaluated using equations (3)-(11) and represented as

$$P_{LJ} = \frac{P_{tj}}{P_{rj}} = \frac{2n_t}{T^2} \int_{t=1}^{T} \frac{(|A_{TN,e}(\hat{t})|^2 + |A_{JN,e}(\hat{t})|^2)}{|s_j(t)|^2}. \tag{13}$$

IV. MODEL ANALYSIS

Our interest in this analysis is to obtain the highest attenuation on the legitimate signal by interfering with the communication process leading to the biofilm formation. This will result in an ideal jamming performance. Consequently, more proteins will reach the biofilm receiver bacteria and activate their internal communications channels. This whole cascade will suppress production of biofilm-forming proteins. The parameter values used to evaluate all the equations in this paper are presented in Table I.

This is the author's version of an article that has been published in this journal. Changes were made to this version by the publisher prior to publication.
The final version of record is available at http://dx.doi.org/10.1109/TNB.2018.2871276

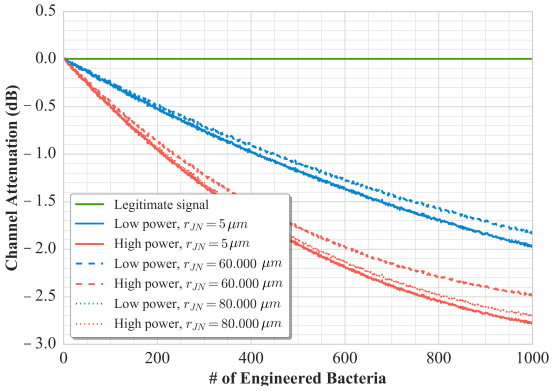

Fig. 11. The path loss in dB for a variable number of engineered bacteria at a fixed distance between JN and RN bacterial populations ($r_{JN} = 5\,\mu$m, $60,000\,\mu$m and $80,000\,\mu$m). There is also no delay associated to both the production and transmission for the legitimate and molecular pulse-based jamming signals, $\tau_d = \tau_p = 0$.

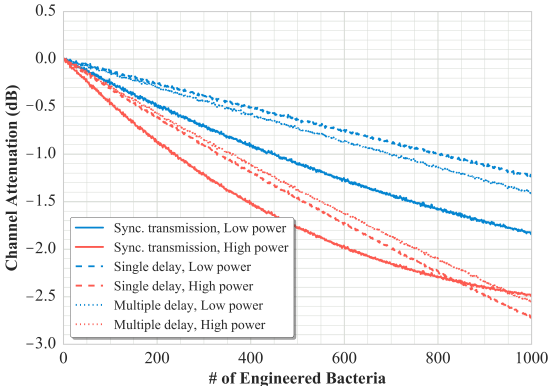

Fig. 12. The channel attenuation when the production of the molecular pulse-based jamming signal is delayed. In this case, the interfering channel has a single propagation delay (for a single partition) and multiple delays (for multiple partitions). We also consider a variable number of engineered bacteria at a fixed distance to the receiver node RN.

A. *Path Loss Analysis*

In this section, we analyse the impact of the molecular pulse-based jamming signals from the engineered bacteria on the TN channel. We analysed equations (12)-(13) by varying the number of engineered bacteria in the jamming node (n_j ranging from 1 to 1000), where each JN bacterium could produce two distinct jamming signals ($[A_{JN}]_{initial} = 0.2$ nM and $[A_{JN}]_{initial} = 1$ nM). We considered that the engineered bacteria population in the jamming node is composed by one single partition ($v = 1$), there is no delay for the production and propagation for the legitimate and interfering signals ($\tau_d = \tau_p = 0$), three different JN-RN distances ($5\,\mu$m, $60.000\,\mu$m and $80.000\,\mu$m), both the legitimate and molecular pulse-based jamming signals were produced within 16 hours and the noise power was considered as $\sigma_n^2 = 1$.

It can be observed from Figure 11 that the attenuation increases proportionally with the number of engineered bacteria. The power of a molecular pulse-based jamming signal also affect the path loss for this system. A greater attenuation is produced by the higher power molecular signal when compared with the lower power. Despite the variations caused by the power of the molecular pulse-based jamming signal, the noise does not produce a strong effect on the path loss and this is due to the low power level ($P_n = 1W$). Figure 11 shows that the path loss can also vary according to the average distance between the engineered and biofilm receiver bacteria r_{JN}. However, small variations in the average distance r_{JN} do not produce noticeable attenuation values. For this particular scenario, within the considered observation time, most of the protein concentration diffused by the engineered bacteria is able to reach the biofilm bacteria receiver. Therefore, they almost do not differ from the case when $r_{JN} = 5\,\mu m$. From this result, we can see that both the average distance r_{JN} and the power of the molecular pulse-based jamming signal are important parameters to ensure a higher interference requirement on the bacterial internal communications channels.

Next, we analyse the impact of both the production and propagation delays in the path loss. We consider an average JN-RN distance ($r_{JN} = 60.000\,\mu$m) and vary the number of engineered bacteria during an observation window of 16 hours. In this case, the propagation delay $\tau_{d,v}$ is produced by the diffusive medium for each partition. Without loss of generality, we considered the propagation delay $\tau_{d,v}$ is random and range from 0 to 4 hours. In Figure 12, we can observe the comparison between the synchronised transmission scenario and when the single and multiple partitions are subjected to random propagation delay values ($\tau_{d,1} = 3.53$ hours, $\tau_{d,2} = 3.94$ hours, $\tau_{d,3} = 1.63$ hours, $\tau_{d,4} = 0.20$ hours). For the single and multiple partitions curves presented in Figure 12 the *quorum sensing* production is delayed by $\tau_p = 3$hours.

The single partition case ($\tau_{d,1} = 3.53$ hours), with a low molecular pulse-based jamming signal power, results in a lower path loss, when compared to all other cases. On the other hand, for a high molecular pulse-based jamming signal power, the same single partition produces

This is the author's version of an article that has been published in this journal. Changes were made to this version by the publisher prior to publication.
The final version of record is available at http://dx.doi.org/10.1109/TNB.2018.2871276

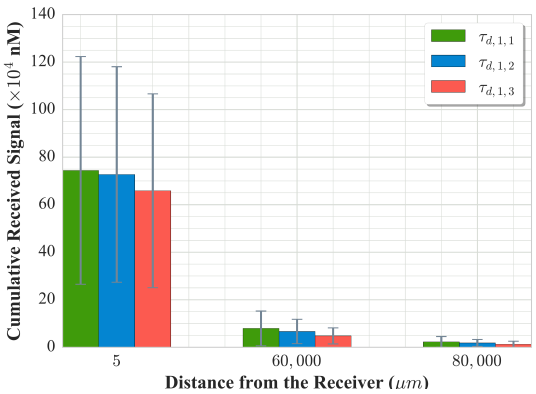

Fig. 13. The effect of the propagation delay $\tau_{d,v}$ on the path loss for a single partition transmission ($\tau_p = 3$ hours). We also considered a fixed number of engineered bacteria ($n_j = 200$) and three different distances to the receiver node values.

a higher path loss. When subjecting this communication system to multiple delays, the path loss is similar to the single partition case, for both low and high power interfering with molecular signals. The worst path loss occurs when the system is affected by a synchronised molecular pulse-based jamming signal. However, is important to note that is possible to achieve a worse path loss scenario if using a higher number of engineered bacteria ($n_j \geq 800$) and a high power molecular pulse-based jamming signal. These results show that the molecular pulse-based jamming signal power can compensate the effects of a single or small delays. They also highlight the importance of using synchronised transmissions to obtain a higher interference.

For the last analysis of this communication system path loss, the following conditions are considered: three r_{JN} average distances were considered ($5\,\mu$m, $60,000\,\mu$m, $80,000\,\mu$m) and a single partition composed by $n_j = 200$ engineered bacteria producing a delayed low power molecular pulse-based jamming signal ($\tau_p = 3$ hours) which is subjected to three propagation delays ($\tau_{d,1,1} = 2.28$ hours, $\tau_{d,1,2} = 2.50$ hours and $\tau_{d,1,1} = 3.16$ hours). Figure 13 shows that when subjected to the lower propagation delay $\tau_{d,1,1}$, more molecular pulse-based jamming signal is able to reach the receiver. The opposite effect occurs for the higher propagation delay value $\tau_{d,1,3}$. It also can be seen in Figure 13 that these results are independent of the distance from the receiver r_{JN}, despite affecting on the total amount of received molecular pulse-based jamming signal. For example, there is a reduction of more than 90% when comparing the shortest and the longest distances (r_{JN}) considered in this analysis.

Figures 11-13 also shows that both the propagation delay and the average distance between the engineered bacteria and the biofilm bacteria receiver are important factors for the design of this communication system. The highest path loss value is achieved for the case of synchronised molecular pulse-based jamming signals, which means that a lower concentration of protein is able to reach the RN bacterial population and activate the defence, stress and energy communications channels. Consequently, to ensure the high interference needed to suppress the biofilm formation, a shorter r_{JN} distance and a lower propagation delay, either for single or multiple sources of interference, are fundamental.

B. Toggle Switch Activation Analysis

In this section, we analyse the toggle switch activation performance based on the results presented in Section IV-A. To activate a toggle switch, a certain amount of molecular pulse-based jamming signal is required to reach the RN bacterial population and induce the production of the biofilm suppression proteins (as described in Section II, each internal communication channel has a target protein to be induced). Since the total amount of received molecular pulse-based jamming signal is important to trigger the switches, we conducted two analyses. In all cases, the number of engineered jamming bacteria and the number of receiver biofilm bacteria are fixed ($n_j = 1000$ and $n_r = 1000$, respectively).

First, we evaluate the amount of pulse-based jamming signal molecules that reach the receiver node within 16 hours. In this case, we assume a fixed distance between the engineered bacteria and the receiver nodes (r_{JN}), synchronised transmission, a single partition subjected to propagation delay $\tau_{d,1} = 0.33$ hours, and multiple partitions subjected to propagation delay $\tau_{d,1} = 0.33$ hours, $\tau_{d,2} = 3.29$ hours, $\tau_{d,3} = 0.23$ hours and $\tau_{d,4} = 0.51$ hours. As seen in Figure 14, the synchronised transmission is the most efficient in reaching the toggle switch threshold (around 8.5hours). However, this result is not so different when compared with the time taken by both the single and multiple partitions (around 8.7hours and 9hours, respectively). We emphasise that the results shown in Figure 14 are dependent on the propagation delay values. It is possible that a single partition reaches the toggle switch threshold later when compared to the multiple partition. However, this is not very likely to occur.

The cumulative molecular pulse-based jamming signal reception for a synchronised and delayed transmission is plotted against the toggle switch activation threshold.

This is the author's version of an article that has been published in this journal. Changes were made to this version by the publisher prior to publication.
The final version of record is available at http://dx.doi.org/10.1109/TNB.2018.2871276

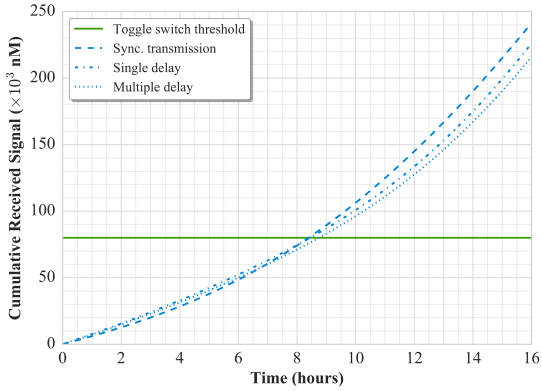

Fig. 14. The cumulative molecular pulse-based jamming signal reception for a synchronised and delayed transmission is plotted against the toggle switch activation threshold.

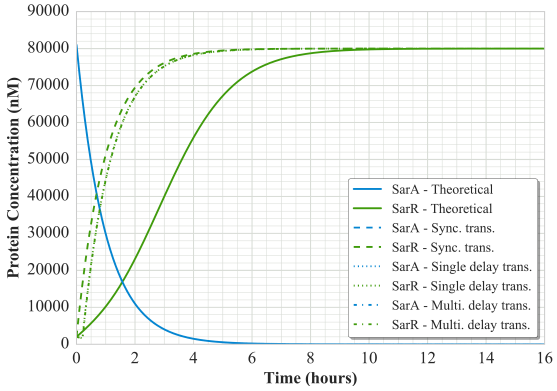

Fig. 15. Toggle switch activation of the cellular stress channel for three different scenarios. For each scenario, a few parameters were modified to observe the different toggle switch behaviours. The parameters used to evaluate these plots are presented in Table I.

Second, we evaluate how fast the received molecular pulse-based jamming signal induces the production of biofilm suppressors. In the previous analysis, we identified that both the production and propagation delays have an impact on the amount of pulse-based jamming signal molecules that reach the receiver node. Furthermore, for both the synchronised and the single partition transmissions, more pulse-based jamming signal molecules were able to reach the toggle switches activation threshold. Therefore, to perform this second analysis, using the same parameter values of Figure 14, we fit the received protein concentration of the previous analysis as two quadratic functions (for the single partition as well as for the multiple partition scenarios) and use it to induce the toggle switches. The other parameters needed to evaluate Equations (1) and (2) are obtained from the experimental data presented in Figure 3, including the starting values for X and Y (81 nM and 2 nM, respectively). For this analysis, we define the activation time as the period taken by the suppressor concentration to become higher than the biofilm formation protein. Figure 15 shows the theoretical curve obtained for the cellular stress communications channel considering a fixed inducer concentration and plotted against the synchronised and delayed molecular pulse-based jamming signal transmissions. There is almost no difference between single and multiple delay transmission activation time. Therefore, in Figure 15 we are only able to compare the theoretical curve with the synchronised and delayed transmissions. As seen in Figure 15 the theoretical activation of the toggle switch occurs around 1.5 hours and takes more than 6 hours for the suppressor signal to reach its maximum value (this is the green solid curve). The fastest toggle switch activation occurs when the molecular pulse-based jamming signal is transmitted without delays. However, the difference between the synchronised and delayed cases is small, where the delayed transmission activates 12 minutes later compared to the case of the synchronised transmission. Additionally, the reducing of the biofilm formation proteins takes the same amount of time in all cases observed. This result suggests that despite the delays can disrupt the communication process related to the biofilm formation, it is not strong enough to affect the activation of the toggle switches and, consequently, it demonstrates the robustness of the proposed molecular pulse-based jamming system. Please note that we only analyse the toggle activation for the cellular defence channel as other two bacterial internal communications channels, namely energy and defence channels, produced similar results to the ones shown in Figure 15.

V. CONCLUSION

Biofilms are responsible for a number of chronic infections, and numerous solutions are continuously being researched to curb their formation. Since this system involves a multi-stage communication process between the bacteria, we show that biofilm formation can be disrupted by applying a molecular pulse-based jamming signal. Based on wet lab experiments, we were able to identify three internal communication channels that lead to the biofilm formation. For each of them, we identified key proteins that need to be targeted for the jamming process. We show that the molecular pulse-based jamming signal degrades the biofilm bacteria

This is the author's version of an article that has been published in this journal. Changes were made to this version by the publisher prior to publication.
The final version of record is available at http://dx.doi.org/10.1109/TNB.2018.2871276

communication to a level that is sufficient to interfere with the biofilm-related protein production, represented by emulated toggle switches. This paper presented an analysis for a number of parameters that include the difference in population between the jamming as well as biofilm-forming bacteria, the distances between these populations and the power of the molecular pulse-based jamming signal from the engineered bacteria. We also analysed the impact caused by the different number of partitions and their respective production and propagation delays on the amount of pulse-based jamming signal molecules arriving at the receiver node RN. Our results suggest that the average distances between the jamming and receiver nodes, as well as the delays that the molecular pulse-based jamming signal is subjected to, have a high impact on the communications process that leads to the biofilm formation. The obtained results lay the foundation for key design parameters that are needed to ensure a fully operational bacteria-based molecular communications jamming system, and this includes: engineering the JN bacterial population and placing them at a strategic distance to the biofilm-forming bacteria, ensuring synchronisation between the jamming signal transmission and molecular signalling between the TN and RN bacterial populations, and synchronising the engineered jamming bacterial population molecular signal production to ensure that sufficient concentration is produced without stressing the engineered bacteria.

ACKNOWLEDGMENT

This work was partially funded by 1) Science Foundation Ireland via the CONNECT research centre (grant no. 13/RC/2077), 2) Irish Research Council under the government of Ireland post-doc fellowship (grant GOIPD/2016/650) and 3) Academy of Finland Research Fellow (grant no. 284531).

REFERENCES

[1] T. Nakano *et al.*,"Molecular Communication Among Biological Nanomachines: A Layered Architecture and Research Issues",*IEEE Transactions on NanoBioscience*, vol. 13, no. 3, pp. 169–197, Sep. 2014.

[2] T. Furubayashi *et al.*,"Design and wet-laboratory implementation of reliable end-to-end molecular communication", *Wireless Networks*, vol. 24, no. 5, pp. 1809–1819, July 2018.

[3] O. B. Akan *et al.*, "Fundamentals of Molecular Information and Communication Science," *Proceedings of the IEEE*, vol. 105, no. 2, pp. 306–318, Feb. 2017.

[4] M. Pierobon and I. F. Akyildiz, "A Physical End-to-End Model for Molecular Communication in Nanonetworks," *IEEE Journal on Selected Areas in Communications*, vol. 28, no. 4, pp. 602–611, Apr. 2010.

[5] L. C. Cobo and I. F. Akyildiz, "Bacteria-based communication in nanonetworks," *Nano Communication Networks*, vol. 1, no. 4, pp. 244–256, Dec. 2010.

[6] S. Balasubramaniam and P. Lio', "Multi-Hop Conjugation Based Bacteria Nanonetworks," *IEEE Transactions on NanoBioscience*, vol. 12, no. 1, pp. 47–59, Mar. 2013.

[7] T. Nakano *et al.*,"Molecular Communication and Networking: Opportunities and Challenges", *IEEE Transactions on NanoBioscience*, vol. 11, no. 2, pp. 135–148, June 2012.

[8] I. F. Akyildiz, F. Brunetti, and C. Blázquez, "Nanonetworks: A new communication paradigm," *Computer Networks*, vol. 52, no. 12, pp. 2260–2279, Aug. 2008.

[9] M. E. Taga and B. L. Bassler, "Chemical communication among bacteria," *Proceedings of the National Academy of Sciences*, vol. 100, no. Supplement 2, pp. 14 549–14 554, Nov. 2003.

[10] K. O'Riordan and J. C. Lee, "Staphylococcus aureus Capsular Polysaccharides," *Clinical Microbiology Reviews*, vol. 17, no. 1, pp. 218–234, Jan. 2004.

[11] A. K. Bhardwaj and K. Vinothkumar, "Evolution of MDRs," in *Quorum Sensing vs Quorum Quenching: A Battle with No End in Sight*, V. C. Kalia, Ed. New Delhi: Springer India, 2015, p. 9.

[12] J. C. Heaton and K. Jones, "Microbial contamination of fruit and vegetables and the behaviour of enteropathogens in the phyllosphere: A review," *Journal of Applied Microbiology*, vol. 104, no. 3, pp. 613–626, Mar. 2008.

[13] B. Kilb *et al.*, "Contamination of drinking water by coliforms from biofilms grown on rubber-coated valves," *International journal of hygiene and environmental health*, vol. 206, no. 6, pp. 563–573, Oct. 2003.

[14] K. Shimizu, "Regulation Systems of Bacteria such as Escherichia coli in Response to Nutrient Limitation and Environmental Stresses," *Metabolites*, vol. 4, no. 1, pp. 1–35, Dec. 2013.

[15] R. Chug, B. Khosla, and M. Singh, "Modulation of the Extracellular Polymeric Substances (EPS) Production by Quorum Sensing (QS) in Bacteria," *Int. J. Curr. Microbiol. App. Sci*, vol. 4, no. 6, pp. 884–896, June 2015.

[16] C. Chang *et al.*, "Non-antibiotic quorum sensing inhibitors acting against N-acyl homoserine lactone synthase as druggable target", *Scientific Reports*, vol. 4, no. 7245, Nov. 2014.

[17] G. Wei *et al.*, "In Silico Evaluation of the Impacts of Quorum Sensing Inhibition (QSI) on Strain Competition and Development of QSI Resistance", *Scientific Reports*, vol. 6, no. 35136, Oct. 2016

[18] D. P. Martins, M. T. Barros, and S. Balasubramaniam, "Using Competing Bacterial Communication to Disassemble Biofilms," in *Proceedings of the 3rd ACM International Conference on Nanoscale Computing and Communication - NANOCOM'16*. New York, New York, USA: ACM Press, Sep. 2016, pp. 1–6.

[19] E. Karatan and P. Watnick, "Signals, Regulatory Networks, and Materials That Build and Break Bacterial Biofilms," *Microbiology and Molecular Biology Reviews*, vol. 73, no. 2, pp. 310–347, June 2009.

[20] G. Wei and R. Marculescu, "Don't Let History Repeat Itself: Optimal Multidrug Quorum Quenching of Pathogens Network," in *Proceedings of the First ACM International Conference on Nanoscale Computing and Communication - NANOCOM'14*. Atlanta, Georgia, USA: ACM Press, May 2014, p. 20.

[21] M. Pierobon and I. F. Akyildiz, "A Statistical-Physical Model of Interference in Diffusion-Based Molecular Nanonetworks," *IEEE Transactions on Communications*, vol. 62, no. 6, pp. 2085–2095, June 2014.

[22] Y. G. Y. Chan *et al.*, "The capsular polysaccharide of Staphylococcus aureus is attached to peptidoglycan by the LytR-CpsA-Psr (LCP) family of enzymes," *Journal of Biological Chemistry*, vol. 289, no. 22, pp. 15 680–15 690, May 2014.

[23] S. Herbert *et al.*, "Regulation of Staphylococcus aureus Type 5 and Type 8 Capsular Polysaccharides by CO2," *Journal of Bacteriology*, vol. 183, no. 15, pp. 4609–4613, Aug. 2001.

This is the author's version of an article that has been published in this journal. Changes were made to this version by the publisher prior to publication.
The final version of record is available at http://dx.doi.org/10.1109/TNB.2018.2871276

[24] L. Zhao *et al.*, "Staphylococcus aureus AI-2 quorum sensing associates with the KdpDE two-component system to regulate capsular polysaccharide synthesis and virulence," *Infection and immunity*, vol. 78, no. 8, pp. 3506–3515, Aug. 2010.
[25] C. R. Arciola *et al.*, "Polysaccharide intercellular adhesin in biofilm: structural and regulatory aspects," *Frontiers in cellular and infection microbiology*, vol. 5, p. 7, Feb. 2015.
[26] Y. Wu *et al.*, "Staphylococcus epidermidis SrrAB regulates bacterial growth and biofilm formation differently under oxic and microaerobic conditions," *Journal of Bacteriology*, vol. 197, no. 3, pp. 459–476, Feb. 2015.
[27] A. A. Pragman, Y. Ji, and P. M. Schlievert, "Repression of Staphylococcus aureus SrrAB using inducible antisense srrA alters growth and virulence factor transcript levels," *Biochemistry*, vol. 46, no. 1, pp. 314–321, Dec. 2007.
[28] J. C. Anderson, C. A. Voigt, and A. P. Arkin, "Environmental signal integration by a modular AND gate," *Molecular Systems Biology*, vol. 3, no. 133, Aug. 2007.
[29] K. Leetanasaksakul and A. Thamchaipenet, "Potential anti-biofilm producing marine actinomycetes isolated from sea sediments in Thailand," *Agriculture and Natural Resources*, vol. 52, no. 3, in-press, 2018.
[30] Y. Liu *et al.*, "Crystal structure of the SarR protein from Staphylococcus aureus," *Proceedings of the National Academy of Sciences of the United States of America*, vol. 98, no. 12, pp. 6877–82, June 2001.
[31] J. J. Collins, T. S. Gardner, and C. R. Cantor, "Construction of a genetic toggle switch in Escherichia coli," *Nature*, vol. 403, no. 6767, pp. 339–342, Jan. 2000.
[32] P. Melke *et al.*, "A cell-based model for quorum sensing in heterogeneous bacterial colonies," *PLoS Computational Biology*, vol. 6, no. 6, pp. 1–13, June 2010.
[33] C. D. Cox *et al.*, "Analysis of noise in quorum sensing," *Omics: a journal of integrative biology*, vol. 7, no. 3, pp. 317–34, Sep. 2003.
[34] I. Llatser *et al.*, "Detection techniques for diffusion-based molecular communication," *IEEE Journal on Selected Areas in Communications*, vol. 31, no. 12, pp. 726–734, Dec. 2013.
[35] L. Rongy and A. De Wit, "Steady Marangoni flow traveling with chemical fronts," *The Journal of Chemical Physics*, vol. 124, no. 16, Apr. 2006.

CHAPTER 8

JOURNAL PAPER: COMPUTATIONAL MODELS FOR TRAPPING EBOLA VIRUS USING ENGINEERED BACTERIA

Journal Title:	IEEE/ACM Transactions on Computational Biology and Bioinformatics
Article Type:	Regular Paper
Complete Author List:	Daniel Perez Martins, Michael Taynnan Barros, Massimiliano Pierobon, Meenkashisundaram Kandhvelu, Pietro Liò, Sasitharan Balasubramaniam
Keywords:	Ebola virus, Genetically engineered bacteria,Microfluidic viral attenuator.
Status:	Published: v. 15, no. 6, p. 2017-2027, November 2018. doi: 10.1109/TCBB.2018.2836430

This is the author's version of an article that has been published in this journal. Changes were made to this version by the publisher prior to publication.
The final version of record is available at http://dx.doi.org/10.1109/TCBB.2018.2836430

Computational Models for Trapping Ebola Virus Using Engineered Bacteria

Daniel P. Martins, *Student Member, IEEE*, Michael Taynnan Barros, *Member, IEEE*, Massimiliano Pierobon, *Member, IEEE*, Meenakshisundaram Kandhavelu, Pietro Lio', Sasitharan Balasubramaniam, *Senior Member, IEEE*

***Abstract*—The outbreak of Ebola virus in recent years has resulted in numerous research initiatives to seek new solutions to contain the virus. A number of approaches that have been investigated include new vaccines to boost the immune system. An alternative post-exposure treatment is presented in this paper. The proposed approach for clearing Ebola virus can be developed through a microfluidic attenuator, which contains the engineered bacteria that traps Ebola flowing through the blood onto its membrane. The paper presents the analysis of the chemical binding force between the virus and a genetically engineered bacterium considering the opposing forces acting on the attachment point, including hydrodynamic tension and drag force. To test the efficacy of the technique, simulations of bacterial motility within a confined area to trap the virus were performed. More than 60% of the displaced virus could be collected within 15 minutes. While the proposed approach currently focuses on *in vitro* environments for trapping the virus, the system can be further developed into the future for treatment whereby blood can be cycled out of the body into a microfluidic device that contains the engineered bacteria to trap viruses.**

***Index Terms*—Ebola virus, Genetically engineered bacteria, Microfluidic viral attenuator.**

I. INTRODUCTION

The recent outbreak of Ebola virus has resulted in concerns by the research community to develop new solutions that can curb and control their spreading process [1]. While the majority of Ebola virus outbreaks are currently found in Africa, their rate of spreading requires immediate attention. The spreading process of Ebola virus is through the exchange of fluids between individuals, animals, as well as within the environment where the virus lies. The poor sanitary conditions in the developing countries also fuel the spreading process, which has detrimental effects on lives and on the socio-economical stability of the affected regions.

Currently, there are preventive and post-exposure treatments available [2] [3]. Two vaccines were developed and are still being tested in Guinea: one developed by Merck Sharp and Dohme and another by Toyama Chemical [4], [5]. Other advanced research for solutions to the Ebola virus disease problem is in the domain of molecular biology and biotechnology [6]. Based on this, a number of therapeutic medications to treat Ebola virus disease has been developed and tested, and this includes TKM-Ebola, amiodarone, dronedarone, verapamil and ZMapp [3], [7], [8]. ZMapp is a cocktail of three monoclonal antibodies produced from Tobacco plants (*Nicotiana benthamiana* species) and provides immunity to the Ebola virus. Successful tests were made on mice and non-human primates [8], [9]. Also, monoclonal antibodies derived from a person who survived Ebola virus disease protected non-human primates when given as late as 5 days after the infection [10], [11]. Other treatments that have compounds capable of blocking Ebola virus-like particles from entry into the cells and a novel peptide vaccine have also been proposed to increase the range of available treatments [12], [13]. While the effectiveness of those vaccines in particular for large scale population is still under investigation, another outbreak can occur. Therefore, we propose an alternative post-exposure treatment using synthetic biology to engineer bacteria that can trap the virus, and utilize this solution through a microfluidic attenuator.

The field of *synthetic biology* has received tremendous attention in recent years, due largely to the potential impact of delivering new solutions for biotechnology [6], [14]. Synthetic biology enables genetic circuits to be designed and inserted into cells in order to create new properties as well as functionalities. For example the field of *molecular communication* [15], [16] aims to construct bio-compatible communication systems based on programming of cells. Engineered bacteria through synthetic biology have also been used as therapeutic agents in the past [17]. For example, HIV-1 infection in CD4+ T cells and macrophages were inhibited using *Lactobacillus jensenii* bacteria [17]. Bacteria have also been used to hunt down and eradicate human lymphomas [18].

In this paper, we propose synthetically engineered bacteria (*Escherichia coli*) that moves and traps Ebola virus in a sponge-like manner [19]. While our theoretical models and analysis presented in this paper are based on *in vitro* environments, the proposed approach has the potential to be used

Daniel P. Martins, Michael T. Barros and Sasitharan Balasubramaniam are with the Telecommunication Software & Systems Group (TSSG), Waterford Institute of Technology (WIT), Ireland.

Sasitharan Balasubramaniam is with the Nano Communications Center (NCC), Department of Electronics and Communication Engineering at Tampere University of Technology (TUT), Finland and Meenakshisundaram Kandhavelu is with the Department of Signal Processing, Tampere University of Technology.

Massimiliano Pierobon is with the Department of Computer Science and Engineering, University of Nebraska-Lincoln, Lincoln.

Pietro Lio' is with the Computer Laboratory, University of Cambridge.

E-mail: dpmartins@tssg.org, mbarros@tssg.org, sasi.bala@tut.fi, maxp@unl.edu, meenakshisundaram.kandhavelu@tut.fi, pl219@cam.ac.uk.

This work was supported by the CIRCLE Project (grant no. 665564) and partially funded by 1) Science Foundation Ireland via the CONNECT research centre (grant no. 13/RC/2077), 2) via the FiDiPro program of Academy of Finland (Nano communication Networks), 2012-2016, 3) Academy of Finland Research Fellow grant, and 4) the US National Science Foundation through grant MCB-1449014.

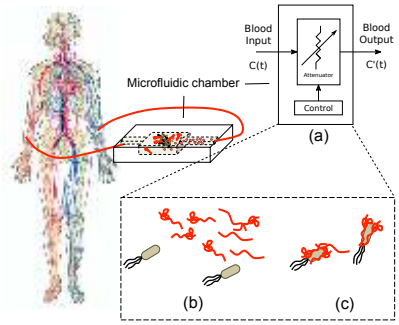

Fig. 1: Illustration of the proposed approach, where blood containing Ebola is passed through an external tube with a microfluidic chamber containing genetically engineered bacteria that are used to trap the Ebola virus, (a) the microfluidic chamber is represented as an attenuator (b) bacteria moves towards the Ebola virus scattered in the chamber, (c) bacteria after trapping the virus once they have bind to their surface membrane.

for treatments in the future as illustrated in Figure 1. The blood contaminated with Ebola virus are transported through a cyclic external tube that goes through a microfluidic attenuator, and back into the body again. Within the chamber are the engineered bacteria that will colide and trap the Ebola through the protein binding process on the surface membrane, resulting in the virus attachment. The proposed system can be described as

$$C'(t) = f_b(t)C, \tag{1}$$

where $C'(t)$ is the Ebola concentration in out-going blood flow, C is the incoming concentration of Ebola virus in the blood stream and $f_b(t)$ is the attenuation function described by the bacterial trapping performance.

The process of virus trapping has been investigated previously. For example, in [19] the red blood cells are used to trap viruses. The red blood cells are ideal for virus trapping due to the fact that they lose their DNA when grown in the bone marrow. Therefore, when the virus infects the red blood cell, it will have no capability of replicating itself due to the missing DNA, and hence, leading to a trapping process. Another example is in [20], where the authors specifically studied the *Phi-6* virus which typically invades *Pseudomonas phaseolica* cell. This particular bacterium attaches itself to the plants by using its hair like structure that extends from their body. The attachment is achieved when the bacteria contracts its body enabling the thick hair to grip onto the surface of the plant. This contracting process will also lead to the virus being able to infect the bacteria. In order to trap the virus, the authors engineered the bacteria to have excessive amount of hair on the surface leading to minimal amount of space to allow the virus to penetrate through the membrane but enough to embed and get stuck on the microbes [20].

The most common mechanism for virus binding on the cell's surface is through the polyvalent interactions between the proteins and the cell's receptors [21]. This process is similar to what we are proposing in this paper. However, there are a number of challenges to be addressed. First, compatible binding process is required between the virus and the bacterium. The compatible receptors on the bacteria can be

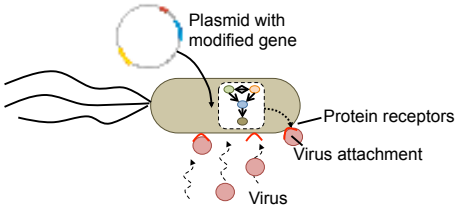

Fig. 2: Genetically engineered bacteria will produce proteins on the surface that will allow the virus to bind.

engineered through synthetic biology as illustrated in Figure 2, where genes that are inserted into the plasmid can lead to expression of proteins on the surface. Second, Ebola virus has a long filamentous structure unlike other types of virus, and usually with a higher molecular weight. Therefore, the binding process may not cover the entire length of the virus, leading to parts of the virus hanging from the bacterium after binding. This means that the binding process must be strong enough to support the momentum of the hanging virus body, and in particular when faced with hydrodynamic tension and drag.

The contributions of this paper include:

- **Design of Ebola virus microfluidic attenuator system**: a cleaning process is proposed, where the bacteria are used to collect and trap the Ebola virus. This trapping process will minimize the virus concentration in blood to curb them from replicating and spreading.
- **Binding force model:** Developed a protein binding force model to trap Ebola virus in free moving bacteria, considering their swimming and tumbling process, as well as opposing forces resulting from the hydrodynamic tension and drag and the weight of the hanging body of the virus.
- **Simulation evaluation:** Simulations of bacteria motility process are conducted to evaluate the effectiveness of trapping an Ebola virus population in a confined area.

The paper is organized as follows. Section II describes the physical properties of Ebola virus. The engineering of proteins on the bacteria surface to bind to the virus is presented in Section III. Section IV describes the binding force models between the bacteria and the virus. The simulation evaluation and results are presented and discussed in Section V. Lastly, Section VI presents the conclusion.

II. BACKGROUND ON EBOLA VIRUS

Ebola virus belongs to the order *Mononegavirales* and the *Filoviridae* family. Upon infection, it can kill up to 50% of the patients within 6 to 16 days [22]. The virus has a filamentous shape, with a uniform width of nearly 80 nm and a length of approximately 970 nm, and its structure is illustrated in Fig. 3. As illustrated in Fig. 3, virus membrane consists of $GP_{1,2}$ (spike glycoprotein) and two other proteins, VP40 and VP24 (primary and secondary matrix proteins). $GP_{1,2}$ is a membrane-spanning protein, and VP40 and VP24 builds the inner matrix [23], [24]. The glycoprotein are 7 nm in diameter and have a spacing of 10 nm between each other. The glycoprotein enables the Ebola virus to bind and

This is the author's version of an article that has been published in this journal. Changes were made to this version by the publisher prior to publication.
The final version of record is available at http://dx.doi.org/10.1109/TCBB.2018.2836430

submerge itself into the host cells (process required for viral internalization) [23].

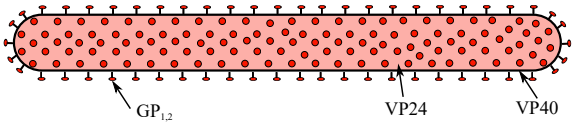

Fig. 3: Structure of an Ebola virus, including the membrane-spanning protein ($GP_{1,2}$) and the proteins that build the inner matrix (VP40 and VP24).

There are three infection routes for the Ebola virus: through mucosal surfaces (mouth, eyes, genitalia), skin abrasions or through the use of contaminated needles [24]. After the virus enters the body, it spreads rapidly [24]–[27], and is capable of overcoming responses from the immune system. The high rate of virus replication inside the immune system cells hinders the human body defenses [25]–[27]. Monocytes, macrophages and dendritic cells are the front door for the Ebola virus infection and preferred sites of replication [26]. In addition, these cells are used as vehicles to spread the Ebola virus through the lymphatic system [24]. Infected monocytes and macrophages secrete soluble factors to recruit other similar cells inside the lymph nodes to increase the infection. In latter stages, hepatocytes and adrenal cortical cells are infected and the production of coagulation factors is decreased which results in internal bleeding [28].

III. ENGINEERING PROTEIN BINDING

A. Synthetic Protein Binding Receptors

The main challenge of lowering the concentration of the Ebola virus using bacteria lies in using synthetic biology to produce the required proteins on the surface membrane to bind the virus. In particular, careful understanding of viral entry and replication mechanisms into the host system is required before suitable genetic circuits can be developed. Past research have used dual color synthetic constructs to observe how a single virus affects the host bacterium and determine the level of infection [29]. Single-virus tracking methods have also been developed to observe the mode of interaction between *E. coli* and bacteriophage lambda [29]. In our proposed model, it is possible to construct a synthetic gene that could increase the expression of Ebola virus protein binding receptors. Facilitating the binding frequency between the viral proteins and over expressed membrane receptor proteins would be an advantage to harvest the target virus. Specifically, reports have suggested that the cell surface receptor *T-cell Immunoglobulin Mucin domain 1* (*TIM-1*) of epithelial cells favourably increases the binding of Ebola virus. A study on over expression of fluorescent tagged *TIM-3* protein in *E. coli* also confirms that TIM-like protein can have a functional property which allows viral protein recognition and binding [30]. Therefore, the TIM-like protein could be one of the possible targets to be expressed in *E. coli* to create engineered bacteria to trap the Ebola virus. Engineering the synthetic circuit of *EnvZ*/*OmpR*/*BolA* genes along with the TIM-like protein-coding genes will facilitate the binding of Ebola virus and simultaneously control the motility of *E.coli* during the binding and trapping of Ebola virus (*EnvZ* is the sensor-transmitter kinase that phosphorylates *OmpR*, a DNA-binding regulatory protein, under stress conditions) [31], [32]. Another requirement is the engineering of the bacteria to prevent the virus entry, and this could be achieved by considering the use of mutant *E.coli* as a host that carries membrane proteins (e.g., Porins) [33], [34].

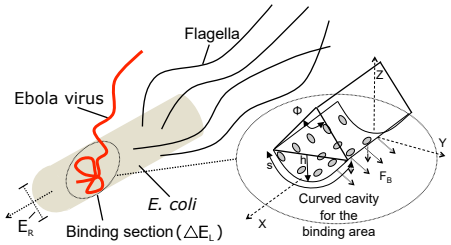

Fig. 4: Expanded view of the partial deformation on the bacterium's surface membrane when the virus binds on its surface.

B. Protein Binding Model

Our model is developed as a function of the binding among bacterial receptors and the viral glycoproteins. We analyse the produced binding force, and how it will counter the opposing forces (due to drag and weight of the virus) that can result in the attachment breakage. During the binding process, the virus deforms the bacterium's surface creating a curved cavity with a submergence angle ϕ (in radians) as shown in Fig. 4 [35]. The cavity segment consist of height h and arc length s. The attachment area B_{Area} between the virus and the bacterium can be evaluated as:

$$\begin{aligned} B_{Area} &= s\Delta E_L \\ &= \phi E_R \Delta E_L \end{aligned}$$

where E_R is the Ebola virus radius and ΔE_L is the length of Ebola virus that attaches to the bacterium. Therefore, the reaction between the bacterial receptors and virus proteins within B_{Area} can be represented as [35]:

$$\mathrm{n[V] + m[B] \overset{K_a}{\rightleftharpoons} [B_m V_n]}, \tag{2}$$

where n is the number of viral proteins that binds to a single bacterial receptor; m is the number of bacterial receptors that binds to a single viral protein; $[\mathrm{V}]$ and $[\mathrm{B}]$ are the concentrations of viral proteins and bacterial receptors, respectively; and K_a is the association binding constant for the reaction. The initial values for the viral and bacterial proteins ($[\mathrm{V_0}]$ and $[\mathrm{B_0}]$) are the ratio between the minimum attachment area and the area occupied by the Ebola glycoprotein and TIM-1, respectively. Therefore, the fraction of the bacterial receptors that are bound by the viral proteins can be defined as p [36]:

$$p = \frac{[\mathrm{B_m V_n}]}{[\mathrm{V}] + [\mathrm{B_m V_n}]}. \tag{3}$$

The total binding energy resulting from the complex formation of the Ebola virus glycoprotein and the bacterium receptors is represented as [37]:

This is the author's version of an article that has been published in this journal. Changes were made to this version by the publisher prior to publication.
The final version of record is available at http://dx.doi.org/10.1109/TCBB.2018.2836430

$$E_{Total} = (E_{Bind} + (p-1)T_a S_0)B_{Area}, \quad (4)$$

where T_a is the absolute temperature; S_0 is the translational and rotational entropy of binding for this complex. The affinity binding energy E_{Bind} can be evaluated as follows:

$$E_{Bind} = -pk_B T_a \ln K_a \quad (5)$$

where k_B is the Boltzmann constant. Based on the E_{Bind}, the binding force F_{Bind} for this process is represented as:

$$F_{Bind} = -\frac{\partial E_{Total}}{\partial \phi}. \quad (6)$$

Since each virus will occupy a small area of the bacterium, the surface area can accommodate a number of Ebola virus. The limit for the number of virus that can bind to each bacterium b_{limit} can be represented as:

$$b_{limit} = bac_{Area} - \sum_{i=0} B^i_{Area} \quad (7)$$

where bac_{Area} is the bacterium surface area and $i = 0, 1, 2, ...$ is the number of attached virus.

IV. FORCE MODEL FOR VIRUS DETACHMENT

In general, to achieve the stability of attachment, the binding force will highly depend on the opposing forces that include hydrodynamic drag force as well as the tensions exerted on the Ebola virus. The equilibrium will depend on B_{Area} and the motion realized by both bodies. After binding, both bodies can move in a straight line or tumble in a fixed location. For each movement, different tensions will affect the attachment. In this section, we discuss the tensions and forces that are exerted onto the virus during the bacterium's movement.

A. Hydrodynamic Drag Force

The medium that we consider is the blood, where the Ebola virus will diffuse through brownian motion. Once the Ebola virus has attached itself to the bacterium, both are subjected to the same hydrodynamic force (drag force) as they mobilize. Since we model the shape of the bacterium as a cylinder, the $\mathbf{F_{Drag}}$ can be expressed as follows [38]:

$$\mathbf{F_{Drag}} = -\frac{1}{2}\rho_f v^2 A C_d, \quad (8)$$

where ρ_f is the fluid medium density, $v = v_b - v_f$ is the relative velocity between the bacterium (v_b) and the fluid (v_f), $A = \pi B_R^2$ is the bacterium's cross-section and B_R is the radius. The drag coefficient C_d is expressed as [38]:

$$C_d = \frac{24}{Re} + \frac{6}{1+\sqrt{Re}} + 0.4, \quad (9)$$

where the Reynolds number (Re) is expressed as [38]:

$$Re = \frac{D_v \rho_f v}{\eta_f}, \quad (10)$$

where η_f is the fluid viscosity, and D_v is the width of the microfluidic chamber.

B. Bacteria Motility

Bacteria have different types of motility, e.g., swarming, swimming, gliding [39]. For swimming, bacteria utilises their flagella to swim in a regular or biased motion towards a source (e.g., nutrients). Bacteria can also move in a coordinated manner across solid or semi-solid surfaces [39]. This motility process is known as swarming and it is performed by group of cells instead of single individuals. This form of motility also depends on the *pili* formation that helps the cells to aggregate into a population [39]. For our model, we consider that the bacteria will swim and will not be allowed to grow or attach onto other surfaces, which is based on the swarming and gliding process. Also our aim is to allow the bacteria the freedom of random movement to trap the Ebola virus, and this could be achieved through their swimming process.

The swimming process of the *E. coli* is based on their *flagella* movement. The flagella are tails that stem from the body of the *E. coli*. The swimming behavior of the bacteria is based on a cycle of run and tumble motion, and is governed by a random walk. During swimming, the flagella will wrap into a single body, and this will rotate as a propeller allowing them to swim forward. The bacteria swims in a straight line for an average period (λ_{Run}) that is based on an exponential distribution [40]. The binding between the bacterium and virus will occur when they come into contact with each other. After swimming for a short period, the flagella will unwrap into individual strands and this will lead to tumbling in a fixed location. Once again the average tumbling period is based on an exponential distribution (λ_{Tumble}) [40]. After the tumbling process, the bacterium will select a random angle to continue swimming.

C. Tension Force for Running Motion

The bacterium's running motion (see Figure 5) produces tension on the binding area that could break the attachment. In order to analyse the forces affecting the binding between two bodies, we use the approach presented in [41]. The description of each variable is as follows: ΔE_L is the length of the Ebola virus that binds to the bacterium's surface (we are assuming here that only a portion of the virus has bound), $\mathbf{F_M}$ is the force exerted by the bacterium's flagella that enables the movement, $\mathbf{W_h}$ is the weight for the hanging section of the Ebola virus, $\mathbf{W_{dl}}$ is the weight for the bound section of the Ebola virus, $\mathbf{T}$ is the tension exerted on the hanging portion of the Ebola virus that attempts to peel it from the bacterium due to resistance, l_1 is the distance between the bound mid-section of the Ebola virus and the bacterium's centre of mass, l_2 is the distance between the centre of the Ebola virus hanging section and its bound mid-section, θ_h is the angle between the hanging portion of the virus and the bacterium. We consider both the Ebola virus and bacterium as homogeneous bodies. Therefore,

$$\mathbf{W_{dl}} = \frac{m_e}{E_L} g \Delta E_L$$

and

$$\mathbf{W_h} = m_e g - \mathbf{W_{dl}} ,$$

This is the author's version of an article that has been published in this journal. Changes were made to this version by the publisher prior to publication.
The final version of record is available at http://dx.doi.org/10.1109/TCBB.2018.2836430

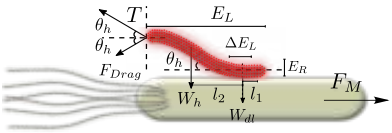

Fig. 5: The binding force representation model between an Ebola virus and the bacterium. The opposing tension force **T** is responsible for peeling the virus from the surface of the bacterium while the other forces act to maintain their attachment stability.

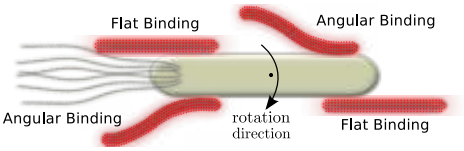

Fig. 6: Illustration of attachment points for angular and flat binding of Ebola virus on the bacterium as its going through a tumbling process. The positions of the flat and angular binding are dependent on the clockwise rotation of the bacterium.

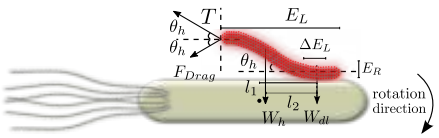

Fig. 7: The force model of an Ebola virus on the bacterium that is going through a tumbling process. This illustration shows the forces acting on the angular binding for Ebola virus. The angular binding only happens on locations of turns when the Ebola virus is being pulled outwards during the tumbling process.

where m_e is the Ebola virus' mass and g is the gravitational constant. In order for the body to move linearly in a particular direction, the sum of momentum has to be equal to zero. Therefore,

$$\sum M = M_{dl} + M_h + M_g + M_d - M_T = 0, \tag{11}$$

where $M_{dl} = \mathbf{W_{dL}} l_1$ is the momentum due to the force exerted on ΔE_L, $M_h = \mathbf{W_h}(l_2 + l_1)\cos\theta_h$ is the momentum due to the force exerted on the hanging section of the Ebola virus, $M_g = \int_0^{\Delta E_L} P_n \; x \; dx$ is the momentum due to the force exerted on the glycoprotein-receptor complexes on the bacterium (where P_n is the adhesive pressure of all the glycoproteins and x is the length of the Ebola virus binding area), $M_d = \mathbf{F_{Drag}} \sin\theta_h E_L$ is the momentum due to the drag force exerted on the edge of the Ebola virus ($\mathbf{F_{Drag}}$ is calculated from Eq. (8)), and $M_T = \mathbf{T} E_L \sin\theta_h$ is the momentum due to the tension exerted on the hanging section of the Ebola virus. Replacing these terms into Eq. (11) as well as the relationship of $l_2 = \left(\frac{E_L}{2} - \frac{\Delta E_L}{2}\right)$, which is the distance between the weights $\mathbf{W_{dL}}$ and $\mathbf{W_h}$, the tension $\mathbf{T}$ can be represented as:

$$T = \left(W_{dl} l_1 + W_h \left(\frac{E_L}{2} - \frac{\Delta E_L}{2} + l_1 \right) \cos\theta_h \right.$$
$$\left. + \frac{P \Delta E_L^2}{2} + F_{Drag} \sin\theta_h E_L \right) (E_L \sin\theta_h)^{-1}. \tag{12}$$

The adhesive pressure of glycoproteins (P) can be expressed as the force exerted within the bound area, and can be represented as follows [41]:

$$P = \frac{\left(F_n + \frac{m_e g}{n_G} \right) n_G \Delta E_L^2}{2\theta_h E_R \Delta E_L}.$$

where n_G is the concentration of glycoproteins required for the minimum attachment area. Inserting P into Eq. (12) will result in:

$$T = \left(W_{dl} l_1 + W_h \left(\frac{E_L}{2} - \frac{\Delta E_L}{2} + l_1 \right) \cos\theta_h \right.$$
$$\left. + \frac{\left(F_n + \frac{m_e g}{n_G} \right) n_G \Delta E_L}{2\theta_h E_R} + F_{Drag} \sin\theta_h E_L \right) (E_L \sin\theta_h)^{-1}. \tag{13}$$

D. Tension Force for Tumbling Motion

When a bacterium tumbles, depending on the position of the Ebola virus binding point, there will be two different types of force models, which are *angular* and *flat* binding. Figure 6 illustrates these binding points on the bacterium. As the bacterium rotates at the centre point of the body, the angular binding will occur when the Ebola virus encounters a pulling force (e.g., at the front of the bacterium when it tumbles clockwise), while the flat binding occurs at the tail end of the body when the virus is pushed through the circular motion. Figure 7 illustrates the force model for the angular binding, while the flat binding model is illustrated in Figure 8.

1) Angular Binding: Since the motion is a continuous rotational spin at a fixed point, the sum of the momentum is represented as follows:

$$\sum M = I\alpha, \tag{14}$$

where I is the inertial momentum of the bacterium as well as the Ebola virus, and the angular acceleration during the tumbling process, which is represented as:

$$\alpha = \frac{d\omega}{dt} = \frac{2\pi f_t}{\lambda_{Tumble}},$$

where f_t is the frequency of tumbling. Therefore, the inertial momentum is represented as:

$$I = \frac{m_B L^2}{12} + m_e \left(E_{hl} \cos\theta_h + \frac{\Delta E_L}{2} + l_1 \right), \tag{15}$$

where E_{hl} is the length of the virus that is hanging, m_B is the mass and L is the half length of the bacterium. For the angular binding, considering Eq. (14) and (15), Eq. (11) can be represented as:

This is the author's version of an article that has been published in this journal. Changes were made to this version by the publisher prior to publication.
The final version of record is available at http://dx.doi.org/10.1109/TCBB.2018.2836430

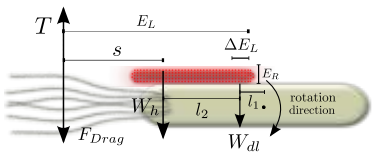

Fig. 8: The force model of the Ebola virus on the bacterium that is going through a tumbling process. This illustration shows the forces acting on the flat binding for the Ebola virus. The flat binding only occurs on locations of turns when the Ebola virus is being pushed up against the bacterium during the tumbling process.

$$I\alpha = W_{dl}l_1 + W_h\left(\frac{E_L}{2} - \frac{\Delta E_L}{2} + l_1\right)\cos\theta_h + \frac{\left(F_n + \frac{m_e g}{n_G}\right) n_G \Delta E_L}{2\theta_h E_R} + F_{Drag}\sin\theta_h E_L - TE_L\sin\theta_h,$$

and from the perspective of the tension **T**, this is represented as:

$$T = \left(W_{dl}l_1 + W_h\left(\frac{E_L}{2} - \frac{\Delta E_L}{2} + l_1\right)\cos\theta_h + \frac{\left(F_n + \frac{m_e g}{n_G}\right) n_G \Delta E_L}{2\theta_h E_R} + F_{Drag}\sin\theta_h E_L - \frac{m_B L^2}{12} - m_e\left(E_{hl}\cos\theta_h - \frac{\Delta E_L}{2} - l_1\right)\alpha\right) * (E_L\sin\theta_h)^{-1}. \quad (16)$$

2) Flat Binding: For the flat binding during the tumbling process, Eq. (16) can be simplified because there is no angle of attachment between the Ebola virus and the bacterium. This means that a large part of the virus will lie flat on the bacterium during rotation. This scenario is presented in Figure 8. In this case, the tension **T** is represented as:

$$T = \left(W_{dl}l_1 + W_h\left(\frac{E_L}{2} - \frac{\Delta E_L}{2} + l_1\right) + \frac{\left(F_n + \frac{m_e g}{n_G}\right) n_G \Delta E_L}{2\theta_h E_R} + F_{Drag}E_L - \left(\frac{m_B L^2}{12} - m_e\left(E_{hl} - \frac{\Delta E_L}{2} - l_1\right)\right)\alpha\right)(E_L)^{-1}. \quad (17)$$

V. ANALYSIS AND SIMULATIONS

Firstly, we will present the analysis of the binding forces and tensions for the virus attachment to an individual bacterium. This will then be followed by simulations that will evaluate the microfluidic attenuator performance of the Ebola collection process. The values for all the parameters used in the binding force analysis and simulations are presented in Table I.

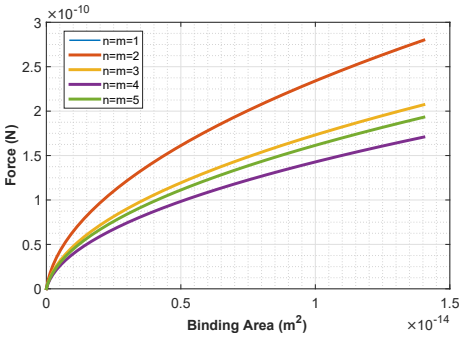

Fig. 9: Analysis of receptor binding force for five different valency configurations.

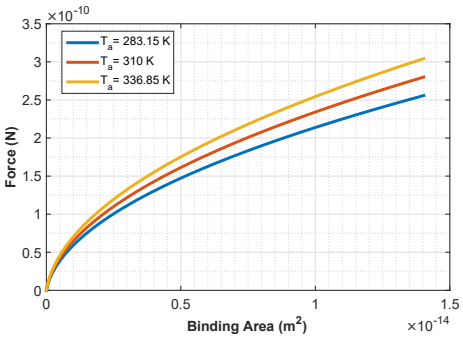

Fig. 10: Analysis of receptor binding force for two different temperatures. The temperature difference was not sufficient to produce significant changes in the attachment force.

A. Binding Force and Tensions Analysis

The aim of the analysis is to evaluate the effect of tension forces acting on the attachment point between the Ebola virus and the bacterium, and how this impacts on the protein binding force. The binding force analysis is presented in Figures 9 and 10, while the opposing forces analysis are presented in Figures 11, 12 and 13.

The binding force relies on the bacterial and viral proteins valency, and its models were presented in Eg. (2)-(6). Therefore, we considered different fixed values of n and m to evaluate their impact on the resulting binding force (see Figure 9). Even if the number of bonds increases, the ratio n/m will still remain the same. For $n = \{1, 2\}$ and $m = \{1, 2\}$, the binding force was almost the same with less than 1% difference, and this was the highest value achieved. The chosen protein, TIM-1, can bind to two or three proteins at same time (i. e. $1 \leq m \leq 3$) and as presented in Figure 9, this resulted in the highest binding force values for all possible attachment area, which also reflects the most suitable protein configuration. In Figure 10, we analysed the effect of temperature on the binding force. We considered three different temperatures to observe different behaviours that can arise. Normal human body temperature is 309.65 K and during fever this is elevated to 313 K. The latter value is also the average temperature of countries where the disease outbreak occurred. As we can observe, the temperature does not produce

This is the author's version of an article that has been published in this journal. Changes were made to this version by the publisher prior to publication.
The final version of record is available at http://dx.doi.org/10.1109/TCBB.2018.2836430

TABLE I: Parameters used to evaluate the receptor binding force, tensions and drag force applied on the bacterium as well as the Ebola virus. * Refers to values chosen by the authors. ** Refers to standard values.

Variable	Value	References
E_R	47×10^{-9} m	[22], [23]
E_L	970×10^{-9} m	[22], [23]
B_R	0.5×10^{-6} m	[42]
B_L	1×10^{-6} m	[42]
v_b	20×10^{-6} m/s	[42]
m_e	5.45×10^{-19} kg	[22], [23]
m_b	1×10^{-18} kg	[42]
$[B_0]$	6.7×10^{-6} proteins/μm^2	*
$[V_0]$	2.8×10^{-2} proteins/μm^2	*
f_t	1.37 tumbles/s	[43]
ϕ	from $\pi/100$ rad to $\pi/10$ rad	*
T_a	310 K	*
k_B	0.00831446211 kJ/mol/K	**
ρ_{blood}	1060 kg.m^{-33}	[38]
g	9.8 m/s^2	**
μ_s	3×10^{-3} Pa.s	**
D_v	5 cm	*

significant changes in the receptor binding force behaviour, even for high temperatures such as $T_a = 336.85$ K.

The opposing forces acting on the attachment area can be increased or lowered depending on variations for a number of parameters: blood velocity, blood viscosity and angle of attachment between the Ebola virus and the bacterium. When the blood enters the microfluidic chamber, it will gain a certain velocity that could be high enough to increase the tension on the attachment point that can lead to breakage. In Figure 11 we considered three different velocities (v_f^1, v_f^2 and v_f^3) and evaluated their impact on the binding force when the bacterium is running in a straight line (worst case). As the velocity increases, we can observe that the tension increases as well. However, if the blood velocity is much higher than the bacteria velocity, this can become an issue. In this case, when the blood flows into the chamber, it will disrupt the bacterial movement by pushing them toward the opposite border of the compartment. To avoid this effect, the bacteria need to be placed inside the microfluidic chamber when the blood is at rest and removed before the blood is pumped back into the body.

The patient's blood can be more or less viscous depending on their health condition. Different viscosity values can produce significant changes on the drag force that could result in higher tension on the attachment point between the virus and the bacterium. Figure 12 shows the effect of three different viscosity values on the tension applied on B_{Area}. Higher viscous blood will have a larger impact when the bacteria is moving, and a less viscous blood will affect the tension when the bacteria is tumbling. For all cases presented in Figure 12, the changes to the tension on the attachment point is reasonably low. This result demonstrates that the blood viscosity will not impact on the proposed attenuator system performance. The same occurs if we change the attachment angle, as shown for both the running and angular binding analysis (Figure 13). For this analysis, we considered three

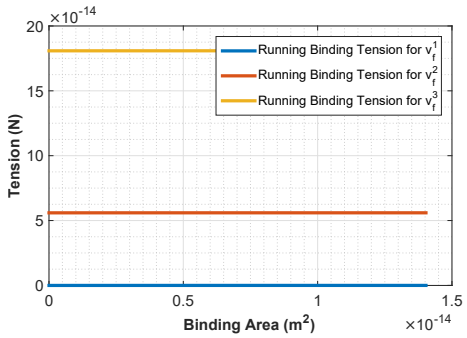

Fig. 11: Analysis of the effect of three different blood velocities on the tension exerted onto the attachment area. We evaluated the opposing forces for $v_f^1 = 0$ μm/s, $v_f^2 = 10$ μm/s and $v_f^3 = 20$ μm/s.

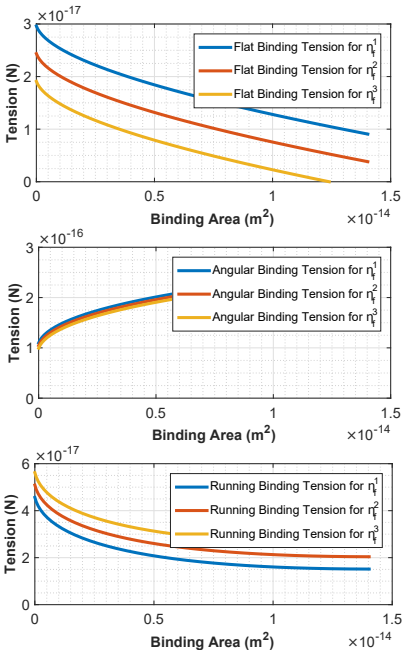

Fig. 12: Analysis of the effect of three different blood viscosities on the tension exerted onto the attachment area. We evaluated the opposing forces for $\eta_f^1 = 3 \times 10^{-3}$ Pa.s, $\eta_f^2 = 4 \times 10^{-3}$ Pa.s and $\eta_f^3 = 5 \times 10^{-3}$ Pa.s.

different attachment angles between the Ebola virus and the bacterium. As we can observe from the plots, when the angle increases, the tension applied to detach the virus from the bacterium decreases. Furthermore, for $\theta \geq 5$ rad, the angular binding tension enhances the attachment rather than oppose to detach the virus.

B. Microfluidic Attenuator Trapping Simulations

In order to validate the Ebola virus trapping process by the bacteria, we conducted several simulations for the different environments that the system could be exposed. We are interested in evaluating the attenuator model performance for

This is the author's version of an article that has been published in this journal. Changes were made to this version by the publisher prior to publication.
The final version of record is available at http://dx.doi.org/10.1109/TCBB.2018.2836430

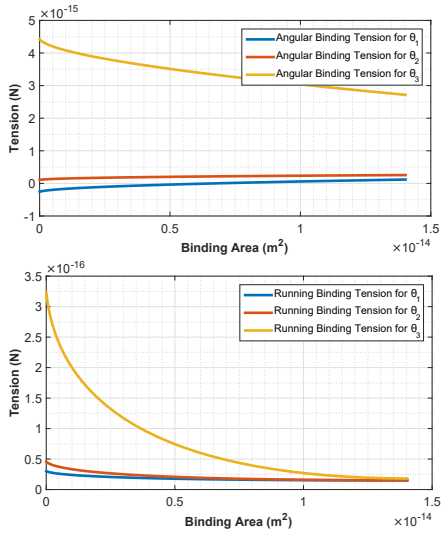

Fig. 13: Analysis of the angular and running binding tensions. Three different attachment angles were considered in this analysis $\theta_1 = 10$ rad, $\theta_2 = 5$ rad, $\theta_3 = 0.5$ rad

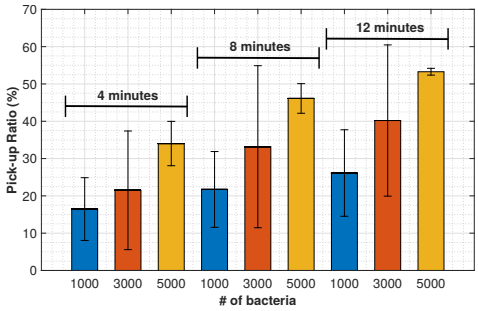

Fig. 14: The pickup ratio increased proportionally to the different simuation times. For 4 minutes more than 30% of the available virus were captured; for 8 minutes, more than 40%; and for 12 minutes, more than 50%.

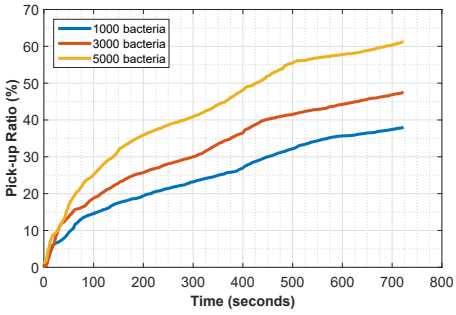

Fig. 15: The quantity of Ebola virus that are captured with respect to time as the quantity of bacteria are varied. The area considered is 5x5 cm.

the initial stage of the infection, where the number of Ebola is approximately 10^4 virus/ml of blood [44]. For all considered scenarios, the Ebola virus were randomly distributed in a

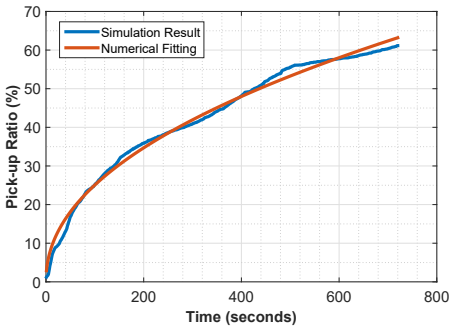

Fig. 16: The filter function $f_b(t)$ was numerically evaluated for 5000 bacteria. This function can be used to predict the time needed to reach the desired pick-up ratio.

microfluidic chamber square area with a size of 25 cm^2, while the bacteria are placed in an external compartment.

The bacteria are released from the compartment ($x = 0$ and along the y-axis) swimming into the chamber to capture the Ebola virus. In our scenario, the number of Ebola virus is higher than the number of bacteria. To ensure a constant blood viscosity value (3×10^{-3} Pa.s), the simulation duration was limited by the amount of time before clotting naturally occurs, which is between 8 and 15 minutes [45]. We also considered a static blood flow ($v_f = 0$), small attachment angle ($\theta \leq 0.5$ rad) and the binding force was generated by a trivalent protein interaction ($n = m = 3$).

Based on the analysis presented in Section V-A, we found that the attachment area has an important effect on the reliability of the binding process. The area limit defined in Eq. (7) is used to determine the maximum number of virus that can attach to each bacterium (this is calculated by considering the bacteria shape as a cylinder, and determining the area of each virus that binds to the surface membrane). In our simulations, for each contact between a bacterium and a virus we evaluate Eq. (7). If the bacterium's area is already full of virus, or if the attachment area is larger than the area available, this means that there are no remaining space on the bacterium's surface. The results presented in Figures 9, 10 and angular binding tension in Figure 12, showed that an increase of B_{Area} resulted in larger binding force or opposing tensions. At the same time, the results presented in Figures 11, 12 (running and flat binding tensions) and 13 showed an inverse relationship with B_{Area}. Therefore, in order to simulate a realistic scenario, we consider various random attachment area between the Ebola virus and the bacteria.

The pick-up ratio was evaluated for different Ebola densities, simulation times and quantity of bacteria. Figure 14 presents the performance of the attenuator, which is the ratio of the average number of Ebola virus captured (10^4, 5×10^4 and 10^5 virus) by 1000, 3000 and 5000 bacteria within 4, 8 and 12 minutes. As we can see from the results, the quantity of virus is reduced with respect to the number of bacteria and duration allowed for the collection process.

Since each bacterium will have an attachment limit in terms of bound Ebola virus, after a certain amount of time the system

This is the author's version of an article that has been published in this journal. Changes were made to this version by the publisher prior to publication.
The final version of record is available at http://dx.doi.org/10.1109/TCBB.2018.2836430

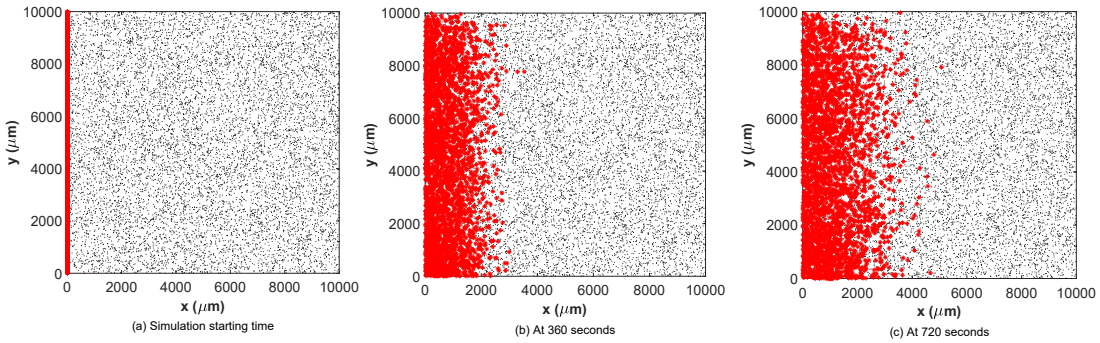

Fig. 17: The placement of bacteria have an impact on the spatial distribution of the virus. (a) At the start of the simulation, the bacteria where placed along the y-axis ($x = 0$) and the virus is randomly distributed within the chamber; (b) at 3600 seconds, bacteria could filter a small portion of the area; (c) at 7200 seconds, bacteria mobilized to more than 30% of the chamber's length.

is expected to became saturated. The next set of experiments is designed to measure the time required before saturation occurs. The number of Ebola virus were fixed at 10,000 and three quantities of bacteria were considered (1000, 3000, 5000), while the simulation time was fixed at a maximum of 720 seconds, and the simulations were executed for 10 cycles. The time 720 seconds is selected to avoid blood clotting. Figure 15 presents the average pick-up ratio, where after 720 seconds, 1000 bacteria achieved $37.89 \pm 12.6\%$ of the total number of virus, 3000 bacteria achieved $47.41 \pm 24.76\%$ and 5000 bacteria achieved $61.15 \pm 13.56\%$. We can also observe in Figure 15 that the bacteria do not achieve their saturation point within the considered period of 720 seconds. The considered number of Ebola (and their random placement) combined with the random nature of bacterial swimming process produce the high variance observed, and limits the bacteria from reaching their saturation point within 720 seconds. We previously defined the model for the attenuator in Eq. (1), which also includes the attenuator function $f_b(t)$ that determines the amount of Ebola virus to be picked up as a function of time. This function can be estimated from the saturation experiments. As an example, considering that 5000 bacteria achieved the highest pick-up ratio, we used this result to evaluate numerically the attenuator function $f_b(t)$ for 10,000 virus, and predict the time required to reach the desired pick-up ratio (see Figure 16), and this is represented as:

$$f_b(t) = 2.903t^{0.4682} \tag{18}$$

The pick-up process can also be observed spatially. In Figure 17, 10,000 Ebola virus were spread randomly within the chamber (with an area of 1 cm^2) and 3,000 bacteria were released along the y-axis ($x = 0$). Within 720 seconds, the number of bacteria reached approximately 5,000 μm. This also demonstates the speed the bacteria takes to move within the area and perform the Ebola pick-up. It can be also observed from Figure 17 that the bacteria is able to only cover a small portion of the area. This result suggest that a proper chamber design is important to optmise the pick-up process. The chamber geometry will depend on the concentration of the virus for the desired blood volume and the number of bacteria used to collect them. This is still a open problem that should be addressed during the attenuator design.

VI. CONCLUSION

The emergence of Ebola virus in recent years has motivated the need for effective treatment solutions to curb the spreading process. In this paper, we presented an approach where bacteria, genetically engineered, are capable of trapping Ebola virus that binds on its surface. The approach requires blood to be temporarily transported through an external tube that is connected through a microfluidic chamber containing the engineered bacteria. Our approach includes the engineering of receptors on the surface of the bacteria that are compatible to the glycoproteins found on the membrane of the Ebola virus. Our analysis found that the binding process of the Ebola virus on the bacteria is highly dependent on the valency of both viral and bacterial proteins as well as the attachment area. The paper also presented a simulation model of the bacteria hunting process of the Ebola virus within a confined area. The analysis includes the saturation time of the Ebola virus collection process, as well as the collection and trapping performance when the number of bacteria and Ebola virus varies. Our results show that for the considered simulation time, the bacteria can collect the virus without reaching its attachment limit, and the performance of the Ebola virus trapping quantity is highly dependent on the number of bacteria that are deployed. Although this paper only concentrated on the *E.coli* bacteria, the approach can also extend to other attenuated strains of bacteria such as *Salmonella* [46] and also to other virus that can bind to TIM-1. The proposed technique also shows the potential of using synthetic biology to build a biomedical machinery to clean human blood from virus.

REFERENCES

[1] K. A. Alexander et al., "What Factors Might Have Led to the Emergence of Ebola in West Africa?", PLoS Neglected Tropical Diseases, vol. 9, no. 6, June 2015.
[2] P. E. Kilgore et al., "Treatment of Ebola Virus Disease", Pharmacotherapy, vol. 35, no. 1, pp. 43-53, Jan. 2015

This is the author's version of an article that has been published in this journal. Changes were made to this version by the publisher prior to publication.
The final version of record is available at http://dx.doi.org/10.1109/TCBB.2018.2836430

[3] World Health Organization (WHO) FAQ, "Ebola vaccines, therapies, and diagnostics", Retrieved from http://www.who.int/medicines/emp_ebola_q_as/en/, Last update in 21 November 2015, 2015.
[4] M. Shuchman, "Ebola vaccine trial in west Africa faces criticism", The Lancet, vol. 385, no. 9981, pp. 1933-1934, May 2015.
[5] M. V. Herp et al, "Favipiravir-a prophylactic treatment for Ebola contacts?", The Lancet, vol. 385 no. 9985, pp. 2350, Jun. 2015.
[6] R. Breitling and E. Takano, "Synthetic biology advances for pharmaceutical production", Current Opinion in Biotechnology, vol. 35, pp.46-51, Mar. 2015.
[7] G. Gehring, et al., "The clinically approved drugs amiodarone, dronedarone and verapamil inhibit filovirus cell entry", Journal of Antimicrobial Chemotherapy Advance Access, vol. 69, no.8, pp. 2123-2131, Aug. 2014.
[8] J. M. Dye et al., "Postexposure antibody prophylaxis protects nonhuman primates from filovirus disease", Proceedings of the National Academy of Sciences, vol. 109 no. 13, pp. 5034-5039. Mar. 2012.
[9] X. Qiu et al., "Reversion of advanced Ebola virus disease in nonhuman primates with ZMapp", Nature, vol. 514, no. 7520, pp. 47-53, Oct. 2014.
[10] J. Misasi et al., "Structural and molecular basis for Ebola virus neutralization by protective human antibodies", Science, Feb. 2016.
[11] D. Corti et al., "Protective monotherapy against lethal Ebola virus infection by a potently neutralizing antibody", Science, Feb. 2016.
[12] J. Kouznetsova et al., "Identification of 53 compounds that block Ebola virus-like particle entry via a repurposing screen of approved drugs", Emerging Microbes and Infections, vol. 3, no. 12, pp. e84, 2014.
[13] A. R. Oany, et al., "Highly conserved regions in Ebola virus RNA dependent RNA polymerase may be act as a universal novel peptide vaccine target: a computational approach", In Silico Pharmacology, vol. 3, no. 7, 2015.
[14] T. Nakano et al., "Molecular Communication among Biological Nanomachines: A Layered Architecture and Research Issues", IEEE Transactions on NanoBioscience, vol. 13, no. 3, pp. 169-197, Sept. 2014.
[15] D. P. Martins et al., "Using Competing Bacterial Communication to Disassemble Biofilms", Proceedings of the 3rd ACM International Conference on Nanoscale Computing and Communication, p. 18, Sep. 2016
[16] C. Piñero-Lambea et al., "Engineered bacteria as therapeutic agents", Current Opinion in Biotechnology, vol. 35, pp. 94-102, Jun. 2015.
[17] L. Vangelista et al., "Engineering of Lactobacillus jensenii to secrete RANTES and a CCR5 antagonist analogue as live HIV-1 blockers", Antimicrobial Agents Chemotherapy, vol. 54, no. 7, pp. 994-3001, Jul. 2010.
[18] P. E. Massa et al., "Salmonella engineered to express CD20-targeting antibodies and a drug-converting enzyme can eradicate human lymphomas", Blood, vol. 122, no. 5, pp. 705-714, Aug. 2013.
[19] D. R. Asher et al., "The erythrocyte viral trap: Transgenic expression of viral receptor on erythrocytes attenuates coxsackievirus B infection", Proceedings of the National Academy of Sciences, vol. 102, no. 36, Sep. 2005.
[20] J. J. Dennehy et al., "Virus population extinction via ecological traps", Ecology Letters vol. 10, no. 3, pp. 230-240, Mar. 2007.
[21] M. Mammen et al., "Polyvalent interactions in biological systems: implications for design and use of multivalent ligands and inhibitors", Angewandte Chemie International Edition, vol. 37, no. 20, pp. 2754-2794, Nov. 1998.
[22] A. M. King et al., "Virus Taxonomy: Ninth Report of the International Committee on Taxonomy of Viruses". Elsevier, 2012.
[23] P. Ascenzi et al., "Ebolavirus and Marburgvirus: insight the Filoviridae family," Molecular aspects of medicine, vol. 29, no. 3 pp. 151-185, Jun. 2008.
[24] A. C. Zampieri et al., "Immunopathology of highly virulent pathogens: insights from Ebola virus", Nature immunology, vol. 8, no. 11, pp. 1159-1164, Nov. 2007.
[25] M. Bray, "Pathogenesis of viral hemorrhagic fever", Current opinion in immunology, vol. 17, no. 4, pp. 399-403, Mar. 2005.
[26] N. Sullivan et al., "Ebola Virus Pathogenesis: Implications for Vaccines and Therapies", Journal of Virology, vol. 77, no. 18, pp. 9733-9737, Sep. 2003.
[27] E. H. Miller and K. Chandran, "Filovirus entry into cells - new insights", Current opinion in virology, vol. 2, no. 2, pp. 206-214, Apr. 2012.
[28] M. Mazzon and J. Mercer, "Lipid interactions during virus entry and infection", Cellular microbiology, vol. 16, no. 10, pp. 1493-1502, Oct. 2014.
[29] E. Rothenberg et al., "Single-virus tracking reveals a spatial receptor-dependent search mechanism", Biophysical Journal, vol. 100, no. 12, pp. 2875-2882, Jun. 2011.
[30] Z. Chen et al., "Interactions of human T cell immunoglobin mucins with apoptotic cells", Journal of Huazhong University of Science and Technology, vol. 32, no. 1, pp. 9-16, Feb. 2012.
[31] C. Dressaire, et al., BolA is a transcriptional switch that turns off motility and turns on biofilm development, MBio, vol. 6, no. 1, pp. 113, 2015.
[32] X. Liu and T. Ferenci, Regulation of porin-mediated outer membrane permeability by nutrient limitation in Escherichia coli, Journal of Bacteriology, vol. 180, no. 15, pp. 39173922, 1998.
[33] M. Morita, et al., Characterization of a virulent bacteriophage specific for Escherichia coli O157:H7 and analysis of its cellular receptor and two tail fiber genes, FEMS Microbiology Letters, vol. 211, no. 1, pp. 7783, 2002.
[34] K. Hantke and V. Braun, Functional interaction of the tonA/tonB receptor system in Escherichia coli, Journal of Bacteriology, vol. 135, no. 1, pp. 190197, 1978.
[35] S. X. Sun, and D. Wirtz, "Mechanics of Enveloped Virus Entry into Host Cells", Biophysical Journal, vol. 90, no. 1, pp. 10-12, Jan. 2006.
[36] V. A. Petrenko and V. J. Vodyanoy, "Phage display for detection of biological threat agents", Journal of Microbiological Methods, vol. 53, no. 2, pp. 253-262, 2003.
[37] V. M. Krishnamurthy et al., "Multivalency in Ligand Design". Fragment-based Approaches in Drug Discovery, 34, pp. 11-53.
[38] L. Arcese et al., "Dynamic behavior investigation for trajectory control of microrobot in blood vessels", IEEE/RSJ International Conference on Intelligent Robots and Systems, IROS 2010 - Conference Proceedings, pp. 5774-5779, Oct. 2010.
[39] R. M. Harshey, "Bacterial Motility on a Surface: Many Ways to a Common Goal", Annual Review of Microbiology, vol. 57, no. 1, pp. 249-273, 2003.
[40] Z. Wang et al., "Validating Models of Bacterial Chemotaxis by Simulating the Random Motility Coefficient", 8th IEEE International Conference on BioInformatics and BioEngineering 2008, BIBE 2008, pp. 1-5, 2008.
[41] M. P. Reyes and R. S. Fearing, "Macromodel for the Mechanics of Gecko Hair Adhesion", Proceedings 2008 IEEE International Conference on Robotics and Automation (ICRA '08), Piscataway, NJ: IEEE Press, 2008, pp. 1602-1607, 2008.
[42] W. R. Schneider and R. N. Doetsch, "Effect of Viscosity on Bacterial Motility", Journal of Bacteriology, vol. 117, no. 2,pp. 696-701, Feb. 1974.
[43] U. Alon, et al., Response regulator output in bacterial chemotaxis, The EMBO Journal, vol. 17, no. 15, pp. 4238-4248, Aug. 1998.
[44] M. de La Vega et al.,"Ebola viral load at diagnosis associates with patient outcome and outbreak evolution", The Journal of Clinical Investigation, vol. 125, n. 12, pp. 4421-4428, Dec. 2015.
[45] L. Silvestri, "Saunders comprehensive review for the NCLEX-RN examination". St. Louis, MO: Elsevier. pp. 116117. 2014.
[46] J. F. Toso et al., "Phase I study of the intravenous administration of attenuated Salmonella typhimurium to patients with metastatic melanoma", Journal of Clinical Oncology, vol. 20, no. 1, pp.142-152, Jan. 2002.

Daniel Perez Martins (S'12) was born in Salvador-BA, Brazil, 1985. Currently, he is a Ph.D. student associated with the with the Telecommunications Software and Systems Group (TSSG) and the Waterford Institute of Technology (WIT – Ireland). Daniel received his M.Sc. degree in Electrical Engineering at the Federal University of Campina Grande (UFCG – Brazil-2013) and B.Sc. degree in Telecommunications Engineering at the University Center Jorge Amado (Unijorge – Brazil-2009). During his Master, he was associated with Institute for Advanced Studies in Communications (Iecom) where worked in a R&D project to identify the acoustical noise's source at an industrial environment using Sound Signal Processing and Stochastic Processes techniques. His experiences concentrates on Mathematical Modelling of Telecommunications Systems, Signal Processing and Analysis, Computer Networks and Molecular Communication. He is also a reviewer for the *Nano Communications Networks* Journal and for the IEEE *Internet of Things Journal*. Interests include Bacteria-Based Nanosystems, Synthetic Biology and Molecular Communication.

This is the author's version of an article that has been published in this journal. Changes were made to this version by the publisher prior to publication.
The final version of record is available at http://dx.doi.org/10.1109/TCBB.2018.2836430

Michael Taynnan Barros was born in Campina Grande, Brazil, 1990. He is currently an Irish Research Council Government of Ireland Postdoctoral research fellow associated with the TSSG, WIT. Michael received his PhD in Telecommunication Software at the Waterford Institute of Technology in 2016, M.Sc. degree in Computer Science at the Federal University of Campina Grande in 2012 and B.Tech. degree in Telematics at the Federal Institute of Education, Science and Technology of Paraiba in 2011. He has published over 40 research papers in diverse journals such as IEEE Transactions on Communications, IEEE Transactions on Nanotechnology, and conferences in the area of wireless communications, optical communications, ad-hoc networks, as well as molecular and nanoscale communications. He is also a reviewer for many journals and participated as technical program committee and reviewer for various international conferences. In 2017, he served as the Technical Program Co-chair for the 3rd International Workshop on Nanoscale Computing and Communications (NsCC) held in conjunction with the NEW2AN conference. Also, he served as the chair of the 5GPPP Network Management, QoS and Security Working Group and the Chair of the 2nd Network Management, QoS and Security for 5G Networks held in conjunction with the EuCNC 2017. His interests are in Molecular Communications, Nanonetworks and 5G Technology for Connected Health.

Massimiliano Pierobon (S05-M13) received the M.S. degree in Telecommunication Engineering from the Politecnico di Milano, Italy, in 2005, and the Ph.D. degree in Electrical and Computer Engineering from the Georgia Institute of Technology, Atlanta, GA, USA, in 2013. Since August 2013, he is an Assistant Professor at the Department of Computer Science and Engineering, University of Nebraska-Lincoln (UNL), NE, USA, where he also holds a courtesy appointment at the Department of Biochemistry. He received the BWN Lab Researcher of the Year Award at the Georgia Institute of Technology for his outstanding research achievements in 2011. He was also named IEEE Communications Letters 2013 Exemplary Reviewer in appreciation for his service as referee, and he is the recipient of the 2016 UNL CSE Upper Level Teaching Award. He is an Editor of the IEEE Transactions on Communications. He was a guest-editor for special issues for the IEEE Internet of Things Journal and the Nano Communication Networks (Elsevier) Journal. He was TPC co-chair for ACM NanoCom 2016, TPC vice-co-chair for the ACM NanoCom 2015. He is a faculty mentor for the UNL iGEM team. His interests are in molecular communication, nanonetworks, synthetic biology, intra-body networks and the Internet of Bio-Nano Things.

Meenakshisundaram Kandhavelu got his undergraduate degree from the American College, Madurai Kamaraj University, India in 2002 and a Masters of Science in Animal Biotechnology from the Bharathidasan University, India in 2005. He was an intern researcher in the stem cell and developmental biology research group, Genomic Institute of Singapore, in 2004-2005. After that, in 2008 he finished a Ph.D. in Pharmaceutical Sciences (research disciplinary, Chemical and Pharmaceutical sciences and biotechnology) from the University of Camerino, Italy (with the mobility research mobility research work at the University of Milan). During 2009 he worked as a Postdoctoral researcher in A.I.Virtanean Institute for Molecular Sciences, Finland. Later, since 2010-2012 he continued his post-doctoral research in the department of signal processing. Since 2013, he is working as a Group leader of Molecular Signaling Lab(MS Lab) and as an Assistant Professor/Adjunct professor in the same department, TUT. He has authored 35+ international refereed publication. He has made contribution to the field of molecular signal processing. His research interest to cover the area of molecular signal processing and health informatics.

Pietro Lio' is a Reader in Computational Biology at the Computer Laboratory, University of Cambridge. His affiliations also include the Cambridge Computational Biology Institute. His work spans Machine Learning and computational models for health Big Data, personalised medicine research, multi-scale/multi-omic/multi-physics modelling and data integration methods, with more than 230 peer reviewed papers. He has edited several books and given over 20 keynote talks

Sasitharan Balasubramaniam (SM'14) received his Bachelor (Electrical and Electronic Engineering) and Ph.D. degrees from the University of Queensland in 1998 and 2005, respectively, and Masters (Computer and Communication Engineering) degree in 1999 from the Queensland University of Technology. He is currently a senior research fellow at the Nano Communication Centre, Department of Electronic and Communication Engineering, Tampere University of Technology, Finland. Previously, Sasitharan was a research fellow at the Telecommunication Software and Systems Group, Waterford Institute of Technology, Ireland, where he worked on a number of Science Foundation Ireland projects. He has published over 70 papers and actively participates in a number of technical programme committee for various conferences. Sasitharan was the TPC co-chair for ACM NANOCOM 2014 and IEEE MoNaCom 2011, both conferences which he co-founded. He is currently an editor for the IEEE Internet of Things journal and Elsevier Nano Communication Networks. His current research interests includes bio-inspired communication networks, as well as molecular communications. Sasitharan is an IEEE Senior member.

CHAPTER 9

JOURNAL PAPER: QUALITY AND CAPACITY ANALYSIS OF MOLECULAR COMMUNICATIONS IN BACTERIAL SYNTHETIC LOGIC CIRCUITS

Journal Title:	IEEE Transactions on Nanobioscience
Article Type:	Regular Paper
Complete Author List:	Daniel Perez Martins, Michael Taynnan Barros, Sasitharan Balasubramaniam
Keywords:	Synthetic logic circuits, Molecular communications, Engineered bacteria.
Status:	In press

This is the author's version of an article that has been published in this journal. Changes were made to this version by the publisher prior to publication.
The final version of record is available at http://dx.doi.org/10.1109/TNB.2019.2930960

Quality and Capacity Analysis of Molecular Communications in Bacterial Synthetic Logic Circuits

Daniel P. Martins, *Student Member, IEEE,* Michael Taynnan Barros, *Member, IEEE,* and Sasitharan Balasubramaniam, *Senior Member, IEEE*

***Abstract*—Synthetic logic circuits have been proposed as potential solutions for theranostics of biotechnological problems. One proposed model is the engineering of bacteria cells to create logic gates, and the communication between the bacteria populations will enable the circuit operation. In this paper, we analyse the quality of bacteria-based synthetic logic circuit through molecular communications that represent communication along a bus between three gates. In the bacteria-based synthetic logic circuit, the system receives environmental signals as molecular inputs and will process this information through a cascade of synthetic logic gates and free diffusion channels. We analyse the performance of this circuit by evaluating its quality and its relationship to the channel capacity of the molecular communications links that interconnect the bacteria populations. Our results show the effect of the molecular environmental delay and molecular amplitude differences over both the channel capacity and circuit quality. Furthermore, based on these metrics we also obtain an optimum region for the circuit operation resulting in an accuracy of 80% for specific conditions. These results show that the performance of synthetic biology circuits can be evaluated through molecular communications, and lays the groundwork for combined systems that can contribute to future biomedical and biotechnology applications.**

***Index Terms*—Synthetic logic circuits, Molecular communications, Engineered bacteria.**

I. INTRODUCTION

RECENT progress in synthetic biology has seen a number of new technologies developed for engineering biological cells utilizing concepts from electrical engineering and computer science [1]–[5]. Unprecedented applications have emerged from synthetic engineering of cells, leading to novel approaches in the fields of biotechnology, medicine, as well as pharmaceutical science [4], [6]–[8]. Example applications have enabled researchers to engineer eukaryotic as well as prokaryotic cells (e.g., animal cells and bacteria, respectively) that can sense enzymes secreted from cancerous cells or treatment of systemic diseases such as Inflammatory Bowel Disease [7]. The multi-disciplinary approach combines principles from both electronics engineering and molecular biology to design the building blocks, where their combination can lead to complex synthetic structures such as logic gates [9]–[13]. However, complex circuits are still an obstacle as the current logic structures are often designed using a single logic gate or simple combinations between them [3].

Daniel P. Martins and Michael Taynnan Barros are with the Telecommunication Software & Systems Group (TSSG), Waterford Institute of Technology (WIT), Ireland. E-mail: dpmartins@tssg.org.

Sasitharan Balasubramaniam is with the Telecommunication Software & Systems Group (TSSG), Waterford Institute of Technology (WIT), Ireland and with the Faculty of Information Technology and Communication Sciences, Tampere University, Finland. Email: sasi.bala@tut.fi.

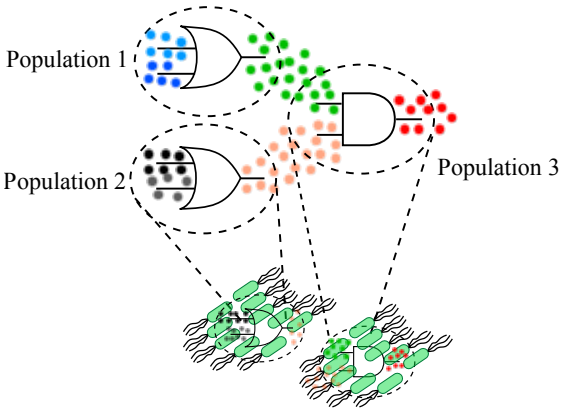

Fig. 1. Illustration of bacteria populations engineered to perform logical operations. For these systems, the input signals are molecules from the environment that are absorbed by the engineered bacteria.

Bacterial cells have been widely used to develop synthetic circuits due to the extensive knowledge about the DNA plasmids, and in particular in genome editing to design synthetic circuits that can lead to specialised functions [6]. Simple logic gates, to toggle switches, as well as oscillators, have already been developed by engineering both single cell and bacterial population [10], [14]. An overall representation of synthetic logic circuits constructed from bacteria is presented in Figure 1. These circuits are usually associated with controlling the bacteria's communication behaviour. As an example, researchers were able to engineer Boolean logic gates by controlling the communications between four *Escherichia coli* populations [15]. With the recent advancements in animal microbiome research, engineered bacteria are being considered as potential biomedical agents that combine diagnostic and individualised treatment (i.e., theranostic) for systemic diseases inside the human microbiome [6], [7], [10]. Specifically, the communication molecules produced by engineered bacteria are the effectors for these applications.

Due to the importance of molecular signals that can be used for the development of biomedical theranostics, researchers

This is the author's version of an article that has been published in this journal. Changes were made to this version by the publisher prior to publication.
The final version of record is available at http://dx.doi.org/10.1109/TNB.2019.2930960

are devoting their attention to understand also how they can be engineered. This new emerging subject is known as **molecular communications** [16]–[20]. This field concentrates on the development of artificial communications systems for biological devices at the nanoscale [16], [17], [21]–[25]. As it is inspired from natural systems, molecular communications systems require the engineering of molecular exchange that can be developed in a biological cell, and this could range from the engineering of cells for ion transfer to design networked communications among nanosystems [16], [17], [19], [20], [25]–[27]. As an example, bacteria-based molecular communications has been proposed to emit molecular signals in a networked model in order to produce jamming signals that interfere with another populations communications [28]–[30].

In this paper, we propose the use of bacteria-based molecular communication systems to evaluate the performance of synthetic logic circuits inside a multi-compartment capsule that contains three bacteria populations (each one is representing a different Boolean logic gate). The logic circuit is then built using the communications among the engineered bacteria confined in each compartment of the chamber. The design of this synthetic logic circuit prevents the engineered bacteria from spreading into the environment while allowing different logic operations to be performed depending on different molecular inputs. The confined chambers have two roles for this bacteria-based molecular communications system. First it limits the bacteria movement, where no organisms will be able to enter or leave the chamber. Second, the chamber prevents larger molecules from diffusing between the compartments. Therefore, these features limit the impact of unwanted effects in the system (e.g., exogenous bacteria hijacking the system or high communications noise due to the presence of unwanted molecules). Based on these assumptions, we focus our investigation on the impact of the noise generated by the engineered bacteria during their production of quorum sensing molecules.

The design principles considered in this paper follows similar approaches for other bacteria-based synthetic circuits. For example, toggle switches, logic gates, biosensors and programmable full-adder were designed using the bacteria signalling molecules as the activator and repressor of gene expression [11], [31]–[34]. Specifically, our bacteria-based synthetic logic circuit is inspired by a similar work in [15], where three *Escherichia coli* populations carried the same NOR gate and another carried the buffer. These bacterial populations were combined in different spatial arrangements to create 16 two-input Boolean logic gates [15]. Their work served as a proof-of-concept for using quorum sensing signalling as chemical 'wires' to interconnect the bacterial populations' logic gates. However, the work presented in this paper does not concentrate on the versatile combination of different synthetic logic gates, but instead on the analysis of molecular information between the gates to determine the quality of the circuit's performance.

Our molecular communications analysis is focused on showing the quality of the proposed bacteria-based synthetic logic circuit in conjunction with the evaluation of the capacity of the channels that interconnect the bacteria populations. Similar to digital circuits that can become faulty due to unreliable interconnection bus [35], [36], we investigate the effect of the free diffusion interconnections and the impact on the quality of the proposed circuit design. The proposed bacteria-based synthetic circuit is capable of sensing environmental variations and actuating accordingly in response to the measurements. This circuit composed of a two-layer synthetic logic circuit that will process the input molecular signals and output the required signal. For this paper, we do not intend to provide further specification on the sensing and actuating functionalities, but only on the communication performance. The main contributions of this paper are

- **Development of a bacteria-based molecular communications end-to-end model that can be used to analyse the reliability performance of a synthetic logic circuit.** We use three bacteria populations to create a synthetic logic circuit that will perform a cascade of logical operations at the molecular level.
- **Computation of quality performance metrics for the synthetic logic circuit operation considering different scenarios.** We analyse the unreliable nature of bacteria-based molecular communications systems that can disrupt the operation of the synthetic circuit, affecting its accuracy and precision.
- **Analysing the channel capacity for the bacteria-based synthetic logic circuit.** Using molecular communications theory, we show how different combination of parameters will affect the reliability of a circuit and how they are associated with the optimum channel capacity for the system.

The rest of the paper is organised as follows. In Section II, we describe the bacteria-based synthetic logic circuit, from both biological and communications engineering perspectives, and how they will be utilized to perform logic operations based on a set of molecular input signals. The communication model that represents the exchange of molecular information between the bacteria populations is presented in Section III. Section V presents the application of this model to determine the quality and the channel capacity for the proposed synthetic circuit. Lastly, in Section VI we present our conclusions.

II. SYSTEM DESIGN

The proposed circuit is a combination of three synthetic logic gates (one OR and two AND gates) that use a set of input molecular signals (see Figure 2). Although this paper only concentrates on this specific circuit, further analysis can be established for other logic gate combinations and circuit size. Each gate, represented in Figure 2(a), is composed of a bacteria population and is situated in a compartment, and is interconnected by free diffusion molecular communications links. These bacteria populations are placed inside a compartmented capsule with isolated chambers. For example, compartment A (OR gate) and B (AND gate) only communicates with the third compartment C (AND gate), through a filter wall (see Figure 2(b)). This thin membrane can be built using an organic compound such as *Polydimethylsiloxane* (*PDMS*), to only allow the molecules but not the bacteria to flow from chambers A and B to C [37]. A general representation of this filtering process is depicted in Figure 3.

This is the author's version of an article that has been published in this journal. Changes were made to this version by the publisher prior to publication.
The final version of record is available at http://dx.doi.org/10.1109/TNB.2019.2930960

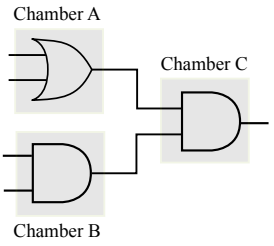

(a) Digital circuit representation of the system.

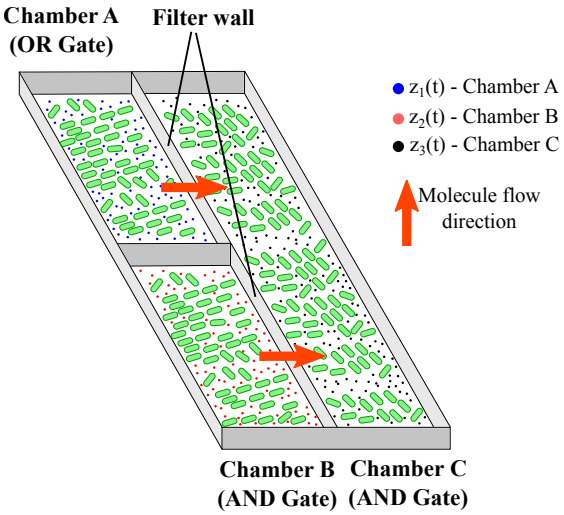

(b) Proposed system's physical design.

Fig. 2. Illustration of the proposed bacteria-based synthetic logic circuit. Each bacteria population is assigned to a compartment, becoming isolated from each other. The molecules produced at chambers A or B access chamber C by passing through a filter wall.

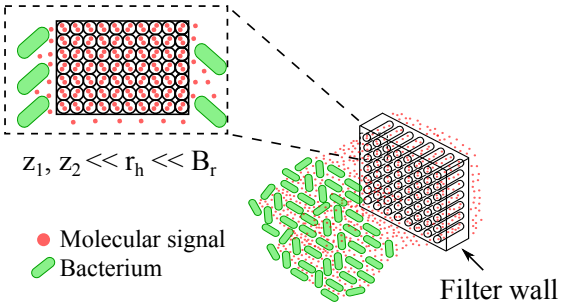

Fig. 3. Representation of the wall that separates the input gates from the output gate. This wall acts like a filter just allowing the molecular signal to pass through. For that purpose, the radius of the holes r_h, depicted in the expanded view of this Figure, must be greater than the molecule signal ($z_1(t)$ and $z_2(t)$) sizes and lesser than the bacterium radius B_r.

We limit the growth of the bacteria populations to fit the finite dimensions of each chamber. This population control can be achieved by applying antibiotics or probiotics, which will lower or increase their population density, respectively [38], [39]. Therefore, we consider that the bacteria population densities are constant. Based on this assumption, our analysis on the circuit's quality and the communications capacity is focused on the maximum bacteria population density.

The circuit operation can be described in two steps. First, each bacterium senses the molecular environmental signals $w_i(t-\tau_i)$ and starts the *quorum sensing* process to produce molecules that will toggle their natural switches (see [30] for further description of this process). The mathematical description of the molecular environmental signal $w_i(t-\tau_i)$ can be found in Section III-A. The molecular environmental delays τ_1, τ_2, τ_3 and τ_4 are produced by the different propagation times of each molecular input signal on the chamber's external medium. Second, all bacteria inside the chambers start to behave similarly to perform the desired logic operations. This process occurs for the first layer of the circuit. From an electronic circuit perspective, this synthetic circuit can be defined as an arrangement of logic gates and RC circuits [40]. This analogy allows us to investigate the quality of the system using the same metrics of a typical electronic circuit [41], [42].

A. Quorum Sensing and Molecule Binding Process

Bacteria can sense and respond to molecular signals that originate from other cells and environment, through a cellular communication process named quorum sensing [43]. This cell-to-cell communication process allows bacteria to display group behaviours through the controlled expression of genes, regulating many of their activities. Bacteria can survive harsh environments, produce virulent factors and form biofilms by using quorum sensing systems [43]. Each bacteria species uses specific molecules to perform this type of communication, and examples include autoinducers and N-Acyl homoserine lactone (AHL's). They also have specific transmembrane receptors to detect these signalling molecules, and examples include LuxN and CqsS [43]. These receptors bind quorum sensing molecules and trigger the expression of genes related to bacteria collective behaviours. Inside each bacterium cell, an initial cluster of genes (operon) will process the molecular signal originated from the transmembrane proteins and promote the second cluster of genes (effector) to transcribe messenger RNAs (mRNAs) [2], [44]. These molecules will be responsible for the translation of the genetic instruction into proteins that will trigger the group behaviours.

Since the first identification of this signalling mechanism, researchers have been proposing synthetic biology techniques that produce different responses for the sensed quorum sensing molecules [9]–[15]. They engineer new reception circuits in the bacteria, through genetic editing, in order to activate a response after sensing a certain concentration level that is tied to the number of individuals in a bacteria population [7]. The molecule binding process has also been applied for the design of molecular communications systems [45], [46]. In this paper, we focus on the use of engineered bacteria to perform logic operations through the use of quorum sensing molecules diffused in a closed space.

This is the author's version of an article that has been published in this journal. Changes were made to this version by the publisher prior to publication.
The final version of record is available at http://dx.doi.org/10.1109/TNB.2019.2930960

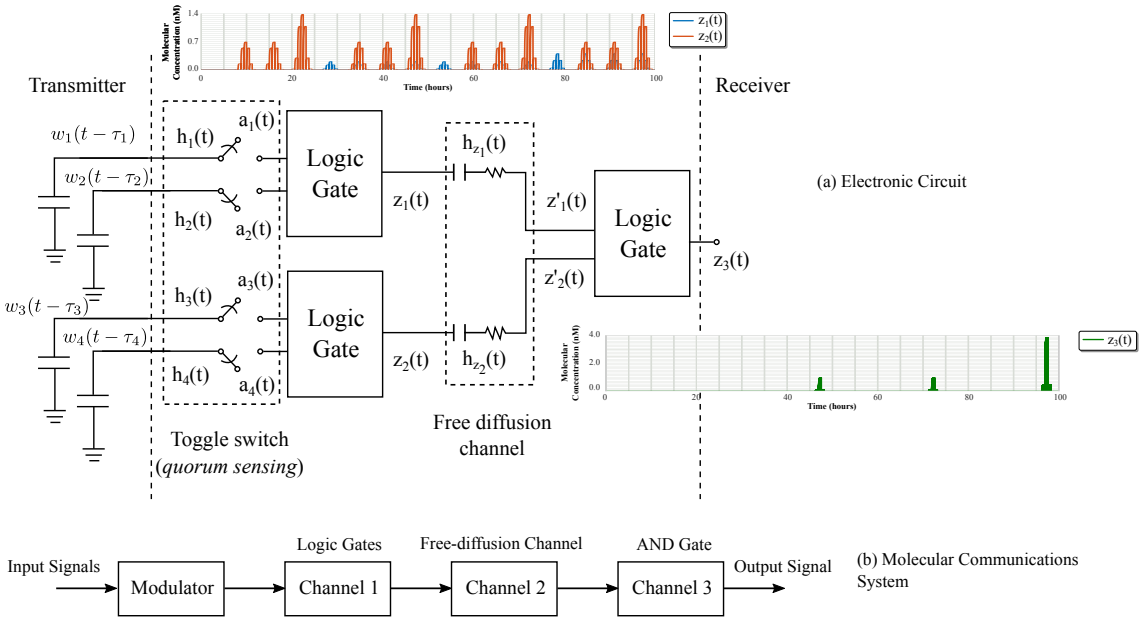

Fig. 4. Illustration of the proposed bacteria-based synthetic logic circuit. The four molecular input signals required to operate the system are processed by a cascade of synthetic logic gates and free diffusion channels. The natural toggle switches, based on the *quorum sensing*, are represented as On-Off systems and the free diffusion channels as an RC circuit. (a) Electronic circuit representation. (b) Molecular communications system representation.

TABLE I
TRUTH TABLE OF THE SYNTHETIC CIRCUIT CONSIDERED FOR THIS WORK. THE HIGH MOLECULAR SIGNAL LEVEL OUTPUT IS HIGHLIGHTED IN GRAY.

$\mathbf{Input_1}$	$\mathbf{Input_2}$	$\mathbf{Input_3}$	$\mathbf{Input_4}$	**Circuit Output**
0	0	0	0	0
0	0	0	1	0
0	0	1	0	0
0	0	1	1	0
0	1	0	0	0
0	1	0	1	0
0	1	1	0	0
0	1	1	1	1
1	0	0	0	0
1	0	0	1	0
1	0	1	0	0
1	0	1	1	1
1	1	0	0	0
1	1	0	1	0
1	1	1	0	0
1	1	1	1	1

B. Synthetic Logic Gates

A synthetic biology system is often described using rate reaction equations [45]. These are mathematical formulations that represent the change in the concentration of chemical substances during a given period. These equations are expressed in terms of the rate of production and consumption of those chemical substances and are described as follows

$$[\mathrm{R}_1] + [\mathrm{R}_2] \underset{\mathrm{k_r}}{\overset{\mathrm{k_f}}{\rightleftharpoons}} [\mathrm{P}], \tag{1}$$

where $[\mathrm{R}_1]$ and $[\mathrm{R}_2]$ are the two chemical substances that react to each other to produce the substance [P]; k_f is the forward reaction rate, in other words, is the speed of $[\mathrm{R}_1]$ and $[\mathrm{R}_2]$ reaction to produce [P]; and k_r is the reverse reaction rate, or the speed of [P] degradation to form $[\mathrm{R}_1]$ and $[\mathrm{R}_2]$.

In this paper, we use rate reaction equations to model the activation of the first layer of the synthetic logic circuit and the production of the molecular output signals from the three synthetic logic gates. Therefore, we describe the natural switch activation (see Figure 4) using the following equations [11]

$$\frac{d[A]}{dt} = \frac{\beta}{1 + K_B^{\alpha}} - \gamma_t [A] \tag{2}$$

and

$$\frac{d[B]}{dt} = \frac{\beta}{1 + K_A^{\alpha}} - \gamma_t [B] \tag{3}$$

where $[A]$ and $[B]$ represents the molecular signal concentrations that trigger and suppresses the operation of the synthetic logic gate, respectively; α and β are the repression constants, and the maximum production rates for both molecular signals $[A]$ and $[B]$; s_A and s_B are the toggle switches' induction signals, $K_A = [A]/(1 + (s_A/K)^{n_t})$ and $K_B = [B]/(1 + (s_B/K)^{n_t})$ define the rates by which the molecular signals bind to the synthetic gate receptor, K is a constant that defines the equilibrium of the chemical reactions involved in the production of a molecular signal, γ_t is the decay constant for both molecular signals, and n_t is the cooperativeness degree of the molecular signal with the synthetic gate receptor (this is also known as the *Hill* coefficient).

This is the author's version of an article that has been published in this journal. Changes were made to this version by the publisher prior to publication.
The final version of record is available at http://dx.doi.org/10.1109/TNB.2019.2930960

After reaching the threshold required to toggle the bacterium's natural switches, the circuit will start to operate. The first two gates shown in Figure 4 are activated by molecular input signals $w_i(t)$, where $i = \{1, 2, 3, 4\}$ are the molecular input's index, diffused from the environment into the synthetic logic circuit. The last logic gate is activated by the outputs ($z_1(t)$ and $z_2(t)$) from the gates in the first layer, producing the molecular signal $z_3(t)$. Considering the specific circuit design (see Figure 4), this last output molecular signal will only have a high concentration signal for the cases highlighted in Table I. Similar to (2) and (3), we use rate reaction equations to describe the production of the molecular signals $z_1(t)$, $z_2(t)$ and $z_3(t)$ by the synthetic logic gates [47]. Therefore, the OR gate is evaluated as

$$\begin{aligned}\frac{d[OR]}{dt} =& \frac{[C]^{n_C}}{K_C^{n_C} + [C]^{n_C}} + \frac{[D]^{n_D}}{K_D^{n_D} + [D]^{n_D}} \\ &- \gamma_{OR}[OR] + N_{OR}(t),\end{aligned} \tag{4}$$

where K_C and K_D define the rates (association constants) by which $[C]$ and $[D]$ bind to the OR gate receptors; γ_{OR} is the decay constant for $[OR]$; n_C, n_D are the Hill coefficients; and $N_{OR}(t)$ is the noise resulting from the chemical reaction for this synthetic logic gate. This noise term is modelled as an Additive White Gaussian Noise – AWGN. The "whitening effect" of the molecular noise in quorum sensing systems was investigated by [48]. Quorum sensing production noise can be modelled as a short noise with a wideband spectrum [49]. Shot noise is often modelled as a Poisson process, but if its mean value is large enough (following the central limit theorem), this noise can be modelled as a Gaussian noise [50]. In this case, if there is a large forward reaction rate compared to the reverse reaction rate, see (1), the noise will spread their frequency spectra and approximate it to an Additive White Gaussian Noise [48]. Following this assumption, our circuit will produce the output molecular signals in higher quantity, which will also prevent reverse reaction in (1) that will lead to the original input molecules. The reaction in (1) for both forward and reverse process generates the noise that is represented as an AWGN noise. Similarly, the AND gate is evaluated as

$$\begin{aligned}\frac{d[AND]}{dt} =& \frac{[E]^{n_E}}{K_E^{n_E} + [E]^{n_E}} \cdot \frac{[F]^{n_F}}{K_F^{n_F} + [F]^{n_F}} \\ &- \gamma_{AND}[AND] + N_{AND}(t),\end{aligned} \tag{5}$$

where K_E, K_F are the association constants for the signals $[E]$ and $[F]$; $\gamma_{AND}$is the decay constants for $[AND]$; n_E and n_F are the Hill coefficients for these molecular signals; and $N_{AND}(t)$ is the AWGN noise for these molecular output signals.

III. COMMUNICATIONS MODEL

An overview representation of the proposed bacteria-based molecular communications model is depicted in Figure 4. This synthetic logic circuit can be viewed, from a communications perspective, as a combination of three channels (see Figure 4b), which processes the molecular signals $a_i(t - \tau_i)$, $z_1(t)$, $z_2(t)$, $z_1'(t)$ and $z_2'(t)$. In this paper, we do not investigate the effects of the aqueous medium over the molecular input signals as they will be generated by sources much larger than the bacteria-based synthetic logic circuit, allowing them to retain their characteristics. In the following, we provide a detailed description of the proposed model for the synthetic logic circuit.

A. End-to-End Model

We model the bacteria-based synthetic logic circuit as a finite 2D aqueous environment where the molecular signals produced in the chambers A and B will freely diffuse towards the chamber C. The first layer of the synthetic circuit is activated by four molecular environmental signals, two different signals for each bacterial population, and is represented as

$$w_i(t - \tau_i) = W_i \frac{\exp\left(\frac{-(t-\tau_i)^2}{2\eta^2}\right)}{\sqrt{2\pi\eta}}, \tag{6}$$

where W_i is the pulse amplitude and η is the spread of the pulse. These four signals will be propagated from the external environment to the synthetic logic circuit and will bind to the receptors inside each bacterium to activate the internal toggle switches (see Figure 4). This internal bacterium system triggering process will result in the On-Off-Keying (OOK) modulation of the molecular signals $w_1(t - \tau_1)$, $w_2(t - \tau_2)$, $w_3(t - \tau_3)$ and $w_4(t - \tau_4)$. Therefore, the resulting molecular input signal is represented as

$$a_i(t - \tau_i) = w_i(t - \tau_i) * h_i(t), \tag{7}$$

where "*" denotes the convolution operator, $h_i(t)$ is a binary sequence that represents the toggle switch activation, modelled by (2) and (3). This sequence is defined as

$$h_i(t) = \begin{bmatrix} s_1 \\ s_2 \\ \vdots \\ s_l \end{bmatrix}, \tag{8}$$

where s_l are either 0 or 1, for the symbol duration t_s, $l = \{1, ..., t_f\}$ is the number of sequences and t_f is the total length of the system's operation (continuous values).

After being modulated, these molecular input signals will be evaluated by the first layer of the bacteria-based synthetic logic circuit (see Figure 4b). Each logic gate will then produce a molecular output signal ($z_1(t)$ for the OR gate and $z_2(t)$ for the AND gate) using (4) and (5) and is represented as

$$\begin{aligned}\frac{dz_1(t)}{dt} &= \frac{a_1(t-\tau_1)^{n_{a_1}}}{K_{a_1}^{n_{a_1}} + a_1(t-\tau_1)^{n_{a_1}}} + \frac{a_2(t-\tau_2)^{n_{a_2}}}{K_{a_2}^{n_{a_2}} + a_2(t-\tau_2)^{n_{a_2}}} \\ &\quad - \gamma_2 z_2(t) + N_2(t), \\ &= \frac{(w_1(t-\tau_1) * h_1(t))^{n_{a_1}}}{K_{a_1}^{n_{a_1}} + (w_1(t-\tau_2) * h_1(t))^{n_{a_1}}} + \\ &\quad \frac{(w_2(t-\tau_2) * h_2(t))^{n_{a_2}}}{K_{a_2}^{n_{a_2}} + (w_2(t-\tau_2) * h_2(t))^{n_{a_2}}} - \gamma_1 z_1(t) + N_1(t),\end{aligned} \tag{9}$$

This is the author's version of an article that has been published in this journal. Changes were made to this version by the publisher prior to publication.
The final version of record is available at http://dx.doi.org/10.1109/TNB.2019.2930960

$$\begin{aligned}\frac{dz_2(t)}{dt} &= \frac{a_3(t-\tau_3)^{n_{a_3}}}{K_{a_3}^{n_{a_3}} + a_3(t-\tau_3)^{n_{a_3}}} \cdot \frac{a_4(t-\tau_4)^{n_{a_4}}}{K_{a_4}^{n_{a_4}} + a_4(t-\tau_4)^{n_{a_4}}} \\ &- \gamma_2 z_2(t) + N_2(t), \\ &= \frac{(w_3(t-\tau_3) * h_3(t))^{n_{a_3}}}{K_{a_3}^{n_{a_3}} + (w_3(t-\tau_3) * h_3(t))^{n_{a_3}}} \\ &\cdot \frac{(w_4(t-\tau_4) * h_4(t))^{n_{a_4}}}{K_{a_4}^{n_{a_4}} + (w_4(t-\tau_4) * h_4(t))^{n_{a_4}}} - \gamma_2 z_2(t) + N_2(t).\end{aligned} \tag{10}$$

The molecular output signals are responsible for activating the next layer of the synthetic circuit. Thus, they are diffused from the chambers A and B to reach the chamber C, where the last layer of the synthetic circuit is located. The molecules that compose each molecular output signal will travel through the fluidic medium between the chambers independently from each other. The thin membrane that separates the chamber C from chambers A and B is composed of nanopores allowing only molecular output signals to pass through. This membrane is designed to limit only the bacterial movement [37]. Therefore, the Brownian motion for this system is characterised using the Fick's law of diffusion resulting in the following diffusion channels [51]

$$h_{z_1}(t_p) = \frac{1}{\sqrt{4\pi D_{z_1}(t_p)}} e^{\frac{-||d_{AC}||^2}{4D_{z_1}(t_p)}}, \tag{11}$$

$$h_{z_2}(t_p) = \frac{1}{\sqrt{4\pi D_{z_2}(t_p)}} e^{\frac{-||d_{BC}||^2}{4D_{z_2}(t_p)}}, \tag{12}$$

where $h_{z_1}(t_p)$ and $h_{z_2}(t_p)$ are the diffusion channel between chambers A and C, and between B and C, respectively; d_{AC} and d_{BC} are the Euclidean distance between chambers A and C, and between B and C, respectively; D_{z_1} and D_{z_2} are the diffusion coefficients for the molecular signals and t_p is propagation time inside the bacteria-based synthetic logic circuit. Each bacterium in the population, placed in both chambers A and B, will produce a molecular output signal concentration that will travel to chamber C. This spatially distributed molecular diffusion will generate a wave that will travel from one chamber to another (from A to C, and B to C). However, as the bacteria are close to each other, we assume that the distances d_{AC} and d_{BC} are between the centres of chambers A and C, and between the centres of chambers B and C. Therefore, this will represent the average distance travelled by the total molecular output signal concentration. Furthermore, this definition also affects the propagation time that is assumed to be small enough to travel from one population centre to another and maintain a high molecular concentration.

After being diffused, only a fraction of the molecular output signals $z_1(t)$ and $z_2(t)$ is able to reach the bacteria population in chamber C. Thus, using the results from (9) and (10) and operating them with the diffusion channels described in (11) and (12), we can obtain the fraction of the molecular output signals $z_1(t)$ and $z_2(t)$, respectively, as

$$z_1'(t) = z_1(t) * h_{z_1}(t-\tau_{z_1}), \tag{13}$$

and

$$z_2'(t) = z_2(t) * h_{z_2}(t-\tau_{z_2}). \tag{14}$$

By substituting (13) and (14) in (5), we are able to finally obtain the molecular output signal $z_3(t)$ as

$$\begin{aligned}\frac{dz_3(t)}{dt} &= \frac{z_1'(t)^{n_{z_1'}}}{K_{z_1'}^{n_{z_1'}} + z_1'(t)^{n_{z_1'}}} \cdot \frac{z_2'(t)^{n_{z_2'}}}{K_{z_2'}^{n_{z_2'}} + z_2'(t)^{n_{z_2'}}} \\ &- \gamma_3 z_3(t) + N_3(t), \\ &= \frac{(z_1(t) * h_{z_1}(t-\tau_{z_1}))^{n_{z_1'}}}{K_{z_1'}^{n_{z_1'}} + (z_1(t) * h_{z_1}(t-\tau_{z_1}))^{n_{z_1'}}} \\ &\cdot \frac{(z_2(t) * h_{z_2}(t-\tau_{z_2}))^{n_{z_2'}}}{K_{z_2'}^{n_{z_2'}} + (z_2(t) * h_{z_2}(t-\tau_{z_2}))^{n_{z_2'}}} - \gamma_3 z_3(t) + N_3(t),\end{aligned} \tag{15}$$

IV. CIRCUIT PERFORMANCE

We analyse the performance of this end-to-end molecular communications system using two distinct metrics: *circuit quality* and *channel capacity*. All the parameters considered for the performance analyses are presented in Table II. We would like to point out that the degradation rates γ_1, γ_2 and γ_3 values are chosen to be small enough, as well as, the association rates K_{a_1}, K_{a_2}, K_{a_3}, K_{a_4}, $K_{z_1'}$ and $K_{z_2'}$ are chosen to be high enough so the noise become AWGN and our analysis can be generalised for a wider range of molecular signal frequencies. The engineered bacteria population densities k_1, k_2 and k_3, as well as, the distances between the chamber compartments centres, d_{AC} and d_{BC}, are constrained by the chambers dimensions ($0.1 \times 0.6\,\text{cm}$), which is equivalent to the size of a drug pill.

The total length of the system's operation t_f, the pulse spread η, the pulse period t_d and the Hill coefficients n_{a_1}, n_{a_2}, n_{a_3}, n_{a_4}, $n_{z_1'}$, $n_{z_2'}$ are chosen to allow the production of a high molecular signal concentration due to the narrow and well-defined molecular input signal pulses (with proper rise and decay times). The molecular input signals arrays ρ_{a_1}, ρ_{a_2}, ρ_{a_3} and ρ_{a_4} have 160 samples each. They are processed by the first layer of the circuit within 25 hours, resulting in a new molecular signal arrays ρ_{z_1}, ρ_{z_2} of $4,000$ samples, which are propagated for $t_p = 0.5$ hours. This will result in higher molecular signal concentration at the centre of the engineered bacteria population placed in compartment C of the chamber, which will subsequently be processed in the following 25 hours by the last synthetic logic gate, resulting in a molecular output signal of $100,000$ samples.

The quality of a system will depend on how it will perform the designed task under certain circumstances [52]. Therefore, to assess the quality of the proposed bacteria-based synthetic circuit, we describe this metric in terms of the *accuracy*, *precision*, *recall*, *false positives (FP)* and *false negatives (FN)* rates, for the molecular output signal $z_3(t)$. The channel

This is the author's version of an article that has been published in this journal. Changes were made to this version by the publisher prior to publication.
The final version of record is available at http://dx.doi.org/10.1109/TNB.2019.2930960

TABLE II
PARAMETERS CONSIDERED FOR THIS ANALYSIS

Variable	Value	Unit	Reference
k_1, k_2, k_3	$10,000$	CFU	*
B_r	0.5	μm	[53]
d_{AC}, d_{BC}	500	μm	*
t_f	50.5	hours	*
t_d	10	hours	*
t_p	0.5	hour	*
D_{z_1}, D_{z_2}	4.9	cm^2/h	[54]
γ_1, γ_2, γ_3	0.1	–	*
K_{a_1}, K_{a_2}, K_{a_3}, K_{a_4}, $K_{z'_1}$, $K_{z'_2}$	10	–	*
n_{a_1}, n_{a_2}, n_{a_3}, n_{a_4}, $n_{z'_1}$, $n_{z'_2}$	2	–	*
η	0.5	–	*
ρ_{a_1}, ρ_{a_2}, ρ_{a_3}, ρ_{a_4}	160	samples	*
ρ_{z_1}, ρ_{z_2}	4,000	samples	*
ρ_{z_3}	100,000	samples	*

* Values chosen by the authors.

capacity represents the maximum throughput that the system can achieve under specific conditions.

A. Circuit Quality

For the first metric, we investigate the impact of the noise and the molecular environmental delay on the production of reliable molecular output signal $z_3(t)$. To evaluate the quality of the proposed synthetic circuit, we first define the minimum molecular concentration levels required for the activation of each bacteria-based synthetic logic gate (for a molecular input signal total length of the system's operation t_f). These thresholds are represented as follows.

$$T_{a_i} = \frac{\max(a_i(t))}{2}, \tag{16}$$

$$T_{z_m} = \frac{\max(z_m(t))}{2}, \tag{17}$$

where a_i represents each $i = \{1, 2, 3, 4\}$ molecular input signal, and z_m represents each $m = \{1, 2, 3\}$ molecular output signal (see Figure 4).

For all of the analyses presented in this paper, we considered each molecular input signal as an array with ρ_{a_i} samples and each molecular output signal as an array with ρ_{z_m} samples. These samples can be defined as positive (high level) when it is above the considered threshold and negative (low level) when it is the opposite. The overall quality of the proposed synthetic circuit will depend on the correct identification of the positive and negative molecular output signal samples. In this case, we first define the *accuracy_ratio*, which is the number of samples that are correctly detected as positive or negative over the total number of samples. This is represented as [52]

$$accuracy\_ratio = \frac{TP + TN}{TP + TN + FP + FN} \times 100, \tag{18}$$

where TP and TN are the number of molecular output signal samples that are correctly detected above and below the defined thresholds, respectively; FP and FN are the number of molecular output signal samples that are not correctly detected above and below the defined thresholds, respectively. The *precision_ratio* is defined as the number of true positive identification over the total positive identifications detected, independent of being either true or false. This is represented as [52],

$$precision\_ratio = \frac{TP}{TP + FP} \times 100. \tag{19}$$

The *recall_ratio* or system sensitivity is defined as the number of true positives over the sum of samples that are detected as positive and the ones that should be detected as high level as well. Therefore [52],

$$recall\_ratio = \frac{TP}{TP + FN} \times 100. \tag{20}$$

Using the detected number of false negatives and false positives, we can define the *false positive_ratio (FP_ratio)* and *false negative_ratio (FP_ratio)* as [52]

$$FN\_ratio = \frac{FN}{FN + TP} \times 100, \tag{21}$$

$$FP\_ratio = \frac{FP}{FP + TN} \times 100. \tag{22}$$

Using (21), we can also express the *recall_ratio* as

$$recall\_ratio = 1 - FN\_ratio. \tag{23}$$

B. Channel Capacity

Using the thresholds defined in (16)–(17), we evaluate the channel capacity based on the probabilities of each sample of for the molecular input signals as well as output signal $z_3(t)$, and this can be for both high or low levels. Therefore, we define $p_0(k)$ and $p_1(k)$ as the probabilities of obtaining a low or high (which are represented as 0 or 1) molecular output signals $z_3(t)$, respectively. These probabilities are agnostic with respect to the definition of true positives and negatives (including their counterparts). For the channel capacity evaluation, we do not focus on classifying the molecular output signal, but in quantifying the received quantity of low and high molecular output signals from the last gate output. We also define $p_0(k|j_1, j_2, j_3, j_4)$ and $p_1(k|j_1, j_2, j_3, j_4)$ as the conditional probabilities of obtaining a high or low level molecular output signal sample k depending on the molecular input signal samples j_1, j_2, j_3, and j_4, where $j_i \in \{0, 1\}$.

Next, we define the information entropy for the molecular output signal $z_3(t)$ as

$$H(z_3(t)) = -\sum_{k=0}^{\rho_{z_3}} p_{0,1}(k) \log_2 p_{0,1}(k). \tag{24}$$

Similarly, the conditional entropy of the molecular output signal $z_3(t)$ for molecular input signals $a_1(t)$, $a_2(t)$, $a_3(t)$

This is the author's version of an article that has been published in this journal. Changes were made to this version by the publisher prior to publication.
The final version of record is available at http://dx.doi.org/10.1109/TNB.2019.2930960

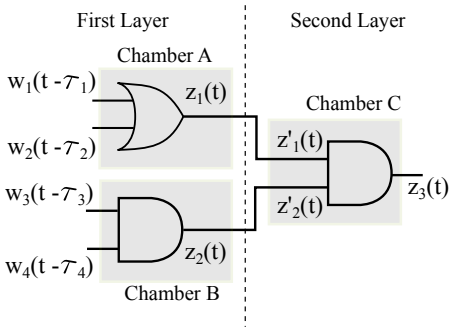

Fig. 5. Representation of the synthetic circuit and the molecular signals considered for this bacteria-based molecular communications system. When the system is not subjected to molecular environmental delays ($\tau_1 = \tau_2 = \tau_3 = \tau_4 = 0$) the molecular output signal is defined as ideal. For the delayed case, we defined $\tau_1 = \tau_3 = 0$ and varied the τ_2 and τ_4 values.

and $a_4(t)$ is defined as

$$H(z_3|a_1(t),a_2(t),a_3(t),a_4(t))) = -\sum_{j_1=0}^{\rho_{a_1}}\sum_{j_2=0}^{\rho_{a_2}}\sum_{j_3=0}^{\rho_{a_3}}\sum_{j_4=0}^{\rho_{a_4}} p_{0,1}(j_1,j_2,j_3,j_4) \cdot \sum_{k=0}^{\rho_{z_3}} p_{0,1}(k|(j_1,j_2,j_3,j_4)) \cdot \log_2 p_{0,1}(k|(j_1,j_2,j_3,j_4)). \quad (25)$$

However, as $p_{0,1}(k|(j_1,j_2,j_3,j_4)) = p_{0,1}(k)$, (25) can be rewritten as

$$H(z_3|a_1(t),a_2(t),a_3(t),a_4(t))) = -\sum_{k=0}^{\rho_{z_3}}[p_{0,1}(k)\log_2 p_{0,1}(k)] \cdot \sum_{j_1=0}^{\rho_{a_1}}\sum_{j_2=0}^{\rho_{a_2}}\sum_{j_3=0}^{\rho_{a_3}}\sum_{j_4=0}^{\rho_{a_4}} p_{0,1}(j_1,j_2,j_3,j_4). \quad (26)$$

The channel capacity for this system is defined by the maximum mutual information between the molecular output signal $z_3(t)$ and the molecular input signals $a_1(t)$, $a_2(t)$, $a_3(t)$ and $a_4(t)$, and is represented as,

$$C_{sys} = \max_{p_{z_3(t)}}[I(z_3(t);a_1(t),a_2(t),a_3(t),a_4(t))], = \max_{p_{z_3(t)}}[H(z_3(t)) - H(z_3(t)|a_1(t),a_2(t),a_3(t),a_4(t))]. \quad (27)$$

We use the entropy and conditional entropy values $H(z_3(t))$ and $H(z_3(t)|a_1(t),a_2(t),a_3(t),a_4(t))$ obtained from (24) and (26) to rewrite (27) as

$$C_{sys} = \max_{p_{z_3(t)}}\Big[-\sum_{k=0}^{s_{z_3}}[p_{0,1}(k)\log_2 p_{0,1}(k)] + \sum_{k=0}^{\rho_{z_3}}[p_{0,1}(k)\log_2 p_{0,1}(k)] \cdot \sum_{j_1=0}^{\rho_{a_1}}\sum_{j_2=0}^{\rho_{a_2}}\sum_{j_3=0}^{\rho_{a_3}}\sum_{j_4=0}^{\rho_{a_4}} p_{0,1}(j_1,j_2,j_3,j_4)\Big]. \quad (28)$$

V. ANALYTICAL RESULTS

In this section, we analyse the operation of the bacteria-based synthetic logic circuit by evaluating its quality and channel capacity. The aim of this analysis is to study the performance of the proposed bacteria-based molecular communications system and define the design parameters required for an accurate operation of the synthetic logic circuit.

Consider a scenario where the system operates under ideal conditions, and this means that the molecular output signal will not suffer from any deterioration in concentration and at the same time the synthetic logic gates of all layers will operate as expected. Figure 5 illustrate the synthetic logic circuit and the molecular signals considered for the proposed system. For our analyses, we considered a synchronised transmission where no molecular environmental delay is present ($\tau_1 = \tau_2 = \tau_3 = \tau_4 = 0$), and delayed scenarios where we considered two molecular environmental delays as $\tau_1 = \tau_3 = 0$ and varied the other two (τ_2 and τ_4). Figure 6 presents four plots to illustrate the synchronized and the delayed operation of the proposed bacteria-based synthetic circuit. Figure 6(a) shows the molecular output signals $z_1(t)$ and $z_2(t)$ when the molecular environmental signals are synchronised with each other (they do not suffer with the molecular environmental delays, $\tau_1 = \tau_2 = \tau_3 = \tau_4 = 0$). Figure 6(b) shows the molecular output signals $z_1(t)$ and $z_2(t)$ when $w_2(t-\tau_2)$ and $w_4(t-\tau_4)$ are delayed by 5 hours (half of the pulse period, $\tau_2 = \tau_4 = t_p/2$). As we can see there are high $z_1(t)$ and low $z_2(t)$ signals produced when compared to the case depicted in Figure 6(a). IIn general, situations where different molecules are produced from the environment, the molecular environmental signals can arrive delayed into the first layer of the synthetic circuit, and aggregated random system effects can also occur, leading to inaccurate outputs from the circuit. This scenario can be observed by comparing the Figures 6(c) and 6(d). The molecular output signal $z_3(t)$ obtained from the ideal operation of the circuit, shown in Figure 6(c), is higher than the one produced in a delayed scenario, shown in Figure 6(d). Furthermore, when subjected to molecular environmental delays, the synthetic logic circuit also produced the wrong molecular output signals. Our interest is to investigate further this phenomenon. We analyse different cases in order to define the most appropriate trade-off between the unwanted effects occurring in the first layer of the circuit and the system performance.

In addition to the delayed molecular environmental signals, we also considered the output bit-1 ratio and the gates inputs

This is the author's version of an article that has been published in this journal. Changes were made to this version by the publisher prior to publication.
The final version of record is available at http://dx.doi.org/10.1109/TNB.2019.2930960

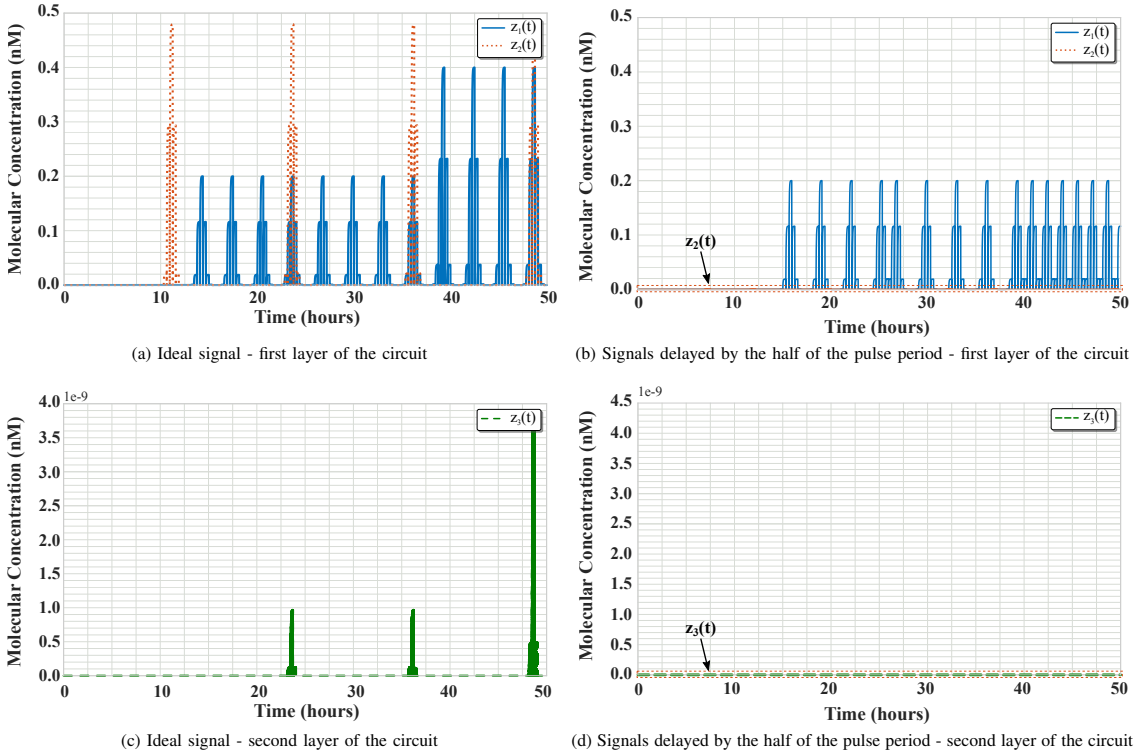

(a) Ideal signal - first layer of the circuit

(b) Signals delayed by the half of the pulse period - first layer of the circuit

(c) Ideal signal - second layer of the circuit

(d) Signals delayed by the half of the pulse period - second layer of the circuit

Fig. 6. Representation of the molecular output signals $z_1(t)$, $z_2(t)$ and $z_3(t)$. For all cases, we considered $h_i(t)$ as deterministic sequence of symbols. (a) Representation of the ideal molecular output signals $z_1(t)$ and $z_2(t)$ from the bacteria-based synthetic logic circuit. (b) When the molecular input signals $w_2(t-\tau_2)$ and $w_4(t-\tau_4)$ are delayed $\tau_2 = \tau_4 = t_d/2$, the molecular output signals $z_1(t)$ and $z_2(t)$ do not have the same concentration levels of the previous case. (c) As $z_1(t)$ and $z_2(t)$ are ideal, the molecular output signal $z_3(t)$ also will be ideal. (d) Due the molecular environmental delays, the molecular output signal have lower concentration levels than when the system works on an ideal conditions and it produces wrong molecular output signals.

concentration difference as possible unwanted effects for the bacteria-based synthetic logic circuit. If the molecular input signal is composed of a large sequence of bit-1, this excess molecular signals can increase the noise that the bacteria populations are being subjected to, and consequently, can degrade the performance of the communications. A similar effect can occur if a large concentration of molecular input signal arrives at the bacteria population in chambers A and B. Therefore, we focus on these three issues to analyse the performance of the molecular communications of the proposed bacteria-based synthetic logic circuit.

A. Circuit Quality Analysis

As discussed in the previous sections, conventional digital circuits can have their quality affected if delays are introduced in the system. Therefore, we first investigate the impact caused by a delayed molecular environmental signal on the accuracy, precision, recall, false negative and false positive rates of the circuit.

For this analysis, we define a pulse period $t_d = 10$ hours, total length of the system's operation $t_f = 50.5$ hours for the molecular input signals $a_1(t)$, $a_2(t)$, $a_3(t)$ and $a_4(t)$; an

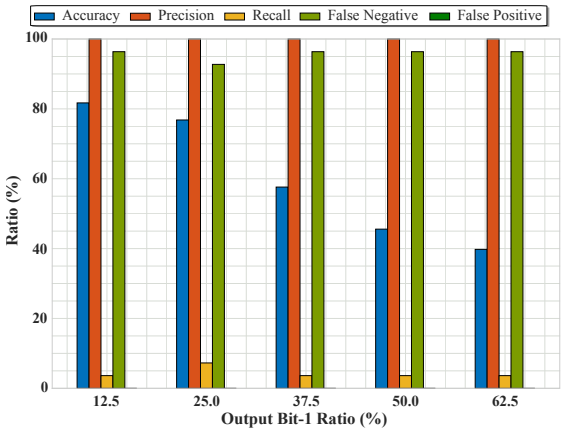

Fig. 7. Quality metrics results for different output bit-1 ratio. For the considered scenario, the circuit worked with 100% of precision, and no false positive was detected.

AWGN noise $N_{A,B}(t)$ with average $\mu_N = 0$ and standard deviation of $\sigma_N^{A,B} = 2 \cdot 10^{-4}$ nM for the bacteria populations

This is the author's version of an article that has been published in this journal. Changes were made to this version by the publisher prior to publication.
The final version of record is available at http://dx.doi.org/10.1109/TNB.2019.2930960

located in chambers A and B; a second AWGN noise $N_C(t)$ with average $\mu_N = 0$ and standard deviation of $\sigma_N^C = 2{\cdot}10^{-13}$ nM for the bacteria population located in chamber C; and we considered the molecular input channels $h_i(t)$ as pseudorandom sequences. These noise values were chosen to represent the small fluctuations that can occur during the molecular output signal production [55]. We also considered that two of the molecular environmental signals are delayed by 5 hours (half of the pulse period), and varied the output bit-1 ratio from 12.5% to 62.5% of the total number of bits present in the pseudorandom sequences $h_1(t)$, $h_2(t)$, $h_3(t)$ and $h_4(t)$. We considered a fixed amplitude for the molecular environmental signals $W_1 = W_2 = 5$ nM and $W_3 = W_4 = 15$ nM. No gate input concentration difference was considered for this case.

We can observe in Figure 7 that the *accuracy_ratio* decreases proportionally with the increase in the output bit-1 ratio. Therefore, higher output bit-1 ratios result in a worse synthetic logic circuit performance. On the other hand, the *precision_ratio* remained 100% for all of the considered output bit-1 ratio values, meaning that there is no false positive detected. In the case considered, the *recall_ratio* remained below 10%, which means that the number of samples wrongly identified as negative is high, and this is based on (20). The *FN_ratio* value observed from Figure 7 validate this observation, and this is based on (23). Specifically, the circuit misses most of the positive samples, therefore classifying them as negative. This issue is directly related to the threshold definition, and its solution is tied to the selection of a better detection technique. It can be deduced from these results that the output bit-1 ratio is an important unwanted effect for this circuit as it can severely affect the accuracy of the results. In the case of the high false negative ratio, this can be addressed by improving the system reception e.g., this could mean engineering bacteria to be more sensitive to molecules in the last chamber C. Furthermore, the timing that the molecular input signals reach the bacteria populations should be well defined to improve the accuracy of the bacteria-based synthetic logic gates.

B. Communications Analysis

Channel capacity is an important metric to describe the performance of any communications system. From this perspective, we investigate the effect of the delayed molecular environmental signals as well as the output bit-1 ratio and the gate input concentration difference on the channel capacity for this bacteria-based molecular communications system. For this analysis, we considered the same AWGN noises from the quality analysis, and the amplitude of the molecular environmental signals as $W_1 = 5$ nM, a variable amplitude of W_2 ranging from 5 to 9 nM, $W_3 = 15$, a variable amplitude of W_4 ranging from 15 to 19 nM. The signal amplitudes were selected to enable the investigation of the impact caused on the channel capacity by the gate inputs concentration difference for the two gates placed in the chambers A and B.

We compared the circuit accuracy with the channel capacity to evaluate their relationship. We considered that the molecular input signals are synchronised, and the molecular input

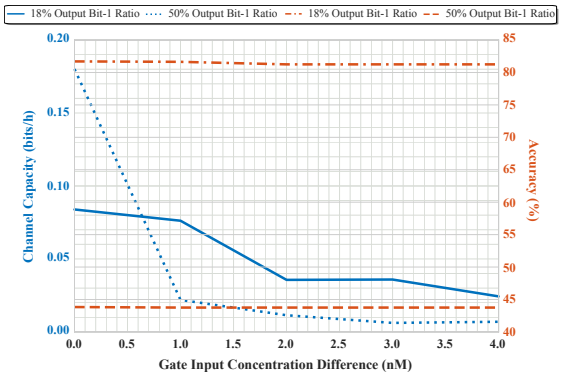

Fig. 8. Evaluation of the channel capacity and circuit accuracy, for a gate inputs concentration difference ranging from 0 to 4 nM.

channels $h_i(t)$ as random sequences, producing two different output bit-1 ratios (18% and 50%). It can be observed from Figure 8 that the *accuracy_ratio*, for both molecular input channels, slightly varies with respect to the gate input concentration difference. On the other hand, the channel capacity shows a noticeable variation when the gate input concentration difference and the output bit-1 ratio are increased. For the 18% output bit-1 ratio (dotted line, see Figure 8), the channel capacity start with a higher value than the 50% case (solid line, see Figure 8), but stays below 0.02 bits/h after increasing the gate input concentration difference to 1 nM. In contrast, the 50% output bit-1 ratio reaches this channel capacity value after 4 nM. This result suggests the existence of a trade-off between a highly accurate system and a high channel capacity, which is related to the output bit-1 ratio. Therefore, this system design imposes a limitation on the amount of molecular signal that can be accurately processed on the circuit's last gate.

Based on the results presented in Figure 8, we decide to investigate the effect of the molecular environmental delay and the gate inputs concentration difference on the channel capacity when the circuit has an accuracy above 80%. Using (27) and considering a molecular input channel $h_i(t)$ that produces a 50% output bit-1 ratio, we evaluate the system's channel capacity when there is no delay associated with the molecular environmental signals arriving at the bacteria populations located in chambers A and B, and when they are delayed by 2 hours ($\tau_2 = \tau_4 = t_p/5$) and 5 hours ($\tau_2 = \tau_4 = t_p/2$). Figure 9 shows that the channel capacity is inversely proportional to the gate input concentration difference. It also can be noted that for both the synchronised and the 2 hours delay cases, there is a small decrease in the channel capacity when compared to the 5 hours delay case. This result shows that the system can tolerate moderate molecular environmental delays and converge to a steady-state value for the channel capacity. If the proposed bacteria-based synthetic circuit is subjected to a high molecular environmental delay, a buffer or other techniques that will adjust the timing of the molecular input signal might be placed in the chambers A and B to counter this unwanted effect.

For our final analysis, we varied the molecular environ-

This is the author's version of an article that has been published in this journal. Changes were made to this version by the publisher prior to publication.
The final version of record is available at http://dx.doi.org/10.1109/TNB.2019.2930960

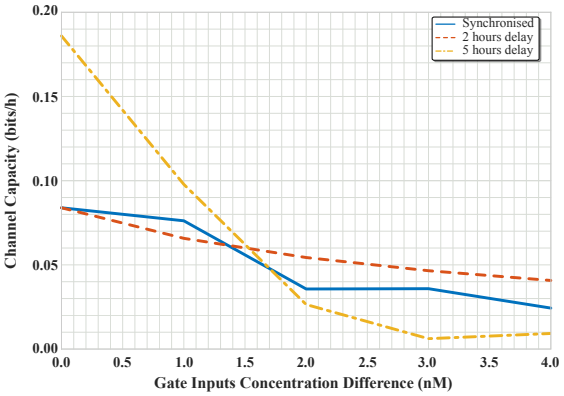

Fig. 9. Evaluation of the channel capacity, for various gate inputs concentration difference for a synchronised and delayed molecular environmental signals.

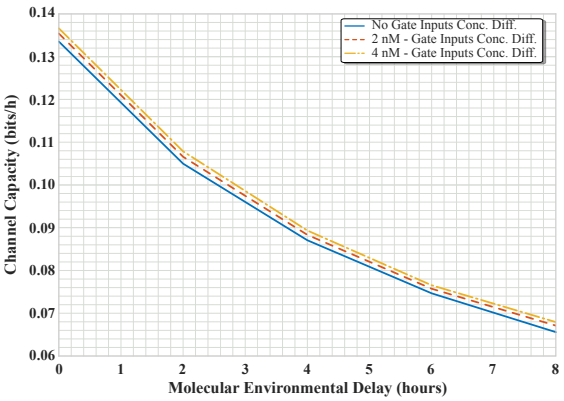

Fig. 10. Channel capacity for different molecular environmental delays, considering three gate inputs concentration difference values.

mental delay, and considered the molecular input channels $h_i(t)$ that produces a 50% output bit-1 ratio, which results in a circuit accuracy of more than 80%. Therefore, Figure 10 shows that the molecular environmental delay can severely affect the channel capacity. On the other hand, greater gate inputs concentration difference result in slightly higher channel capacity. This result corroborates with the result presented in Figure 9 and demonstrates the impact of the gate input concentration difference and the delay on the bacteria-based synthetic logic circuit.

VI. CONCLUSION

In recent years, new applications have emerged for molecular communications, and in particular through the application of synthetic biology. In this paper, we present the use of molecular communications between bacteria populations that can be used to create synthetic logic circuits. Each population represents a gate, and the communication bus between the gates is established through molecular communications. Given the stochastic property of molecular communications, the paper investigates the quality of the synthetic circuit to determine its accuracy that is dependent on variations of molecular signal input delays, as well as the amplitude of the molecular environmental signals. We also utilized communications theory in terms of channel capacity between the gates and its impact on the quality of the circuit. We found that the molecular concentration difference between the inputs of the circuit can disrupt the operation of the synthetic logic gate, and this can also be affected by the reception thresholds. The molecular concentration difference between the circuit's inputs can impact on the wrong definition in the high and low molecular concentration levels, which can degrade both the quality and channel capacity. Our results suggest that the system can operate with an accuracy above 80%, and the output bit-1 ratio plays a major role in the evaluation of the quality and system performance. These metrics could be further improved by optimising the molecular signal reception on the circuit's last gate. From the obtained results, we can infer that the combination of synthetic biology and molecular communications is an important tool for the design, performance and quality evaluation of bacteria-based synthetic logic circuits.

ACKNOWLEDGMENT

This work was partially funded by 1) Science Foundation Ireland via the CONNECT research centre (grant no. 13/RC/2077), 2) Science Foundation Ireland via the Vistamilk research centre and 3) Academy of Finland Research Fellow (grant no. 284531).

REFERENCES

[1] I. F. Akyildiz, J. M. Jornet, and M. Pierobon, "Nanonetworks: A New Frontier in Communications", *Communications of the ACM*, vol. 54, no. 11, pp. 84-89, Nov. 2011.
[2] A. Marcone, M. Pierobon, and M. Magarini, "Parity-Check Coding Based on Genetic Circuits for Engineered Molecular Communication Between Biological Cells," *IEEE Transactions on Communications*, vol. 66, no. 12, pp. 6221–6236, Dec. 2018.
[3] J. R. Porter and E. Batchelor, "Using Computational Modeling and Experimental Synthetic Perturbations to Probe Biological Circuits," in *Computational Methods in Synthetic Biology*, ser. Methods in Molecular Biology, M. A. Marchisio, Ed. New York, NY: Springer New York, 2015, vol. 1244, pp. 259–276.
[4] C. Sabu *et al.*, "Bioinspired and biomimetic systems for advanced drug and gene delivery," *Journal of Controlled Release*, vol. 287, no. June, pp. 142–155, Aug. 2018.
[5] R. Sarpeshkar, "Analog synthetic biology," *Philosophical Transactions of the Royal Society A: Mathematical, Physical and Engineering Sciences*, vol. 372, no. 2012, pp. 20 130 110–20 130 110, Feb. 2014.
[6] D. T. Riglar and P. A. Silver, "Engineering bacteria for diagnostic and therapeutic applications," *Nature Reviews Microbiology*, vol. 16, no. 4, pp. 214–225, Feb. 2018.
[7] Y. Higashikuni, W. C. Chen, and T. K. Lu, "Advancing therapeutic applications of synthetic gene circuits," *Current Opinion in Biotechnology*, vol. 47, pp. 133–141, Aug. 2017.
[8] H. K. Allen *et al.*, "Finding alternatives to antibiotics," *Annals of the New York Academy of Sciences*, vol. 1323, no. 1, pp. 91–100, sep 2014.
[9] P. Hillenbrand, G. Fritz, and U. Gerland, "Biological Signal Processing with a Genetic Toggle Switch," *PLoS ONE*, vol. 8, no. 7, p. e68345, Jul. 2013.
[10] B. Saltepe *et al.*, "Cellular Biosensors with Engineered Genetic Circuits," *ACS Sensors*, vol. 3, no. 1, pp. 13–26, Nov. 2018.
[11] J. J. Collins, T. S. Gardner, and C. R. Cantor, "Construction of a genetic toggle switch in Escherichia coli," *Nature*, vol. 403, no. 6767, pp. 339–342, Jan. 2000.

This is the author's version of an article that has been published in this journal. Changes were made to this version by the publisher prior to publication.
The final version of record is available at http://dx.doi.org/10.1109/TNB.2019.2930960

[12] N. Dalchau *et al.*, "Computing with biological switches and clocks," *Natural Computing*, vol. 17, no. 4, pp. 761–779, June 2018.
[13] A. Urrios *et al.*, "Plug-and-Play Multicellular Circuits with Time-Dependent Dynamic Responses," *ACS Synthetic Biology*, vol. 7, no. 4, pp. 1095–1104, Mar. 2018.
[14] A. Sengupta, H. B. Pakrasi, and P. P. Wangikar, "Recent advances in synthetic biology of cyanobacteria," *Applied Microbiology and Biotechnology*, pp. 1–15, May 2018.
[15] A. Tamsir, J. J. Tabor, and C. A. Voigt, "Robust multicellular computing using genetically encoded NOR gates and chemical 'wires'", *Nature*, vol. 469, no. 7329, pp. 212–215, Jan. 2011.
[16] T. Nakano, A. W. Eckford, and T. Haraguchi, "Molecular communication", Cambridge University Press, 2013.
[17] L. Felicetti *et al.*, "Applications of molecular communications to medicine: A survey," *Nano Communication Networks*, vol. 7, pp. 27–45, Mar. 2016.
[18] O. B. Akan *et al.*,"Fundamentals of molecular information and communication science",*Proceedings of the IEEE*, vol. 105, no. 2, pp. 306–318, Feb. 2017.
[19] M. T. Barros, "Ca2+-signaling-based molecular communication systems: Design and future research directions," *Nano Communication Networks*, vol. 11, pp. 103–113, Mar. 2017.
[20] Y. Chahibi, "Molecular communication for drug delivery systems: A survey," *Nano Communication Networks*, vol. 11, pp. 90–102, Mar. 2017.
[21] V. Loscrì, A. M. Vegni, and G. Fortino, "On the Interaction between a Nanoparticulate System and the Human Body in Body Area Nanonetworks," *Micromachines*, vol. 6, no. 9, pp. 1213-1235, Aug. 2015.
[22] B. Atakan, O. B. Akan, and S. Balasubramaniam, "Body area nanonetworks with molecular communications in nanomedicine", *IEEE Communications Magazine*, vol. 50, no. 1, pp. 28–34, Jan. 2012.
[23] T. Nakano *et al.*, "Molecular Communication and Networking: Opportunities and Challenges," *IEEE Transactions on NanoBioscience*, vol. 11, no. 2, pp. 135–148, Jun. 2012.
[24] G. Wei and R. Marculescu, "Miniature Devices in the Wild: Modeling Molecular Communication in Complex Extracellular Spaces," *IEEE Journal on Selected Areas in Communications*, vol. 32, no. 12, pp. 2344–2353, Dec. 2014.
[25] A. O. Bicen, J. J. Lehtomäki, and I. F. Akyildiz, "Shannon Meets Fick on the Microfluidic Channel: Diffusion Limit to Sum Broadcast Capacity for Molecular Communication," *IEEE Transactions on NanoBioscience*, vol. 17, no. 1, pp. 88–94, 2018.
[26] L. Felicetti *et al.*, "TCP-like molecular communications", *IEEE Journal on Selected Areas in Communications*, vol. 32, no. 12, pp. 2354–2367, Dec. 2014.
[27] V. Loscrì, L. Matekovits, I. Peter, and A. M. Vegni, "In-body Network Biomedical Applications: from Modeling to Experimentation,", *IEEE Transaction on Nanobioscience*, vol. 15, no. 1, pp. 53-61, Jan. 2016.
[28] L. C. Cobo and I. F. Akyildiz, "Bacteria-based communication in nanonetworks," *Nano Communication Networks*, vol. 1, no. 4, pp. 244–256, Dec. 2010.
[29] A. Einolghozati, M. Sardari, and F. Fekri, "Design and Analysis of Wireless Communication Systems Using Diffusion-Based Molecular Communication Among Bacteria," *IEEE Transactions on Wireless Communications*, vol. 12, no. 12, pp. 6096–6105, Dec. 2013.
[30] D. P. Martins *et al.*, "Molecular Communications Pulse-Based Jamming Model for Bacterial Biofilm Suppression," *IEEE Transactions on NanoBioscience*, vol. 17, no. 4, pp. 533–542, Oct. 2018.
[31] D. Ausländer *et al.*, "Programmable full-adder computations in communicating three-dimensional cell cultures," *Nature Methods*, vol. 15, no. 1, p. 57, Dec. 2018.
[32] Z. Li *et al.*,"Bacteria-based AND logic gate: a decision-making and self-powered biosensor", *Chemical Communications*, vol. 47, no. 11, pp. 3060–3062, Mar. 2011.
[33] K. Kim *et al.*,"Logic circuit upon angiogenic response controlled by enzyme-linked iron oxide microparticles–towards biocomputing in human cells", *Chemical Communications*, vol. 48, no. 55, pp. 6918–6920, May 2012.
[34] Y. Hu *et al.*, "Programming the quorum sensing-based AND gate in Shewanella oneidensis for logic gated-microbial fuel cells",*Chemical Communications*, vol. 51, no. 20, pp. 4814–4817, Feb. 2015.
[35] J. Qian, S. Pullela, and L. Pillage, "Modeling the "Effective capacitance" for the RC interconnect of CMOS gates," *IEEE Transactions on Computer-Aided Design of Integrated Circuits and Systems*, vol. 13, no. 12, pp. 1526–1535, Dec. 1994.
[36] F. Dartu, N. Menezes, and L. Pileggi, "Performance computation for precharacterized CMOS gates with RC loads," *IEEE Transactions on Computer-Aided Design of Integrated Circuits and Systems*, vol. 15, no. 5, pp. 544–553, May 1996.
[37] J. Shim *et al.*, "Controlling the contents of microdroplets by exploiting the permeability of PDMS," *Lab on a Chip*, vol. 11, no. 6, p. 1132, Mar. 2011.
[38] D. E. Contois, "Kinetics of Bacterial Growth: Relationship between Population Density and Specific Growth Rate of Continuous Cultures",*Microbiology*, vol. 21, no. 1, pp. 40–50, Aug. 1959.
[39] C. C. Spicer, "The Theory of Bacterial Constant Growth Apparatus", *Biometrics*, vol. 11, no. 2, pp. 225–230, June 1955.
[40] M. Pierobon and I. F. Akyildiz, "A Physical End-to-End Model for Molecular Communication in Nanonetworks," *IEEE Journal on Selected Areas in Communications*, vol. 28, pp. 602–611, May 2010.
[41] T. Sakurai, "Closed-Form Expressions for Interconnection Delay, Coupling, and Crosstalk in VLSI's," *IEEE Transactions on Electron Devices*, vol. 40, no. 1, pp. 118–124, Jan. 1993.
[42] S. Krishnaswamy *et al.*, "Probabilistic transfer matrices in symbolic reliability analysis of logic circuits," *ACM Transactions on Design Automation of Electronic Systems*, vol. 13, no. 1, pp. 1–35, Jan. 2008.
[43] P. Mehta *et al.*, "Information processing and signal integration in bacterial quorum sensing," *Molecular Systems Biology*, vol. 5, no. 1, p. 325, Jan. 2009.
[44] W. K. Purves *et al.*, *Life: The Science of Biology*. Macmillan, 2001.
[45] M. Kuscu and O. B. Akan, "Maximum Likelihood Detection With Ligand Receptors for Diffusion-Based Molecular Communications in Internet of Bio-Nano Things," *IEEE Transactions on NanoBioscience*, vol. 17, no. 1, pp. 44–54, Jan. 2018.
[46] M. Pierobon and I. F. Akyildiz, "Noise Analysis in Ligand-Binding Reception for Molecular Communication in Nanonetworks," *IEEE Transactions on Signal Processing*, vol. 59, no. 9, pp. 4168–4182, 2011.
[47] J. Bonnet *et al.*, "Amplifying Genetic Logic Gates," *Science*, vol. 340, no. 6132, pp. 599–603, May 2013.
[48] C. D. Cox *et al.*, "Analysis of noise in quorum sensing," *Omics: a journal of integrative biology*, vol. 7, no. 3, pp. 317–34, Sep. 2003.
[49] M. L. Simpson *et al.*, "Frequency domain analysis of noise in autoregulated gene circuits", *Proceedings of the National Academy of Sciences*, vol. 100, no. 8, pp. 4551–4556, Apr. 2003.
[50] A. Papoulis, and S. Unnikrishna Pillai, "Probability, random variables, and stochastic processes", Tata McGraw-Hill Education, 2002.
[51] I. Llatser *et al.*, "N3Sim: Simulation framework for diffusion-based molecular communication nanonetworks," *Simulation Modelling Practice and Theory*, vol. 42, pp. 210–222, Dec. 2013.
[52] D. L. Olson and D. Delen, *Advanced Data Mining Techniques*. Springer Science & Business Media, 2008.
[53] W. R. Schneider and N. R. Doetsch, "Effect of Viscosity on Bacterial Motility," *Journal of Bacteriology*, vol. 117, no. 2, pp. 696–701, Feb. 1974.
[54] P. Melke *et al.*, "A Cell-Based Model for Quorum Sensing in Heterogeneous Bacterial Colonies," *PLoS Computational Biology*, vol. 6, no. 6, pp. 1–13, June 2010.
[55] M. Thattai and A. van Oudenaarden,"Intrisic noise in gene regulatory networks", *Proceedings of the National Academy of Science*, vol. 98, no. 15, pp. 8614–8619, July 2001.

CHAPTER 10

JOURNAL PAPER: FREQUENCY ANALYSIS OF LOGIC COMPUTATION FOR BACTERIA-BASED BIOSENSOR MOLECULAR COMMUNICATION SYSTEM

Journal Title:	IEEE Transactions on Communications
Article Type:	Regular Paper
Complete Author List:	Daniel Perez Martins, Michael Taynnan Barros, Thitipol Sinkruasuan, Lee Coffey, Paul D. Cotter, Donagh P. Berry, and Sasitharan Balasubramaniam
Keywords:	Cellular logic, Communication systems, Frequency domain analysis.
Status:	Submitted

Frequency Analysis of Logic Computation for Bacteria-based Biosensor Molecular Communication System

Daniel P. Martins, *Student Member, IEEE,* Michael Taynnan Barros, *Member, IEEE,* Lee Coffey, Paul D. Cotter, Donagh P. Berry, and Sasitharan Balasubramaniam, *Senior Member, IEEE*

***Abstract*—Synthetic biology has facilitated the engineering of biological cells to mimic electrical components, and systems targeting a diverse range of applications. One example is the design of logic gates that can sense and compute molecular signals. However, the capabilities and performance of these logic gates deployed in a natural environment remain unclear due to the challenge of understanding the impact of molecular signal flows. In this paper, we investigate the performance of engineered bacterial logic gates that act as biosensors by computing incoming molecular signals through an AND operation. Our frequency domain analysis incorporates concepts from molecular communications to investigate the channel's effect on the operation of a bacteria-based biosensor. Furthermore, our analysis includes an electronic circuit equivalent model to map the sensing, processing and emission of molecular signals by the bacteria-based biosensors, and wet lab experiments to evaluate the required concentration of molecular input signals for the biosensor operation. Based on our wet lab experiment setup, we found that the biosensor requires input signals to be produced for three hours to achieve sufficient concentration to trigger the logic operation. Moreover, our results show that a low molecular signal frequency has a positive impact on the logic computation performance.**

Daniel P. Martins and Sasitharan Balasubramaniam are with the Telecommunication Software & Systems Group (TSSG), Waterford Institute of Technology (WIT), Waterford, Ireland, X91 P20H. E-mail: {dpmartins, sasib}@tssg.org.

Lee Coffey is with the Pharmaceutical & Molecular Biotechnology Research Centre, Waterford, Ireland, X91 K0EK. E-mail: lcoffey@wit.ie

Paul D. Cotter is with the Teagasc, Food Research Centre, Moorepark, Ireland, P61 C996. E-mail: paul.cotter@teagasc.ie

Donagh P. Berry is with the Teagasc, Animal & Grassland Research and Innovation Centre, Moorepark, Ireland, P61 C997. E-mail: donagh.berry@teagasc.ie

Michael Taynnan Barros is with the Telecommunication Software & Systems Group (TSSG), Waterford Institute of Technology (WIT), Waterford, Ireland, X91 P20H, and with the Computational Biophysics and Imaging Group, BioMediTech, Faculty of Medicine and Health Technology, Tampere University, FI-33014 Tampere, Finland. Email: michael.barros@tuni.fi

***Index Terms*—Cellular logic, Communication systems, Frequency domain analysis.**

I. INTRODUCTION

BACTERIA commonly exchange molecular signals to trigger population-level functions, and one example process is known as *Quorum Sensing* [1]–[3]. This signalling process contributes towards their survival strategy and is based on the exchange of different molecule types, where examples include *N-Acyl Homoserine Lactone* (*AHL*) and processed *Oligo-peptides* [2], [3]. A number of synthetic biology models are based on the engineering of bacterial Quorum Sensing [1]–[4]. For example, logic gates can be engineered into a bacterial population by controlling their detection thresholds and inducing them to collectively respond to specific molecules. This customised design is needed to enable the bacterial population to recognize the complex combination of signals found in nature. For example, AND gates can be engineered into cells to detect the presence of environmental pollutants, such as arsenic and xylene [5]. Other potential applications can result from engineering bacterial logic gates for various molecular levels, such as the targeted production of therapeutic molecules [1], [4].

Molecular communications is a new communication paradigm devoted to creating artificial communication systems that are engineered from nanoscale biological systems [6]–[10]. Bacteria have been used in developing molecular communications systems, which includes engineering molecular diffusion to modulate information as well as transporting small DNA plasmid molecules [6], [7], [11]–[17]. This has resulted in applications

that includes modulation of molecular signals for multi-hop network of bacterial populations [18], and emission of molecules for jamming biofilm communication to prevent the production of proteins that lead to biofilm formation [19]. While experimental validations have demonstrated the operations of logic computation using bacterial populations, the analysis of molecular communication flow of signals to the gates, and its reliability, has not been fully investigated.

In this paper, we introduce an electronic equivalent circuit model to investigate the molecular communication performance of a biosensor composed of a synthetic AND bacteria-based logic gate. We propose the use of an engineered bacterial population to sense and process molecules secreted from a target system, which we term as a **molecular generator**. The bacteria-based biosensor will detect the input molecules produced from the molecular generator and, depending on the computation, produce secondary molecular signals that can be applied to the sensing of, for example, a disease or any other type of indicators. Other example applications for our proposed system can include sensing enzymes from the environment that represent indicators for a particular contaminant [20]. Both the bacterial population and the molecular generator are interconnected through diffusion channels, which are further elaborated in Section II. We focus our analysis on three aspects. First, we investigate the production of molecular signal by the generator and its impact on the computation by the bacteria-based biosensor. Second, we provide a frequency domain analysis of the proposed electronic equivalent circuit, including a impedance and power spectrum density analysis. Finally, we compute the communications capacities of the diffusion channel and the bacteria-based biosensor. Our main contributions are as follows:

- **Electronic equivalent circuit model to map molecular communication system to a bacteria-based biosensor:** We propose an electronic equivalent circuit representation for the reception of incoming molecules into the logic gate, for the synthetic bacteria-based biosensor operation and to enable the transmission of the molecular output signal.
- **Frequency domain analysis of the bacteria-based biosensor:** We study how the generated molecular signal is affected by the fluid diffusion channel and its impact on the operation of the bacteria-based biosensor through a frequency domain analysis.
- **Communications performance evaluation for the end-to-end bacteria-based biosensor:** We compute the channel capacity for the end-to-end system starting from the molecular generator (source that produce molecules to be computed), as well as the computation process, and the output of molecular signal from the biosensor.

The rest of the paper is organised as follows. In Section II, we describe the electronic equivalent circuit model, followed by the communications model in Section III. Then, we present our analysis methods for this bacteria-based molecular communications system. In Section IV, we present the numerical results for the frequency domain analysis of the bacteria-based biosensor and communications channels in Section V. Our wet lab experiment is described in Section VI. Lastly, in Section VII we present our conclusions.

II. SYSTEM MODEL

Our bacteria-based biosensor molecular communications system, illustrated in Figure 1, represents an interaction between two biological entities: a molecular generator and the bacteria-based biosensor, which is represented by a synthetic AND gate, and will act as a biosensor that detects the molecular signal concentration diffused by the generator [12], [20]. The molecules produced by each biological entity considered in this paper will travel through the channel independently of each other. Moreover, we opt to restrict the engineered bacterial population size, and, in a living host, this can be achieved through the use of probiotics, prebiotics, phage, bacteriocins, antibiotics and/or another factor [21], [22]. This will enable us to investigate the molecular communication system for this specific scenario, which can also limit the level of unwanted effects in the system.

As shown in Figure 1, this bacteria-based biosensor molecular communications system is composed of two devices, which is the molecular generator and the bacteria-based biosensor engineered from bacteria, with a diffusion channel connecting them. This system is investigated through three steps, where two involves the propagation of molecules. First, the generator produces a molecular signal $x_1(t)$

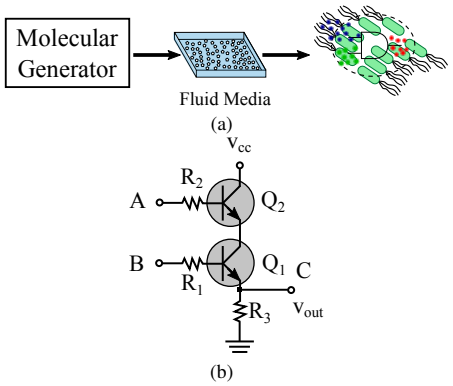

Fig. 1. Representation of the bacteria-based biosensor molecular communications system proposed in this paper. The considerd application scenario is based on a molecular generator that produces and diffuses molecules through a fluidic channel towards an engineered bacteria biosensor. (a) The bacteria-based biosensor represents an AND gate operation that computes the molecular signals from the generator, and this could be used to sense specific types of molecules. (b) Analog circuit equivalent of a digital AND gate.

that diffuses into a fluid environment (which can suffer a molecular input delay of τ_1 hours). Next, the bacteria-based biosensor detects the transmitted signal $y_1(t+t_p+\tau+\tau_1)$ after a propagation period t_p, and computes the molecules through the AND logic operation.

The second signal $s_2(t_f)$ required for the logic operation is from the surrounding environment. Resulting from this operation, a molecular signal $x_2(t_f)$ is then emitted from the bacteria-based biosensor, which may be an indicator (e.g., fluorescent proteins and dyes) that represents a computation by the synthetic logic gate, where $t_f = t+t_p+\tau$.

A. Mapping of Electronic Circuit Models to Biological Processes

Synthetic logic gates can be built using biological entities, such as bacteria, archaea and mammalian cells [23]. For this purpose, signalling molecules are used to activate cellular internal pathways, which will lead to the production of specific molecular concentration output as a response to the input signalling molecules [24]–[26]. To model this dynamic process, biologists often use rate reaction equations that describes the chemical concentrations changes with respect to time [24]–[26].

In this paper, the synthetic AND gate is modelled using an analog circuit that is able to perform the Boolean operation, as illustrated in Figure 1b. For that end, we considered that engineered bacterial population is immotile and the system is placed in a location that the fluid is not flowing. The analog circuit model of the bacteria-based biosensor (see Figure 2) is further extended to include the reception and the transmission of molecular signals that is communicated to the bacteria-based biosensor (see Figure 2). The equivalent analog circuit model will be composed of diodes, capacitors, transistors and resistors, which are represented as biological processes. This approach is inspired by the seminal work in [27] where the diffusion of molecular signals is represented with electronic engineering analysis [27]. However, in this paper, an equivalent circuit is proposed to represent the chemical reactions (in the population level) related to the bacteria-based computing of molecules, which is a different approach from [27].

We model the molecular input signal $s_1(t_f+\tau_1)$, the molecular environmental signal $s_2(t_f)$, and the molecular output signal $x_2(t_f)$ as the equivalent voltages of the proposed analogue circuit model ($t_f = t+t_p+\tau$). Therefore,

$$s_1(t_f+\tau_1) \equiv s_{in1}(t_f+\tau_1), \quad (1)$$

$$s_2(t_f) \equiv s_{in2}(t_f), \quad (2)$$

$$x_2(t_f) \equiv s_{out}(t_f), \quad (3)$$

where $s_{in1}(t_f+\tau_1)$ and $s_{in2}(t_f)$ are the voltages applied to the base of the transistors Q_1 and Q_2, respectively (see Figure 2); and $s_{out}(t_f)$ is the molecular output signal produced by the bacteria-based biosensor. If the engineered bacterial population density is time-dependent, the absorption and production rates will vary accordingly with the bacterial population density (see Figure 2a). However, if there is any form of control to the engineered bacterial population density, their growth will become time-independent, and the absorption and production rate will assume fixed values (see Figure 2b). In this paper, we assume that the engineered bacteria population will have a fixed density. Therefore, from an electronics perspective, this assumption transforms the variable resistors shown in Figure 2a into fixed value resistors illustrated in Figure 2b, simplifying the model. Consequently, for the proposed circuit, all resistors will be modelled using fixed binding, absorption, production and transportation or degradation rate values for the molecules [27].

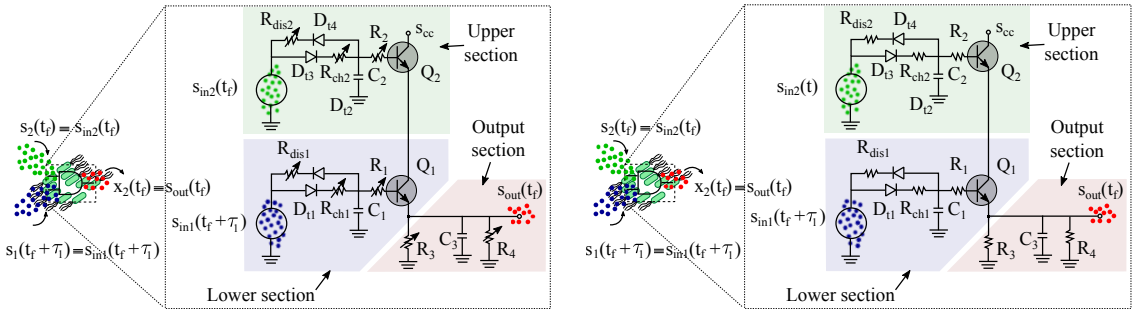

Fig. 2. The bacteria-based biosensor represented using an electronic circuit (please observe that $t_f = t + t_p + \tau$). (a) When the bacterial population size varies with respect to time, the absorption and production rates can be represented as variable resistors (in this paper we only investigate a fixed bacterial population size). (b) When the bacterial population size is time-independent, the absorption and production rates can be represented as static resistors.

To activate the bacteria-based biosensor, the diffused molecular signal concentration will first bind to the bacterial surface membrane receptors and activates the internal signalling pathways that is responsible for the production of a secondary molecular signal (sensing indicator). This process is equivalent to the activation of an electronic trigger that enables the signal to flow through an analog circuit. This biological reception process is equivalent to an association of two resistors and two diodes (see Figure 2). The resistors R_{ch1}, R_{ch2}, R_{dis1} and R_{dis2} are the resistance values for the charging and discharging phase of the capacitor C_1 and C_2, respectively. These resistors and their equivalence to the molecular binding process are represented as follows [27]

$$R_{ch1} = R_{dis1} \equiv k_{b1}, \tag{4}$$

$$R_{ch2} = R_{dis2} \equiv k_{b2}, \tag{5}$$

where k_{b1} and k_{b2} are the binding rates for the input molecular signals $s_1(t_f + \tau_1)$ and $s_2(t_f)$ that will bind onto the bacterial membrane, respectively. The binding rate is chosen to be the same as the unbinding rate, represented by (4) and (5), to model a scenario where there is a continuous renewal of molecular reception by the engineered bacterial population. Additionally, due to the small frequency analysis, the diodes will be considered as short circuits, and therefore, will not be mapped to any biological process [27].

The capacitors C_1 and C_2 placed after the diode-resistor association are modelled as equivalent to the number of bacterial receptors responsible for absorbing the input molecular signal [27]. Therefore,

$$C_1 \equiv n_{r1}, \tag{6}$$

$$C_2 \equiv n_{r2}, \tag{7}$$

where n_{r1} and n_{r2} are the number of bacterial receptors for the molecular signals $s_1(t_f + \tau_1)$ and $s_2(t_f)$, respectively. A fraction of the input voltages, after passing the diode-resistor association, is absorbed by the resistors R_1 and R_2 placed at the transistors' bases. These resistors are defined as being equivalent to the molecular absorption rates, k_{t1} and k_{t2}, for the engineered bacterial population [27]. Therefore,

$$R_1 \equiv \frac{1}{k_{t1}}, \tag{8}$$

$$R_2 \equiv \frac{1}{k_{t2}}. \tag{9}$$

Each NPN transistor has an internal resistance which draws some of the voltage that passes from the base to its emitter (see Figure 1b). From a molecular biological perspective, these internal resistance are equivalent as the degradation rates for each molecular input signal. Therefore,

$$R_{Q1} \equiv \frac{1}{\gamma_1}, \tag{10}$$

$$R_{Q2} \equiv \frac{1}{\gamma_2}, \tag{11}$$

where γ_1 and γ_2 are the degradation rates of the molecular input signals for the proposed analog

circuit. The resistor R_3 connected to the emitter of the transistor Q_1 draw a certain voltage that feeds to the output portion of the electronic circuit. For the proposed synthetic circuit modelling, the resistor R_3 uses a fraction of the molecular signal concentration emitted by the transistor Q_1 to produce the required molecular output signal $s_{out}(t_f)$. This resistor is represented as [27],

$$R_3 \equiv \frac{1}{k_o}, \tag{12}$$

where k_o is the molecular production rate of the engineered bacterial population.

For the circuit shown in Figure 2, the capacitor C_3 stores the voltage that reaches the output section, and the resistor R_4 controls the discharge rate of the stored voltage in this capacitor. The equivalent biological process for capacitor C_3 is the ratio between the molecular output signal concentration outside and inside the bacterial cells, and the resistor R_4 is the resistance value generated by the diffusion channel [27]. Therefore,

$$C_3 \equiv \frac{p_{out}}{p_{in}}, \tag{13}$$

and

$$R_4 \equiv \frac{1}{D}, \tag{14}$$

where p_{in} and p_{out} are the transportation rates of molecules secreted from the cytoplasm out to the membrane of the bacterial cells, respectively, and D is the diffusion coefficient in aqueous media.

The collector end of the transistor Q_2 is applied a minimum voltage level s_{cc} that is required for the circuit's operation. This can be represented in the biological process as the molecular basal level s_{basal} that is the minimum concentration of a specific chemical substance inside a cell [24]. This equivalence is defined as

$$s_{cc} \equiv s_{basal}. \tag{15}$$

III. COMMUNICATIONS MODEL

An overall representation of the end-to-end bacteria-based biosensor molecular communications system is presented in Figure 3. We considered the molecular generator as a transmitter that diffuses a molecular signal $x_1(t)$ into the communications channel $h_c(t_p + \tau)$. This molecular signal is modelled as [28],

$$x_1(t) = \frac{X}{1 + e^{-2k(t-0.5)}} + n_1(t), \tag{16}$$

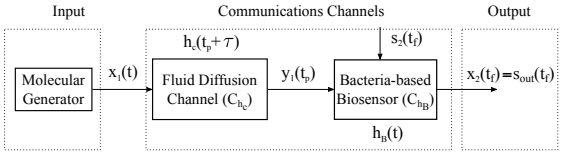

Fig. 3. End-to-end channel model for the bacteria-based biosensor molecular communications system proposed in this paper. This model is used to characterize the flows of molecules between the entities, and to determine how their variations can impact the operation of the system.

where X is the molecular signal amplitude, $n_1(t)$ is the molecular production fluctuation; where k is a parameter that approximates this output pattern to the Heaviside function, and t is the transmission period. By defining $k \geq 10$, we are able to find a good approximation to compute this continuous pulse molecular signal [28]. The communications channel $h_c(t_p + \tau)$ interconnect the molecular generator to the bacteria-based biosensor, and τ is the propagation delay. Using the solution for the Fick's diffusion equation [29], we characterize this communications channel as follows

$$h_c(t_p + \tau) = \frac{1}{\sqrt{4\pi D(t_p + \tau)}} e^{\frac{-d^2}{4D(t_p + \tau)}}, \tag{17}$$

where $h_c(t_p + \tau)$ is the fluidic channel between the molecular generator and the bacteria-based biosensor; and d is the Euclidean distance.

The molecular signal $y_1(t + t_p + \tau + \tau_1)$ shown in Figure 3, results from the interaction between the molecular signal $x_1(t)$ and the communications channel $h_c(t_p + \tau)$, and is received by the bacteria-based biosensor. Therefore,

$$y_1(t+t_p+\tau+\tau_1) = x_1(t) * h_c(t_p+\tau) + n_c(t), \tag{18}$$

where $n_c(t)$ is the molecular noise present in the environment from different molecules. Depending on the medium type, different molecular signals concentration reaches the bacteria-based biosensor composed of engineered bacterial population density n_{bac}, and invoke each individual cell to produce a response molecular signal $s_1(t_f)$, which is represented as follows

$$s_1(t_f + \tau_1) = n_{bac}.y_1(t + t_p + \tau + \tau_1). \tag{19}$$

The signals $s_1(t_f)$ and the second molecular signal $s_2(t_f)$ that exists in the environment will be processed by the bacteria-based biosensor to produce

the molecular signal $s_{out}(t_f)$. We consider that the molecular concentration level of $s_1(t_f)$ and $s_2(t_f)$ are higher than the required threshold to activate the bacteria-based biosensor operation. However, asynchronous signals for each of the inputs can arrive at the gate with a lag. We define this time difference as the molecular input delay τ_1, and its impact on the reliability of the computation has been investigated in [31]. In this paper we consider that there is no propagation delay (τ) affecting the communications process, $\tau = \tau_1 = 0$.

IV. System Analysis

A. Channel Capacity Analysis

The proposed bacteria-based biosensor molecular communications system is composed of two independent communications channels as shown in Figure 3. The capacity of the fluid channel C_{h_c} and of the bacteria-based biosensor operation C_{h_B} are modelled as follows [32]

$$C_{h_c} = B_f \log_2 \left(1 + \frac{P_{y_1}}{P_{n_1}}\right), \tag{20}$$

$$C_{h_B} = B_f \log_2 \left(1 + \frac{P_{s_{out}}}{P_{n_2}}\right), \tag{21}$$

where B_f is the molecular signal frequency band; P_{y_1}, and $P_{s_{out}}$ are the molecular signal power for $y_1(t + t_p + \tau + \tau_1)$, and $s_{out}(t_f)$, respectively; and P_{n_1}, P_{n_2} are the power of the noise generated during the production of the molecular signals $y_1(t + t_p + \tau + \tau_1)$, and $s_{out}(t_f)$, respectively. The power of the molecular signal $y_1(t + t_p + \tau + \tau_1)$ and $s_{out}(t_f)$ are described as follows

$$P_{y_1} = \frac{1}{2T} \int_{T=0}^{T=t_f+\tau_1} |y_1(t + t_p + \tau + \tau_1)|^2 dt_p, \tag{22}$$

and

$$P_{s_{out}} = \frac{S_{out}(f_s)^2}{Z_{OUT}}, \tag{23}$$

where $T = t_f$ is the molecular signal duration. The noise power can be represented as follows

$$P_{n_1} = \sigma_1^2, \tag{24}$$

and

$$P_{n_2} = \sigma_2^2, \tag{25}$$

where σ_1 and σ_2 are the standard deviation of the molecular noise generated during the production of the molecular signals $y_1(t + t_p + \tau + \tau_1)$ and $s_{out}(t_f)$. The biological noise model for bacteria-based computation is still unknown (this can be further improved with the help of wet lab experiments). Therefore, in this work we opted to represent the computation noise as the small fluctuations resulting from the production of the molecular output signal $s_{out}(t_f)$ and can be modelled as an AWGN noise [31].

B. Frequency Domain Analysis

We also analyze the operation of the logic biosensor and evaluate the engineered bacterial communications channel $h_B(t)$ in the frequency domain, which is required for expressing the molecular output signal $s_{out}(t_f)$. Therefore,

$$s_{out}(t_f) = s(t) * h_B(t) + n_2(t), \tag{26}$$

where $s_t = s_{in1}(t_f).s_{in2}(t_f)$. By applying the Fourier transform to (26), this equation can be rewritten as

$$\frac{S_{out}(f_s)}{S(f_s)} = H_B(f_s) + \frac{N_2(f_s)}{S(f_s)}, \tag{27}$$

where $H_B(f_s)$ is the frequency domain representation of the communications channel $h_B(t)$; $S_{out}(f_s)/S(f_s)$ is the ratio between the frequency domain representation of the molecular signal output, $S_{out}(f_s)$, and input, $S(f_s)$, concentration; and $N_2(f_s)/S(f_s)$ represents the random fluctuations associated with the production of the molecular signals. Using the proposed equivalent electronic circuit, the communications channel $H_B(f_s)$ is evaluated as follows

$$H_B(f_s) = Z_{IN1} + Z_{IN2}. \tag{28}$$

where Z_{IN1} and Z_{IN2} are the equivalent impedances for the lower and upper sections of the proposed circuit illustrated in Figure 4, respectively. Figure 4 shows the two parts of the equivalent circuit for the evaluation of (28). First, we evaluate the circuit's output section equivalent impedance (Figure 4c), and then, the lower section of the circuit which is associated with the reception of the molecular signal transmitted by the molecular generator (Figure 4b). Lastly, we evaluate the equivalent impedance of the upper part of the circuit which receives the molecular signal that lies around the bacteria-based biosensor (Figure 4a).

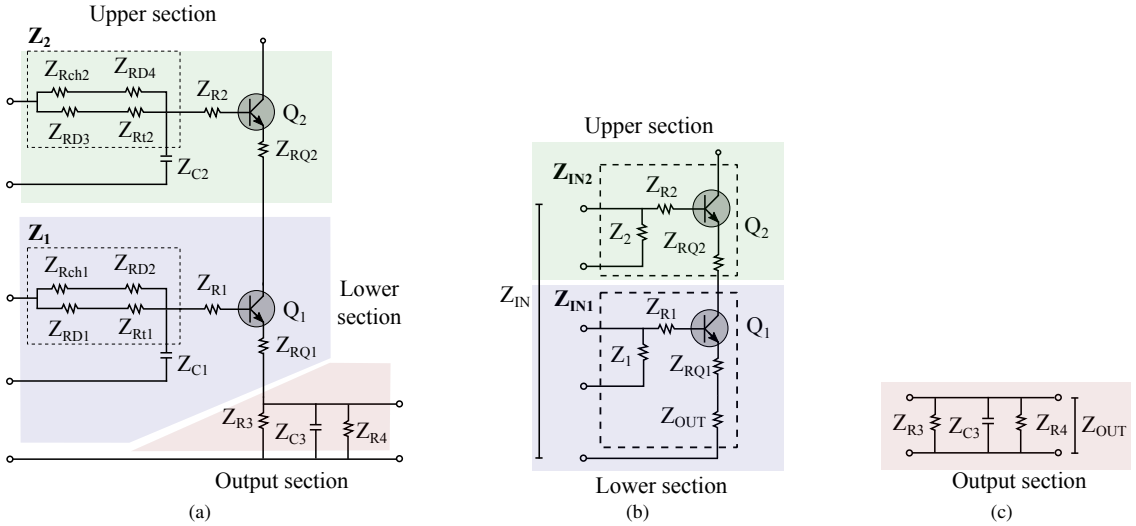

Fig. 4. Frequency domain representation of the bacteria-based biosensor circuit for the evaluation of its impedance equivalence. (a) Representation of the full bacteria-based biosensor circuit. (b) Equivalent impedance of the upper and lower sections of the circuit (the lower and upper sections represent inputs 1 and 2 into the gate, respectively). (c) Equivalent impedance of the output section of the gate.

The equivalent output impedance for the circuit shown in Figure 4c is represented as

$$Z_{OUT} = \frac{R_4 + 2\pi f_s R_3 R_4 C_3}{R_3 + R_4 + 2\pi f_s R_3 R_4 C_3}, \quad (29)$$

where Z_{R3} and Z_{R4} are the impedance of resistors R_3 and R_4, respectively; f_s is the molecular signal frequency; and Z_{C3} is the impedance of capacitor C_3. As the diodes were assumed to be short circuits then, $Z_{RD1} = Z_{RD2} = Z_{RD3} = Z_{RD4} = 0$ [27]. The equivalent impedance for the lower section of the circuit, shown in Figure 4, is represented as

$$Z_1 = \frac{R_{ch1}}{R_{dis1} + R_{ch1}}, \quad (30)$$

where Z_1 is the impedance for the lower section of the proposed circuit; Z_{Rch1} and Z_{Rdis1} are the impedance for the resistors, R_{ch1} and R_{dis1}, respectively. For this representation, the diodes are modelled as resistors because we consider that the system will operate with a low molecular signal frequency [33]. By knowing the impedance value Z_1, the equivalent impedance for the lower section of the circuit can be represented as

$$Z_{IN1} = \frac{2\pi f_s C_1 (R_1 + R_{Q1} + Z_{OUT})}{1 + 2\pi f_s C_1 (R_1 + R_{Q1} + Z_{OUT})}, \quad (31)$$

where Z_{RQ1} is the impedance of the transistor's internal resistor R_{Q1}, and Z_{R1} is the impedance of resistor R_1. The upper section of the circuit can be described in a similar manner as the lower section. Therefore,

$$Z_2 = \frac{R_{ch2}}{R_{dis2} + R_{ch2}}, \quad (32)$$

and

$$Z_{IN2} = \frac{2\pi f_s C_2 (R_2 + R_{Q2})}{1 + 2\pi f_s C_2 (R_2 + R_{Q2})} \quad (33)$$

where Z_{RQ2} is the impedance of the transistor's internal resistor R_{Q2}; Z_2 is the input impedance for the upper section of the proposed circuit; Z_{Rch2} and Z_{Rdis2} are the impedance for the resistors, R_{ch2} and R_{dis2}, respectively; and Z_{C2} is the impedance for the capacitor C_2.

TABLE I
PARAMETERS CONSIDERED FOR THIS ANALYSIS

Variable	Value	Unit	Reference
k_{b1}, k_{b2}	0.1	–	*
k_{t1}, k_{t2}, p_{out}, p_{in}	10	–	*
k_o	0.002	–	*
D	4.9	cm^2/h	*
γ_1, γ_2	0.5×10^3	–	*
n_{r1}, n_{r2}	100	receptors	*
P_{n_1}	10^{-2}	mM	*
P_{n_2}	10^{-22}	mM	*

* Obtained through the analysis of the wet lab experimental data.

V. NUMERICAL ANALYSIS

In this section, we analyse the bacteria-based biosensor operation by evaluating the molecular output signal concentration $s_{out}(t_f)$ for different scenarios and utilize it to also evaluate its channel capacity and the diffusion channel capacity. The aim of these analyses is to investigate the communications that enable the logic computation of two molecular input signals for the bacteria-based biosensor. The results described in this section were obtained through simulation and analytical evaluation of the proposed electronic equivalent model. The parameters and their values are presented in Table I.

A. Molecular Generator Signal Production

The production of the molecular signal by the generator is the first step of the communications system's operation. Depending on the molecular signal concentration $y_1(t+t_p+\tau+\tau_1)$ that is able to reach the bacteria-based biosensor after diffusing through the channel $h_c(t_p+\tau)$, the engineered bacteria will be required to produce a molecular output signal $s_{out}(t_f)$. Therefore, we use (16) to generate an unit step signal that will diffuse through the channel to determine the molecular signal concentration that sufficient enough to activate the bacteria-based biosensor.

We considered two scenarios for this analysis. First, we defined five amplitude values ($X = \{3, 5, 7, 9, 11\}$ M) for the molecular signal produced by the generator and measured the cumulative molecular signal concentration $y_1(t+t_p+\tau+\tau_1)$ for the propagation period of $t + t_p = 14,400$ seconds (time required to produce sufficient the molecular signal that can be detected based on our wet lab experiment, described in Appendix A). We also defined a fixed distance between the molecular generator and the bacteria-based biosensor ($d = 0.5$ cm). Figure 5a presents the results for this scenario. Despite the high amplitude value of the molecular generated signal $x_1(t)$, the system takes several hours to receive a high molecular signal concentration $y_1(t + t_p + \tau + \tau_1)$. In the second scenario, we chose a fixed value for the amplitude of the molecular generated signal and varied the distance between the generator and the proposed equivalent circuit. Figure 5b presents the results and shows that takes several hours to receive a high molecular signal concentration $y_1(t + t_p + \tau + \tau_1)$. Nonetheless, the second scenario will result in a higher quantity of molecular signal concentration $y_1(t+t_p+\tau+\tau_1)$ that will be received at the lower section of the circuit compared to the first scenario, which can result in higher probability of activating the bacteria-based biosensor.

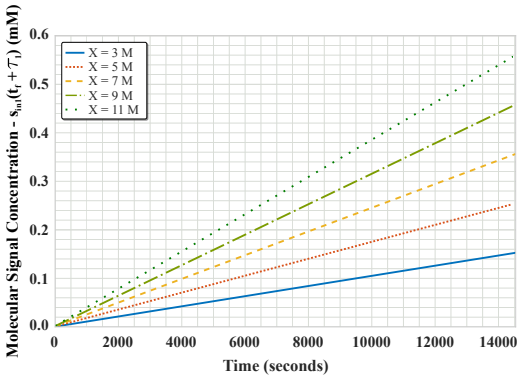

(a)

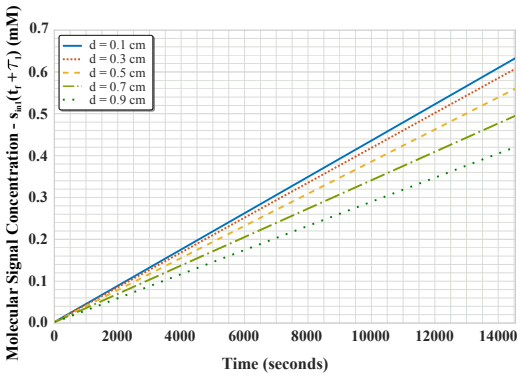

(b)

Fig. 5. Cumulative molecular signal concentration received at the lower section of the circuit shown in Figure 2. (a) We first consider a fixed distance $d = 0.5$ cm and different molecular input signals concentration amplitudes X to evaluate the cumulative molecular signal concentration. (b) Second, we fixed the molecular input signal amplitude $X = 11$ M and vary the distance d between the generator and the bacteria-based biosensor.

The results presented in Figures 5a and 5b shows that the engineered bacteria of the bacteria-based biosensor requires high molecular signal concentration to accumulate in order to activate the signalling pathway, then the molecular generator should ideally have a distance $d \leq 0.1$ cm. At the same time, the generator is also required to produce molecules at the highest quantity possible, $X \geq 11$ M, and these values are used in our biosensor operation

analyses. Nevertheless, we define a low range for the cumulative molecular signal concentration (between 0 mM and 0.1 mM) to investigate the communications performance of the system as this is the same range that is used in our wet lab experiments (a further description can be found in Appendix A).

B. Circuit Operation

The logic operation starts when the molecular signals $s_{in1}(t_f + \tau_1)$ and $s_{in2}(t_f)$ binds to the receptors of the bacterial membrane. When the molecular concentration is above a certain threshold, the circuit will be triggered and perform a Boolean AND operation. In our first analysis, we investigate the impact of the molecular signal frequency on the production of a high level of molecular output signal concentration $s_{out}(t_f)$. Our objective is to produce a sufficient quantity of molecular output signal concentration that will improve the posterior detection by the bacteria-based biosensor. For this scenario, we considered different molecular signal frequency values (ranging from $1\,\mu$Hz to 1 Hz) and the results are shown in Figure 6. In this analysis, we simulated the circuit considering that the amplitude of the molecular signal $s_{in2}(t_f)$ was equal to 0.5 mM (value defined by our wet lab experiment restrictions) and the amplitude is varied for the molecular signal $s_{in1}(t_f+\tau_1)$ from 0 mM to 0.1 mM. In this scenario, there was no molecular input delay considered ($\tau_1 = 0$). It can be noted from Figure 6 that for the frequencies ranging from 1×10^{-6} Hz to 1×10^{-5} Hz the bacteria-based biosensor produces higher molecular output signal concentrations $s_{out}(t_f)$. This result is due to the direct relationship between the molecular signal frequency and the circuit's components and their biological properties described earlier. Therefore, using molecular signals with a frequency that is higher than this range will result in a different circuit design, and require the specification of different components. Additionally, it is important to note that the low magnitude on the molecular output signal concentration shown in Figure 6 (and in the other results presented in this paper) is due to the small size of the engineered bacterial population considered in this paper.

For the next analyses, we define a specific molecular signal frequency that will take several hours to be consumed by the engineered bacterial population. The molecular signal frequency can be defined as

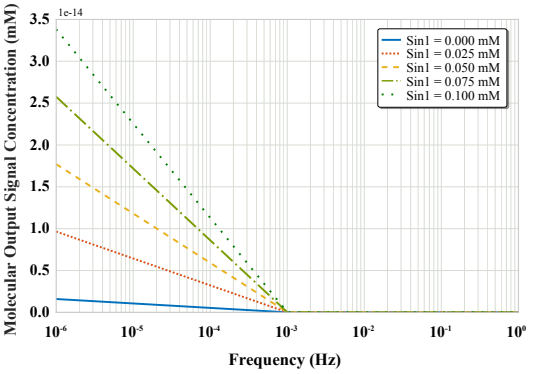

Fig. 6. Molecular output signal concentrations with respect to varying signal frequency f_s of lower section (input 1 to the gate) and fixed upper section input concentration amplitude $Sin2 = 0.5$ mM.

the inverse of this signal period. Therefore, for a long pulse period (20 hours), the molecular signal frequency can be evaluated as

$$f_s = \frac{1}{20\,\text{h}} = \frac{1}{72000\,\text{s}} = 1.39 \times 10^{-5}\,\text{Hz}. \quad (34)$$

This long pulse period assumption is based on the standard duration that exists in natural biological processes and the result obtained in our first analysis [34].

We use the molecular signal frequency value in (34) to generate the molecular signals $s_{in1}(t_f + \tau_1)$ and $s_{in2}(t_f)$ and analyse their impact on the production of the molecular output signal concentration $s_{out}(t_f)$. Moreover, we create a linear relationship between the amplitudes of the molecular signals concentration $s_{in1}(t_f + \tau_1)$ and $s_{in2}(t_f)$ to simulate the bacteria-based biosensor. For the first scenario of this analysis, we defined five fixed molecular signal $s_{in1}(t_f + \tau_1)$ amplitudes, and varied the amplitudes of the molecular signal $s_{in2}(t)$ from 0 mM to 0.5 mM. Figure 7a shows the result of this simulation. Despite the linear relationship, the resulting molecular output signal concentration $s_{out}(t_f)$ is nonlinear (sigmoid curve). We obtained a different result in our second scenario of this analysis when we varied the molecular signal concentration $s_{in1}(t_f + \tau_1)$ amplitude from 0 mM to 0.1 mM, and considered five fixed values for the molecular signal concentration $s_{in2}(t_f)$ amplitudes. In this scenario, the molecular output signal concentration $s_{out}(t_f)$ slightly increases (almost linear) with respect to the $s_{in1}(t_f+\tau_1)$, as illustrated in Figure 7b. We can infer

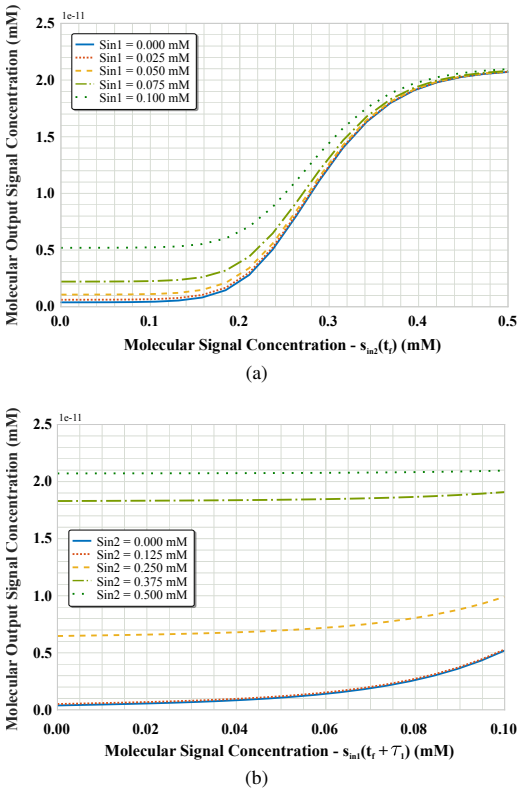

Fig. 7. Evaluation of the molecular output signal concentration for two different scenarios. (a) Different lower section input molecular concentration amplitude $Sin1$ with a fixed upper section input concentration amplitude $Sin2$. (b) Different upper section input molecular concentration amplitude $Sin2$ with a fixed lower section input concentration amplitude $Sin1$.

from these results that the molecular signal concentration $s_{in1}(t_f+\tau_1)$ biases the circuit transistor Q_1 in the linear region, while the bias presented in Figure 7a is for the nonlinear region of the transistor Q_2. Despite the different circuit behaviour displayed in Figures 7a and 7b, high molecular output signal concentration $s_{out}(t_f)$ is obtained when the amplitude of the molecular signals concentration $s_{in1}(t_f+\tau_1)$ and $s_{in2}(t_f)$ are 0.1 nM and 0.5 nM, respectively.

Following the results obtained in the previous scenario, we now simulate the proposed equivalent circuit for $14,400$ seconds (5 hours) to investigate the behaviour of molecular signals $s_{in1}(t_f+\tau_1)$, $s_{in2}(t_f)$ and $s_{out}(t_f)$ in the time and frequency domains. These analyses will ensure that the bacteria-based biosensor will operate as expected in the long term, and to understand how the different channels that compose the bacteria-based molecular communications system would affect its operation. We also considered the molecular signals concentration $s_{in1}(t_f+\tau_1)$ and $s_{in2}(t_f)$ as cosine molecular signals with amplitude equal to $Sin1 = 0.1$ mM and $Sin2 = 0.5$ mM, respectively; and molecular signal frequency equal to (34). The molecular signal concentration are shown in Figure 8. Due to the selected frequency value, the pulse period of both molecular signals $s_{in1}(t_f+\tau_1)$ and $s_{in2}(t_f)$ are too large, and consequently, their oscillatory behaviour is not shown in Figure 8a. The molecular output signal $s_{out}(t_f)$ resulting from this scenario is shown in Figure 8b and its behaviour is similar to the molecular output signal of a synthetic logic gate operation modelled using a set of ordinary differential equations (which is the standard model for synthetic systems) [19], [31]. For the frequency domain that is shown in Figure 8c, we evaluated the power spectrum density of the molecular signals $S_{in1}(f_s)$ and $S_{in2}(f_s)$ which shows two distinct behaviours dependent on the molecular signal frequency value. Both molecular signals $S_{in1}(f_s)$ and $S_{in2}(f_s)$ have a linear decrease as the frequency value increases from 1×10^{-5} Hz to 1×10^{-4} Hz. Nonetheless, around the frequency value of 1×10^{-4} Hz, both curves present their second behaviour and start to decrease exponentially towards the zero concentration value. A different behaviour is observed in the power spectrum density plot of the molecular output signal $S_{out}(f_s)$. It can be noted from Figure 8d that only one behaviour is displayed by the molecular output signal $S_{out}(f_s)$, which exponentially decreases as the molecular signal frequency value is increased from 1×10^{-5} Hz to 1×10^{-3} Hz towards the zero molecular signal concentration value. This behaviour results from the long molecular signal period that is considered in our study.

C. Channel Capacity

Next we evaluate the capacity for the molecular channel $h_c(t_p+\tau)$ and the circuit $h_B(t)$. In this analysis, we aim to evaluate the communication limits for this bacteria-based system. We first investigate the diffusion channel $h_c(t_p+\tau)$ capacity by considering the same scenarios in Section V-A. Moreover, as required by (20), we evaluate the power spectrum density of the molecular signal concentration $y_1(t+t_p+\tau+\tau_1)$ using (22). Figure 9a presents the

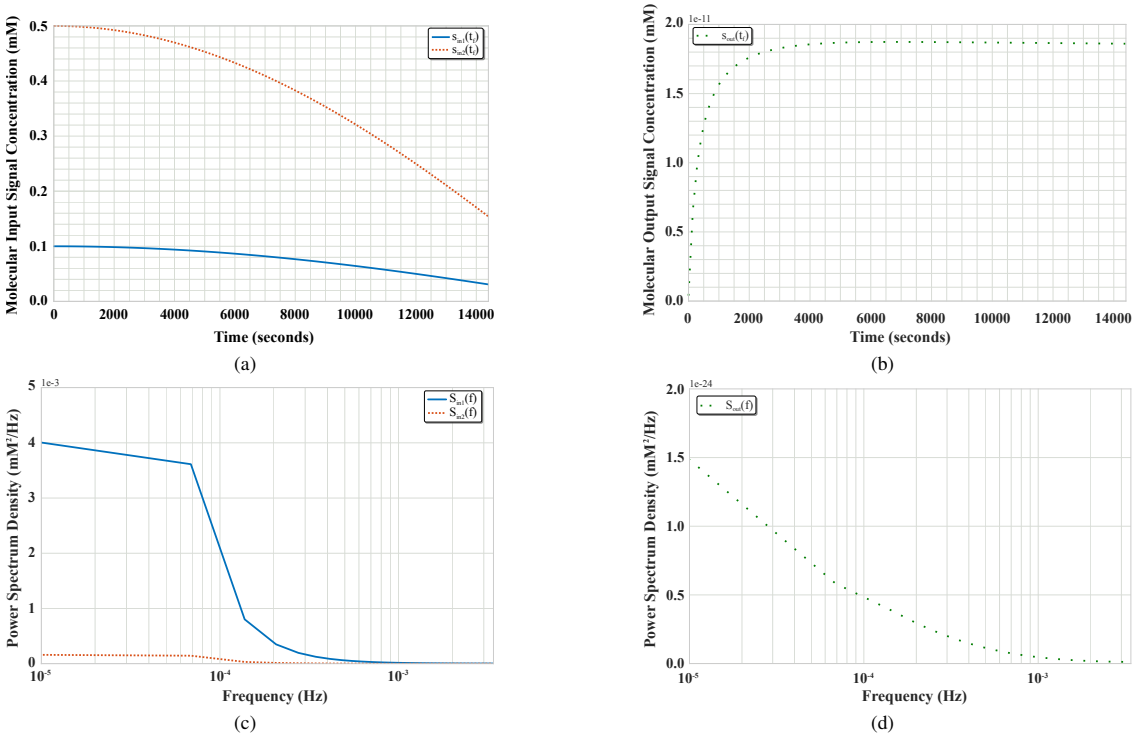

Fig. 8. Time and frequency representation of the molecular input and output signals simulated on the proposed circuit. (a) Circuit molecular input signals concentration $s_{in1}(t_f + \tau_1)$ and $s_{in2}(t_f)$ generated by a oscillatory source with frequency $f_s = 1.39 \times 10^{-5}$ Hz. (b) Circuit molecular output signal concentration $s_{out}(t_f)$ obtained using the oscillatory sources with frequency $f_s = 1.39 \times 10^{-5}$ Hz. (c) Power spectrum density of the circuit molecular input signals concentration $S_{in1}(f_s)$ and $S_{in2}(f_s)$. (d) Power spectrum density of the circuit molecular output signal concentration $S_{out}(f_s)$.

fluid medium channel capacity for five molecular generated signal amplitudes at a fixed distance of $d = 0.5$ cm between the molecular generator and the bacteria-based biosensor. In this case, the channel capacity reduces with respect to the increase in the molecular signal frequency. It also can be noted that the channel capacity is severely reduced for higher molecular generated signal amplitudes. For our next analysis, we fixed the molecular generated signal amplitude $X = 11\,\mathrm{M}$ and evaluated the channel capacity for five distances between the molecular generator and the proposed equivalent circuit. As shown in Figure 9b the distance d produces a linear channel capacity that is lower than the result shown in Figure 9a. Moreover, there is also an inverse relationship between the distance d and the channel capacity due to the lower molecular signal concentration reaching the bacteria-based biosensor.

For the evaluation of the channel $h_B(t)$ capacity, we first need to obtain the circuit's emitted power. Therefore, we simulate the circuit (see Figure 2) using the oscillatory molecular signals concentration $s_{in1}(t_f)$ and $s_{in2}(t_f)$ with amplitude equal to $Sin1 = 0\,\mathrm{mM}$ and $Sin2 = 0.5\,\mathrm{mM}$, respectively, to evaluate the power spectrum density of the molecular output signal $S_{out}(f_s)^2$. We also consider a second scenario where we modify the amplitude of the molecular signal concentration to $0.1\,\mathrm{mM}$ and use the same amplitude of the molecular signal concentration $s_{in2}(t_f)$ from the previous scenario. Next, we evaluate the bacteria-based biosensor impedance using (31), (33), (34) as well as the parameter values displayed in Table I, and resulted in the value of $0.99\,\Omega$. Using these results and (21), we numerically evaluate the bacteria-based biosensor channel capacity. This analysis is depicted in Figure 10. We can observe that for both amplitudes of the molecular signal concentration, the $s_{in1}(t_f)$ results

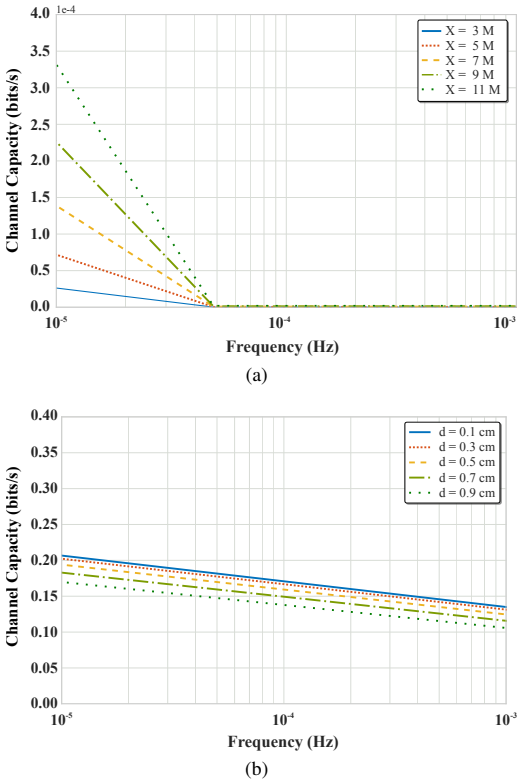

Fig. 9. Evaluation of the diffusion channel capacity for two different scenarios. (a) First, we fixed the distance $d = 0.5\,\text{cm}$ between the molecular generator and bacteria-based biosensor and varied the molecular input signals amplitude X. (b) Second, we fixed the molecular input signal amplitude $X = 11\,\text{M}$ and varied the distance d between the molecular generator and the bacteria-based biosensor.

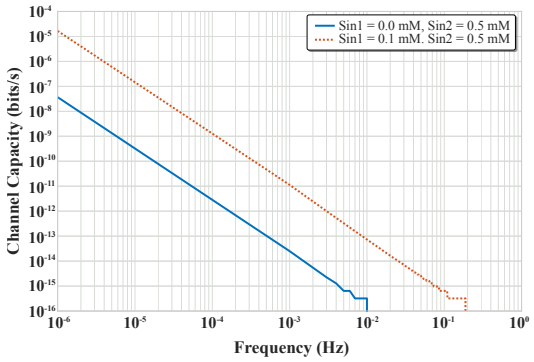

Fig. 10. Channel capacity of the bacteria-based biosensor for different molecular signal concentrations amplitudes $Sin1$ and $Sin2$.

in a linear decreasing channel capacity. This result is similar to the linear region of the fluid medium channel capacity depicted in Figure 9a. This means that the operation of the bacteria-based biosensor is impacted from the channel effects from the fluid channel. Therefore, we infer that the bacteria-based biosensor channel capacity could be improved by modifying certain parameters such as the molecular generated signal amplitude and the distance between the generator and the engineered bacterial population.

From the results presented in this section, we infer that the main parameter affecting the bacteria-based biosensor operation is the molecular signal frequency. We also observed that lower frequencies of signals generated approximates the simulation and theoretical models to the natural systems. On the other hand, higher frequencies will require a more robust bacterial population engineering to increase the reaction rates, but they are expected to result in higher molecular output signal concentrations, which eases its integration with other systems. Furthermore, the results suggest that fine tuning of the molecular frequency value will result in better communications performance for the bacteria-based biosensor. Lower molecular signal frequencies produces large pulse periods, resulting in a molecular signal similar at a constant value (a DC source, instead of an AC source). This constant value acts longer for the bacteria-based biosensor computation, and have a narrow molecular signal frequency band as shown in Figure 8c.

VI. WET LAB EXPERIMENT

We performed wet-lab experiments to validate our analytical model, where the full description of the experiment is described in Appendix A. In the experiment that is illustrated in Figure 11a, we directly applied the molecular signal concentration amplitude $Sin1 = 0.1\,\text{mM}$ and molecular environmental signal concentration amplitude $Sin2 = 0.5\,\text{mM}$ into an engineered bacterial population that represents the biosensor and measured the molecular output signal (to obtain a better control of the bacteria-based biosensor operation experimental observations). The output from the successful AND operation of two high inputs result in yellow stains as illustrated in the Figure 11b.

We measured the experimental cumulative molecular output signal concentration during $14,400$ seconds (5 hours) and compared with the cumulative

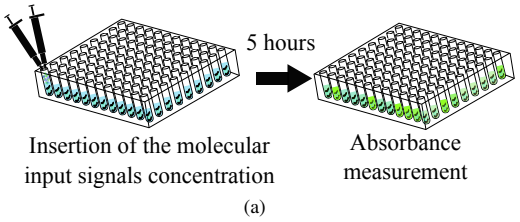

(a)

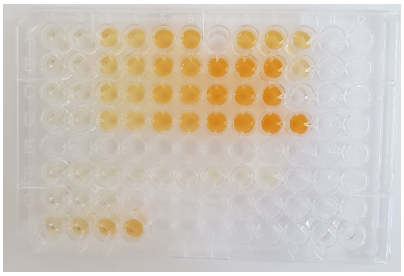

(b)

Fig. 11. A 96-well plate assay for the synchronized production of the molecular signal $s_{out}(t_f)$. The molecular signal $s_{in1}(t_f)$ was inducer IPTG, which activates the genes to produce the required proteins. The molecular signal $s_{in2}(t_f + \tau)$ was the substrate nitrile that is converted by the enzyme to acid and ammonia. (a) Illustration of the wet lab experiment demonstrating the operation of a synthetic AND gate (this process is fully discussed in [35]). Regular readings of the absorbance levels were taken for a period of 5 hours. (b) The yellow color indicates two 1 input into the AND gate, resulting in a 1 output. In the case of clear color, this means that either the inputs were 1 and 0 (or vice versa), or two 0's.

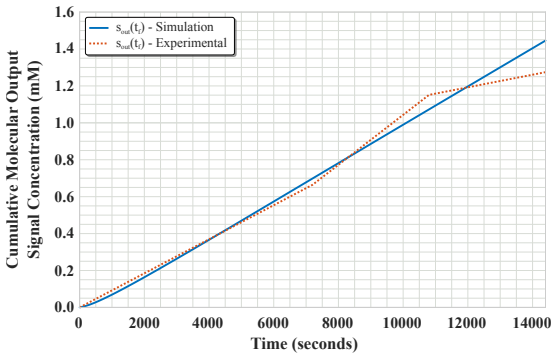

Fig. 12. Comparison between the molecular output signal concentration obtained from the simulation and the wet lab experiment. This is for an AND operation that resulted in a 1 output signal.

molecular output signal obtained from the simulations using the data from Figure 8b. For both the simulations as well as wet lab experiments, the molecular output signals are obtained through the use of quasi-continuous molecular input signals by considering longer periods for the pulse of molecular transmission. Therefore it is expected that the cumulative molecular output signal $s_{out}(t_f)$ will be represented as a linear function [36]. Additionally, we considered that each engineered bacterium of the population has the same characteristics and behaviour, where there is no social impact such as competition for shared goods. These conditions allow us to fit the simulation to the experimental results by a multiplying factor (related to the difference between the population sizes on the wet lab experiment and the simulation scenario), which in this case was equal to $800,000,000$. Figure 12 shows the comparison between these two molecular output signals and the simulated curve, which has close correlation to the experimental result. In this case, we obtained a mean square error of 7.33×10^{-3} M. Therefore, the proposed electronic equivalent circuit (see Figure 2) is a valid model to describe a synthetic Boolean AND gate computation and can be used to design more complex synthetic circuits.

VII. CONCLUSION

Synthetic biology research has facilitated the engineering of biological cells to function in a similar manner to electronic components and systems (e.g., logic gates, oscillators). Nevertheless, one of the main drawbacks for this approach is how to address the impact that environmental factors can have on the operation of the engineered cells, and in particular on the signals that flow towards the cells to be computed. In this paper, we introduce an electronic equivalent circuit model of a bacteria-based biosensor that operates as a synthetic AND gate, and investigate the performance of the system when computing external molecular signals concentration. To evaluate our proposed model, we abstracted the incoming molecular signal concentration as being artificially produced by a generator, which can represent any source, such as a diseased cells. Based on these abstractions, we proposed two analyses to investigate its operation performance, and this includes analysing the signals in the frequency domain and channel capacity. Our analyses suggests that the molecular signal frequency is an important parameter for the system's design as it severely affects both the molecular output signal concentration amplitude and the channel capacities (diffusion channel and circuit operation). Numerical

analysis concluded that low frequency molecular signals is ideal, in order for the bacteria-based biosensor to produce sufficient molecular output concentration. This study also shows the validation of the electronic equivalent model through a wet lab experiment of an AND gate developed from engineered bacteria. The comparison between the simulation and experimental data resulted in a mean square error of 7.33×10^{-3} M.

The joint analysis between the numerical analysis and the wet lab experiments indicates the feasibility of using an electronic equivalent circuit model for the design of molecular communications systems that incorporates synthetic logic gates for computation. Additionally, a variety of different fluorescent proteins (green, yellow, red) that are often used for molecular biology analysis, could be employed into our proposed system as the final outputs to be read and linked to a variety of different promotors, each responding to different molecular input signals. Some of these signals can be designed to be read by IVIS imaging (*in vivo in situ* imaging) using a camera [37] that detects, in real time, a signal transmitted by microbes located inside of a sedated animal (e.g., mouse). Therefore, the proposed approach in this paper can support the development of robust biosensors that specifically react to a related molecular signal for precise use of herbicides and theranostics applications in humans, animals and plants, as well as for quality tests of food samples.

APPENDIX A
WET LAB EXPERIMENT

A nitrilase gene from a *Burkholderia* bacteria was PCR amplified and cloned to an expression vector. Each $15\,\mu$L PCR reaction mixture contained $7.5\,\mu$L Platinum™SuperFi™Green PCR Master Mix (ThermoFisher Scientific, Cat. No. 12359010), $15\,\mu$M of each primer and $1\,\mu$L cell suspension with a final cell O.D. @$600\,$nm $= 0.04$. The following PCR conditions were used: 1 cycle of $95\,^{\circ}$C for 5 min, 30 cycles of $95\,^{\circ}$C for 1 min, $56\,^{\circ}$C for 1 min, $72\,^{\circ}$C for 2 min, followed by 1 cycle of $72\,^{\circ}$C for 5 min. The PCR product was cleaned using the Zymo Research clean and concentrator™-5 (Zymo Research, Cat. No. D4013) as per the manufacturer instructions with elution in water. The pRSF-2 Ek/LIC vector (Novagen, Cat. No. 71364) was used for expression of the nitrilase. Cloning procedures were followed as per manufacturer's instructions, with ligations transformed to E. coli BL21 (DE3) as per manufacturer's guidelines for heat shock transformations.

The detection of the molecular output signal (ammonia) was carried out using the Nessler's microscale ammonia assay [35]. Assays were carried out in $150\,\mu$L format containing potassium phosphate buffer pH 7, a final cell O.D. @$600\,$nm of 0.5 and a final substrate (molecular input signal $s_{in2}(t_f + \tau)$) concentration of $0\,$mM, $5\,$mM or 10mM (no, low or high molecular signal amplitude $Sin2$, respectively). The amounts of enzyme expression inducer, IPTG (Isopropyl-β-D-thiogalactopyranoside, Zymo Research, L1001-5), (molecular input signal $s_{in1}(t_f)$) was either $0\,$mM, $0.1\,$mM or $0.5\,$mM (no, low or high molecular signal amplitude $Sin1$, respectively). The biotransformation was carried out over 5 hours with regular readings taken throughout. To quench the continued generation of signal, $37.5\,\mu$L of $250\,$mM HCl (Sigma-Aldrich, Cat. No. 435570) was added to stop the reaction. Cell biomass was removed at 500 x g for 10 minutes at $4\,^{\circ}$C. We transferred $20\,\mu$L of the quenched reaction supernatant to a microtiter plate and to this $181\,\mu$L of the Nessler's master mix was added ($151\,\mu$L deionised H_2O, $1.0\,\mu$L 10N NaOH (Sigma-Aldrich, Cat. No. 765429) and $25\,\mu$L Nessler's reagent (Sigma-Aldrich, 72190). Reaction was incubated at room temperature ($22\,^{\circ}$C) for 10 minutes and the absorbance was read at $425\,$nm. The appropriate controls were used at all stages of experiments, with no $s_{in1}(t_f)-$, no $s_{in2}(t_f+\tau)-$ or no cell-controls used. All experiments were replicated and performed three times.

ACKNOWLEDGMENT

This work was partially funded by 1) Science Foundation Ireland via the CONNECT research centre (grant no. 13/RC/2077), 2) Science Foundation Ireland via the VistaMilk research centre (grant no. 16/RC/3835).

REFERENCES

[1] P. Melke, *et al.*, "A Cell-Based Model for Quorum Sensing in Heterogeneous Bacterial Colonies," *PLoS Computational Biology*, vol. 6, no. 6, pp. 1–13, June 2010.

[2] B. L. Bassler. "How Bacteria Talk to Each Other: Regulation of Gene Expression by Quorum Sensing", *Current opinion in microbiology*, vol. 2, no. 6, pp. 582–587, Dec. 1999.

[3] M. B. Miller and B. L. Bassler. "Quorum Sensing in Bacteria", *Annual Reviews in Microbiology*, vol. 55, no. 1, pp. 165–199, Oct. 2001.

[4] A. Tamsir, J. J. Tabor, and C. A. Voigt. "Robust multicellular computing using genetically encoded NOR gates and chemical 'wires'." *Nature*, vol. 469, no. 7329, pp. 212–215, Jan. 2011.

[5] B. Wang, *et al.*, "Engineering modular and orthogonal genetic logic gates for robust digital-like synthetic biology" *Nature Communications*, vol. 2, no. 508, Oct. 2011.

[6] O. B. Akan *et al.*,"Fundamentals of molecular information and communication science", *Proceedings of the IEEE*, vol. 105, no. 2, pp. 306–318, Feb. 2017.

[7] I. F. Akyildiz, M. Pierobon, and S. Balasubramaniam, "Moving Forward With Molecular Communication: From Theory to Human Health Applications", *Proceedings of the IEEE*, vol. 107, no. 5, pp. 858–865, May 2019.

[8] T. Nakano, "Biological computing based on living cells and cell communication", *In 2010 13th International Conference on Network-Based Information Systems, IEEE*, pp. 42–47, Sep. 2010.

[9] Y. Chahibi, and I. F. Akyildiz, "Molecular Communication Noise and Capacity Analysis for Particulate Drug Delivery Systems", *IEEE Transactions on Communications*, vol. 62, no. 11, pp. 3891–3903, Nov. 2014.

[10] T. Nakano, and T. Suda, "Molecular communication using dynamic properties of oscillating and propagating patterns in concentration of information molecules", *IEEE Transactions on Communications*, vol. 65, no. 8, pp. 3386–3398, May 2017.

[11] L. C. Cobo and I. F. Akyildiz, "Bacteria-based communication in nanonetworks," *Nano Communication Networks*, vol. 1, no. 4, pp. 244–256, Dec. 2010.

[12] D. T. Riglar and P. A. Silver, "Engineering bacteria for diagnostic and therapeutic applications," *Nature Reviews Microbiology*, vol. 16, no. 4, pp. 214–225, Feb. 2018.

[13] Y. Okaie *et. al*, "Bacterium-based mobile bionanosensor networks for target tracking: a biologically realistic model", *In Proceedings of the 8th International Conference on Bioinspired Information and Communications Technologies*, pp. 188–190, Dec. 2014.

[14] C. Lo, G. Wei, and R. Marculescu, "Towards autonomous control of molecular communication in populations of bacteria", *In Proceedings of the Second Annual International Conference on Nanoscale Computing and Communication*, p. 29, Sep. 2015.

[15] C. Lo, K. Bhardwaj, and R. Marculescu, "An autonomous and adaptive bacteria-based drug delivery system", *In Proceedings of the 3rd ACM International Conference on Nanoscale Computing and Communication*, p. 19, Sep. 2016.

[16] B. D. Unluturk, A. O. Bicen, and I. F. Akyildiz, "Genetically Engineered Bacteria-based BioTransceivers for Molecular Communication", *IEEE Transactions on Communications*, vol. 63, no. 4, pp. 1271–1281, Apr. 2015.

[17] A. Marcone, M. Pierobon, and M. Magarini, "Parity-Check Coding Based on Genetic Circuits for Engineered Molecular Communication Between Biological Cells", *IEEE Transactions on Communications*, vol. 66, no. 12, pp. 6221–6236, Dec. 2018.

[18] A. Einolghozati, M. Sardari, and F. Fekri, "Design and Analysis of Wireless Communication Systems Using Diffusion-Based Molecular Communication Among Bacteria," *IEEE Transactions on Wireless Communications*, vol. 12, no. 12, pp. 6096–6105, Dec. 2013.

[19] D. P. Martins *et al.*, "Molecular Communications Pulse-Based Jamming Model for Bacterial Biofilm Suppression," *IEEE Transactions on NanoBioscience*, vol. 17, no. 4, pp. 533–542, Oct. 2018.

[20] K. Yagi,"Applications of whole-cell bacterial sensors in biotechnology and environmental science", *Applied Microbiology and Biotechnology*, vol. 73, no. 6, pp. 1251–1258, Jan. 2007.

[21] D. E. Contois, "Kinetics of Bacterial Growth: Relationship between Population Density and Specific Growth Rate of Continuous Cultures",*Microbiology*, vol. 21, no. 1, pp. 40–50, Aug. 1959.

[22] C. C. Spicer, "The Theory of Bacterial Constant Growth Apparatus", *Biometrics*, vol. 11, no. 2, pp. 225–230, June 1955.

[23] D. E. Cameron, C. J. Bashor and J. J. Collins, "A brief history of synthetic biology". *Nature Reviews Microbiology*, vol. 12, no. 5, p. 381, May 2014.

[24] C. A. Voigt, "Genetic parts to program bacteria". *Current Opinion in Biotechnology*, vol. 17, no. 5, pp.548–557, Oct. 2006.

[25] L. Goers *et al.*, "Engineering microbial biosensors", In *Methods in Microbiology*, vol. 40, pp. 119–156, Academic Press, 2003.

[26] M. Kuscu, and O. B. Akan. "Modeling convection-diffusion-reaction systems for microfluidic molecular communications with surface-based receivers in Internet of Bio-Nano Things," *PloS one*, vol. 13, no. 2, pp. e0192202, Feb. 2018.

[27] M. Pierobon and I. F. Akyildiz, "A Physical End-to-End Model for Molecular Communication in Nanonetworks," *IEEE Journal on Selected Areas in Communications (JSAC)*, vol. 28, no. 4, pp. 602–611, May 2010.

[28] A. I. Iliev, N. Kyurkchiev, and S. Markov, "On the approximation of the cut and step functions by logistic and Gompertz functions", *Biomath*, vol. 4, no. 2, pp. 1510101, Oct. 2015.

[29] I. Llatser *et al.*, "N3Sim: Simulation framework for diffusion-based molecular communication nanonetworks," *Simulation Modelling Practice and Theory*, vol. 42, pp. 210–222, Dec. 2013.

[30] Y. M. Gumnitskii and O. V. Lyuta, "Molecular-diffusion mass transfer of substance in soil medium", *Theoretical Foundations of Chemical Engineering*, vol. 48, no. 4, pp. 414–419, Jul. 2014.

[31] D. P. Martins, M. T. Barros and S. Balasubramaniam, "Quality and Capacity Analysis of Molecular Communications in Bacterial Synthetic Logic Circuits," *To appear at IEEE Transactions on NanoBioscience*, 2019.

[32] B. P. Lathi, and Z. Ding, "Modern Digital and Analog Communication Systems", Oxford University Press, Oxford, 2010

[33] Robert L. Boylestad, and L. Nashelsky. "Electronic Devices and Circuit Theory", Pearson New International Edition, Essex, 2014.

[34] E. Renshaw, "Modelling Biological Populations in Space and Time". Vol. 11. Cambridge University Press, 1993.

[35] T. M. Coady *et al.*, "A high throughput screening strategy for the assessment of nitrile-hydrolyzing activity towards the production of enantiopure β-hydroxy acids", *Journal of Molecular Catalysis B: Enzymatic*, vol. 97, no. 0, pp.150–155, Dec. 2013.

[36] S. S. Dey *et al.*, "Orthogonal control of expression mean and variance by epigenetic features at different genomic loci", *Molecular Systems Biology*, vol. 11, no. 5, p. 806, May 2015.

[37] A. Campion *et al.*, "In vivo activity of Nisin A and Nisin V against Listeria monocytogenes in mice", *BMC Microbiology*, vol. 13, no. 1, pp. 23, Feb. 2013.

CHAPTER 11

JOURNAL PAPER: A RELIABILITY ANALYSIS FOR BACTERIAL MOLECULAR COMPUTING ON A CHIP

Journal Title:	IEEE Transactions on Emerging Topics in Computing
Article Type:	Short Paper
Complete Author List:	Daniel Perez Martins, Michael Taynnan Barros, Thitipol Sinkruasuan, Benjamin O'Sullivan, Alan O'Riordan and Sasitharan Balasubramaniam
Keywords:	Synthetic logic gate, Engineered bacteria population, Continuous pulse analysis.
Status:	Submitted

A Reliability Analysis for Bacterial Molecular Computing on a Chip

Daniel P. Martins, *Student Member, IEEE,* Michael Taynnan Barros, *Member, IEEE,* Thitipol Sinkruasuan, Benjamin O'Sullivan, Alan O'Riordan, and Sasitharan Balasubramaniam, *Senior Member, IEEE*

Abstract—Synthetic oscillators and logic gates have been designed in the past years to perform computing function that can lead to new applications for monitoring the environment or even treat metabolic diseases. In this paper, we analyse the reliability of a logic AND gate by an engineered bacterial population that is sensed by an electrochemical sensor on a chip. Our analysis incorporates concepts from molecular communications between the entities to determine how unwanted effects (e.g., delays and noises) impact on the reliability of the logic computation, as well as conditions of pH limits and current ranges that need to be passed through the nanowire for sensing. Our numerical analysis found that a small variation in the production delay of molecules by the bacteria can have a major impact on the reliability of the computation. Our results show that the electrochemical sensors can detect small pH changes created by the acidification of the fluid medium due to the emission of the molecules produced from the engineered bacteria. The integration of molecular communications with synthetic logic gates and sensing systems can provide a new breed of bio-electronic chips that enables computing to be performed by both biological cells as well as silicon technology.

Index Terms—Synthetic logic gate, Bacterial molecular computing, Internetof Bio-Nano Things.

1 INTRODUCTION

BACTERIA communicate to coordinate, or interfere, on individual and population level tasks through *quorum sensing* signalling [1]. For example, bacteria can protect themselves from environmental changes through their signalling pathways related to energy consumption [1]. At the same time, they can promote the synthesis of antibiotic molecules that interfere with other bacterial populations [2]. In the past years, researchers have been investigating this signalling process to synthetically induce bacterial populations to display behaviours that mimic their natural traits [1], [3]. These molecular computing systems are often based on synthetic logic gates and have been applied towards the production of therapeutic molecules [4].

Bacteria signalling processes can also be applied to the design of engineered nanoscale biological systems that exchange molecular information [5], [6]. This recent communications paradigm is named **Molecular Communications**, and it is devoted to modeling the exchange of molecular information in a similar manner as conventional communications systems [6]. Through the investigation of these systems, a number of applications have been proposed, such as the jamming of the communications processes involved with the biofilm formation, and the construction of a bacteria-based synthetic logic circuits [7], [8]. A particular application that has resulted in a number of biotechnology applications is logic circuit computing, and a number of works have developed such molecular computing systems from bacterial cells. This in turn can enable new forms of bio-electronic chips where computing are performed by both biological cells as well as silicon technology. In our case, we term our particular application as *Bacterial Molecular Computing on a Chip*. Nevertheless, the reliability analysis of the computing of molecular signals combined with the constraints of electro-chemical sensing for such a chip has not been fully investigated.

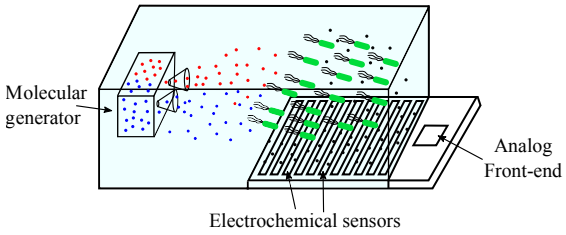

Fig. 1. Illustration of the integration of a bacteria-based molecular communications system with an electrochemical sensing device proposed in this paper. The electrochemical sensor detects the pH level change due to the molecular signal produced from the computing operation, and process this signal using an analog front-end.

We analyse the reliability of the molecular computing output signal that is detected by electrochemical sensors that is part of the chip (see Figure 1). Example applications for chips that incorporate logic computing may include the remote monitoring of contaminant levels on a particular

- *Daniel P. Martins and Sasitharan Balasubramaniam are with the Telecommunication Software & Systems Group (TSSG), Waterford Institute of Technology (WIT), Waterford, Ireland, X91 P20H. E-mail: {dpmartins, sasib}@tssg.org.*
- *Michael Taynnan Barros is with the Telecommunication Software & Systems Group (TSSG), Waterford Institute of Technology (WIT), Waterford, Ireland, X91 P20H, and with the Computational Biophysics and Imaging Group, BioMediTech, Faculty of Medicine and Health Technology, Tampere University, FI-33014 Tampere, Finland. Email: michael.barros@tuni.fi*
- *Thitipol Sinkruasuan is with the Chulalongkorn University, Bangkok, Thailand, 10330. E-mail: thitipol8599@gmail.com*
- *Benjamin O'Sullivan and Alan O'Riordan are with Tyndall National Institute, Cork, Ireland, T12 R5CP. E-mail:{benjamin.osullivan, alan.oriordan}@tyndall.ie*

environment and precision healthcare monitoring [9], [10]. Specifically, the real-time telemetry of clinical analytes such as pH level can provide non-invasive methods for health condition surveillance of chronic disease patients. In this paper, we use a similar electrochemical sensing system design as in [10]. However, our focus is to measure the pH level change due to the emission of molecular signals from the engineered bacterial population that represents a logic gate.

In this paper, we propose a simple biosensor design that can be applied on the future development of a Internet of Bio-Nano Things framework [11], [12]. In this case, a bacterial population is engineered to detect two molecular signals secreted from a nanoscale system, which we term as a **molecular generator**, and depending on its computation process it will produce secondary molecular signals that will be emitted and further detected by electrochemical sensors. In this particular case, the computation is performed by an AND logic gate engineered bacteria. The secondary molecular signal when propagating into the environment, changes the pH level of the media around the engineered bacterial population, allowing it to be indirectly measured by the electrochemical sensors. Therefore, we focus our analysis on the probability of correct detection of molecular concentration values at the electrochemical sensors based on the molecular propagation through a fluid media. The evaluation includes analysing the impact of the molecular pulse amplitude on the integrity of the received signal concentration at the molecular generator. We also consider other unwanted effects such as molecular input delays and signal production fluctuations that can affect the performance of the system.

Our main contributions are as follows:

- **Analysing the reliability of molecular environmental signals computation:** We analyse two factors that includes the delay and signal amplitude, that can affect the reliable processing of molecular generated signals and, consequently, the signal to be analyzed by the chip.
- **Bacterial molecular computing and electrochemical sensing reliability analysis:** We analyse and combine the reliability of the generated molecular signals in conjunction with the constraints of the pH levels as well as current signals through the nanowires of the chip.

The rest of the paper is organised as follows. In Section 2, we describe the system model. Then, in Section 3 we present the analytical results for the reliability evaluation of the logical computation by the engineered bacterial population. Lastly, in Section 4 we present our conclusions.

2 SYSTEM MODEL

The molecular communications system for the chip, illustrated in Figure 2, represents an interaction between a molecular generator and an engineered bacterial population, and its interface to an electro-chemical sensor. This source is an abstract representation of the different artificial or biological systems that can be used to produce and emit

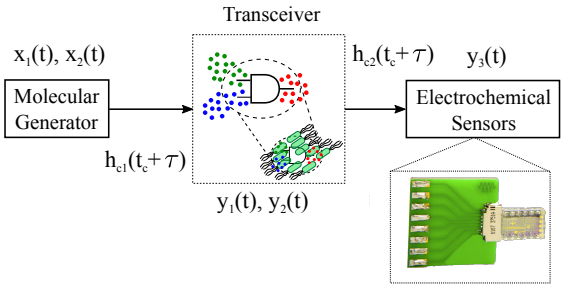

Fig. 2. Communications model of the bacteria-based system investigated in this paper. The two signals produced and transmitted by the molecular generator can reach the engineered bacterial population and be processed into a molecular output signal that will affect the pH level of the fluid media, which is detected by the electrochemical sensors embeded into a chip.

molecular signals. For example, this bacteria-based molecular communications system can be composed of a plant root that represents a molecular generator, and engineered soil bacteria that represents a logic gate, or two engineered bacterial populations in an agar plate that interacts and produces molecular output signals that will affect the pH level of the media around these entities.

As introduced in the previous section, pH level changes can be detected by electrochemical sensors, and this could enable molecular signals to be transmitted to the Internet. These devices transduce chemical signals into electrical currents or potential that is measured in amperes or volts, respectively. Figure 2 shows the communication model representation for this process. The pH level change is transduced into an electrical signals by a readout circuit that is composed of a potentiostat and an instrumental amplifier [10]. These analog signals are multiplexed and converted into digital signals before being processed by the microcontroller on the chip.

Due to the sensitivity of the electrochemical sensors, the molecular output signal concentration produced by the engineered bacterial population need to be as accurate as possible to not generate the inaccurate pH variations. Therefore, we focus our analysis on the accuracy of the detection of the molecular output signal by the electrochemical sensor. We also consider that the three entities (molecular generator, engineered bacterial population and electrochemical sensors) are immersed in a fluid media. Furthermore, the engineered bacterial population, represented by an AND gate, will act as a concentration sensor for the molecular signal diffused by the generator and produce the secondary signal that will be detected by the electrochemical sensors [5], [9].

The molecules produced by each biological entity considered in this paper will travel through the channel independently of each other. Therefore, the channel $h_c(t_c + \tau)$ can be characterised by using the solutions for fluid media which is the Fick's diffusion equation [13], and represented as follows

$$h_{c1}(t_c+\tau) = \frac{1}{\sqrt{4\pi D_c(t_c+\tau)}} e^{\frac{-d_{TS1}^2}{4D_c(t_c+\tau)}}, \quad (1)$$

where, $h_{c1}(t_c+\tau)$ is the fluid channel that interconnect the three entities; D_c is the diffusion coefficient for the molecular signals propagation in the fluid channel; τ is the propagation delay; and d_{TS1} is the Euclidean distance between the molecular generator and the bacteria-based AND gate population centre. The distance assumption is to ensure that all the bacteria-based AND gate will equally contribute to the molecular signal sensing, as well as production of the feedback molecular signals to the generator.

The molecular generator produces the signals $x_1(t)$ and $x_2(t)$ as train of pulses with amplitude X_1 and X_2, respectively. These signals will propagate through the channel $h_{c1}(T_c+\tau)$, resulting in the molecular signals $y_1(t_c)$ and $y_2(t_c)$ (shown in Figure 1), that are received by the engineered bacterial population. Therefore, the molecular signals $y_1(t)$ and $y_2(t)$ can be evaluated as follows

$$\begin{cases} y_1(t) = x_1(t) * h_c(t_c+\tau) + n_1(t), \\ y_2(t) = x_2(t) * h_c(t_c+\tau) + n_2(t), \end{cases} \quad (2)$$

where $n_1(t)$ and $n_2(t)$ are the propagation noises, which are modelled as a Poisson distributions with λ_1 and λ_2 equal to the number of molecules emitted through the channel [14]. As both the molecular generator and the engineered bacterial population output a signal concentration, the number of molecules can be determined as follows

$$\begin{cases} \lambda_1 = y_1(t)N_0, \\ \lambda_2 = y_2(t)N_0, \end{cases} \quad (3)$$

where $N_0 = 6.022 \times 10^{23}$ is the Avogadro's constant [15].

Depending on the propagation behaviour through the fluid, either high or low molecular signals concentration will reach the engineered bacterial population and are logically computed to produce the response molecular signal $x_3(t)$. We consider that the molecular concentration level of $y_1(t)$ and $y_2(t)$ are higher than the required threshold to activate the engineered bacterial population molecular computing process. The molecular signal $x_3(t)$ produced by the molecular computing is, therefore, evaluated as

$$\begin{aligned} \frac{dx_3(t)}{dt} =& \frac{y_1(t)^n}{k_{y1}^n + y_1(t)^n} \cdot \frac{y_2(t)^n}{k_{y2}^n + y_2(t)^n} - \gamma x_3(t) \\ &+ N_x(t), \end{aligned} \quad (4)$$

where, $N_x(t)$ is the signal production fluctuation, which is modeled as an AWGN noise (average μ_c and standard deviation σ_c) for the molecular signal $x_2(t)$.

The molecular signal $x_2(t)$ that is output from the bacteria-based AND gate is emitted towards the electrochemical sensors in a process similar to (2). Therefore, the diffusion channel is represented as

$$h_{c2}(t_c+\tau) = \frac{1}{\sqrt{4\pi D_c(t_c+\tau)}} e^{\frac{-d_{TS2}^2}{4D_c(t_c+\tau)}}, \quad (5)$$

where d_{TS2} is the Euclidean distance between the bacteria-based AND gate population centre and the electrochemical sensors. Then, the molecular output signal can be evaluated as

$$y_3(t) = x_3(t) * h_{c2}(t_c+\tau) + n_3(t), \quad (6)$$

where $n_3(t)$ is the propagation noise, which is modelled as a Poisson distribution (similarly to $n_1(t)$ and $n_2(t)$), with $\lambda_3 = y_3(t)N_0$.

When emitted by the engineered bacterial population, the molecular output signal $y_3(t)$ will produce protons decreasing the pH of the surrounding fluid media. This pH level change will be detected by the electrochemical sensors measuring the oxidation/reduction potentials of a signalling mediator molecule. This measurement will be continuous to enable the system to be applied for the fast biosensing of harmful chemical agents spread in the environment. To simulate this detection process, we use a finite element software, COMSOL Multiphysics®(version 5.3). A similar process was applied by Wahl et. al to simulate the electric current on a gold nanowire electrode [16]. Furthermore, we use *ferrocene monocarboxylic acid* (FcCOOH), a signalling molecule, to detect the production of protons (in this case, H^+) and the consequent decrease in pH [16], [17]. The redox potential E_0 of FcOOH has a pH dependence of $+30$mV/pH at a polypyrrole modified reference electrode [16]. By varying this molecular signalling mediator molecules redox potential (tendency in acquire or lose electrons), we can investigate the impact of the molecular output signal $y_3(t)$ on the pH level change over the range of pH 7 to 9.

TABLE 1
Parameters considered for this analysis

Variable	Value	Unit	Reference
k_{y1}, k_{y2}	10	–	[8]
d_{TS}	50	μm	*
D_c	1.37×10^{-7}	m^2/s	[8]
γ	0.01	–	[8]
n	2	–	[8]
N_0	6.022×10^{23}	–	[15]
t_c	30	minutes	*
t	6	hours	*

* Value chosen by the authors.

3 SYSTEM ANALYSIS

Our analysis considers the molecular generator produces two trains of molecular signal concentration pulses with different amplitudes ($X_1 = X_2 = \{1.0, 1.2, 1.4, 1.6, 1.8, 2.0\}$ mM). These molecular signals will propagate through the fluid channel (it can suffer a propagation delay τ), and are detected by the bacteria-based logic gate population. We evaluate the logic operation reliability when the gate processing is instantaneous or delayed by 1 hour (hereinafter defined as production delay). Finally, the molecular output signal $x_2(t)$, computed by the gate, will be propagated to the electrochemical sensors, through the same channel.

For our analysis, we use the parameter values presented in Table 1 and consider an AWGN noise to model the

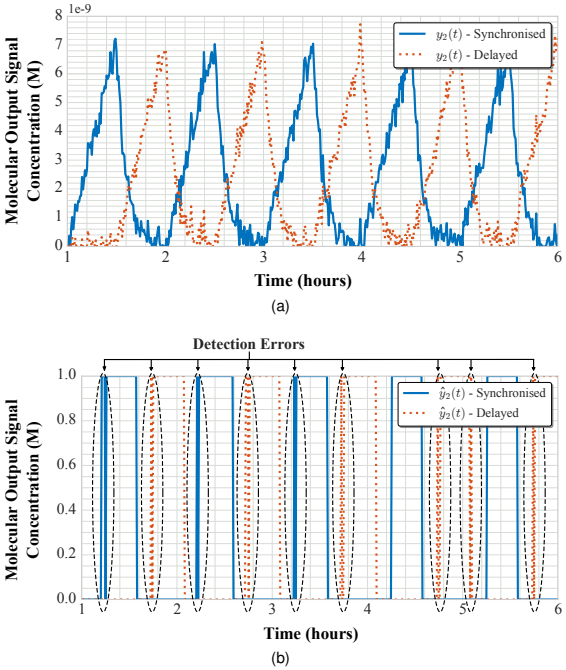

Fig. 3. Representation of molecular signal $y_2(t)$ that is received by the system when transmitted through a fluid channel. (a) Depiction of a synchronised and a delayed (30 minutes) molecular signals transmission. (b) Normalised version of the molecular received signal $y_2(t)$. Some detection errors are found due to the noise and channel effects on the transmitted molecular signal.

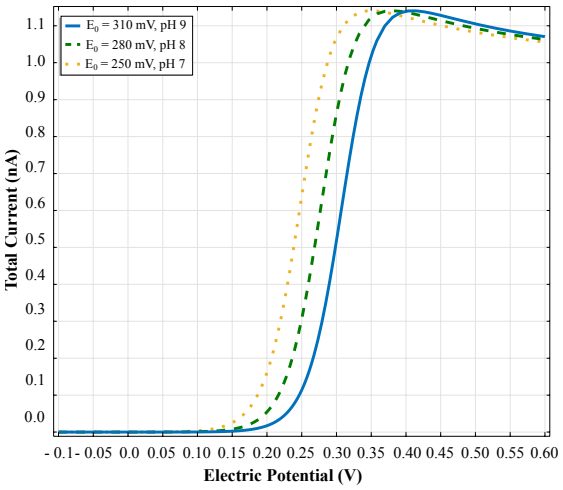

Fig. 4. Cyclic voltammograms over the pH range of 7 to 9. As the pH decreases (as more molecules are generated), a lower redox potential E_0 of ferrocene is needed.

fluctuation on the production of molecular signals (see [8] for a further explanation about this assumption). This molecular production noise will have an average of $\mu_c = 0$ and variance of $\sigma_c = 0.3$ nM. Due to the molecular diffusion through a fluid medium, this system will suffer from propagation noise that was modelled as a Poisson distribution dependent on the number of molecules emitted through the diffusion channel [14]. We consider the diffusion coefficient for the fluid channel as $D_c = 1.37 \times 10^{-7}\,\mathrm{m}^2/\mathrm{s}$. The molecular output signal $x_2(t)$ is produced for 6 hours, the propagation through the diffusion channels are expected to last for $t_c = 30$ minutes, and the molecular generator outputs signals during 1 hour and rests for another 1 hour before producing the next molecular pulse. The bacteria-based logic gate and the molecular generator have a distance of $d_{TS} = 50\,\mu$m between each other.

We can observe the impact from the production and propagation delays and both noises considered in this paper in Figure 3. Due to these unwanted effects, the obtained molecular output signal $y_2(t)$ become slightly different from the expected well-defined train of pulses (see Figure 3a). The effects due to both delays and noise (production and propagation) can be easily noted when the obtained molecular output signal $y_2(t)$ is normalised. Therefore, certain errors distorting the signal reception at the electrochemical sensors can be detected (see Figure 3b). This issue is present for both synchronised and delayed molecular output signals $y_2(t)$. However, the delayed signals will produce larger numbers of detection errors due to the difficulty in identifying the positive and negative samples in the molecular output signal $y_2(t)$.

We further investigate the impact of the delays and noises (production and propagation) on this bacteria-based molecular communications system by evaluating the reliability of the logic computation probability for different scenarios. First, we investigate the electrochemical sensor detection threshold in order to study the probability of the correct detection of positive and negative values. When the molecular signal concentration is above the electrochemical sensor threshold, we define it as a positive value, and as negative when it is below the same limit. Therefore, to define this threshold, we used the sensitivity of the electrochemical sensors. Due to the small concentration of protons 3.2 nM (or pH 8.5) produced by the engineered bacterial population (see Figure 3), the acidification of the fluid medium will be more sensitive in the pH range of 9 to 7 (from 1 nM to 100 nM). Therefore, we set the electrochemical sensors to detect a variation of $[\mathrm{H}^+]_{added} = 3.2$ nM protons. Assuming a 1:1 molecular concentration relationship, this proton addition would reduce the pH_f of a fluid as follows

$$\begin{aligned}\mathrm{pH}_f &= -\log_{10}([\mathrm{H}^+]_{initial} + [\mathrm{H}^+]_{added}) \\ &= -\log_{10}(1 \times 10^{-9} + 3.2 \times 10^{-9}) = 8.38.\end{aligned} \tag{7}$$

In the case of $[\mathrm{H}^+]_{initial} = 100$ nM, the pH_f of a fluid would change as follows

$$\begin{aligned}\mathrm{pH}_f &= -\log_{10}([\mathrm{H}^+]_{initial} + [\mathrm{H}^+]_{added}) \\ &= -\log_{10}(100 \times 10^{-9} + 3.2 \times 10^{-9}) = 6.99.\end{aligned} \tag{8}$$

From (7) and (8), it can be noted that the defined molecular signal concentration 3.2 nM can produce a greater pH level change if the fluid has a pH 9 than if it had a pH 7. These pH level changes result in the production

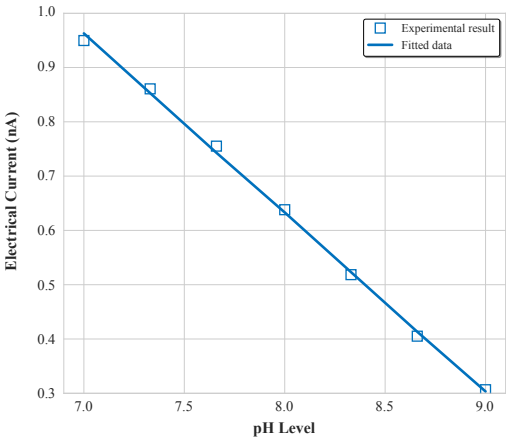

Fig. 5. Plot of the electrical current values for different pH levels when the electric potential is fixed at 0.28 V. The decrease rate was measured as -32.97 mV/pH. The sensitivity of the nanowire sensors [18] means the current value at 0.28 V can be used as a probe for the pH change in a solution.

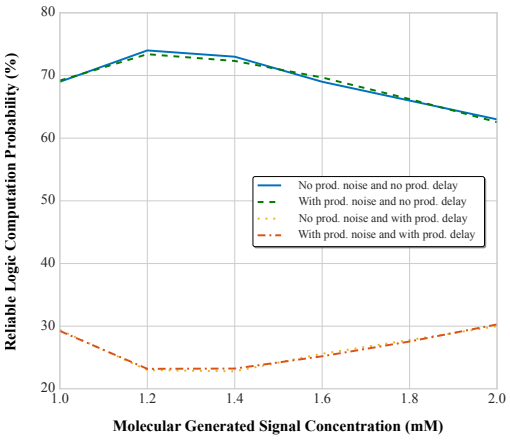

Fig. 6. Reliability logic computation probability for different amplitudes of the molecular generated signals when the system is both affected or not affected by the production and propagation noise, as well as production delay.

of different electrical currents when measured at a given electric potential, as shown in Figure 4. A small increase on the pH level result in a significantly different electric current value when measured at a fixed potential of 0.28 V, facilitating, the detection of small molecular output signal concentrations.

FcCOOH at a polypyrrole reference electrode has a higher redox potential for high pH levels, meaning that when more protons are present, a smaller electric potential is required for oxidisation). Based on our previous analysis, we defined an electric potential of 0.28 V to simulate the detection of the molecular output signal by the electrochemical sensors and define the electric current value required to oxidate the signalling molecule (FcCOOH). The result obtained from this analysis is depicted on Figure 5. . It can be noted that when the fluid channel has a pH of 7, a higher electrical current passes through the electrochemical sensors at the fixed potential than when it has a pH of 9. Therefore, a small ion concentration change, such as 3.2 nM, is harder to be detected for a fluid with a lower pH level. From this result, we also can propose a linear equation to fit the data and predict the electric current level for other pH levels, which is described as

$$I_c = -0.3219\text{pH}_c + 3.1867, \tag{9}$$

where pH_c is the pH level of the considered fluid media. Using (9), we found that for the defined threshold value (3.2 nM, or pH 8.5), the electrical current produced by the electrochemical sensors was equal to $I_c = 0.45$ nA.

We apply the threshold value of 3.2 nM to investigate the system's reliability logic computation probability when it is not affected and not affected by the production delay and noise for different molecular generated signals amplitudes $X_1 = X_2 = \{1.0, 1.2, 1.4, 1.6, 1.8, 2.0\}$ mM. The results presented in Figure 6 shows that the reliability increases between 1 mM and 1.2 mM and decreases from 1.2 mM to 2 mM when the molecular output signal does not suffer

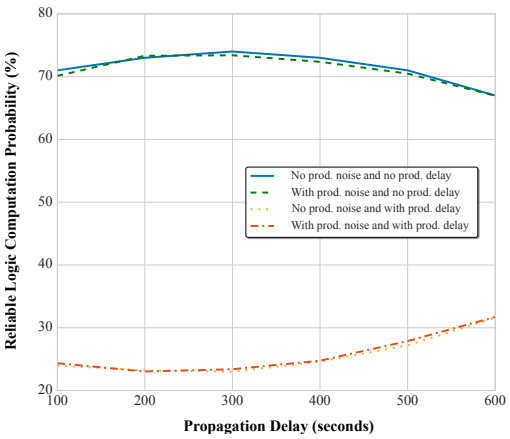

Fig. 7. Reliability logic computation probability for different propagation delay values when the system is affected or not affected by the production and propagation noise, as well as production delay.

from production delays. A symmetric result is obtained when this bacteria-based molecular communications system is affected by the production delay. It can also be observed from Figure 6 that the production delay is the main factor to reduce the reliability of this logic computation system.

Lastly, we evaluate the reliability logic computation probability for different propagation delay values $\tau = \{100, 200, 300, 400, 500, 600\}$ seconds. For this scenario, we used the same threshold value (3.2 nM, or pH 8.5) from the previous analyses, and fixed the amplitude of the molecular generated signal at 1.2 mM. When the molecular signals are not subjected to production delay, the reliability logic computation probability is slightly increased, for a specific range of propagation delay (between 100 and 300 seconds) as illustrated in Figure 7. In this case, the maximum reliability logic computation probability achieved was 73%. It

can also be noted from Figure 7 that when the molecular signals are affected by the production delay, the reliability logic computation probability improves exponentially with the increase of the propagation delay, but it is much lower than the case of no production delay (maximum value of 33%). This means that the propagation delay counters the effects of the production delay, improving the reliability logic computation probability of this bacteria-based molecular communications system.

The results presented in this section showed that even small molecular signal concentrations can be detected by the electrochemical sensors. Furthermore, this molecular signal detection has a high accuracy (73% for the best case scenario) depending of the channel conditions and synchronisation in the production of molecules. The reliability analysis showed that both the molecular generated signal concentration and the propagation delay can worsen the reliability of the logic computation when no production delay is affecting the system. On the other hand, these same parameters can improve the obtained reliability logic computation probability when the molecular signals are generated asynchronously.

4 CONCLUSION

While synthetic biology research have enabled biological cells to be engineered into electrical components and systems (e.g., logic gates, oscillators), little attention has been dedicated to understanding how variations in the molecular inputs can affect the computation performance. This is a challenge when we consider future bio-electronic chips that require biological specimens to output signals to electronic devices for analysis. This challenge is further amplified when we consider that these biological specimens are required to perform computing functions to create output signals for analysis. In this paper, we investigated the reliability for logic gate computing from engineered bacterial population on a chip, which we term as Bacterial Molecular Computing on a Chip. The output of this logic gate computing is a molecular output signal that is measured by an electrochemical sensors that will detect the acidification of the medium. The reliability analysis investigates the impact of unwanted effects (e.g., production and propagation delay and noise) for both the molecular generated and output signals and its impact on variations of pH that can affect the reliability of the sensor.

Our analyses found that the propagation delay is an important parameter that can counter the effect of the production delay and improve the reliability of the system. Furthermore, the best results were obtained when the bacteria-based molecular communications system that represents an AND gate is not affected by the production delays (73%). We also found that considering a detection threshold of $3.2\,\text{nM}$ (or pH 8.5), the electrochemical sensors can operate better if the fluid medium has a pH 9 instead of a pH 7. This threshold was also translated into a minimal electrical current level ($I_c = 0.45\,\text{nA}$) for the detection of molecular output signal concentration.

This study shows that molecular communications can be used to enable logic computing performed by biological cells and sensed by electrochemical sensors for future bacteria on a chip application. This system can be the basis for the development of a Internet of Bio-Nano Thigns framework, where new types of devices have their sensing capababilities further extended by integrating low-power wireless circuits to allow remote control by other devices within a local access network or even through the Internet.

ACKNOWLEDGMENTS

This work was partially funded by 1) Science Foundation Ireland via the CONNECT research centre (grant no. 13/RC/2077), 2) Science Foundation Ireland via the VistaMilk research centre (grant no. 16/RC/3835).

REFERENCES

[1] P. Mehta et. al, "Information processing and signal integration in bacterial quorum sensing," *Molecular Systems Biology*, vol. 5, no. 1, Jan. 2009.

[2] M. J. Ferdele and B. Bassler, "Interspecies communication in bacteria", *The Journal of Clinical Investigation*, vol. 112, no. 9, pp. 1291–1299, Nov. 2003

[3] A. Tamsir, J. J. Tabor, and C. A. Voigt. "Robust multicellular computing using genetically encoded NOR gates and chemical 'wires'." *Nature*, vol. 469, no. 7329, pp. 212-215, Jan. 2011.

[4] Y. Higashikuni, W. CW Chen and T. K. Lu, "Advancing therapeutic applications of synthetic gene circuits", *Current Opinion in Biotechnology*, no. 47, pp. 133–141, Oct. 2017.

[5] D. T. Riglar and P. A. Silver, "Engineering bacteria for diagnostic and therapeutic applications," *Nature Reviews Microbiology*, vol. 16, no. 4, pp. 214–225, Feb. 2018.

[6] O. B. Akan, H. Ramezani, T. Khan, N. A. Abbasi, and M. Kuscu,"Fundamentals of molecular information and communication science", *Proceedings of the IEEE*, vol. 105, no. 2, pp. 306–318, Feb. 2017.

[7] D. P. Martins et. al, "Molecular Communications Pulse-Based Jamming Model for Bacterial Biofilm Suppression," *IEEE Transactions on Nanobioscience*, vol. 17, no. 4, pp. 533–542, Oct. 2018.

[8] D. P. Martins, M. T. Barros and S. Balasubramaniam, "Quality and Capacity Analysis of Molecular Communications in Bacterial Synthetic Logic Circuits," *IEEE Transactions on NanoBioscience*, vol. 18, no. 4, pp. 628–639, July 2019.

[9] K. Yagi,"Applications of whole-cell bacterial sensors in biotechnology and environmental science", *Applied Microbiology and Biotechnology*, vol. 73, no. 6, pp. 1251–1258, Jan. 2007.

[10] W. S. Wang et. al, "Real-time telemetry system for amperometric and potentiometric electrochemical sensors", *Sensors*, vol. 11, no. 9, pp. 8593–8610, Sep. 2011.

[11] I. F. Akyildiz, J. M. Jornet, "The Internet of Nano Things", *IEEE Wireless Communications*, vol. 17, n0. 6, pp.58–63, Dec. 2010.

[12] I. F. Akyildiz, M. Pierobon and S. Balasubramaniam, "The Internet of Bio-Nano Things", *IEEE Communications Magazine*, vol. 53, n0. 3, pp.32–40, Mar. 2015.

[13] I. Llatser, D. Demiray, A. Cabellos-Aparicio, D. T. Altilar, and E. Alarcón, "N3Sim: Simulation framework for diffusion-based molecular communication nanonetworks," *Simulation Modelling Practice and Theory*, vol. 42, pp. 210–222, Dec. 2013.

[14] M. Pierobon, and I. F. Akyildiz, "Diffusion-based Noise Analysis for Molecular Communication in Nanonetworks", *IEEE Transactions on Signal Processing*, vol. 59, no. 6, pp. 2532–2547, June 2011.

[15] L. Pauling, "General Chemistry", Dover Publications Inc., New York, United States of America, p. 96, 1970.

[16] A. Wahl et. al, "Electroanalysis at Ultramicro and Nanoscale Electrodes: A Comparative Study", *Journal of Electrochemical Society*, vol. 161, no. 2, pp. B3055–B3060, Jan. 2014.

[17] J. B. Raoof, R. Ojani and F. Chekin, "Electrochemical Analysis of D-Penicillamine Using a Carbon Paste Electrode Modified with Ferrocene Carboxylic Acid", *Electroanalysis: An International Journal Devoted to Fundamental and Practical Aspects of Electroanalysis*, vol. 19, no. 18, pp. 1883–1889, Sep. 2007.

[18] K. Dawson et. al, "Fully integrated on-chip nano-electrochemical devices for electroanalytical applications", *Electrochimica Acta*, vol. 115, no. 1, pp. 239–246, Jan. 2014.

CHAPTER 12

DISCUSSION

This PhD research work has investigated bacteria-based molecular communications systems by using conventional communications engineering metrics, such as end-to-end delay of molecular signals, channel noise from the environment, path loss of molecular signals, channel capacity, and attenuation of the molecular signal. Due to the uniqueness of this type of communications system, the mapping of the conventional communications theory onto bacteria-based systems faces numerous challenges. Moreover, beyond the mapping of the different systems, specific biological parameters such as different bacterial population strains and sizes, chemical rates, molecular signal production noise and diffusion coefficient, can affect the performance of the bacteria-based molecular communications systems and create challenges in their analysis. This chapter summarises the lessons learnt as well as understandings from designing and analysing different bacteria-based molecular communications systems.

12.1 DISASSEMBLING AND PREVENTING BIOFILMS

Biofilm formation has been associated to a number of harmful effects within the human body as well as the environments, and examples includes chronic diseases and biofouling.

Therefore, this PhD research aims to solve this issue by both disassembling as well as preventing biofilms formation using bacteria-based molecular communications systems. First, the thesis proposed the disassembling of biofilms by starving the bacteria from nutrients that will sustain the biofilm structure. The bacteria that are used to hijack the nutrients was engineered to detect the biofilm and position itself at a close location to deplete the nutrients around the biofilm. For the investigated scenario, the media where both bacterial populations are located does not affect their placement, the molecular diffusion, or the supply of external nutrients for the biofilm surroundings (in other words, there is no flow). This research focussed on the population growth and nutrient consumption dynamics for both free-moving bacteria and bacteria within the biofilm to show the impact of this induced nutrient competition on the disassembling process, when the free-moving bacteria forms the wall to absorb the nutrients. Therefore, this analysis did not investigated the impact of the proposed solution on the EPS production. Instead, this research considered any change in EPS production as an after effect based on the amount of nutrients consumed by the biofilm-forming bacteria. The analysis depicted in Figure 12.1a shows that when the bacteria cooperates (i.e. forming the wall), the free-moving bacteria is able to deplete the nutrients faster and consequently accelerate the biofilm decay, forcing its disassembling. Furthermore, the ability of the free-moving bacteria to attract other bacteria to form the wall was also investigated. Figure 12.1b shows that for the scenario studied, a small number of bacteria is more effective in attracting others microbes to the same location, which can enable us to determine that this parameter can be applied towards customisation of the system depending on the target scenario.

To prevent biofilm formation, a bacteria-based molecular communications system was devised to target the bacteria pathways (here modelled as communications channels) related to this process. Through wet lab experiments, the biofilm-related communications channels were identified for the *S. aureus* bacteria and the main proteins related to these channels were

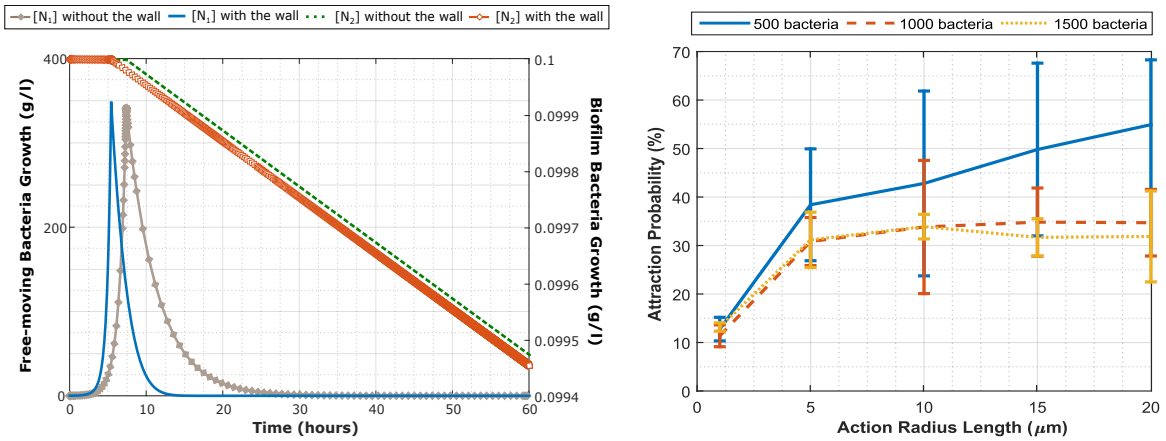

(a) (b)

Fig. 12.1 (a) Comparison between free-moving bacteria, $[N_1]$, and biofilm, $[N_2]$, growth rate when co-existing an there is no wall formed and when the wall is formed [51]. (b) Simulation of the attraction probability for three free-moving bacterial population sizes (500, 1000, 1500) [51].

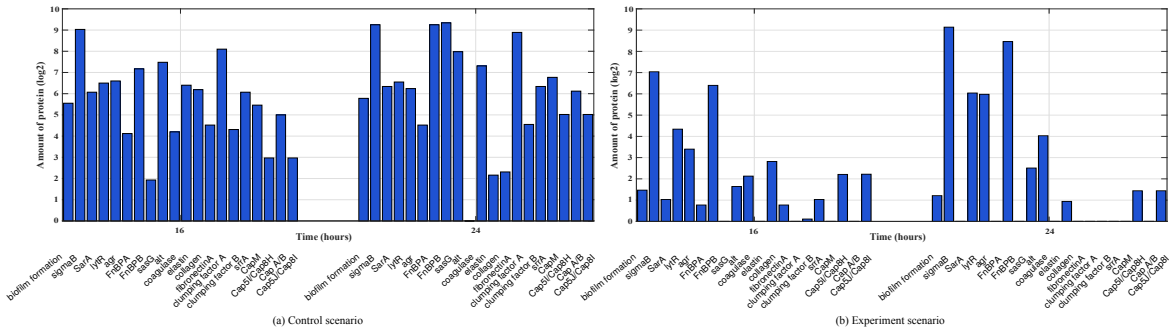

Fig. 12.2 A highlight of the most significant 19 proteins extracted from more than 1500 different types that were detected in the wet lab experiment. These concentration were considered for characterising the communications channels and the main proteins that are essential towards biofilm formation and maintenance. [51].

used as targets for molecular interference signals. These proteins (see Figure 12.2) showed a greater variation in their concentration levels and are directly related to the bacteria's ability to respond to the environmental changes [154–159]. It is important to note that there is no need to disrupt all the communications channels to prevent the biofilm formation. This process can be effective by influencing any of the identified channels [154–159]. The proposed model assumes that there is enough resources to sustain prolonged production of the molecular jamming signal by the engineered bacteria population to focus the analysis

on the communications performance of a bacteria-based molecular communications system subjected to this continuous molecular interference. Using conventional communications theory (see Figure 12.3a), the impact of the molecular interference signal on the biofilm-related communications channel was evaluated as path loss. This representation enabled us to identify specific molecular channels of corresponding proteins that can be disrupted from molecular interference signals (in other words jamming the signals to disrupt the legitimate molecular signals). Figure 12.3b shows the channel attenuation for different scenarios, and it can be noted that the greater attenuation for this bacteria-based molecular communications system occurs for a synchronised pulse-based jamming signal. Synchronisation in this case means that the interference is synchronised with the normal communication signals used by the bacteria to form the biofilm. This scenario not only attenuates the transmission required for the biofilm formation, but also quickly activates their communications channels in order to facilitate the interference on the target proteins (see Chapter 7). This was achieved when we jammed corresponding molecular proteins that will reverse the toggle-switch within the bacterium that will prevent signalling for channels that lead to formation of the biofilm.

The systems discussed in this section are biocompatible alternative solutions for preventing and disassembling biofilms. These approaches were based on bacterial natural behaviour and showed to be feasible, under the right conditions. To further investigate these scenarios, the computational modelling of the bacteria movement and population dynamics for the disassembling approach (Chapter 6), as well as for the signalling reception and signalling pathways used for preventing the biofilm (Chapter 7) were fundamental. Moreover, it also provided a mechanism in determining the systems' performance. It also could be observed that most of the complexity in design these bacteria-based approaches resides in the precise definition of the systems' parameters to be engineered as well as their values.

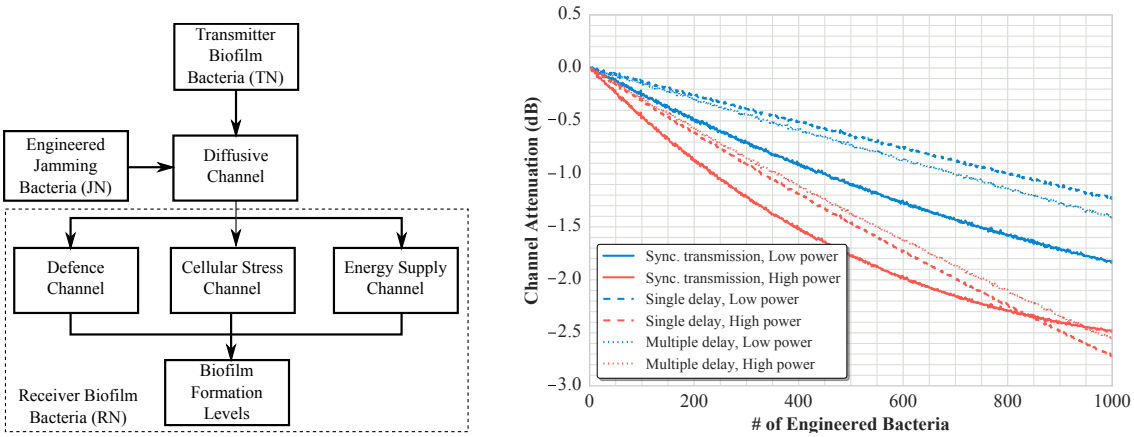

Fig. 12.3 (a) Molecular communications system model to disrupt the biofilm formation [144]. (b) Analysis of the channel attenuation when the production of the molecular pulse-based jamming signal suffers from single and multiple delays for a variable number of engineered bacteria at a fixed distance to the receiver bacterial population, which are the bacteria used to create the biofilm.

12.2 Design of Bacteria-based Molecular Communications Devices

The obtained results from the biofilm studies supported the development of more complex bacteria-based molecular communications systems. Devices ranging from an attenuator for virus filtration to a wireless bacteria-based biosensor were proposed in this PhD research. These devices also aimed to provide biocompatible alternatives to current issues that includes Ebola disease treatment (Chapter 8), and biotechnological applications that can utilize logic computing for biosensing chemical substances within the environment (Chapters 9 and 10, respectively).

The first bacteria-based device proposed in this PhD research was applied for the attenuation of Ebola virus concentration in the patient's blood. To avoid worsening the patient's condition, the engineered bacteria (the main component of this system) is placed inside an

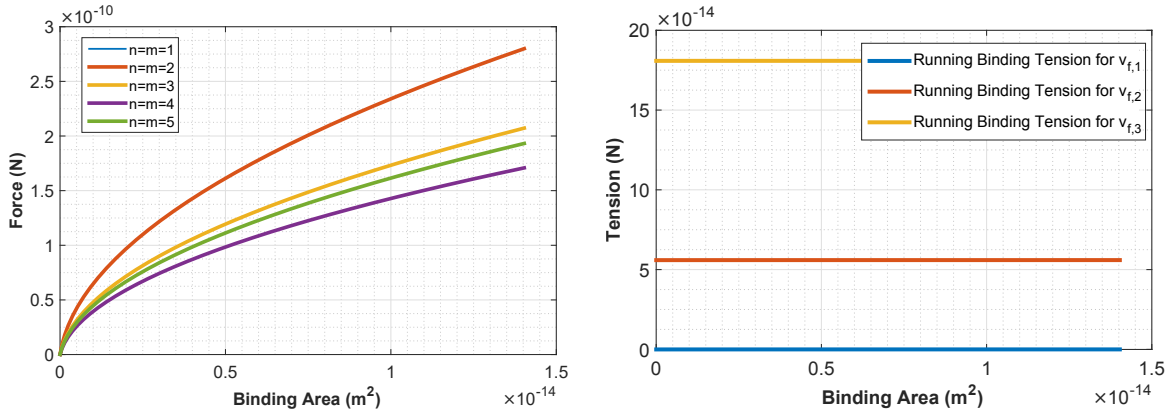

Fig. 12.4 (a) Analysis of the binding force for five different binding arrangements between the viral and bacterial proteins [146]. (b) Binding area tension analysis for different blood velocities ($v_{f1} = 0\mu$m/s, $v_{f2} = 10\mu$m/s and $v_{f3} = 20\mu$m/s) [146].

external microfluidic chamber that cycles the blood in a dialysis-like medical procedure. In this solution, the bacteria membrane is engineered to create a strong binding process to the viral membrane proteins upon contact. This strong adhesion is several magnitudes higher than any other tension exerted in the binding area (see Figures 12.4a and 12.4b). These results indicates that the focus for the future implementation of such a device will require the engineered bacteria to find as much Ebola virus as possible to bind with them in a short time period. As shown in Figure 12.5a, the placement of the engineered bacteria in the microfludic chamber affects the efficiency of the virus attenuation. Furthermore, the chamber design can also affect the virus pick-up process as it allow the engineered bacteria to freely move (as shown in Figure 12.5a) or provide a specific direction for them to move. This pick-up process was simulated for 720 seconds (to avoid blood clotting) for a fixed number of virus ($10,000$) and three engineered bacterial population sizes (1000, 3000 and 5000). It can be noted from Figure 12.5b that the pick-up ratio increases logistically with respect to the simulation time. Additionally, as more engineered bacteria is placed in the microfluidic chamber, more virus can be collected (reaching 60% when using 5000 engineered bacteria). These results shows the feasibility of the proposed bacteria-based device for supporting the

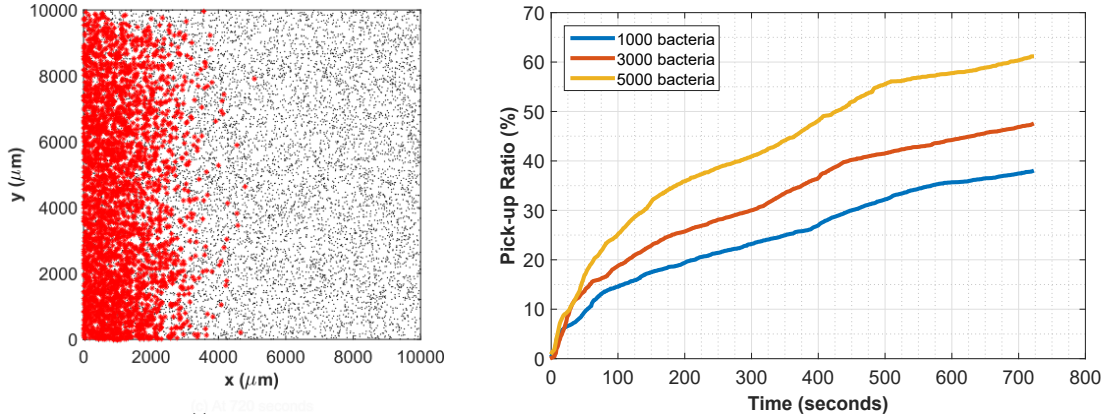

(a) (b)

Fig. 12.5 (a) The placement of bacteria have an impact on the spatial distribution of the virus. At 720 seconds, bacteria is able to cover more than 30 percent of the chamber's area. Adapted from [146]. (b) The virus pick-up ratio is dependent on the number of engineered bacteria and the time that they are allowed to swim and collect the Ebola virus [146].

treatment of this particular disease, and can pave the way for similar system design for other deadly virus-related diseases.

This PhD research also investigated the performance of a logic circuit composed by three bacteria-based logic gates interconnected by two fluid diffusion channels. Specifically, this bacteria-based molecular communications systems was designed to study the possible trade-off between an accurate molecular generation and the end-to-end channel capacity of this system. Therefore, communications parameters like, input delay, noise and input amplitude mismatch were applied as variables for this study. It is important to note that the noise considered in this work is the fluctuation in the molecular concentration output by each synthetic logic gate. Therefore, this assumption focuses on the system performance analysis of an ideal scenario that can be used as a benchmark for this specific device. Two of this analysis' results are shown in Figure 12.6. First, the results in Figure 12.6a shows that the channel capacity decreases as the gate input concentration difference (i.e., input amplitude mismatch) increases, which is a similar result for the *accuracy_ratio*. However, Figure 12.6a also shows that there is an inverse relationship between the channel capacity and

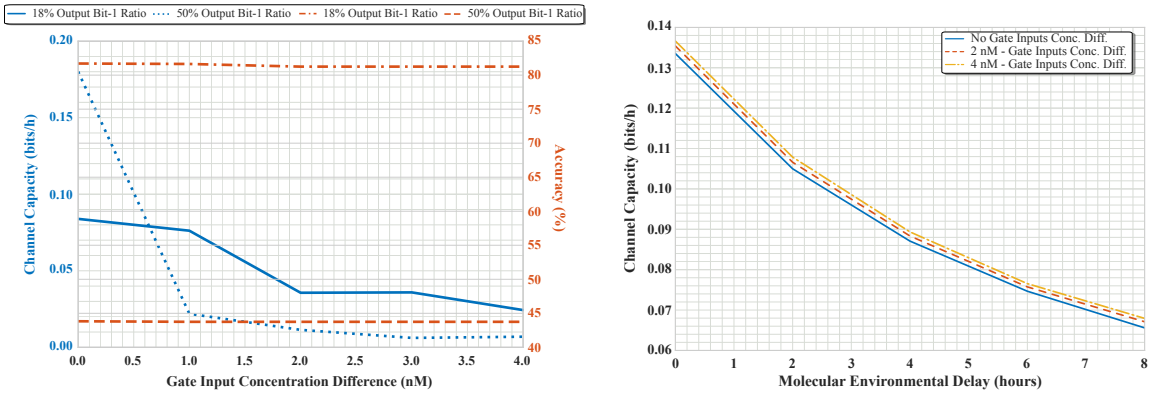

(a) (b)

Fig. 12.6 (a) Evaluation of the channel capacity and circuit accuracy, for a gate inputs concentration difference ranging from 0 to 4 nM [147]. (b) Channel capacity for different molecular environmental delays for three gate input concentration difference values [147].

the *accuracy_ratio*, which are also dependent on the output bit-1 ratio (number of bit-1 over the total number of bits output from the system). This means that the system performance can be adjusted if necessary, by modifying the thresholds used to define what is a bit '0' or '1'. These adjustments might be made in cases where a more accurate system is needed (noisy environments) or when more information needs to be transmitted (fast detection of disease biomarkers). The channel capacity was also investigated when the system is subjected to molecular environmental delays (i.e., input delays). Figure 12.6b shows the result of this analysis for three gate input concentration difference values, and it can be noted that the channel capacity exponentially decreases with respect to the molecular environmental delays. Additionally, it shows that a higher gate input concentration difference can counter the effect of the delay and improve the end-to-end channel capacity.

An electronic equivalent model for a bacterial population that performs logic gate computing using molecular signals was proposed in this PhD research. This system acts as a wireless bacteria-based biosensor that senses a molecular signal concentration, in this case nitrile ($R-C\equiv N$), produced by a distant generator and outputs ammonia (NH_3) and acid (H^+) in response (see Chapter 10). Three distinct processes of the wireless bacteria-based

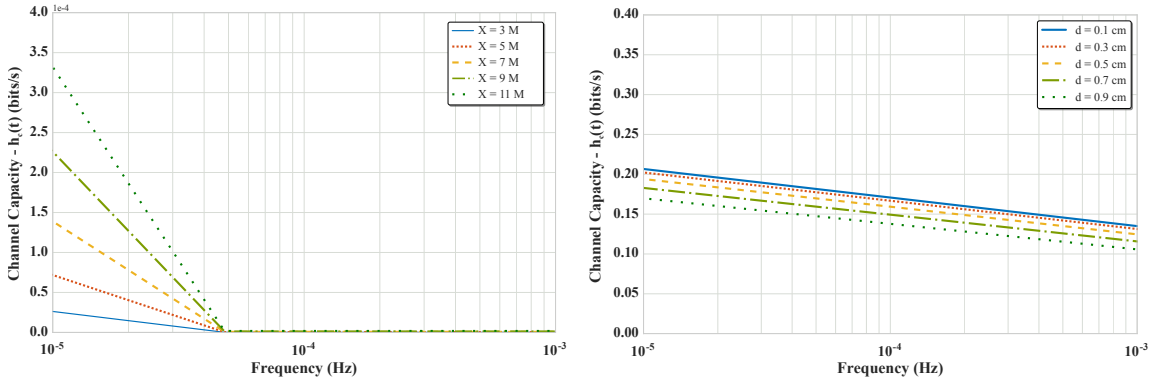

(a) (b)

Fig. 12.7 Evaluation of the diffusion channel capacity. (a) In this case, a fixed distance $d = 0.5\,\text{cm}$ and different molecular input signals amplitude X were considered [148]. (b) In this scenario, a fixed molecular input signals $X = 11\,\text{M}$ and different distances d between the molecular generator and the wireless bacteria-based biosensor were considered [148].

biosensor were described using electronic components (resistors, capacitors and transistors) and grouped into a single circuit that is equivalent to the bacterial natural processes of receiving, computing and emitting a molecular signal. A frequency domain analysis was used to study this system's performance (see Figure 12.7). Therefore, the capacity of the diffusive channel that interconnects the molecular generator and the bacterial population was evaluated with respect to the frequency of the nitrile molecular signal. The distance between the molecular generator and the bacterial population, as well as the amplitude of the molecular signal produced by the generator were considered for the evaluation of the diffusive channel capacity. It can be noted from Figure 12.7a that the channel capacity sharply decreases with respect to the molecular signal frequency and that higher molecular signal amplitudes results in higher channel capacity values. Figure 12.7b shows the evaluation of the diffusive channel capacity for different distances d. It can be inferred from this result that the distance barely affects the diffusive channel capacity. These results allowed the identification of the main parameters needed to build the wireless bacteria-based biosensor.

Integration between bacteria-based molecular communications systems and electrochemical sensors was proposed to reliably compute molecular signals based on the acidification

of the fluid media, where engineered bacteria were placed. The indirect measurement of the molecular output signal was possible due to the high sensitivity of the pH level change by the electrochemical sensors. Therefore, the electrical signal (current or voltage) was investigated to ensure that these electrochemical sensors reliably detect the pH level change. Figure 12.8a show the different electrical current and potential produced due to different pH levels of the fluid. It can be noted from this result that small variations on pH level result in noticeable electrical signals. To further this investigation, the electrical potential was fixed at 0.28 V and the electrical current was measured for different pH levels. The result of this scenario is shown in Figure 12.8b and it can be noted that the electrical current has an inverse relationship with the pH level. Furthermore, these results were fitted to a mathematical equation to evaluate the electrical current for any pH level from 7 to 9. From these results, the detection threshold of 3.2 nM for the electrochemical sensors was defined, which can be translated as a pH 8.5 and consequently produce an electrical current of 0.45 nA.

In Chapter 10 and 11, similar bacteria-based systems were proposed to detect environmental harmful chemical agents. However, in Chapter 10, the analysis focused on the propagation of the signals emitted by a molecular source and its effect on the operation of the synthetic logic gate. Furthermore, the molecular output of the AND gate can be measured by an optical imaging system. In comparison with the work described in Chapter 10, this device was proposed to investigate the reliable and quicker detection of molecular signals output by the engineered bacteria using electrical signals, instead of optical imaging. On all the four devices investigated in this PhD research work, bacteria-based molecular communications systems was built to allow the wireless exchange of molecular signals. Thus, communication metrics can be applied on the numerical and simulation analyses of their performances and presents fine details of the nature of these devices. For example, the amplitude of the input signals have a greater impact on the channel capacity of simple systems, like the wireless bacteria-based biosensor, than in the complex cases (e.g. capsular bacteria-based

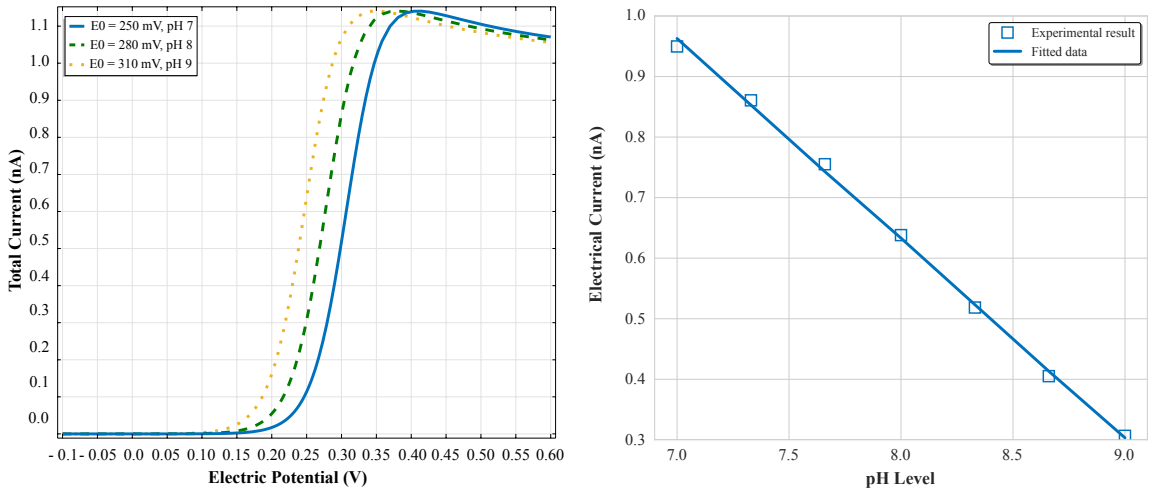

(a) (b)

Fig. 12.8 Evaluation of the electrical signal produced by the detection of the pH level change. (a) As the pH increases (as more molecules are generated), the total current value increases for the same electric potential. [160]. (b) Plot of the electrical current values for different pH levels when the electric potential is fixed at 0.28 V. [160].

logic circuit). Therefore, these results demonstrates the importance of accurate definitions of the target scenarios and the parameter values for designing bacteria-based molecular communications devices.

12.3 RELIABILITY ANALYSIS OF WIRELESS BACTERIA -BASED SYNTHETIC LOGIC GATES

Biological systems can be affected by several factors that would impact on the predictability and control required by conventional communications systems. Therefore, it becomes critical to specify accurate and precise bacteria-based molecular communications system parameters to have reliable outputs and support the implementation of long-term operating devices. In this PhD research work, three bacteria-based molecular communications systems were devised to study the reliability of synthetic logic gates. Firstly, a study was conducted on the capsular bacteria-based logic circuit and its reliability in terms of the produced molecular

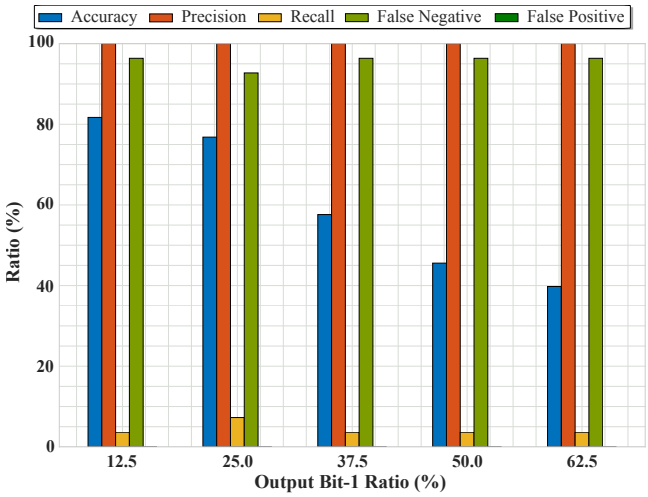

Fig. 12.9 Circuit quality evaluated for different output bit-1 ratio. The circuit produced a 100% precise molecular output signal and no false positive was detected [147].

output signal. A nitrile wireless bacteria-based biosensor's accuracy was investigated through a comparison between simulation and experimental results. Lastly, two different diffusive channels have their impact evaluated based on the reliable operation of a synthetic AND gate.

Four molecular input signals with different amplitudes were considered for the logic operation of a bacteria-based synthetic logic circuit, which is placed inside a compartmented capsule. Each gate of the synthetic logic circuit is composed of a bacterial population, which are interconnected by diffusion channels. The reliable logic computation of these molecular signals, by the synthetic logic gates, is assessed in terms of the *accuracy*, *precision*, *recall*, *false positive* and *false negative* ratio for the molecular output signal. Figure 12.9 shows that no *false positive_ratio* were measured for all considered output bit-1 ratio (number of bit 1 over the total of output bits), which resulted in a 100% precise system. On the other hand, the *accuracy_ratio* reduced with respect to the increase of the output bit-1 ratio, showing that the correct reception of the signal becomes more complex and less reliable as the number of bit 1 in the molecular output signal increases. Another important result from this analysis is the high *false negative_ratio* that is due to the definition of a high detection threshold. Therefore, fine tuning of the threshold value may improve the computation of these molecular signals.

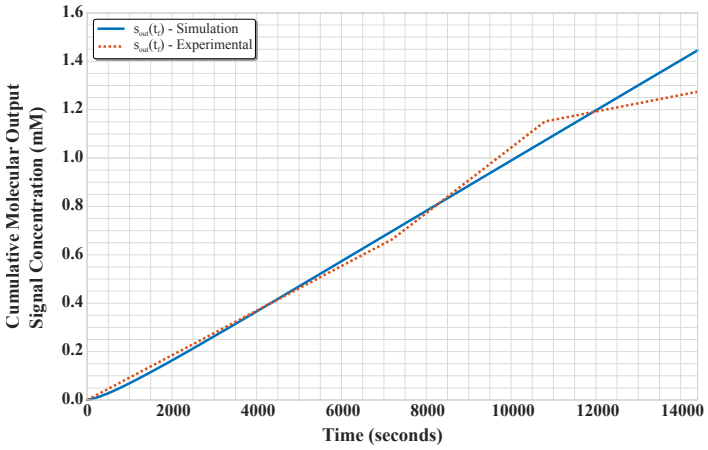

Fig. 12.10 Comparison of the cumulative molecular output signal concentration obtained from the simulation and wet lab experiment (adapted from [148]).

A molecular communications system, where a wireless bacteria-based biosensor (composed of a synthetic logic gate) designed to detect nitrile (R−C≡N) and output ammonia (NH_3) and acid (H^+) was developed as part of the wet lab experiments in this PhD research. This system had its reliability studied through a comparison between wireless bacteria-based biosensor circuit simulation and a wet lab experiment. Two molecular input signal amplitudes were applied directly on the plates containing the engineered bacteria for the wet lab experiment. For the simulation, these same molecular signals were emitted from a distance $d = 0.5\,\text{cm}$ to activate the proposed circuit. Additionally, the simulated molecular signals were modelled as a quasi-constant function (see Chapter 10) and evaluated through the cumulative molecular output signal of this system. This modelling simplified the validation process and this is because in the wet lab experiment, the pipetting process often produces a constant molecular signal concentration. Due to the unknown number of engineered bacteria used in the experiment, we considered for the circuit simulation that each engineered bacterium of the population has the same characteristics, and they cooperate towards the production of the molecular output signal. These conditions allowed to fit the simulation to the experimental results by using a multiplying factor equal to $800,000,000$. Figure 12.10 shows the obtained result from this comparison, and it can be noted that both approach produces similar cumula-

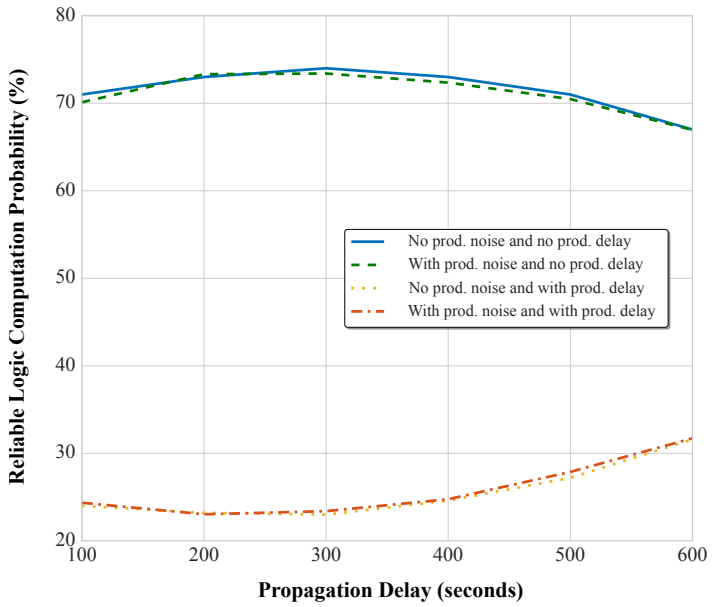

Fig. 12.11 Reliability logic computation probability for a increasing propagation delay values when the system is subjected or not to production and propagation noise and delay. [160].

tive molecular output signal concentrations (the mean squared error for this comparison was equal to 7.33×10^{-3}). Therefore, the proposed molecular communications systems could be validated and showed to be an accurate representation of this sensing and actuation scenario.

The performance and the reliability of a simple synthetic logic gate will depend on the environment where it is placed, among other factors. For example, it is expected that a molecular communications system applied to a fluid scenario will have a higher channel capacity and reliability if no noise and delay is applied to the system. Therefore, a bacteria-based molecular communications system was proposed for studying its reliability when subjected to different unwanted effects. This investigation, presented in Chapter 11, analysed the impacts of the reliable operation of a synthetic logic gate based on the transmission of molecular signals over a fluid media and can acidify it (step required for the detection of a molecular signal using electrochemical sensors). Figure 12.11 shows that the maximum reliable logic computing probability achieved was 73%. It can also be observed that the increase in propagation delay can reduce reliable logic computing probability for the system's operation without production delay. On the other hand, the propagation delay counter the

effect of the production delay, see Figure 12.11. For the scenarios analysed, the delay is shown as the parameter that most affects the reliability of this proposed bacteria-based molecular communications system.

The reliability of the three wireless bacteria-based synthetic logic circuits studied in this PhD research was shown to be mostly dependent on the scenario considered for their analyses. Thus, a proper definition of the restrictions and associated parameter values will result in more reliable logic computation of the molecular signals. In addition, it could be inferred that the molecular communications systems can be used as a supporting tool to design reliable wireless bacteria-based synthetic logic circuits.

CHAPTER 13

CONCLUSION

A number of bacteria-based molecular communications systems have been studied in the past ten years (e.g., bacteria-based nanosensors) [14, 43, 161]. Nonetheless, just a few of these works focus on the design of devices that utilize engineered bacteria to do specialised functions at the hardware level that are able to exchange molecular signals to improve it's reliability[52, 91]. These studies mostly focus on the analysis of using molecular signals taken from conventional communications techniques. A similar situation occurred for the biology facets of this PhD thesis. Bacteria-based synthetic biology systems (hardware level) have been extensively investigated in the past twenty years [4, 45–50, 96, 104, 108, 109, 111–114, 118–124, 133–137]. For example, synthetic transmitters and receivers have been designed to emit and receive molecular signals, respectively. Despite this, limited research works have focused on the communications analysis at the software level for synthetic systems. Therefore, the union of these two complementary subjects that includes molecular communications and synthetic biology, will enable the development of biocompatible applications that will improve life quality and expectancy of animals, plants and humans.

This PhD thesis follows this union premise and is focused on the design of computational bacteria-based synthetic biology systems that communicate using molecular signals. Notably, this thesis investigated the operation using spatio-temporal and frequency domain analysis,

performance analysis in terms of channel capacity and path loss, and reliability analysis using metrics such as accuracy and precision. The contributions of this PhD research were grouped into three main topics: disassembling and preventing biofilms, design of bacteria-based molecular communications devices that utilized engineered bacteria, and reliability analysis of wireless bacteria-based synthetic logic gates.

Biofilms have been related to chronic infections and industrial biofouling, hence the necessity of controlling its formation and inducing its dispersal is an important issue facing the biotechnology industry today. Two molecular communications systems were devised to apply natural bacteria signalling to affect a formed biofilm that will induce its dispersion, or interfering with the biofilm formation to prevent its formation. For the first case, the population dynamics and bacteria communications capabilities were simulated to evaluate how fast an induced biofilm disassembling can occur, and how effective the bacteria signalling can be utilized to induce this process. In the second case, a pulse-based jamming system produced the attenuation required to affect the internal bacterial communications channels, which consequently will prevent the biofilm formation. The molecular environmental delay, the power of the jamming signal and the distance between the engineered jamming bacteria and the biofilm were considered for the evaluation of the channel attenuation. These results showed that a bacteria-based molecular communications system can be established to negatively interact with a biofilm towards its disassembling and prevention.

More complex bacteria-based molecular communications systems were also proposed to attenuate the amount of Ebola virus in the patient's blood, to logically compute molecular signals and to biosense nitrile in the environment. These devices were analysed in the spatial, temporal and frequency domains in addition to communications performance analysis. Other metrics that includes pick-up ratio for the virus attenuator, gate input concentration difference in the synthetic logic circuit, and the power spectrum density for there wireless bacteria-based biosensor were also considered. For the virus attenuator, it was found that due to the number

of bacteria placed inside the microfluidic chamber, this device could be fitted to a particular level of infection, enabling it to become a customisable system. In the synthetic logic circuit analysis, the research found a trade-off between the circuit accuracy and its channel capacity that should be optimised during the implementation of the proposed device. The analysis of the wireless bacteria-based biosensor showed the dependence of the sensing operation on the frequency of the molecular signal inputs to the system. These bacteria-based devices allowed the exchange of molecular signals and the investigation of their performance contributes for future implementation of such bacteria-based molecular communications systems.

Lastly, this PhD thesis further studied the reliability of bacteria-based synthetic circuits to identify the main parameters and factors that could preclude the correct operation of these systems. Therefore, quality metrics were evaluated for the proposed synthetic logic device, a wet lab experiment was used to validate the wireless bacteria-based biosensor, and different diffusive communications channel were considered for the computing of the reliable logic operation probability for a synthetic AND gate. In the case of the synthetic logic device, the results showed that reliable computation depends on the accurate definition of the detection threshold for the system to be sensitive to minimal variations. For the wireless bacteria-based biosensor, the cumulative molecular output signal simulated using an electronic equivalent circuit model is similar to the case obtained through the wet lab experiment and only requiring the definition of a multiplying factor. In conclusion, the fluid channel produced reliable operations overall, despite the porous channel having a better performance when a lower bacterial population size was considered.

The results obtained from the study of the aforementioned topics demonstrated the operation of synthetic systems when considered as the hardware physical layer of a bacteria-based molecular communications systems. They can be used for the future development of more complex systems, and also be applied to further investigation of other bacteria behaviours such as population control, and exploration of other aspects of the molecular

communications and synthetic biology integration. In the following section, the future works that will address some of the topics not covered by this PhD thesis are outlined.

13.1 FUTURE WORKS

The synergistic effect when molecular communications and synthetic biology systems are put together have a number of ramifications, in addition to the challenges that were presented in this PhD thesis. Thus, other investigations based on the results obtained through this PhD research can be further investigated to understand these ramifications. In the following subsections, some works that can be further investigated from this PhD thesis are introduced.

13.1.1 INVESTIGATION OF OTHER BACTERIA BEHAVIOURS

This PhD thesis focused on some of the common bacterial behaviours. However, other behaviours can also be investigated towards the development of novel bacteria-based molecular communications systems. For example, the bacteria signalling pathways that produce virulence factors can be modelled using a similar approach to the pulse-based jamming system that was presented in Chapter 7 to create alternative treatments for bacterial infections. Similarly, population control and other ecological relationships of the microbes (i.e., commensalism, mutualism and parasitism) can also be applied to the design of bacteria-based molecular communications systems.

13.1.2 REAL IMPLEMENTATION OF BACTERIA-BASED DEVICES

The numerical and simulation analyses performed in this PhD thesis were based and adapted from other synthetic biology works that often had other goals compared to the cases investigated in this PhD research. Thus, the next step would be the design of proof-of-concept systems to validate the theoretical models, and to develop prototypes for novel future devices.

To take this synergistic approach for the implementation of real bacteria-based devices will require collaborations with professionals from other fields. For example, to build such devices, molecular microbiologists and electrochemists are needed. Then, at a later stage, pharmacists, physicians and veterinarians will be necessary to test the bacteria-based devices in humans and animals.

13.1.3 FURTHER INTEGRATION BETWEEN MOLECULAR COMMUNICATIONS AND SYNTHETIC BIOLOGY

The synergy demonstrated for bacteria-based molecular communications systems and synthetic biology can be also seen in Ca^{2+}-signalling-based, neuronal-based and virus-based systems [13, 162, 163]. However, there are several other biological processes that have not been modelled using molecular communications systems (e.g., inter-kingdom communications). Bacteria can communicate with protozoans, insects, plants and animal cells [164–166]. These processes could be modelled as a heterogenous communications systems and it will help to understand the effects of other cells on the design of bacteria-based system. Biocompatible devices and procedures can result from this approach as an alternative to the conventional methods that have been related to the emergence of antibiotic resistant microbes.

13.1.4 INTERNET OF BIO-NANO THINGS

Wireless bacteria-based biosensors can be interconnected in a conventional network manner to monitor more complex scenarios. Furthermore, the molecular outputs of these systems can be transformed into electrical signals that can connect to the Internet. This scenario was introduced by Akyildiz et. al and describe the potential use of a biological nanonetworks to exchange molecular signals towards the development of healthcare applications, among others [43]. Bacteria-based devices were showed in this PhD research to be feasible options

for the development of the Internet of Bio-Nano Things, leading to improved monitoring and controling of biological systems.

REFERENCES

[1] M. J. Smanski, H. Zhou, J. Claesen, B. Shen, M. A. Fischbach, and C. A. Voigt, "Synthetic biology to access and expand nature's chemical diversity," *Nature Reviews Microbiology*, vol. 14, no. 3, p. 135, Mar. 2016.

[2] Y. Higashikuni, W. C. Chen, and T. K. Lu, "Advancing therapeutic applications of synthetic gene circuits," *Current Opinion in Biotechnology*, vol. 47, pp. 133–141, Oct. 2017.

[3] L. You, R. S. Cox, R. Weiss, and F. H. Arnold, "Programmed population control by cell–cell communication and regulated killing," *Nature*, vol. 428, no. 6985, pp. 868–871, Apr. 2004.

[4] A. Tamsir, J. J. Tabor, and C. A. Voigt, "Robust multicellular computing using genetically encoded NOR gates and chemical 'wires'," *Nature*, vol. 469, no. 7329, pp. 212–5, Jan. 2011.

[5] T. Großkopf and O. S. Soyer, "Synthetic microbial communities," *Current opinion in microbiology*, vol. 18, pp. 72–77, Apr. 2014.

[6] M. A. Marchisio and J. Stelling, "Computational design tools for synthetic biology," *Current opinion in biotechnology*, vol. 20, no. 4, pp. 479–485, Aug. 2009.

[7] C. A. Hutchison, R.-Y. Chuang, V. N. Noskov, N. Assad-Garcia, T. J. Deerinck, M. H. Ellisman, J. Gill, K. Kannan, B. J. Karas, L. Ma, *et al.*, "Design and synthesis of a minimal bacterial genome," *Science*, vol. 351, no. 6280, aad6253, Mar. 2016.

[8] S. Robert, C. Gysemans, T. Takiishi, H. Korf, I. Spagnuolo, G. Sebastiani, K. Van Huynegem, L. Steidler, S. Caluwaerts, P. Demetter, C. H. Wasserfall, M. A. Atkinson, F. Dotta, P. Rottiers, T. L. Van Belle, and C. Mathieu, "Oral delivery of glutamic acid decarboxylase (GAD)-65 and IL10 by lactococcus lactis reverses diabetes in recent-onset NOD mice," *Diabetes*, vol. 63, no. 8, pp. 2876–2887, Aug. 2014.

[9] I. Y. Hwang, M. H. Tan, E. Koh, C. L. Ho, C. L. Poh, and M. W. Chang, "Reprogramming microbes to be pathogen-Seeking killers," *ACS Synthetic Biology*, vol. 3, no. 4, pp. 228–237, Apr. 2014.

[10] E. Andrianantoandro, S. Basu, D. K. Karig, and R. Weiss, "Synthetic biology: new engineering rules for an emerging discipline," *Molecular Systems Biology*, vol. 2, no. 1, May 2006.

[11] T. Nakano, M. J. Moore, F. Wei, A. V. Vasilakos, and J. Shuai, "Molecular Communication and Networking: Opportunities and Challenges," *IEEE Transactions on NanoBioscience*, vol. 11, no. 2, pp. 135–148, Jun. 2012.

[12] G. A. Truskey, F. Yuan, and D. F. Katz, "Transport phenomena in biological systems," 2004.

[13] M. T. Barros, "Ca2+-signaling-based molecular communication systems: Design and future research directions," *Nano Communication Networks*, vol. 11, pp. 103–113, Mar. 2017.

[14] L. C. Cobo and I. F. Akyildiz, "Bacteria-based communication in nanonetworks," *Nano Communication Networks*, vol. 1, no. 4, pp. 244–256, Dec. 2010.

[15] E. Gul, B. Atakan, and O. B. Akan, "Nanons: A nanoscale network simulator framework for molecular communications," *Nano Communication Networks*, vol. 1, no. 2, pp. 138–156, Jun. 2010.

[16] T. E. Gorochowski, A. Matyjaszkiewicz, T. Todd, N. Oak, K. Kowalska, S. Reid, K. T. Tsaneva-Atanasova, N. J. Savery, C. S. Grierson, and M. Di Bernardo, "Bsim: An agent-based tool for modeling bacterial populations in systems and synthetic biology," *PloS one*, vol. 7, no. 8, e42790, Aug. 2012.

[17] L. Felicetti, M. Femminella, and G. Reali, "Simulation of molecular signaling in blood vessels: Software design and application to atherogenesis," *Nano Communication Networks*, vol. 4, no. 3, pp. 98–119, Sep. 2013.

[18] G. Wei, P. Bogdan, and R. Marculescu, "Efficient modeling and simulation of bacteria-based nanonetworks with bnsim," *IEEE Journal on Selected Areas in Communications*, vol. 31, no. 12, pp. 868–878, Dec. 2013.

[19] I. Llatser, D. Demiray, A. Cabellos-Aparicio, D. T. Altilar, and E. Alarcón, "N3sim: Simulation framework for diffusion-based molecular communication nanonetworks," *Simulation Modelling Practice and Theory*, vol. 42, pp. 210–222, Mar. 2014.

[20] Y. Jian, B. Krishnaswamy, C. M. Austin, A. O. Bicen, A. Einolghozati, J. E. Perdomo, S. C. Patel, F. Fekri, I. F. Akyildiz, C. R. Forest, *et al.*, "Nanons3: A network simulator for bacterial nanonetworks based on molecular communication," *Nano communication networks*, vol. 12, pp. 1–11, Jun. 2017.

[21] M. Gregori and I. F. Akyildiz, "A new nanonetwork architecture using flagellated bacteria and catalytic nanomotors," *IEEE Journal on selected areas in communications*, vol. 28, no. 4, pp. 612–619, May 2010.

[22] V. Petrov, D. Moltchanov, and Y. Koucheryavy, "Analytical model for link reliability in bacteria nanonetworks," in *Proceedings of ACM The First Annual International Conference on Nanoscale Computing and Communication*, ACM, May 2014, p. 17.

[23] M. Komarov, B. Deng, V. Petrov, and D. Moltchanov, "Performance analysis of simultaneous communications in bacterial nanonetworks," *Nano Communication Networks*, vol. 8, pp. 55–67, Jun. 2016.

[24] N. Michelusi and U. Mitra, "Capacity of electron-based communication over bacterial cables: The full-csi case," *IEEE Transactions on Molecular, Biological and Multi-Scale Communications*, vol. 1, no. 1, pp. 62–75, Mar. 2015.

[25] N. Michelusi, J. Boedicker, M. Y. El-Naggar, and U. Mitra, "Queuing models for abstracting interactions in bacterial communities," *IEEE Journal on Selected Areas in Communications*, vol. 34, no. 3, pp. 584–599, Mar. 2016.

[26] S. Balasubramaniam and P. Lio', "Multi-Hop Conjugation Based Bacteria Nanonetworks," *IEEE Transactions on NanoBioscience*, vol. 12, no. 1, pp. 47–59, Mar. 2013.

[27] S. Balasubramaniam, N. Lyamin, D. Kleyko, M. Skurnik, A. Vinel, and Y. Koucheryavy, "Exploiting bacterial properties for multi-hop nanonetworks," *IEEE Communications Magazine*, vol. 52, no. 7, pp. 184–191, Jul. 2014.

[28] G. Wei, P. Bogdan, and R. Marculescu, "Bumpy rides: Modeling the dynamics of chemotactic interacting bacteria," *IEEE Journal on Selected Areas in Communications*, vol. 31, no. 12, pp. 879–890, Dec. 2013.

[29] G. Wei, C. Walsh, I. Cazan, and R. Marculescu, "Molecular tweeting," in *Proceedings of the 6th ACM Conference on Bioinformatics, Computational Biology and Health Informatics - BCB '15*, New York, New York, USA: ACM Press, Sep. 2015, pp. 366–375.

[30] C. Bai, M. S. Leeson, and M. D. Higgins, "Performance of sw-arq in bacterial quorum communications," *Nano Communication Networks*, vol. 6, no. 1, pp. 3–14, Mar. 2015.

[31] ——, "Analysis of arq protocols for bacterial quorum communications," *Nano Communication Networks*, vol. 7, pp. 65–79, Mar. 2016.

[32] A. Einolghozati, M. Sardari, A. Beirami, and F. Fekri, "Data gathering in networks of bacteria colonies: Collective sensing and relaying using molecular communication," in *2012 Proceedings IEEE INFOCOM Workshops*, IEEE, Mar. 2012, pp. 256–261.

[33] A. Einolghozati, M. Sardari, and F. Fekri, "Design and Analysis of Wireless Communication Systems Using Diffusion-Based Molecular Communication Among Bacteria," *IEEE Transactions on Wireless Communications*, vol. 12, no. 12, pp. 6096–6105, Oct. 2013.

[34] ——, "Networks of bacteria colonies: A new framework for reliable molecular communication networking," *Nano Communication Networks*, vol. 7, pp. 17–26, Mar. 2016.

[35] Y. Gao, S. Lakshmanan, and R. Sivakumar, "On attractant scheduling in networks based on bacterial communication," in *2011 IEEE Conference on Computer Communications Workshops (INFOCOM WKSHPS)*, IEEE, Apr. 2011, pp. 419–424.

[36] W.-K. Hsu, M. R. Bell, and X. Lin, "Carrier allocation in mobile bacteria networks," in *2015 49th Asilomar Conference on Signals, Systems and Computers*, IEEE, Nov. 2015, pp. 59–63.

[37] V. Petrov, S. Balasubramaniam, R. Lale, D. Moltchanov, Y. Koucheryavy, *et al.*, "Forward and reverse coding for chromosome transfer in bacterial nanonetworks," *Nano Communication Networks*, vol. 5, no. 1-2, pp. 15–24, Mar. 2014.

[38] V. Petrov, D. Moltchanov, S. Balasubramaniam, and Y. Koucheryavy, "Incorporating bacterial properties for plasmid delivery in nano sensor networks," *IEEE Transactions on Nanotechnology*, vol. 14, no. 4, pp. 751–760, Jul. 2015.

[39] V. Petrov, B. Deng, D. Moltchanov, S. Balasubramaniam, and Y. Koucheryavy, "Performance comparison of message encoding techniques for bacterial nanonetworks," in *2016 IEEE Wireless Communications and Networking Conference*, IEEE, Apr. 2016, pp. 1–7.

[40] B. Krishnaswamy, C. M. Henegar, J. P. Bardill, D. Russakow, G. L. Holst, B. K. Hammer, C. R. Forest, and R. Sivakumar, "When bacteria talk: Time elapse communication for super-slow networks," in *2013 IEEE International Conference on Communications (ICC)*, IEEE, Jun. 2013, pp. 6348–6353.

[41] B. Krishnaswamy, C. M. Austin, J. P. Bardill, D. Russakow, G. L. Holst, B. K. Hammer, C. R. Forest, and R. Sivakumar, "Time-elapse communication: Bacterial communication on a microfluidic chip," *IEEE Transactions on Communications*, vol. 61, no. 12, pp. 5139–5151, Dec. 2013.

[42] B. Atakan, "Molecular communications among nanomachines," in *Molecular Communications and Nanonetworks*, Springer, 2016, ch. 1, pp. 1–24.

[43] I. F. Akyildiz, M. Pierobon, and S. Balasubramaniam, "Moving forward with molecular communication: From theory to human health applications," *Proceedings of the IEEE*, vol. 107, no. 5, pp. 858–865, May 2019.

[44] S. Hennig, G. Rödel, and K. Ostermann, "Artificial cell-cell communication as an emerging tool in synthetic biology applications," *Journal of biological engineering*, vol. 9, no. 1, p. 13, Dec. 2015.

[45] P. Hillenbrand, G. Fritz, and U. Gerland, "Biological Signal Processing with a Genetic Toggle Switch," *PLoS ONE*, vol. 8, no. 7, M. Isalan, Ed., e68345, Jul. 2013.

[46] J. J. Collins, T. S. Gardner, and C. R. Cantor, "Construction of a genetic toggle switch in Escherichia coli," *Nature*, vol. 403, no. 6767, pp. 339–342, Jan. 2000.

[47] B. Saltepe, E. Ş. Kehribar, S. S. Su Yirmibeşoğlu, and U. Ö. Şafak Şeker, "Cellular Biosensors with Engineered Genetic Circuits," *ACS Sensors*, vol. 3, no. 1, pp. 13–26, Nov. 2018.

[48] N. Dalchau, G. Szép, R. Hernansaiz-Ballesteros, C. P. Barnes, L. Cardelli, A. Phillips, and A. Csikász-Nagy, "Computing with biological switches and clocks," *Natural Computing*, vol. 17, no. 4, pp. 761–779, Jun. 2018.

[49] A. Urrios, E. Gonzalez-Flo, D. Canadell, E. De Nadal, J. Macia, and F. Posas, "Plug-and-Play Multicellular Circuits with Time-Dependent Dynamic Responses," *ACS Synthetic Biology*, vol. 7, no. 4, pp. 1095–1104, Mar. 2018.

[50] A. Sengupta, H. B. Pakrasi, and P. P. Wangikar, "Recent advances in synthetic biology of cyanobacteria," *Applied Microbiology and Biotechnology*, pp. 1–15, May 2018.

[51] D. P. Martins, M. T. Barros, and S. Balasubramaniam, "Using competing bacterial communication to disassemble biofilms," in *Proceedings of the 3rd ACM International Conference on Nanoscale Computing and Communication*, ACM, Sep. 2016, p. 18.

[52] B. D. Unluturk, A. O. Bicen, and I. F. Akyildiz, "Genetically Engineered Bacteria-Based BioTransceivers for Molecular Communication," *IEEE Transactions on Communications*, vol. 63, no. 4, pp. 1271–1281, Apr. 2015.

[53] R. Weiss, S. Basu, S. Hooshangi, A. Kalmbach, D. Karig, R. Mehreja, and I. Netravali, "Genetic circuit building blocks for cellular computation, communications, and signal processing," *Natural Computing*, vol. 2, no. 1, pp. 47–84, Mar. 2003.

[54] A. A. Nielsen, B. S. Der, J. Shin, P. Vaidyanathan, V. Paralanov, E. A. Strychalski, D. Ross, D. Densmore, and C. A. Voigt, "Genetic circuit design automation," *Science*, vol. 352, no. 6281, aac7341, Apr. 2016.

[55] R. Manzoni, A. Urrios, S. Velazquez-Garcia, E. de Nadal, and F. Posas, "Synthetic biology: Insights into biological computation," *Integrative Biology*, vol. 8, no. 4, pp. 518–532, Apr. 2016.

[56] W. Ji, H. Shi, H. Zhang, R. Sun, J. Xi, D. Wen, J. Feng, Y. Chen, X. Qin, Y. Ma, W. Luo, L. Deng, H. Lin, R. Yu, and Q. Ouyang, "A Formalized Design Process for Bacterial Consortia That Perform Logic Computing," *PLoS ONE*, vol. 8, no. 2, Feb. 2013.

[57] M. Mimee, P. Nadeau, A. Hayward, S. Carim, S. Flanagan, L. Jerger, J. Collins, S. McDonnell, R. Swartwout, R. J. Citorik, *et al.*, "An ingestible bacterial-electronic system to monitor gastrointestinal health," *Science*, vol. 360, no. 6391, pp. 915–918, 2018.

[58] D. Puchberger-Enengl, S. Podszun, H. Heinz, C. Hermann, P. Vulto, and G. A. Urban, "Microfluidic concentration of bacteria by on-chip electrophoresis," *Biomicrofluidics*, vol. 5, no. 4, p. 044 111, 2011.

[59] T. M. Wassenaar, "Bacteria: The benign, the bad, and the beautiful," in. Wiley Online Library, 2012, ch. How Old Are They?

[60] C. Anetzberger and K. Jung, "Introduction," in *Bacteria Signalling*, R. Kramer and K. Jung, Eds., Wiley-Blackwell, 2010, ch. 1, pp. 3–5.

[61] R. M. Harshey, "Bacterial motility on a surface: Many ways to a common goal," *Annual Reviews in Microbiology*, vol. 57, no. 1, pp. 249–273, Oct. 2003.

[62] Z. Wang, M. Kim, and G. Rosen, "Validating models of bacterial chemotaxis by simulating the random motility coefficient," in *2008 8th IEEE International Conference on BioInformatics and BioEngineering*, IEEE, Oct. 2008, pp. 1–5.

[63] J. A. Wolff, J. J. Ludtke, G. Acsadi, P. Williams, and A. Jani, "Long-term persistence of plasmid dna and foreign gone expression in mouse muscle," *Human molecular genetics*, vol. 1, no. 6, pp. 363–369, Sep. 1992.

[64] M. Amos, I. M. Axmann, N. Blüthgen, F. de la Cruz, A. Jaramillo, A. Rodriguez-Paton, and F. Simmel, "Bacterial computing with engineered populations," *Philosophical Transactions of the Royal Society A: Mathematical, Physical and Engineering Sciences*, vol. 373, no. 2046, p. 20 140 218, Jul. 2015.

[65] M. Hajimorad and J. Gralnick, "Towards enabling engineered microbial-electronic systems: Rk2-based conjugal transfer system for shewanella synthetic biology," *Electronics Letters*, vol. 52, no. 6, pp. 426–428, Jan. 2016.

[66] P. Mehta, S. Goyal, T. Long, B. L. Bassler, and N. S. Wingreen, "Information processing and signal integration in bacterial quorum sensing," *Molecular systems biology*, vol. 5, no. 1, p. 325, Jan. 2009.

[67] M. B. Miller and B. L. Bassler, "Quorum sensing in bacteria," *Annual Reviews in Microbiology*, vol. 55, no. 1, pp. 165–199, Oct. 2001.

[68] B. L. Bassler, "How bacteria talk to each other: Regulation of gene expression by quorum sensing," *Current opinion in microbiology*, vol. 2, no. 6, pp. 582–587, Dec. 1999.

[69] C. M. Waters and B. L. Bassler, "Quorum sensing: Cell-to-cell communication in bacteria," *Annu. Rev. Cell Dev. Biol.*, vol. 21, pp. 319–346, Nov. 2005.

[70] W. K. Purves, D. E. Sadava, G. H. Orians, and H. C. Heller, *Life: the science of biology*. Macmillan, 2001, p. 349.

[71] A. Marcone, M. Pierobon, and M. Magarini, "Parity-check coding based on genetic circuits for engineered molecular communication between biological cells," *IEEE Transactions on Communications*, vol. 66, no. 12, pp. 6221–6236, Dec. 2018.

[72] D. Roszak and R. Colwell, "Survival strategies of bacteria in the natural environment.," *Microbiological reviews*, vol. 51, no. 3, p. 365, Sep. 1987.

[73] C. de la Fuente-Núñez, F. Reffuveille, L. Fernández, and R. E. Hancock, "Bacterial biofilm development as a multicellular adaptation: antibiotic resistance and new therapeutic strategies," *Current Opinion in Microbiology*, vol. 16, no. 5, pp. 580–589, Oct. 2013.

[74] K. Shimizu, "Regulation systems of bacteria such as escherichia coli in response to nutrient limitation and environmental stresses," *Metabolites*, vol. 4, no. 1, pp. 1–35, Mar. 2014.

[75] H.-C. Flemming and J. Wingender, "The biofilm matrix," *Nature Reviews Microbiology*, vol. 8, no. 9, p. 623, Sep. 2010.

[76] A. K. Bhardwaj and K. Vinothkumar, "Evolution of mdrs," in *Quorum Sensing vs Quorum Quenching: A Battle with No End in Sight*, Springer, New Delhi, 2015, pp. 9–22.

[77] B. Kilb, B. Lange, G. Schaule, H.-C. Flemming, and J. Wingender, "Contamination of drinking water by coliforms from biofilms grown on rubber-coated valves," *International journal of hygiene and environmental health*, vol. 206, no. 6, pp. 563–573, Jan. 2003.

[78] E. Karatan and P. Watnick, "Signals, regulatory networks, and materials that build and break bacterial biofilms," *Microbiol. Mol. Biol. Rev.*, vol. 73, no. 2, pp. 310–347, Jun. 2009.

[79] W. N. Chaudhry, J. Concepcion-Acevedo, T. Park, S. Andleeb, J. J. Bull, and B. R. Levin, "Synergy and order effects of antibiotics and phages in killing pseudomonas aeruginosa biofilms," *PloS one*, vol. 12, no. 1, e0168615, Jan. 2017.

[80] M. Sadekuzzaman, S. Yang, M. Mizan, and S. Ha, "Current and recent advanced strategies for combating biofilms," *Comprehensive Reviews in Food Science and Food Safety*, vol. 14, no. 4, pp. 491–509, Jul. 2015.

[81] L. Goers, N. Kylilis, M. Tomazou, K. Y. Wen, P. Freemont, and K. Polizzi, "Engineering microbial biosensors," in *Methods in Microbiology*, vol. 40, Elsevier, 2013, pp. 119–156.

[82] M. Kuscu and O. B. Akan, "Modeling convection-diffusion-reaction systems for microfluidic molecular communications with surface-based receivers in Internet of Bio-Nano Things," *PLOS ONE*, vol. 13, no. 2, P.-P. Liu, Ed., e0192202, Feb. 2018.

[83] D. Tilman, "Tests of Resource Competition Theory Using Four Species of Lake Michigan Algae," *Ecology*, vol. 62, pp. 802–815, Jun. 1981.

[84] P. Melke, P. Sahlin, A. Levchenko, and H. Jönsson, "A cell-based model for quorum sensing in heterogeneous bacterial colonies," *PLoS Computational Biology*, vol. 6, no. 6, pp. 1–13, Jun. 2010.

[85] Y. Hu, Y. Yang, E. Katz, and H. Song, "Programming the quorum sensing-based and gate in shewanella oneidensis for logic gated-microbial fuel cells," *Chemical Communications*, vol. 51, no. 20, pp. 4184–4187, Feb. 2015.

[86] P. Siuti, J. Yazbek, and T. K. Lu, "Synthetic circuits integrating logic and memory in living cells," *Nature biotechnology*, vol. 31, no. 5, p. 448, May 2013.

[87] U. Alon, *An introduction to systems biology: design principles of biological circuits*. Chapman and Hall/CRC, 2006.

[88] P. E. M. Purnick and R. Weiss, "The second wave of synthetic biology: from modules to systems," *Nature Reviews Molecular Cell Biology*, vol. 10, no. 6, pp. 410–422, Jun. 2009.

[89] B. Wang, R. I. Kitney, N. Joly, and M. Buck, "Engineering modular and orthogonal genetic logic gates for robust digital-like synthetic biology," *Nature communications*, vol. 2, p. 508, Oct. 2011.

[90] J. S. Hallinan, O. Gilfellon, G. Misirli, and A. Wipat, "Tuning receiver characteristics in bacterial quorum communication: An evolutionary approach using standard virtual biological parts," in *2014 IEEE Conference on Computational Intelligence in Bioinformatics and Computational Biology*, IEEE, May 2014, pp. 1–8, ISBN: 978-1-4799-4536-8.

[91] A. O. Bicen, C. M. Austin, I. F. Akyildiz, and C. R. Forest, "Efficient Sampling of Bacterial Signal Transduction for Detection of Pulse-Amplitude Modulated Molecular Signals," *IEEE Transactions on Biomedical Circuits and Systems*, vol. 9, no. 4, pp. 505–517, Sep. 2015.

[92] M. Pierobon and I. F. Akyildiz, "Noise analysis in ligand-binding reception for molecular communication in nanonetworks," *IEEE Transactions on Signal Processing*, vol. 59, no. 9, pp. 4168–4182, 2011.

[93] H. Jaffe and D. Berlincourt, "Piezoelectric transducer materials," *Proceedings of the IEEE*, vol. 53, no. 10, pp. 1372–1386, Oct. 1965.

[94] R. Mesleh and A.-O. Ayat, "Acousto-optical modulators for free space optical wireless communication systems," *Journal of Optical Communications and Networking*, vol. 10, no. 5, pp. 515–522, May 2018.

[95] C. Kung, B. Martinac, and S. Sukharev, "Mechanosensitive channels in microbes," *Annual review of microbiology*, vol. 64, pp. 313–329, Oct. 2010.

[96] A. Prindle, J. Liu, M. Asally, S. Ly, J. Garcia-Ojalvo, and G. M. Süel, "Ion channels enable electrical communication in bacterial communities," *Nature*, vol. 527, no. 7576, p. 59, Nov. 2015.

[97] F. Sachs and C. E. Morris, "Mechanosensitive ion channels in nonspecialized cells," in *Reviews of Physiology Biochemistry and Pharmacology, Volume 132*, Springer, 1998, pp. 1–77.

[98] H. H. Tuson and D. B. Weibel, "Bacteria–surface interactions," *Soft Matter*, vol. 9, no. 17, pp. 4368–4380, Mar. 2013.

[99] L. Gomes, L. Silva, M. Simões, L. Melo, and F. Mergulhão, "Escherichia coli adhesion, biofilm development and antibiotic susceptibility on biomedical materials," *Journal of Biomedical Materials Research Part A*, vol. 103, no. 4, pp. 1414–1423, Apr. 2015.

[100] H. J. Busscher and H. C. van der Mei, "How do bacteria know they are on a surface and regulate their response to an adhering state?" *PLoS pathogens*, vol. 8, no. 1, e1002440, Jan. 2012.

[101] C. Piñero-Lambea, G. Bodelón, R. Fernández-Periáñez, A. M. Cuesta, L. Álvarez-Vallina, and L. Á. Fernández, "Programming controlled adhesion of e. coli to target surfaces, cells, and tumors with synthetic adhesins," *ACS synthetic biology*, vol. 4, no. 4, pp. 463–473, Jul. 2014.

[102] R. Sadamoto, K. Niikura, T. Ueda, K. Monde, N. Fukuhara, and S.-I. Nishimura, "Control of bacteria adhesion by cell-wall engineering," *Journal of the American Chemical Society*, vol. 126, no. 12, pp. 3755–3761, Mar. 2004.

[103] G. Georgiou, H. L. Poetschke, C. Stathopoulos, and J. A. Francisco, "Practical applications of engineering gram-negative bacterial cell surfaces," *Trends in biotechnology*, vol. 11, no. 1, pp. 6–10, Jan. 1993.

[104] T. Danino, O. Mondragón-Palomino, L. Tsimring, and J. Hasty, "A synchronized quorum of genetic clocks," *Nature*, vol. 463, no. 7279, p. 326, Jan. 2010.

[105] D. Shrestha, Z. Pang, and D. Dzung, "Precise clock synchronization in high performance wireless communication for time sensitive networking," *IEEE Access*, vol. 6, pp. 8944–8953, Feb. 2018.

[106] K. A. Dyar, D. Lutter, A. Artati, N. J. Ceglia, Y. Liu, D. Armenta, M. Jastroch, S. Schneider, S. de Mateo, M. Cervantes, *et al.*, "Atlas of circadian metabolism reveals system-wide coordination and communication between clocks," *Cell*, vol. 174, no. 6, pp. 1571–1585, Sep. 2018.

[107] N. C. Reading and V. Sperandio, "Quorum sensing: The many languages of bacteria," *FEMS microbiology letters*, vol. 254, no. 1, pp. 1–11, Jan. 2006.

[108] M. B. Elowitz and S. Leibler, "A synthetic oscillatory network of transcriptional regulators," *Nature*, vol. 403, no. 6767, p. 335, Jan. 2000.

[109] J. Stricker, S. Cookson, M. R. Bennett, W. H. Mather, L. S. Tsimring, and J. Hasty, "A fast, robust and tunable synthetic gene oscillator," *Nature*, vol. 456, no. 7221, p. 516, Nov. 2008.

[110] C. Mollén, E. G. Larsson, and T. Eriksson, "Waveforms for the massive mimo downlink: Amplifier efficiency, distortion, and performance," *IEEE Transactions on Communications*, vol. 64, no. 12, pp. 5050–5063, Apr. 2016.

[111] J. Zeng, J. Teo, A. Banerjee, T. W. Chapman, J. Kim, and R. Sarpeshkar, "A synthetic microbial operational amplifier," *ACS synthetic biology*, vol. 7, no. 9, pp. 2007–2013, Aug. 2018.

[112] G. J. Nistala, K. Wu, C. V. Rao, and K. D. Bhalerao, "A modular positive feedback-based gene amplifier," *Journal of biological engineering*, vol. 4, no. 1, p. 4, Dec. 2010.

[113] H.-S. Lee and C. G. Sodini, "Analog-to-digital converters: Digitizing the analog world," *Proceedings of the IEEE*, vol. 96, no. 2, pp. 323–334, Feb. 2008.

[114] J. Zeng, A. Banerjee, J. Kim, Y. Deng, T. W. Chapman, R. Daniel, and R. Sarpeshkar, "A novel bioelectronic reporter system in living cells tested with a synthetic biological comparator," *Scientific reports*, vol. 9, no. 1, p. 7275, May 2019.

[115] L. D. Paarmann, *Design and analysis of analog filters: a signal processing perspective*. Springer Science & Business Media, 2006, vol. 617.

[116] R. J. Cameron, C. M. Kudsia, and R. R. Mansour, *Microwave filters for communication systems: fundamentals, design, and applications*. John Wiley & Sons, 2018.

[117] N. Marsidi, H. A. Hasan, and S. R. S. Abdullah, "A review of biological aerated filters for iron and manganese ions removal in water treatment," *Journal of Water Process Engineering*, vol. 23, pp. 1–12, Jun. 2018.

[118] T. Sohka, R. A. Heins, R. M. Phelan, J. M. Greisler, C. A. Townsend, and M. Ostermeier, "An externally tunable bacterial band-pass filter," *Proceedings of the National Academy of Sciences*, vol. 106, no. 25, pp. 10 135–10 140, Jun. 2009.

[119] M.-T. Lin, C.-Y. Wang, H.-J. Xie, C. H. Y. Cheung, C.-H. Hsieh, H.-F. Juan, B.-S. Chen, and C. Lin, "Novel utilization of terminators in the design of biologically adjustable synthetic filters," *ACS synthetic biology*, vol. 5, no. 5, pp. 365–374, Mar. 2016.

[120] K. Brenner, D. K. Karig, R. Weiss, and F. H. Arnold, "Engineered bidirectional communication mediates a consensus in a microbial biofilm consortium," *Proceedings of the National Academy of Sciences*, vol. 104, no. 44, pp. 17 300–17 304, Oct. 2007.

[121] B. Drees, M. Reiger, K. Jung, and I. B. Bischofs, "A modular view of the diversity of cell-density-encoding schemes in bacterial quorum-sensing systems," *Biophysical journal*, vol. 107, no. 1, pp. 266–277, Jul. 2014.

[122] F. Sedlmayer, D. Hell, M. Müller, D. Ausländer, and M. Fussenegger, "Designer cells programming quorum-sensing interference with microbes," *Nature communications*, vol. 9, no. 1, p. 1822, May 2018.

[123] F. K. Balagaddé, H. Song, J. Ozaki, C. H. Collins, M. Barnet, F. H. Arnold, S. R. Quake, and L. You, "A synthetic escherichia coli predator–prey ecosystem," *Molecular systems biology*, vol. 4, no. 1, p. 187, Jan. 2008.

[124] W. Kong, D. R. Meldgin, J. J. Collins, and T. Lu, "Designing microbial consortia with defined social interactions," *Nature Chemical Biology*, vol. 14, no. 8, p. 821, Aug. 2018.

[125] S. P. Barros, R. Williams, S. Offenbacher, and T. Morelli, "Gingival crevicular fluid as a source of biomarkers for periodontitis," *Periodontology 2000*, vol. 70, no. 1, pp. 53–64, Feb. 2016.

[126] C. Chowdhury, S. Chun, A. Pang, M. R. Sawaya, S. Sinha, T. O. Yeates, and T. A. Bobik, "Selective molecular transport through the protein shell of a bacterial microcompartment organelle," *Proceedings of the National Academy of Sciences*, vol. 112, no. 10, pp. 2990–2995, Mar. 2015.

[127] Y. Chahibi, I. F. Akyildiz, S. Balasubramaniam, and Y. Koucheryavy, "Molecular communication modeling of antibody-mediated drug delivery systems," *IEEE Transactions on Biomedical Engineering*, vol. 62, no. 7, pp. 1683–1695, Feb. 2015.

[128] M. Pierobon, "A systems-theoretic model of a biological circuit for molecular communication in nanonetworks," *Nano Communication Networks*, vol. 5, no. 1-2, pp. 25–34, Mar. 2014.

[129] B. P. Van Milligen, P. Bons, B. A. Carreras, and R. Sanchez, "On the applicability of fick's law to diffusion in inhomogeneous systems," *European journal of physics*, vol. 26, no. 5, p. 913, Jul. 2005.

[130] Y. V. Kalinin, L. Jiang, Y. Tu, and M. Wu, "Logarithmic sensing in escherichia coli bacterial chemotaxis," *Biophysical journal*, vol. 96, no. 6, pp. 2439–2448, Mar. 2009.

[131] Q. Wang and T. Zhang, "Review of mathematical models for biofilms," *Solid State Communications*, vol. 150, no. 21-22, pp. 1009–1022, Jun. 2010.

[132] J. D. Chambless, S. M. Hunt, and P. S. Stewart, "A three-dimensional computer model of four hypothetical mechanisms protecting biofilms from antimicrobials," *Appl. Environ. Microbiol.*, vol. 72, no. 3, pp. 2005–2013, Mar. 2006.

[133] L. E. Weiss, J. P. Badalamenti, L. J. Weaver, A. R. Tascone, P. S. Weiss, T. L. Richard, and P. C. Cirino, "Engineering motility as a phenotypic response to luxi/r-dependent quorum sensing in escherichia coli," *Biotechnology and bioengineering*, vol. 100, no. 6, pp. 1251–1255, Aug. 2008.

[134] S. Bi, A. M. Pollard, Y. Yang, F. Jin, and V. Sourjik, "Engineering hybrid chemotaxis receptors in bacteria," *ACS synthetic biology*, vol. 5, no. 9, pp. 989–1001, Jun. 2016.

[135] J. C. Anderson, E. J. Clarke, A. P. Arkin, and C. A. Voigt, "Environmentally controlled invasion of cancer cells by engineered bacteria," *Journal of molecular biology*, vol. 355, no. 4, pp. 619–627, Jan. 2006.

[136] L. L. Looger, M. A. Dwyer, J. J. Smith, and H. W. Hellinga, "Computational design of receptor and sensor proteins with novel functions," *Nature*, vol. 423, no. 6936, p. 185, May 2003.

[137] M. Dwyer, L. Looger, and H. Hellinga, "Computational design of a zn2+ receptor that controls bacterial gene expression," *Proceedings of the National Academy of Sciences*, vol. 100, no. 20, pp. 11 255–11 260, Sep. 2003.

[138] O. B. Akan, H. Ramezani, T. Khan, N. A. Abbasi, and M. Kuscu, "Fundamentals of molecular information and communication science," *Proceedings of the IEEE*, vol. 105, no. 2, pp. 306–318, Nov. 2016.

[139] O. Tsave, I. Kavakiotis, K. Kantelis, S. Mavridopoulos, P. Nicopolitidis, G. Papadimitriou, I. Vlahavas, and A. Salifoglou, "The anatomy of bacteria-inspired nanonetworks: Molecular nanomachines in message dissemination," *Nano Communication Networks*, May 2019.

[140] T. E. Gorochowski, "Agent-based modelling in synthetic biology," *Essays in biochemistry*, vol. 60, no. 4, pp. 325–336, Nov. 2016.

[141] K. Kantelis, G. Papadimitriou, P. Nikopolitidis, I. Kavakiotis, O. Tsave, and A. Salifoglou, "Fick's law model revisited: A new approach to modeling multiple sources message dissemination in bacterial communication nanosystems," *IEEE Transactions on Molecular, Biological and Multi-Scale Communications*, vol. 3, no. 2, pp. 89–105, Jun. 2017.

[142] Y. Zhu and R. Sivakumar, "Challenges: Communication through silence in wireless sensor networks," in *Proceedings of the 11th annual international conference on Mobile computing and networking*, ACM, Aug. 2005, pp. 140–147.

[143] S. H. Sellke, C.-C. Wang, S. Bagchi, and N. Shroff, "Tcp/ip timing channels: Theory to implementation," in *IEEE INFOCOM 2009*, IEEE, Apr. 2009, pp. 2204–2212.

[144] D. P. Martins, K. Leetanasaksakul, M. Taynnan Barros, A. Thamchaipenet, W. Donnely, and S. Balasubramaniam, "Molecular communications pulse-based jamming model for bacterial biofilm suppression," *IEEE Transactions on Nanobioscience*, vol. 17, no. 4, pp. 533–542, Oct. 2018.

[145] K. Leetanasaksakul, S. Kittisenachai, S. Roytrakul, and A. Thamchaipenet, *Investigation of Staphylococcus aureus biofilm inhibition by a marine Streptomyces sp. GKU 223 using a proteomic approach*, submitted to PLoS ONE, 2018.

[146] D. P. Martins, M. Taynnan Barros, M. Pierobon, M. Kandhavelu, P. Lio', and S. Balasubramaniam, "Computational models for trapping ebola virus using engineered bacteria," *IEEE/ACM Transactions on Computational Biology and Bioinformatics*, vol. 15, no. 6, pp. 2017–2027, Nov. 2018.

[147] D. P. Martins, M. Taynnan Barros, and S. Balasubramaniam, "Quality and capacity analysis of molecular communications in bacterial synthetic logic circuits," *IEEE Transactions on Nanobioscience*, vol. 18, no. 4, pp. 628–639, Oct. 2019.

[148] D. P. Martins, M. Taynnan Barros, L. Coffey, P. D. Cotter, D. P. Berry, and S. Balasubramaniam, "Frequency analysis of logic computation for bacteria-based biosensor molecular communication system," *Submitted to IEEE Transactions on Communications*, 2019.

[149] P. E. Kilgore, J. D. Grabenstein, A. M. Salim, and M. Rybak, "Treatment of ebola virus disease," *Pharmacotherapy: The Journal of Human Pharmacology and Drug Therapy*, vol. 35, no. 1, pp. 43–53, Jan. 2015.

[150] S.-M. Tien, C.-Y. Hsu, and B.-S. Chen, "Engineering bacteria to search for specific concentrations of molecules by a systematic synthetic biology design method," *PloS one*, vol. 11, no. 4, e0152146, Apr. 2016.

[151] T. Danino, A. Prindle, G. A. Kwong, M. Skalak, H. Li, K. Allen, J. Hasty, and S. N. Bhatia, "Programmable probiotics for detection of cancer in urine," *Science translational medicine*, vol. 7, no. 289, 289ra84, May 2015.

[152] C. A. Swofford, N. Van Dessel, and N. S. Forbes, "Quorum-sensing salmonella selectively trigger protein expression within tumors," *Proceedings of the National Academy of Sciences*, vol. 112, no. 11, pp. 3457–3462, Mar. 2015.

[153] S. Tauriainen, M. Karp, W. Chang, and M. Virta, "Luminescent bacterial sensor for cadmium and lead," *Biosensors and Bioelectronics*, vol. 13, no. 9, pp. 931–938, Oct. 1998.

[154] Y. G.-Y. Chan, H. K. Kim, O. Schneewind, and D. Missiakas, "The capsular polysaccharide of staphylococcus aureus is attached to peptidoglycan by the lytr-cpsa-psr (lcp) family of enzymes," *Journal of Biological Chemistry*, vol. 289, no. 22, pp. 15 680–15 690, 2014.

[155] S. Herbert, S. W. Newell, C. Lee, K.-P. Wieland, B. Dassy, J.-M. Fournier, C. Wolz, and G. Döring, "Regulation of staphylococcus aureus type 5 and type 8 capsular polysaccharides by co2," *Journal of bacteriology*, vol. 183, no. 15, pp. 4609–4613, 2001.

[156] L. Zhao, T. Xue, F. Shang, H. Sun, and B. Sun, "Staphylococcus aureus ai-2 quorum sensing associates with the kdpde two-component system to regulate capsular polysaccharide synthesis and virulence," *Infection and immunity*, vol. 78, no. 8, pp. 3506–3515, 2010.

[157] C. R. Arciola, D. Campoccia, S. Ravaioli, and L. Montanaro, "Polysaccharide intercellular adhesin in biofilm: Structural and regulatory aspects," *Frontiers in cellular and infection microbiology*, vol. 5, p. 7, 2015.

[158] Y. Wu, Y. Wu, T. Zhu, H. Han, H. Liu, T. Xu, P. Francois, A. Fischer, L. Bai, F. Götz, *et al.*, "Staphylococcus epidermidis srrab regulates bacterial growth and biofilm formation differently under oxic and microaerobic conditions," *Journal of bacteriology*, vol. 197, no. 3, pp. 459–476, 2015.

[159] A. A. Pragman, Y. Ji, and P. M. Schlievert, "Repression of staphylococcus aureus srrab using inducible antisense srra alters growth and virulence factor transcript levels," *Biochemistry*, vol. 46, no. 1, pp. 314–321, 2007.

[160] D. P. Martins, M. Taynnan Barros, T. Sinkruasuan, B. O'Sullivan, A. O'Riordan, and S. Balasubramaniam, "A reliability analysis for bacterial molecular computing on a chip," *Submitted to IEEE Transactions on Emerging Technologies in Computing*, 2019.

[161] J. L. Marzo, J. M. Jornet, and M. Pierobon, "Nanonetworks in biomedical applications," *Current drug targets*, vol. 20, no. 8, pp. 800–807, Jun. 2019.

[162] M. Veletić and I. Balasingham, "Synaptic communication engineering for future cognitive brain-machine interfaces," *Proceedings of the IEEE*, vol. 107, no. 7, pp. 1425–1441, Jul. 2019.

[163] F. Walsh and S. Balasubramaniam, "Reliability and delay analysis of multihop virus-based nanonetworks," *IEEE Transactions on Nanotechnology*, vol. 12, no. 5, pp. 674–684, Jun. 2013.

[164] Y. Uriel, R. Gries, L. Tu, C. Carroll, H. Zhai, M. Moore, and G. Gries, "The fly factor phenomenon is mediated by interkingdom signaling between bacterial symbionts and their blow fly hosts," *Insect science*, Jul. 2018.

[165] R. Gregor, S. David, and M. Meijler, "Chemical strategies to unravel bacterial–eukaryotic signaling," *Chemical Society Reviews*, vol. 47, no. 5, pp. 1761–1772, Mar. 2018.

[166] B. G. Coutinho, E. Mevers, A. L. Schaefer, D. A. Pelletier, C. S. Harwood, J. Clardy, and E. P. Greenberg, "A plant-responsive bacterial-signaling system senses an ethanolamine derivative," *Proceedings of the National Academy of Sciences*, vol. 115, no. 39, pp. 9785–9790, Sep. 2018.